2019

Staphylococcus Aureus Evasion of the Innate Immune System

James Paul Grayczyk

LOYOLA UNIVERSITY CHICAGO

STAPHYLOCOCCUS AUREUS EVASION OF THE INNATE IMMUNE SYSTEM

A DISSERTATION SUBMITTED TO

THE FACULTY OF THE GRADUATE SCHOOL

IN CANDIDACY FOR THE DEGREE OF

DOCTOR OF PHILOSOPHY

PROGRAM IN MICROBIOLOGY AND IMMUNOLOGY

BY

JAMES PAUL GRAYCZYK

CHICAGO, ILLINIOS

AUGUST 2019

ACKNOWLEDGEMENTS

First and foremost, I would like to thank my mentor and advisor Dr. Francis Alonzo for guiding me through my PhD. The words “thank you” are not adequate to express my gratitude for the immense amount of patience, wisdom, and guidance he provided me throughout my time in his lab. His tireless work ethic, vast scientific expertise, phenomenal scientific communication skills, and curiosity all set the stage for what an excellent scientist and mentor he is. As I continue to venture through my scientific career, I will be forever shaped by his guidance and mentorship he has instilled upon me over these past years. I look forward to seeing the great things in store for the Alonzo lab over the coming years.

Secondly, I would like to thank all members of the Alonzo lab for making my time in lab not only enjoyable but also a wonderful scientific journey. I am indebted for the instances where fellow members have assisted in experiments and provided valuable insights into my data. Thank you Azul Zorzoli, Chelsea White, Ryan Novak, Irina Laczkovich, Tracy Chen, Alex Argianas, Cameron Harvey, Dr. Wei Ping Teoh, Sarah Flury, CJ Cosgriff, Zach Resko and even Won Paik for everything over the years. My experience in lab would not have been as great as it was if I were not surrounded by wonderful people.

Also, I would like to acknowledge my dissertation committee, Drs. Alan Wolfe, Phong Le, Nancy Freitag, and Andrew Ulijasz for their insight and guidance into my project. Furthermore, thank you to everyone in the Department of Microbiology and

Immunology providing a scientific stimulating and fun environment. Thank you to Pat Simms for your expertise in flow cytometry.

I would like to also thank my family for always supporting and believing in me during this journey. Sarah you have provided more support and compassion to me than I deserve.

TABLE OF CONTENTS

LIST OF TABLES

LIST OF FIGURES

LIST OF ABBREVIATIONS

CDC	Centers for Disease Control and Prevention
MRSA	methicillin-resistant *S. aureus*
MLST	multilocus sequence typing
PFGE	pulsed-field gel electrophoresis
CC	clonal complex
DNA	deoxyribonucleic acid
HA	healthcare-associated
CA	community-associated
MSSA	methicillin-susceptible *S. aureus*
AMP	antimicrobial peptide
IL	interleukin
Ig	immunoglobulin
TNF	tumor necrosis factor
MHC	major histocompatibility complex
CD	cluster of differentiation
Th	T helper
Luk	Leukotoxin
PMN	polymorphonuclear
MCP-1	monocyte chemotactic protein 1
LPS	lipopolysaccharide

IFN	interferon
TGF	transforming growth factor
PRR	pattern recognition receptor
RNA	ribonucleic acid
PAMP	pathogen-associated molecular pattern
TLR	Toll-like receptor
CLR	C-type lectin receptor
RIG-I	retinoic acid-inducible gene-I
FPR	formylated protein receptor
NOD	nucleotide binding-oligomerization domain
S	Svedberg
LTA	lipoteichoic acid
PSM	phenol-soluble modulin
NLR	NOD-like receptor
TIR	Toll/IL-1 receptor domain
LRR	leucine-rich repeats
NF-κB	nuclear factor kappa B
MyD88	myeloid differentiation primary response 88
IRAK-4	IL-1receptor associated kinase 4
IRAK-1	IL-1receptor associated kinase 1
TRAF6	tumor necrosis factor receptor associated factor 6
NEMO	nuclear factor kappa B essential modulator
TAK1	transforming growth factor activated kinase 1

IKK	I kappa B kinase
MAPK	mitogen-activated protein kinases
AP-1	activation factor-1
CC	chemokine C-C motif
MIP	macrophage inflammatory protein
KC	keratinocyte-derived cytokine
ATP	adenosine triphosphate
NET	neutrophil extracellular trap
MPO	myeloperoxidase
Fe	iron
Zn	zinc
Mn	manganese
ROS	reactive oxygen species
NADPH	nicotinamide adenine dinucleotide phosphate
Phox	phagocyte oxidase
Rac	ras-related C3 botulinum toxin substrate
$O_2^{-\bullet}$	superoxide
$\bullet$	radical
H_2O_2	hydrogen peroxide
CGD	chronic granulomatous disease
mROS	mitochondrial reactive oxygen species
$NO^{\bullet}$	nitric oxide
iNOS	inducible nitric oxide synthetase

$ONOO^-$	peroxynitrite
RNS	reactive nitrogen species
SCIN	*Staphylococcus* complement inhibitor
SAK	Staphylokinase
SpA	Staphylococcal protein A
Sbi	Staphylococcal binder of immunoglobulin
Efb	extracellular fibrinogen binding molecule
Ecb	extracellular complement binding molecule
SSL	superantigen-like
Eap	extracellular adherence protein
CHIPS	chemotaxis inhibitory protein of *S. aureus*
FLIPr	formyl peptide receptor-like 1 inhibitor
SelX	Staphylococcal enterotoxin-like protein
PSGL1	P-selectin glycoprotein ligand 1
ICAM1	intercellular adhesion molecule 1
ADAM10	A disintegrin metalloproteinase domain containing protein 10
Hla	alpha-hemolysin
Hlg	gamma-hemolysin
PVL	Panton-Valentine leukocidin
SodA/M	superoxide dismutase A or M
Msr	methionine sulfoxide reductase
Sok	surface factor promoting resistance to oxidative killing
DARC	duffy antigen chemokine receptor

Hmp	flavohemoglobin
Ldh1	lactate dehydrogenase
GAPDH	glyceraldehyde-3-phosphate
Atl	autolysin
PDH	pyruvate dehydrogenase
OGDH	2-oxoglutarate dehydrogenase
BCODH	branched-chain 2-oxoacid dehydrogenase
GCS	glycine cleavage system
AoDH	acetonin dehydrogenase
TCA	tricarboxylic acid
coA	coenzyme A
WT	wild type
LAC	Los Angeles County
RPMI	Roswell Park Memorial Institute
TSB	tryptic soy broth
TSA	tryptic soy agar
LB	lysogeny broth
Erm	erythromycin
Kan	kanamycin
Neo	neomycin
Cam	chloramphenicol
BCFA	branched chain fatty acids
°C	degree Celsius

µg	microgram
pg	picogram
µL	microliter
µM	micromolar
mL	milliliter
mM	millimolar
nM	nanomolar
nm	nanometer
rpm	rotations per minute
O/N	overnight
M	molar
PCR	polymerase chain reaction
SOEing	splicing by overlap extension
AnTet	anhydrous tetracycline
BMM	bone marrow derived macrophage
DMSO	dimethyl sulfoxide
DMEM	Dulbecco modified Eagle medium
ACK	ammonium chloride potassium
PBS	phosphate buffered saline
FBS	fetal bovine serum
HI	heat inactivated
CBA	cytometric bead array
FACS	fluorescence activated cell sorting

OD	optical density
PES	polyethersulfone
L	liter
PMSF	phenylmethane sulfonyl fluoride
DTT	dithiothreitol
BCA	bicinchoninic acid
SDS-PAGE	sodium dodecyl sulfate polyacrylamide gel electrophoresis
IB	immunoblot
CB	Coomassie blot
kDa	kilodalton
TBST	tris-buffered saline tween
PBST	phosphate-buffered saline tween
HRP	horseradish peroxidase
BSA	bovine serum albumin
TCA	trichloroacetic acid
ELISA	enzyme-linked immunosorbent assay
IP	intraperitoneal
IV	intravenous
DPI	diphenyleneiodonium
L-NIL	N6-(1-Iminoethyl)-lysine hydrochloride
CFU	colony forming unit
MOI	multiplicity of infection
ANOVA	analysis of variance

ns	not significant
SD	standard deviation
MFI	mean fluorescent intensity
DC	dendritic cell

ABSTRACT

Upon entry into the host, pathogens must overcome innate immunity in order to cause disease. The innate immune system is a fast-acting initial line of defense to prevent infection. In order to withstand innate defenses, bacterial pathogens like the Gram-positive bacterium *Staphylococcus aureus* produce a wide array of virulence factors that can inhibit innate immune cell recruitment and antimicrobial activity, or directly target and kill phagocytic leukocytes thereby facilitating pathogenesis. Infection with *S. aureus* can cause disease in virtually any tissue site and is a significant burden to human health. In this thesis, we sought to understand how *S. aureus* counters the host innate immune system to cause disease. Macrophages are professional phagocytic leukocytes that are central to innate defenses. As such, we hypothesized that *S. aureus* must be able to overcome macrophage inflammatory responses to aid in its pathogenesis.

Data from a forward genetic screen using *S. aureus* cell free supernatants derived from a transposon mutant library uncovered that a mutation in the gene encoding the lipoic acid synthetase (LipA), which is required for the *de novo* synthesis of the cofactor lipoic acid, resulted in enhanced TLR2-dependent activation of macrophages. We found that the hyper-inflammatory response elicited by a Δ*lipA* mutant correlated with the absence of lipoylation on the E2 subunit of the pyruvate dehydrogenase complex (E2-PDH). In wild type cells, the release of lipoyl-E2-PDH occurred during exponential growth and required the major staphylococcal autolysin Atl.

Purified *S. aureus* lipoyl-E2-PDH prevented TLR1/2 activation by triacylated lipopeptides. Moreover, the absence of lipoyl-protein production in vivo resulted in the recruitment of activated inflammatory macrophages that are better able to restrict *S. aureus* growth through production of bactericidal reactive oxygen and nitrogen species. Despite enhanced antimicrobial immunity upon primary infection with a Δ*lipA* mutant, we found that the host fails to mount an improved recall response to secondary infection.

Overall, data in this thesis indicate that *S. aureus* lipoylated E2-PDH moonlights as a novel immune evasion protein by suppressing TLR-mediated macrophage activation. Our data also suggest that lipoic acid synthesis in *S. aureus* promotes bacterial persistence during infection through limitation of reactive oxygen and nitrogen species generation by macrophages. Broadly, this work furthers our understanding of the intersections between bacterial metabolism and the immune response to infection. Furthermore, work in this thesis provides a potential therapeutic target for *S. aureus* that can cripple bacteria replication and promote host immunity.

CHAPTER ONE

REVIEW OF LITERATURE

Section 1: *Staphylococcus aureus* and Human Health

Nearly 140 years have passed since Sir Alexander Ogston first isolated an infectious bacterium from a patient's leg abscess and named it *Staphylococcus aureus* (1, 2). *S. aureus* is a Gram-positive coccus which causes a significant amount of human disease. Up to one-third of humans are asymptomatic carriers of *S. aureus* where it mainly resides in the nasal cavities, but recent data demonstrates that other sites of the body can be colonized as well (3-9). In addition to these carriers, a large proportion of people are transiently colonized with *S. aureus* (3-5). The pool of asymptomatic and transient carriers contributes to a large carrier population. Though *S. aureus* is highly pathogenic and potentially lethal, it is considered to be part of normal bacterial flora in asymptomatic carriers (5). Moreover, these carriers may facilitate the transmission of *S. aureus* throughout the population both in healthcare and community settings (10).

S. aureus Disease and Morbidity.

The most common manifestation of *S. aureus* disease is skin and soft-tissue infections such as impetigo, boils, scalded skin syndrome, or abscesses, and atopic dermatitis. Though the skin is the most common infection site of *S. aureus*, the bacterium can breach skin barriers and colonize almost every tissue site in the host. Upon access to these other tissues of the host, *S. aureus* infections lead to more severe

diseases including osteomyelitis, pneumonia, toxic shock syndrome, necrotizing fasciitis, food borne illness, endocarditis, bacteremia, and sepsis.

S. aureus is an opportunistic pathogen. Immunocompromised individuals, as well as those undergoing device implantations or procedures like catheterization are all at higher risk of contracting a severe *S. aureus* infection (11). In 2013, the Centers for Disease Control and Prevention (CDC) estimated an incidence of 80,000 severe infections and 11,000 deaths caused by *S. aureus* (12). Alarmingly, a recent report cites that the number of reported severe infections has increased to just under 200,000 cases and around 20,000 deaths (13). A contributing factor to the mortality of patients with severe infections is the inability to treat *S. aureus* infections due to antibiotic resistance.

Antibiotic Resistance in *S. aureus*.

The first successful antibiotic to treat *S. aureus* infections was penicillin. However, resistance by *S. aureus* to penicillin quickly appeared (14, 15). In 1960, a synthetic derivative of penicillin, named methicillin, was created as an alternative aimed to treat penicillin-resistant *S. aureus* infections. However, after only one year of use the first incidence of methicillin-resistant *S. aureus* (MRSA) was identified (16). Resistance to methicillin is conferred by the presence of the *mecA* gene which is mobilized by a mobile genetic element called the staphylococcal cassette chromosome *mec* (17). The presence of methicillin resistance on a mobile genetic element leads to robust horizontal transfer between different *S. aureus* strains (18). A large number of genes that encode antibiotic resistance mechanisms and virulence factors are found on mobile genetic elements which are transferred by phage transduction (19). Transduction by phage is the most common route for gene transfer as *S. aureus* is not naturally competent.

Though resistance to methicillin is considered a dangerous adaptation, MRSA can still be treated with the antibiotic vancomycin. Similarly, as with methicillin, the emergence of vancomycin resistance in *S. aureus* isolates appeared quickly after its implementation (20, 21). Despite its high level of antimicrobial resistance, there are several antibiotics in use or in development that can still control this pathogen. Derivatives of vancomycin such as telavancin, dalbavancin, and oritavancin all can kill *S. aureus* in vitro (22, 23). In the clinic, the cephalosporins ceftobiprole and ceftaroline were shown to be effective against skin and soft-tissue infections (24, 25). In summary, the emergence of antibiotic resistant isolates of *S. aureus* highlights the adaptability of this human pathogen.

Epidemiology of *S. aureus*.

There are many different infectious strains and isolates of *S. aureus* that have been characterized over the years. Three main typing methods such as multilocus sequence typing (MLST), staphylococcal protein A gene (*spa*) typing, and pulsed-field gel electrophoresis (PFGE) have been used to molecularly classify the different types of *S. aureus* isolates (26). MLST is a sequence-based genotyping method based on single nucleotide variations of seven *S. aureus* housekeeping genes that lead to distinct profiles known as sequence type (ST) (27, 28). Furthermore, *S. aureus* genomes are categorized into clonal complexes (CC) based on MLST, of which four CC cover 90% of all known *S. aureus* genomes (29, 30). *spa* typing is based on the variable tandem repeats in the *spa* gene (31). Lastly, PFGE incorporates fragmentation of the DNA with restriction enzymes followed by separation of the fragments PFGE. In the United States, PFGE was chosen as a standard over other typing methods and classified eight different lineages designated as pulsed-field types USA100 through USA800 (32).

Although infections occur on a global scale, a global pandemic strain has never emerged, rather infectious strains tend to only regionally dominate. A recent example of a strain that emerged in the healthcare setting was CC30 in North America and Europe (33, 34). In focusing on current predominant strains in the United States, USA300 is the most common strain of *S. aureus* that spreads mainly in the community causing skin and soft-tissue infections (35). USA300 first emerged in 2000 as a cause of skin and soft-tissue infections among college football players in Pennsylvania and prisoners in Missouri (36, 37). Since 2000, it has continued to spread among the community in the United States and was isolated from cases of severe infections (38). The spread of USA300 is attributed to virulence characteristics like resistance to numerous antibiotics such as methicillin, erythromycin, levofloxacin, mupirocin, and tetracycline (35). Though USA300 is a dominant strain in the United States, it has been isolated in Europe, South America, and Australia (39-41).

With the first report of MRSA in 1961, that bacterium was believed to be transmitted in the healthcare setting. However, in the 1990s, cases of MRSA were beginning to be reported in the community in individuals that had no prior hospitalization leading to both healthcare-associated (HA) and community-associated (CA) infections (42). MRSA and methicillin-susceptible *S. aureus* (MSSA) infections are dominant in both the healthcare and community setting (43, 44). As such, in 2013 MRSA was classified as a serious threat to public health due to widespread infections and associated morbidity in the United States (45). Although a recent report by the CDC details a steady decline in the incidence of HA-MRSA infections from 2005-2012, between 2013-2016 this decline has slowed (13). Furthermore, CA-MRSA infection

rates have decreased at a much slower rate (13). Alarmingly, the rates of HA-MSSA infections have not decreased and CA-MSSA infections are still steadily increasing (13). The severity of infections caused by *S. aureus* and the continued dominance in hospital and community settings, underscore the need to find ways to treat *S. aureus* infections that do not rely on antibiotics or lead to resistance.

Section 2: Host Defense Against *S. aureus*

The success of *S. aureus* as a human pathogen is aided by its ability to overcome host defenses such as the innate immune system. In this section, we will introduce components of the innate immune system that *S. aureus* faces upon invasion of the host focusing most heavily on macrophages. This will be followed by a section detailing how the innate immune system can recognize *S. aureus*. Then we will describe ways in which the innate immune system controls *S. aureus* during infection. After introducing how the host innate immune system interacts, recognizes, and controls *S. aureus* infection we then will cover the myriad adaptations of *S. aureus* that function to overcome the host response to infection.

Physical and Chemical Barriers to *S. aureus* Infection.

The most common manifestation of *S. aureus* infection is skin and soft-tissue infection. Therefore, the first line of defense that *S. aureus* must overcome to cause disease is the host skin layer. The skin layer acts as physical barrier to prevent *S. aureus* from accessing deep tissues of the host. In the skin, epithelial cells linked together by tight junctions form a barrier to prevent *S. aureus* entry into the body. Besides these physical components, chemical components of the skin also work to defend against *S. aureus* infection. The skin is free of infection due to its slight acidic pH

and antimicrobial lipid composition (46). In saliva and tears, antibacterial enzymes including lysozyme and secretory phospholipase A_2 function to kill *S. aureus* (47, 48). In addition, skin cells produce more than 20 different types of antimicrobial peptides (AMPs) such as defensins or cathelicidins, and make antibacterial fatty acids to prevent *S. aureus* infection (46, 49, 50).

Cellular Arm of the Innate Immune System.

When chemical and physical barriers to infection fail, the spread of a pathogen is countered by an innate inflammatory response mediated by recruited effector leukocytes and associated molecules. These leukocytes are derived from the myeloid lineage of cells which include macrophages, monocytes, neutrophils, dendritic cells, mast cells, eosinophils, and basophils. Though non-myeloid derived cells such as natural killer cells and $\gamma\delta$ T-cells also have innate-like functions. Cells that comprise the innate immune system are characterized by their ability to recognize microbes and mount fast responses to infection. The majority of innate immune cells are present in the blood and can access almost any tissue site during an infection. All of these innate immune cells are described to interact with *S. aureus* in some capacity and are outlined below.

Eosinophils, Basophils, and Mast Cells.

Eosinophils, basophils and mast cells are highly granular cells of the innate immune system that have many overlapping functions. All of these cells contribute to responses in allergic inflammation. Eosinophils produce a wide range of cytokines, though their production of cytotoxic granule proteins such as major basic protein, eosinophil peroxidase, eosinophil cationic protein, and eosinophil-derived neurotoxin

(51, 52). Granule proteins produced by eosinophils aid in host control of helminth infections. Eosinophils can also respond to inflammatory signals and release mitochondrial DNA forming traps with granule proteins that are known to have antibacterial activity (53).

Like eosinophils, basophils facilitate host defense to parasites. Basophils have little proliferative capacity, but upon activation produce histamine in addition to interleukin (IL) 4 and IL-13 all of which are potent mediators of allergic responses (54). Mast cells have many overlapping functions with basophils including the production of granule proteins such as histamines, but they also produce IL-5 and IL-13 upon activation (55). Again, mast cells are widely recognized for their role in allergic responses but can also aid in control of bacteria or viruses.

While the role of eosinophils, basophils, and mast cells in facilitating host defense to *S. aureus* infection is not well understood, there are numerous studies that describe activation of these granular cells in response to *S. aureus* exposure. *S. aureus* can exacerbate allergic diseases like atopic dermatitis (56). In atopic dermatitis the functions of these granular cells contribute to the pathology associated with disease. Eosinophils were found to be targeted and killed by a *S. aureus* toxin in the supernatant called alpha-hemolysin (57). The *S. aureus* mediated killing of eosinophils is proposed to increase tissue injury during allergic disease (57). Moreover, Staphylococcal protein A, which binds to Fc regions of antibodies, is reported to bind and crosslink IgE and IgG on the surface of basophils causing the release of histamine (58). Lastly, mast cells can recognize the presence of *S. aureus* and activate inflammatory responses such as production of IL-8 and tumor necrosis factor-α (TNFα) (59). Interestingly, *S. aureus* can

invade and persist in mast cells (60). While *S. aureus* can activate mast cells in vitro, mice lacking mast cells were not more sensitive to *S. aureus* infection (61). In summary, while there is a small amount of published work related to how granulocytes such as eosinophils, basophils, and mast cells interact with *S. aureus*, the biological relevance of these interactions needs to be further explored.

Dendritic Cells.

Dendritic cells are aptly named for their stellate morphology, when first described in the 1970s (62, 63). They are a heterogenous population of cells with distinct functions and subsets that are present in peripheral tissues. A main function of dendritic cells is their proficient ability to ingest matter through phagocytosis, micropinocytosis, and receptor-mediated endocytosis (64). Upon engulfment of a pathogen or activation by pro-inflammatory signals, dendritic cells can migrate from the tissue into secondary lymphoid organs and undergo a maturation event culminating in antigen presentation (64, 65). In antigen presentation, the internalized pathogen is processed and broken down into small components or antigens that are then presented on major histocompatibility class I or II (MHC) to activate naïve T cells (64, 65). In addition to antigen presentation on MHC, T cells also require co-stimulation which is provided by a variety of surface expressed molecules on dendritic cells including cluster of differentiation (CD) 40, CD80 and CD86 (66). Furthermore, dendritic cells secrete cytokines such as IL-12 that are involved in differentiation and activation of Th1 cells (67). In mice, dendritic cells are usually defined by the expression of an integrin named CD11c and high levels of MHC-II. A subset of dendritic cells that respond to viral pathogens are known as plasmacytoid dendritic cells. Relevant to *S. aureus* are the

classic/conventional dendritic cells, which secrete cytokines and chemokines necessary for establishing protection against *S. aureus* (68).

Dendritic cells also interact with *S. aureus* in different ways that can have major consequences for the innate and adaptive immune system. For example, wall teichoic acid of *S. aureus* drives dendritic cell maturation and activation in vitro (69). Without proper dendritic cell activation, they do not efficiently present antigen nor activate T cells. EsxA/EsxB are virulence factors of *S. aureus* and were found to be important for dendritic cells to condition the Th1/Th17 response to *S. aureus* (70). Conditional knockout of dendritic cells in mice during infection with *S. aureus* led to higher bacterial loads, inflammation, and mortality (71). A recent example of *S. aureus* interaction with dendritic cells revolves around the *S. aureus* toxin LukAB, which can kill dendritic cells and interfere with their activation of T cells (72). All together, these examples highlight a few of the interactions between *S. aureus* and dendritic cells that can influence the host response to infection.

Neutrophils.

Neutrophils are the most abundant cell of the innate immune system (73-75). Neutrophils are mainly present in the blood, though they can be found in the bone marrow, spleen, lung and the liver (76, 77). Because of their unique multi-lobulated nucleus, neutrophils are termed polymorphonuclear leukocytes (PMNs), which include other innate immune cells such as basophils and eosinophils. An additional characteristic of neutrophils is their large abundance of granules and secretory vesicles present in the cytoplasm (78, 79). Neutrophils are considered to be short-lived cells, but during inflammation their longevity is expanded (76, 80). Upon invasion of *S. aureus* or

other pathogenic microbes into host tissues, neutrophils are rapidly recruited from the vasculature to site of infection by extravasation (81). During extravasation, P- and E-selectin on the surface of endothelial cells in blood vessels bind to glycosylated ligands on the surface of neutrophils, causing free-flowing neutrophils to tether to the endothelium (82). The flow of circulating blood causes neutrophils to roll along the endothelium until they adhere via binding to integrins (83). Neutrophil specific chemokine gradients on the endothelium promote the crawling of neutrophils during extravasation (84). Finally, this process culminates upon transmigration of neutrophils through the endothelial cell layer and into the tissue by either paracellular or transcellular routes (85).

Neutrophils are considered to be highly pro-inflammatory cells with potent killing capacities. Though less proficient than macrophages and dendritic cells, neutrophils also phagocytose extracellular material. In mice, neutrophils are characterized by surface expression of the integrin CD11b and the protein Ly6G. It is unknown if there are different subsets of neutrophils like dendritic cells and macrophages.

In the context of *S. aureus* infection, neutrophils are critical to infection control, as their absence leads to a higher susceptibility to infection (86, 87). During MRSA infection, distinct types of neutrophils were isolated from mice, based on their surface expression of proteins and production of cytokines, that either resisted or were susceptible to infection (88). The neutrophils isolated from resistant mice were more mature and displayed pro-inflammatory characteristics in contrast to the anti-inflammatory phenotype of neutrophils from susceptible mice (88). It is unknown if there

are different lineages of neutrophils that arise during infection with *S. aureus* or if neutrophils change functions based on diverse signals.

Macrophages.

Described by their ability to phagocytose bacteria and apoptotic cells over 100 years ago, macrophages have long been considered to be important cells of the innate immune system (89). In the host, macrophages have critical immune roles in pathogen defense and are major mediators in a multitude of host homeostatic functions. In addition to engulfment of pathogens and cellular debris, macrophages secrete an abundant array of cytokines and chemokines that function to regulate other innate immune cells and regulate the adaptive immune response to infection (90).

Tissue resident macrophages. Nearly every tissue in the body has a resident population of macrophages, including immune privileged sites such as the brain and testes (91). In these tissues, macrophages can orchestrate critical functions in tissue development, sense damage, and mediate tissue repair. Originally, these tissue resident macrophages were thought to be populated by circulating blood monocytes that can differentiate into macrophages. However, we now understand that this is not the case. Instead these tissue resident macrophages are derived from the yolk sac and fetal liver, with only a small component derived from hematopoietic stem cells in the bone marrow (92, 93). These resident macrophages are then maintained by continuous self-renewal (94-96). Moreover, tissue resident macrophages have distinct tissue-specific transcriptional and epigenetic profiles that highlight their heterogenous tissue specific functions based on the anatomical location in which they reside (97-100). Brief examples of the diverse functions of tissue resident macrophages are the following:

osteoclasts, bone macrophages, are highly specialized cells that can remodel bone (101); microglia present in the central nervous system contribute to brain development and function (102); lung alveolar macrophages clear surfactants produced by lung cells in addition to inhaled particulates and microbes (103); Kupffer cells in the liver remove harmful metabolites and pathogens (104); splenic red-pulp macrophages remove senescent red blood cells from circulation and recycle heme and iron (105).

Peritoneal macrophages. A large reservoir of tissue resident macrophages is present in the peritoneal cavity. Peritoneal macrophages comprise two major subsets, the large and the small peritoneal macrophage (106). These two macrophages populations were first separated based on high surface levels of the integrin CD11b and the surface glycoprotein F4/80 in the large peritoneal macrophages compared to the small peritoneal macrophages (107). Large peritoneal macrophages are thought to originate from the yolk sac and self-renew in contrast to small peritoneal macrophages which have bone-marrow origins (108). During an infection in the peritoneal cavity, small peritoneal macrophages increase in number and are derived from recruited monocytes (107). Furthermore, small peritoneal macrophages are more phagocytotic and produce oxidative molecules to a higher extent than large peritoneal macrophages.

Recruitment of macrophages during infection. During the course of acute inflammation or infection, macrophages are recruited to facilitate the host immune response. Macrophages that are present at the site of infection or inflammation can be from the tissue resident cells or derived from circulating monocytes. Monocytes originate from hematopoietic stems cells derived from the bone marrow and themselves have important functions in innate immunity (109, 110). However, monocytes infiltrate

the site of inflammation or infection where they differentiate into macrophages or dendritic cells (111). In response to environmental stimuli, these monocyte-derived macrophages can accentuate inflammatory responses or dampen the inflammatory response. These recruited monocytes are innate effectors that can kill pathogens through phagocytosis, produce a range of antimicrobial reactive oxygen species, and secrete inflammatory cytokines (112). In contrast, monocytes can promote angiogenesis to facilitate wound healing (113). Monocyte recruitment is driven by two main chemokines, the monocyte chemotactic protein 1 (MCP-1/CCL2) and CX3CL1 that bind to receptors, CCR2 and CX3CR1 (114, 115). These chemokines are produced by fibroblasts, epithelial cells, and endothelial cells in response to inflammation and thus facilitate the recruitment of monocytes to the site of inflammation.

M1 and M2 macrophages. Macrophages are grouped into two main categories based on polarization states in response to various stimuli, M1 or classically activated macrophages and M2 or alternatively activated macrophages (116). The dogma is that M1 macrophages are polarized from the presence of lipopolysaccharide (LPS) and/or interferon-γ (IFN-γ) and M2 macrophages arise from IL-4 and IL-13 signaling (117, 118). Expression of specific transcription factors in M1 and M2 macrophages contribute to their polarization. Upon activation, M1 macrophages are more phagocytic, produce pro-inflammatory cytokines such as IL-12, IL-1α/β, IL-6, TNFα, upregulate surface molecules, and have increased pathogen-killing capacity. In contrast, M2 macrophages are considered to be any macrophage that is not pro-inflammatory, which can include both wound healing and anti-inflammatory macrophages. These anti-inflammatory M2 macrophages exert immunosuppression through production of cytokines such as IL-10

or transforming growth factor β (TGF-β) (119). Besides immunosuppressive functions, other M2 macrophage roles can include promotion of allergic inflammation, aiding tumor growth, and also serving as reservoirs of pathogen survival. The M1 and M2 distinction of macrophages was proposed to mimic the T cell literature, as distinct classes of T cells are well characterized. However, the idea of defining macrophages as M1 or M2 is now regarded as too simplistic and narrow based on the varied roles that heterogeneous populations of macrophages can assume. Moreover, unlike other immune cells that upon differentiation are committed in lineage, macrophages are not irreversibly committed to a certain polarization state and can exert functions that encompass both M1 and M2 activities (120). Thus, some have proposed that due to the remarkable plasticity of macrophages, their classification should not be thought of as a linear scale, but rather representing a color wheel in which a blending of phenotypes leads to a larger spectrum that encompasses heterogeneous macrophage populations (90).

***S. aureus* interaction with macrophages.** Like neutrophils, macrophages are part of the initial cellular response to infection. As such, *S. aureus* and macrophages interact with each other during infection. Mice that are depleted of macrophages are exquisitely sensitive to *S. aureus* infection. For example, during *S. aureus*-induced peritonitis in mice, the absence of macrophages led to increased bacterial loads in organs as well as significantly higher mortality (121). Likewise, in a pulmonary model of infection, absence of alveolar macrophages significantly increased the mortality of mice but did not alter bacterial loads in the lung (122). *S. aureus* is readily internalized by macrophages, where it can survive and persist (123, 124). It is hypothesized that, as a

consequence of this persistence, *S. aureus* uses macrophages as a means of dissemination during infection (123, 124). In cystic fibrosis, *S. aureus* can cause recurrent pneumonia which is attributed to the intracellular persistence of *S. aureus* in alveolar macrophages (125). Thus, alveolar macrophages from the cystic fibrotic lung may serve as a reservoir of *S. aureus* leading to chronic pneumonia. Recently, it was reported that in a model of recurrent skin and soft-tissue infections by *S. aureus* that the host's ability to mount a greater recall response to recurrent infections is mediated by the innate-like memory of macrophages (126). Altogether, the interactions between *S. aureus* and macrophages during infection are a critical determinant to the outcome of infection.

Concluding Remarks.

In this section, we have introduced the main cellular components of the innate immune system that interface with *S. aureus*. These include eosinophils, basophils, mast cells, dendritic cells, neutrophils, and macrophages. We defined general features of these cells and highlighted some literature evidence that supports interactions of these innate cells with *S. aureus*. In the next section we will introduce how cells of the innate system detect *S. aureus*.

Section 3: Innate Recognition of *S. aureus*

After breaching physical barriers, the innate immune system is the first line of defense against *S. aureus*. The recognition of *S. aureus* by the innate immune system is mediated through germline-encoded pattern recognition receptors (PRRs). PRRs are able to recognize microbial components like essential cell membrane and cell wall components of bacteria, bacterial toxins, DNA, RNA, bacterial lipoproteins, and

components of bacteria motility organelles. These microbial components are collectively known as pathogen-associated molecular patterns (PAMPs). PRRs are found either on the surface or reside within the cytosol of the cell. Interactions with cognate PAMPs leads to activation of specific signaling pathways that culminate in antimicrobial responses. PRRs modulate responses to various stimuli, are independent of immunological memory, and are present both internally and externally in cells that express PRRs (127). Almost every cell in the innate immune system, as well as endothelial and epithelial cells, and some cells of the adaptive immune system express PRRs. The first family of PRRs to be studied in detail is the Toll-like receptor (TLR) family. The name stems from the unanticipated role of the Toll protein in *Drosophila melanogaster* in responding to fungal infection (128). Currently there are 10 TLRs in humans and 13 known TLRs in mice that recognize a range of PAMPs. The primary ligands of these TLRs are summarized in Table 1. Other classes of PRRs include C-type lectin receptors (CLRs), RIG-I-like helicases, formylated protein receptors (FPR1 and FPR2) or the nucleotide binding-oligomerization domain (NOD)-like receptors. The diverse location, range of cell types, recognition of numerous PAMPs, and activation of antimicrobial signaling pathways of PRRs arm the innate immune system to mount rapid responses to invading pathogens.

Table 1. Toll-like Receptors and Ligands.

Toll-like Receptor (TLR) (Location)	Primary Ligand(s)	Reference(s)
1/2 (Surface)	Triacylated lipoproteins/ lipopeptides	(129)
2 (Surface)	Lipoprotein/lipopeptides, peptidoglycan (controversial), lipoteichoic acid, zymosan	(130-133)
3 (Internal)	Viral double-stranded RNA	(134)
4 (Surface)	Lipopolysaccharide	(135)
5 (Surface)	Flagellin	(136)
6/2 (Surface)	Diacylated lipoproteins/lipopeptides, lipoteichoic acid	(137, 138)
7 (Internal)	Viral single-stranded RNA	(139, 140)
8 (Internal)	Viral single-stranded RNA or bacterial RNA	(140, 141)
9 (Internal)	CpG-containing DNA	(142)
10 (human only)	N/A	N/A
11 (only in mice) (Internal)	Profilin-like molecule; and unknown ligand from uropathogenic bacteria	(143, 144)
12 (only in mice)	Profilin-like molecule	(145)
13 (only in mice) (Internal)	23S ribosomal RNA	(146)

PRR Recognition of *S. aureus*.

Recognition of *S. aureus* by PRRs is rapidly achieved due its many PAMPs including: lipoteichoic acid (LTA), peptidoglycan, lipoproteins, DNA, and RNA. *S. aureus*-derived PAMPs include the cell wall, which is comprised of thick peptidoglycan layers embedded with LTA, as well as membrane anchored lipoproteins. *S. aureus* is considered to be an extracellular pathogen in that it does not depend on invading a host cell for its pathogenesis or replication. As such, the dominant PRRs that recognize *S. aureus* are found on the surface of PRR-expressing cells. This includes TLR2 that recognizes bacterial lipids, CLRs that sense carbohydrates, and formyl peptide

receptors that bind to secreted bacterial proteins containing a formylated methionine or to lytic small molecules made by *S. aureus* named phenol-soluble modulins (PSMs) (147). However, *S. aureus* can be internalized by professional phagocytes such as neutrophils, macrophages or dendritic cells, and by non-professional phagocytes including human keratinocytes. Internalized *S. aureus* is then recognized by endosomal and cytosolic PRRs including TLR8/9 that sense RNA and DNA respectively, and NLRs that detect peptidoglycan structures (141, 148, 149).

TLR2 Recognition of *S. aureus*.

The most important and well characterized PRR that recognizes *S. aureus* is TLR2. Like other surface TLRs, TLR2 is part of the type I integral membrane glycoprotein family (150). The extracellular N-terminal ectodomain is responsible for PAMP detection and consists of 16-28 leucine-rich repeats (LRR) (151). The conserved intracellular C-terminal domain bears homology to the IL-1 receptor and is known as the Toll/IL-1 receptor domain (TIR) (152). This intracellular TIR domain is necessary for the interaction of adaptor molecules, which aid in activating downstream signaling pathways upon receptor engagement (153). Recognition of TLR2 native ligands occurs through heterodimerization with either TLR1 or TLR6. Upon dimerization with a native ligand, crystallography studies with bound ligands reveal that the ectodomain of each monomer form a horse-shoe shaped structure containing the LRRs and the two monomers collectively form an “m” shaped complex with the ligand, stabilizing the two receptors (154-157). TLR1/2 heterodimers bind to triacylated lipoproteins and TLR2/6 heterodimers primarily recognize diacylated lipoproteins and LTA (which is diacylated)

(158). Recognition of lipoproteins by TLR2 in the absence of TLR1 or TLR6 does not occur (159).

S. aureus produces abundant amounts of lipoproteins that are both diacylated and triacylated, but under most growth conditions *S. aureus* lipoproteins are triacylated (160, 161). Therefore, recognition of *S. aureus* lipoproteins is most often mediated by TLR1/2. Co-crystallization of TLR1/2 heterodimer with a synthetic triacylated lipopeptide demonstrates that the ectodomain of TLR1 has a channel that binds the amide-linked lipid chain of the triacylated lipopeptide (157). This channel is blocked by phenylalanine residues in TLR6, providing a structural explanation for the specificity of diacylated or triacylated lipoproteins by TLRs (162). TLR2 has a hydrophobic pocket that interacts with the cysteine-linked diacylglycerol in a less specific manner that allows for functional plasticity in recognition of fatty acid chains with varying length or chemical structure (162).

The cell wall of *S. aureus* is made up of thick layers of peptidoglycan. Countless studies and reviews list bacterial peptidoglycan as a TLR2 ligand (132, 163, 164). Many of the initial studies that determined peptidoglycan was a TLR2 ligand used commercially purified preparations of peptidoglycan. The use of commercial purified peptidoglycan may contain other TLR2 activating components. A study by Travassos et al. detailed that the TLR2-activating function of purified peptidoglycan stems from contaminating cell wall LTA and lipoproteins that are easily co-purified with peptidoglycan (165). Furthermore, they show that, with added steps in the procedure to isolate peptidoglycan by including treatments with amylase, trypsin, sodium dodecyl sulfate, acetone, and hydrofluoric acid, that peptidoglycan fails to activate cells through

TLR2 (165). Importantly, the hydrofluoric acid treatment step deactivates bacterial lipoproteins and LTA, which abrogates the TLR2 activating function of purified peptidoglycan. Treatment of *S. aureus* cell wall components with lipase, to hydrolyze the esterified lipids attached to lipoproteins also abrogates the TLR2 activating ability of the purified cell wall fractions (166, 167). Shortly after, another group reported that by treating bacteria with penicillin, which prevents peptidoglycan transpeptidation and allows for purification of soluble peptidoglycan fragments that are not incorporated into the cell wall or linked to other cell wall components, peptidoglycan still activates TLR2 responses (168). A study using chemically synthesized fragments of peptidoglycan structure and surface plasma resonance found that only some but not all of the synthesized fragments could bind to TLR2 (169). However, these synthetic fragments were never put onto TLR2 expressing cells. Peptidoglycan isolated from *Bacillus anthracis*, which lacks LTA, needed to be internalized by cells in order to activate immune signaling cascades (170). In this instance, the cytosolic NLRs, which are definitive peptidoglycan receptors, are likely recognizing the internalized peptidoglycan. The variation in peptidoglycan structure from different bacterial species in conjunction with the slightly different methodologies of peptidoglycan purification compound the controversy of defining it as a TLR2 ligand (171). Thus, peptidoglycan is not likely to be a ligand of TLR2.

TLR2 co-receptors. Besides working with TLR1 and TLR6 to increase the range of TLR2 substrate recognition, other molecules such as CD14, CD36 and asialo-GM1 also interact with TLR2 to facilitate ligand recognition. These molecules are not necessary for TLR2 to recognize PAMPs, but instead function to enhance responses by

lowering the concentrations of ligand needed for receptor recognition (172, 173). CD14 is a glycosylphosphatidylinositol-anchored membrane protein with no intracellular domain that can be found expressed on phagocytes such as macrophages. Besides being critical for facilitating TLR4 recognition of LPS, CD14 is an accessory molecule that helps to load both LTA and diacylated lipoproteins onto TLR2/6 heterodimers as well as deliver triacylated lipoproteins to TLR1/2 heterodimers (174-176). CD36, a membrane glycoprotein involved in scavenging, can load diacylated LTA or lipoproteins onto TLR2/6, but CD36 itself cannot bind to triacylated lipoproteins (177). CD36 plays a critical role during infection as CD36 knockout mice were found to be highly susceptible to *S. aureus* infection (172). Moreover, CD36 deficient macrophages could not produce cytokines after stimulation by LTA or different forms of diacylated lipoproteins, but other diacylated and triacylated lipoproteins were found to activate these CD36 deficient macrophages (178). Thus, CD36 may only recognize LTA and diacylated lipoproteins with certain structures. A study identified that CD36 may bind ligands and transfer them to CD14, which are both localized in lipid rafts that contain TLR1/2 or TLR2/6, and then load the ligands to the relevant TLR2 heterodimer (177). Besides CD14 and CD36, asialylated glycolipids like asialo-GM1, which are found in lung epithelial cells, are hypothesized to facilitate TLR2 recognition of *S.* aureus (179, 180). On the surface of airway epithelial cells, TLR2 and asialo-GM1 associate in lipid rafts and generate the synthesis of IL-8 after exposure to *S. aureus* (181). Therefore, the association of TLR2 with TLR1, TLR6, CD14, CD36 and asialo-GM1 help to generate a large variety of stimuli for TLR2.

The TLR2 signaling pathway. Upon ligand binding to either heterodimer pair of TLR2, a signaling cascade induces nuclear translocation of the transcription factor nuclear factor kappa B (NF-κB), which controls the expression of pro-inflammatory genes. As diagramed in Figure 1, upon ligand recognition and dimerization of TLR2 the TIR domain of TIRAP/Mal proteins bind to the TIR domain of TLR2 and recruits the common adaptor molecule MyD88 (182). MyD88 then recruits IL-1R-associated kinase 4 (IRAK-4) that then phosphorylates IRAK-1 to then initiate autophosphorylation (183). The phosphorylated IRAK-1 subsequently associates with TNFR-associated factor 6 (TRAF6), which acts as an ubiquitin protein ligase (E3) to ubiquitinate itself in addition to the IKK-γ/NF-κB essential modulator (NEMO) (184, 185). This ubiquitination activates a complex of TGF-β-activated kinase 1 (TAK1) and its associated proteins, leading to the phosphorylation of NEMO and activation of the inhibitor of nuclear factor-κ (IKK) complex (186). Phosphorylated IκB undergoes K48-linked ubiquitination and degradation by the proteasome. This frees NF-κB to then translocate to the nucleus to initiative its transcriptional program of pro-inflammatory gene expression (187). At the same time, TAK1 activates the mitogen-activated protein kinases (MAPKs) cascades, leading to activation factor-1 (AP-1) induction, which also induces the expression of genes encoding pro-inflammatory factors (184). Together, NF-κB and AP-1 lead to the production of cytokines and chemokines such as IL-6, TNF, KC/IL-8, and Chemokine (C-C motif) ligand 3 or 4 (CCL3 and CCL4) also known as macrophage inflammatory protein 1-alpha or beta (MIP-1α and MIP-1β). This is just a very small sampling of the wide range of inflammatory changes mediated by these transcription factors.

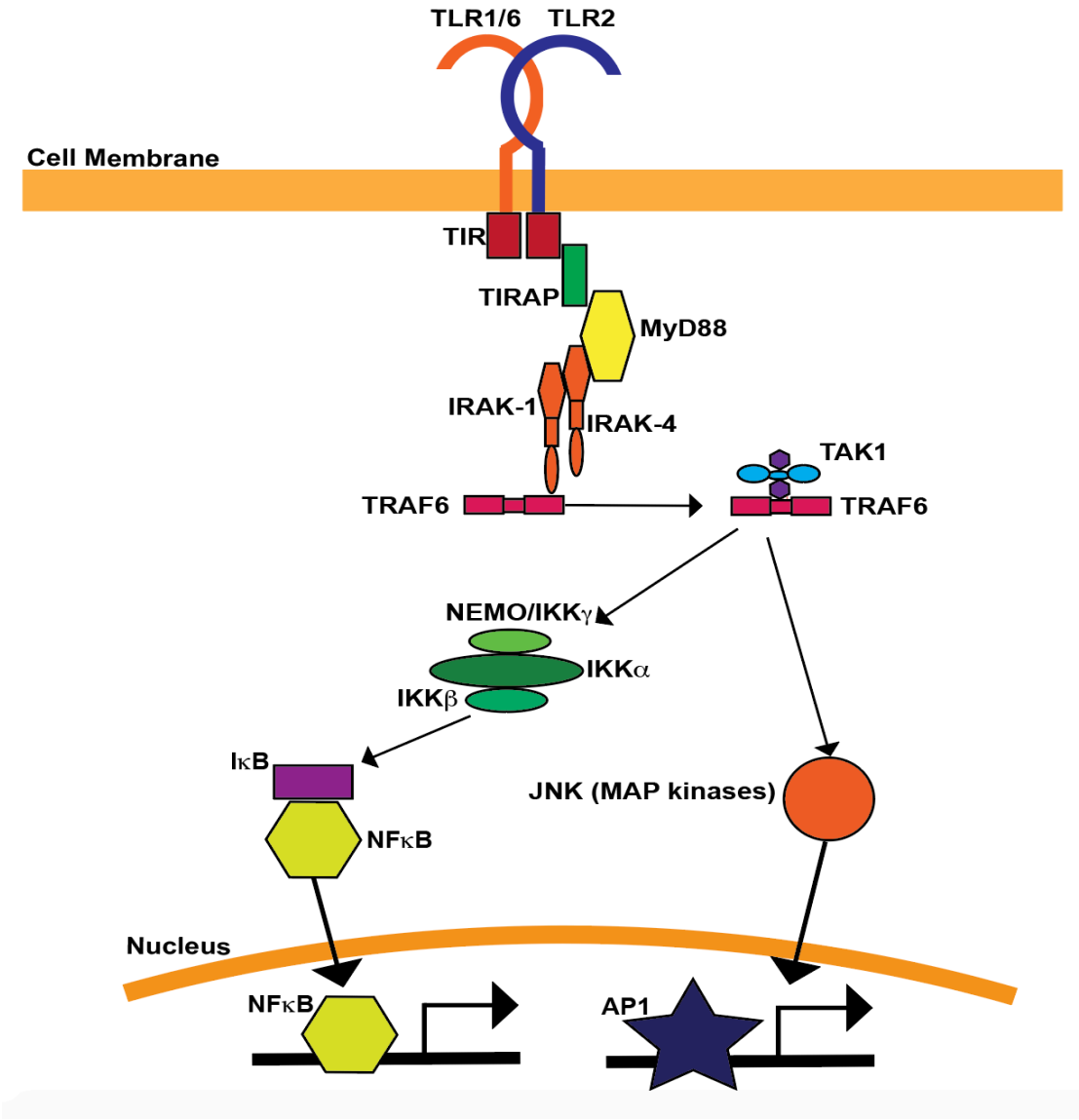

Figure 1. Model of TLR2 Signaling Pathway. After ligand recognition and dimerization of TLR2 with TLR1 or TLR6, the TIR domain of TLR2 recruits the common adaptor protein MyD88. MyD88 then recruits IRAK-4 which phosphorylates IRAK-1. The phosphorylated IRAK-1 subsequently associates with TRAF6, which ubiquitinates itself in addition to the IKK-γ/NEMO complex. This ubiquitination activates a complex of TAK1 and its associated proteins, leading to the phosphorylation of NEMO and activation of the IKK complex. Phosphorylated IκB undergoes K48-linked ubiquitination and degradation by the proteasome. This frees NF-κB to then translocate to the nucleus to initiative its transcription program of pro-inflammatory genes. At the same time, TAK1 activates the MAP kinases cascades, leading to AP-1 induction, which also induces the expression of genes encoding pro-inflammatory factors.

Concluding Remarks.

In this section, we introduced how the host innate immune system recognizes *S. aureus*. This is carried out by the expression of various types of PRRs such as TLRs on innate cells as well as other non-innate immune cells including epithelial cells and keratinocytes in the skin. In particular, we focused on how *S. aureus* PAMPs are potently recognized by TLR2. PAMP recognition leads to a signaling cascade that culminates in the synthesis or activation of mediators of inflammation by innate immune cells. In this next section, we will introduce how the host controls or eliminates *S. aureus* upon recognition of the bacterium.

Section 4: Host Control of *S. aureus*

Extracellular Mechanisms of Host Defense.

Antimicrobial peptides. A chemical defense strategy by innate cells and skin cells is the production of AMPs. AMPs are made by cells that are the primary defenders against *S. aureus* such as mast cells, eosinophils, dendritic cells, neutrophils, monocytes, macrophages, and keratinocytes. In total, there are over 1200 known or predicted AMPs with a diverse range of structure and activities (188). However, there are common features of these peptides, such as being small, containing positive charged residues, and having an amphipathic structure. Different types of AMPs including α-defensins, β-defensins, and cathelicidins are known to have antibacterial activity against *S. aureus* (189). The unique features of AMPs allow them to attach and insert into membrane bilayers to form pores through ‘barrel-stave’, ‘carpet’ or ‘toroidal-pore’ mechanisms (190-192). The formation of transmembrane pores in bacteria lead to lysis and death of the targeted bacterium. However, pore formation is not the only

mechanism of bacterial killing, as AMPs can enter bacteria to inhibit cell-wall synthesis, or block DNA and protein synthesis. Besides the potent killing capacity of AMPs, they can also possess a variety of immune regulating functions (193). AMPs can serve as chemoattractants to promote leukocyte recruitment to the site of infection, induce production of chemokines and cytokines by innate immune cells, influence cell differentiation, modulate immune signaling pathways, and initiate adaptive immune responses. Thus, AMP production by the host in response to *S. aureus* infection is a broad defense mechanism.

Complement. Another critical mediator of innate immunity is the complement system, initially discovered for its ability to induce bacterial lysis. The complement system is a cascade of soluble proteins produced by the liver that function mainly in the serum as well as in tissues, on surfaces, or within the cell. There are three separate pathways of the complement system: classical pathway, lectin pathway, and the alternative pathway (194, 195). All of these pathways end in formation of surface-bound C3 convertases that cleave C3 to C3a and C3b.

The classical pathway is initiated when C1q, C1r, and C1s bind to the Fc portion of IgG or IgM that is bound to *S. aureus*. C1s is then activated to cleave C4 and C2 to yield the C3 convertase C4bC2a. This is similar to the lectin pathway which is activated when mannose binding lectin or Ficolin bind to carbohydrate moieties on pathogens (196, 197). Proteins associated with mannose binding lectin autoactivate upon binding to carbohydrate moieties on pathogens, cleaving C4 into C4a and C4b as well as C2 into C2b and C2a. C4b and C2a form the C3 convertase C4bC2a. In the alternative pathway, C3 is constitutively hydrolyzed to form C3b which binds to bacteria. This

attracts factor B and factor D to form the C3 convertase C3bBb of the alternative pathway (198). Furthermore, cleavage of C3 by the C3 convertases forms C3a and C3b, which combine with other complement proteins to the generate two C5 convertases, C4bC2aC3b and C3bBb. The cleavage of C5 by the C5 convertases produces C5a and C5b.

Activated complement leads to generation of three different types of immune effectors. First, C3a and C5a are anaphylatoxins that can attract and activate leukocytes through interaction with the C3a and C5a receptor (C3aR or C5aR) on leukocytes (199, 200). Second, C5b is part of the membrane attack complex that directly lyses Gram-negative bacteria. Last, the complement cascade produces opsonins like C3b, iC3b, and C3d that covalently bind to bacterial cells to facilitate phagocytosis by innate immune cells. In summary, the complement system is a large and complex cascade of cleavage and binding events that culminates in directly or indirectly killing invading bacteria like *S. aureus*.

Cytokine and chemokine production. Another component of innate immune system control of *S. aureus* infection is the ability to produce and secrete cytokines and chemokines that help to regulate both the innate and adaptive immune system. Cytokines are small soluble proteins that initiate specific pro- and anti-inflammatory responses by binding to specific receptors on cells. There are over 100 proteins described as cytokines (201). In focusing on a small subset of the pro-inflammatory cytokines produced mainly by macrophages and/or neutrophils, the most common cytokines are IL-6, TNF, keratinocyte-derived cytokine (KC or IL-8 in humans), IL-1 family, and IL-12. IL-6, TNF, and the IL-1 family (including IL-1α, IL-1β, and IL-1Ra) are

potent pyrogens and all cause a fever response (202). IL-6 pro-inflammatory functions include recruitment of monocytes to the site of infection, maintenance of Th17 cells, and inhibition of T cell apoptosis (203, 204). TNF induces vasodilation and loss of vascular permeability, which aids immune cell tissue infiltration. The IL-1 family of cytokines especially IL-1α and IL-1β are strongly pro-inflammatory and share overlapping functions. IL-1β stimulates histamine release from mast cells thereby causing vasodilation and increased local inflammation. Moreover, IL-1β assists in CD4 T cell differentiation and expansion, increases the surface expression of adhesion molecules on various cell types, and is a chemoattractant for granulocytes (205). KC is a potent chemoattractant for neutrophil recruitment (206, 207). IL-12, comprised of the p35 and p40 subunits, promotes inflammation through stimulation of Th1 cells resulting in production of IFN-γ, which potently stimulates pro-inflammatory functions of macrophages (208).

Chemokines are a type of cytokine, but they serve as chemoattractants to recruit specific cell types to the site of injury (209). Macrophages and neutrophils, among other cells, secrete CCL2, CCL3, and CCL4 in response to pro-inflammatory stimuli. After the binding of these chemokines to their cognate receptors, CCR2 for CCL2, and CCR5 for CCL3 and CCL4, monocytes and macrophages recruitment to the site of infection is enhanced. Altogether, the production of pro-inflammatory cytokines and chemokines in recognition of *S. aureus* infection serves to amplify the immune response to clear *S. aureus* from the host.

Cellular Mediated Control of *S. aureus*.

Phagocytosis and phagosome formation. Professional phagocytes of the innate immune system, including neutrophils, eosinophils, dendritic cells, macrophages, and monocytes work to ingest and eliminate invading pathogens like *S. aureus*. The process of phagocytosis and subsequent killing of internalized bacteria is best understood in neutrophils and macrophages. For neutrophils, initiation of phagocytosis requires the deposition of opsonins on the surface of the bacterium (210). In the serum, the predominant factors that serve as opsonins are immunoglobulins IgG and complement components such as C3b. Once deposited on the bacterial surface, receptors on neutrophils such as the Fc receptors, complement receptors, or other PRRs can then trigger phagocytosis. Macrophages generally do not need bacteria or other material to be opsonized to trigger phagocytosis. Macrophages are constitutively undergoing dynamic actin-based rearrangement to produce extracellular protrusions that probe the surrounding environments (211-213). Upon recognition of opsonized bacteria by different surface receptors, signal transduction in the interior of the cell works to promote localized lipid remodeling and rearrangement of the actin cytoskeleton within the plasma membrane (214, 215). Actin polymerization is required at the leading edge of the membrane pseudopodia to envelop the bacterium and concurrently actin depolymerization at the base of the pseudopod forms the phagocytic cup to allow entry of the newly internalized bacterium (216-218). The internalized bacterium is present in a structure called the phagosome, which is an outside-in compartment inside the cell. The phagosome then immediately undergoes a maturation process to become a highly localized site of bacterial killing. This process is driven by a series of sequential

interactions/fusions with different vesicles of the endocytic pathway, each transforming the phagosome in a unique way (219). Maturation of the phagosome is comprised of early, intermediate, and late stages. The final stage of phagosome maturation occurs when the maturing phagosome fuses with a lysosome, forming the phagolysosome. During the entire maturation process, the lumen of the phagosome becomes increasingly acidic from the activity of proton-pumping V-ATPases, which creates an unfavorable bacterial growth environment (220). The acidic environment in the lumen is not only important for inhibiting the growth of the resident bacteria but also provides the optimum pH in which many hydrolytic enzymes function (221, 222).

Neutrophil mediated killing of *S. aureus.* Neutrophils, which are one the first immune cells recruited to the site of infection, can extracellularly kill *S. aureus* through neutrophil extracellular trap (NETs) formation in a process named NETosis or by degranulation. NETs are large, web-like extracellular structures that contain decondensed chromatin with embedded antimicrobial molecules that function to kill bacteria, viruses, fungi, and parasites (223). *S. aureus* is known to initiate two different types of NETosis, one that results in cell death and one that is independent of cell death. In the cell death version of NETosis, nucleus delobulation precedes disassembly of the nuclear envelope and loss of cellular polarization (224). Next, the chromatin decondenses and the plasma membrane ruptures leading to expelling of the NET and cell death. The non-lytic form of NETosis leads to expulsion of chromatin and granule contents. The remaining cell, called an anucleated cytoplast, can continue to ingest pathogens (225, 226).

Degranulation is another key killing mechanism of neutrophils. The process of degranulation occurs when PRR engagement stimulates neutrophils to translocate granules to the plasma membrane where they then can release their contents in the extracellular milieu through exocytosis (227). Four different types of granules exist in neutrophils: primary or azurophilic granules, secondary or specific granules, tertiary granules, and secretory vesicles (228). Of these granules, the primary granules contain the most reactive molecules such as elastase, myeloperoxidase (MPO), cathepsins, and defensins (229). Secondary and tertiary granules contain overlapping contents such as lactoferrin, matrix metalloprotease nine, and other materials (230). The release of these toxic granule contents by degranulation facilitate the strong bactericidal ability of neutrophils. In addition to the extracellular release of granules, they can be delivered to the phagosome. Lactoferrin in neutrophil secondary and tertiary granules acts as a scavenger of iron, aiding in bacterial growth restriction (231). A similar bacteriostatic activity is carried out by the membrane protein, named natural resistance-associate macrophage protein 1, which extrudes divalent metals such as Fe^{2+}, Zn^{2+} and Mn^{2+} from the phagosomal lumen (232-234). Furthermore, neutrophils produce calprotectin, which can bind and sequester zinc and manganese from bacteria (231). This sequestration of essential metals or other trace nutrients is a general process called nutritional immunity (235).

Macrophage and neutrophil ROS production. A major antimicrobial activity of neutrophils and macrophages is a process known as respiratory burst, which generates potent reactive oxygen species (ROS) (236). The generation of ROS occurs through the nicotinamide adenine dinucleotide phosphate (NADPH) phagocyte oxidase complex

that is assembled on the phagosomal membrane (237). The NADPH oxidase complex is comprised of two transmembrane proteins, gp91*phox* and p22*phox*, in addition to four cytosolic proteins denoted as p47*phox*, p67*phox*, p40*phox*, and Rac1 or Rac2 (237-240). Upon assembly and activation of the NADPH oxidase complex, it transfers electrons from NADPH to molecular oxygen releasing superoxide ($O_2^{-\bullet}$) in the phagosome (239). Superoxide can undergo spontaneous dismutation into hydrogen peroxide (H_2O_2) or hydroxyl radical and other ROS (237, 239, 241-243). H_2O_2 can then be converted into hypochlorous acid and chloramines by MPO (229, 241). These ROS lead to oxidization of internalized bacterial DNA, mobilization of iron from iron-sulphur-containing dehydratases promoting toxic Fenton chemistry, and oxidation of protein residues (237, 244, 245). All of these collectively facilitate killing of the internalized bacteria by ROS. NADPH oxidase dysfunction leads to chronic granulomatous disease (CGD) (246, 247). Patients with CGD commonly suffer from recurrent infections with *S. aureus* as well as the fungal pathogen *Aspergillus*, highlighting the importance of NADPH oxidase in host defense (246, 247). In addition to NADPH oxidase-derived ROS, mitochondrial respiration also generates ROS that contribute to the destruction of internalized bacteria (248). These mitochondrial ROS (mROS) are generated when electrons from the oxidative phosphorylation machinery escape and react with molecular oxygen (249, 250). Recent work demonstrates that mROS are packaged into mitochondrial-derived vesicles and delivered to the phagosome to facilitate the inhibition of internalized *S. aureus* (251, 252). Compared to macrophages, neutrophils are capable of producing higher amounts of ROS in response to bacterial pathogens. In

summary, the production of ROS by phagocytes is important for restricting *S. aureus* growth.

Macrophage and neutrophil RNS production. Synthesis of nitric oxide ($NO^{\bullet}$) also inhibits internalized bacterial pathogens and is produced in high amounts by macrophages (237). In response to engulfed pathogens, inducible nitric oxide synthetase (iNOS) is activated and leads to the formation of $NO^{\bullet}$ and citrulline in large amounts from L-arginine and oxygen (253). It is known that $NO^{\bullet}$ alone is not a highly reactive molecule and has an expansive range of cellular functions (254). Rather, $NO^{\bullet}$ only becomes highly reactive when it is converted by the presence of oxygen into nitrogen dioxide, peroxynitrite ($ONOO^{-}$), dinitrogen trioxide, and other nitrogen-based reactive species collectively forming reactive nitrogen species (RNS) (237, 255). The synthesized $NO^{\bullet}$ and RNS inhibit bacterial respiration, perturb DNA replication, interfere with metal centers and tyrosine residues in proteins, and alter lipid integrity (237, 254, 256). $NO^{\bullet}$ and RNS are produced in higher abundance in activated macrophages rather than neutrophils. Given the similarities in the reactivity and formation of ROS and RNS, under certain conditions they can have synergistic antimicrobial activities (257). In particular, the production of the powerfully reactive RNS, $ONOO^{-}$, is formed from NADPH oxidase-derived $O_2^{-\bullet}$ and iNOS-generated $NO^{\bullet}$, establishing a link between ROS and RNS production (237, 254).

Concluding Remarks.

In this section, we introduced the various ways in which the innate immune system can kill pathogens like *S. aureus*. AMP production and activation of the complement system both contribute to the elimination of *S. aureus*. Also, production of

inflammatory cytokines and chemokines are necessary to coordinate innate and adaptive responses to *S. aureus* infection. The best studied antimicrobial functions of the innate system are the antibacterial activities of neutrophils and macrophages. Many of the antibacterial functions occur within neutrophils and macrophages, through a coordinated attack of *S. aureus* internalized by phagocytosis. In the next section, we cover the known virulence factors of *S. aureus* that work to counter these innate immune responses.

Section 5: Innate Immune Evasion Mechanisms of *S. aureus*

S. aureus has acquired a vast array of virulence factors that inhibit innate responses and facilitate disease. Table 2 highlights many virulence factors encoded by *S. aureus* and the immune components they target.

Table 2. Virulence Factors of *S. aureus*

Virulence Factor	Function	Immune Target	Reference
Aureolysin	Metalloprotease, cleaves C3 and LL-37	Complement System, blocks deposition of C3b; AMP function	(258, 259)
***Staphylococcal* complement inhibitor (SCIN)**	Binds and stabilizes C3bBb and C4b2a	Complement system, impairs C3a/C3b/C5a production	(260, 261)
Staphylokinase (SAK)	Activate plasminogen to generate plasmin	Complement system, AMP production, and opsonization	(262, 263)
Protein A (SpA)	Binds to Fc region of Immunoglobins	Phagocytosis; complement system	(264, 265)
***Staphylococcal* binder of immunoglobin (Sbi)**	Binds to Fc region of IgG	Phagocytosis; complement system	(266-268)
Extracellular fibrinogen binding molecule (Efb)	Binds to fibrinogen and C3d	Phagocytosis; complement system	(260, 269)
Extracellular complement binding molecule (Ecb)	Binds to C3d	Phagocytosis; complement system	(260)
Superantigen-like proteins (SSL 3/5/6/7/10/11)	Binds to IgA/IgG1, PSGL1, CD47, CXCR4	Complement system; phagocytosis; Neutrophil migration; TLR2 signaling	(270-276)
coagulase and von Willebrand factor-binding protein	generate staphylothrombin	Blocks agglutination and phagocytosis	(277)
DltABCD	Modifies wall teichoic acids with d-alanine	AMP	(278)

MprF	Modification of phosphatidylglycerol with l-lysine	AMP	(279)
OatA	Peptidoglycan acetylation	Lysozyme activity	(280)
Extracellular adherence protein and homologs (Eap, EapH1, EapH2)	Inhibition of serine proteases; bind to ICAM1	Neutrophil antibacterial activity; Leukocyte migration	(281, 282)
SelX	Bind to PSGL1	Leukocyte migration	(274)
Staphopain A	Cleaves CXCR2	Neutrophil migration	(283)
chemotaxis inhibitory protein of *S. aureus* (CHIPS)	Bind FPR1 and C5aR	Neutrophil migration	(284, 285)
formyl peptide receptor-like 1 inhibitor and its homolog (FLIPr/FLIPrL)	Bind FPR1 and FPR2	Recognition of formylated proteins; Neutrophil migration	(286)
Phenol Soluble Modulins (PSMs)	Lysis of immune cells	Innate immune cells	(287, 288)
Alpha-hemolysin (Hla)	Lysis of innate immune cells, erythrocytes, epithelial cells	Various cell types	(289, 290)
Leukotoxins (HlgAB, HlgCB, LukAB/HG, LukED, PVL)	Lysis of immune cells and erythrocytes	Cellular innate immunity and T-cells	(291-293)
adenosine synthase A (AdsA)	Generates adenosine	Inhibit neutrophil degranulation and respiratory burst	(294)
staphyloxanthin	antioxidant	ROS detoxification	(295)
Catalase and alkylhydroperoxide reductase	antioxidant	ROS detoxification	(296)
SodA and SodM	Superoxide dismutases	ROS detoxification	(297)
methionine sulfoxide reductase (Msr)	Repair oxidized methionine residues	ROS detoxification	(298)
surface factor promoting resistance to oxidative killing (Sok)	Resists oxidative killing	Inhibit antimicrobial function of ROS	(299)
Flavohemoglobin (Hmp)	$NO^{\bullet}$ scavenger	RNS detoxification	(300)
Lactate dehydrogenase (Ldh1)	Maintain bacterial redox homeostasis	Nitrosative stress in phagosome	(301)

Perturbation of Phagocytosis and Complement.

Phagocytosis and the complement system are the targets of many *S. aureus* virulence factors. The presence of a thick peptidoglycan layer prevents the complement-mediated membrane attack complex from lysing *S. aureus*. In addition, some clinical isolates of *S. aureus* contain genes that encode a polysaccharide capsule which can disrupt phagocytosis (302). One way that *S. aureus* targets the complement system

directly is through the activity of a zinc-dependent metalloprotease called Aureolysin (258). Aureolysin targets the complement system by cleaving C3 to form C3a and C3b. Then, the host complement factor I and factor H degrade C3b to prevent it from binding to *S. aureus*. The degradation of C3b also limits the release of C5a, interfering with production of opsonins. *Staphylococcus* complement inhibitor (SCIN) is a small protein that binds and stabilizes the C3bBb and C4b2a convertases preventing production of important complement mediators such as C3a, C3b, and C5a (260, 261). Staphylokinase (SAK), a secreted enzyme, activates host plasminogen attached on the bacterial surface to form plasmin, a potent serine protease (263). Plasmin is then able to cleave fibrin to break up blood clots and degrades C3b and human IgG. Collectively this blocks phagocytosis by eliminating potential complement-derived opsonins.

Besides complement-derived opsonins, immunoglobins like IgG can serve as opsonins. Staphylococcal protein A (SpA) and Staphylococcal binder of immunoglobulin (Sbi) both bind to the Fc domain of IgG (264, 265, 268, 303). SpA and Sbi interfere with Fc receptor mediated phagocytosis and block the complement protein C1q from binding to IgG thereby disrupting complement activation (266, 267). Moreover, extracellular fibrinogen binding molecule (Efb) and extracellular complement-binding protein (Ecb) bind to the C3d region of cleaved C3b blocking complement-mediated opsonization (260, 269).

Also involved in complement system inhibition are the staphylococcal superantigen-like proteins (SSLs) that are closely related to superantigens of *S. aureus* but lack the functional T cell receptor binding domain (304). The 14 *ssl* genes are arranged as tandem repeats in two different areas on the chromosome, in genomic

island-α and immune evasion cluster 2 (305). Most SSLs are only specific for humans and not animal host factors. SSL7 can interfere with the complement system by binding to human IgA and C5, leading to impaired IgA binding with its receptor FcαRI (270). Similarly, SSL10 binds to the Fc region of human IgG1 and blocks FcγR-mediated phagocytosis (306). Moreover, SSL3 can bind to the extracellular domain of TLR2, blocking macrophages from optimally recognizing native TLR2-activating ligands (276). Thus, many virulence factors of *S. aureus* function to block components of the complement system as well as interfere with phagocytosis.

Disruption of Coagulation.

Coagulation is another innate response mechanism by the host that is initiated by activated thrombin, converting fibrinogen to a crosslinked fibrin meshwork structure that can immobilize bacteria and attract phagocytic immune cells to clear the entrapped bacteria. All *S. aureus* isolates secrete coagulase and von Willebrand factor-binding protein, which are two coagulase degrading enzymes (305). These coagulases associate with prothrombin to generate staphylothrombin, which cleaves fibrinogen yielding fibrin without activating other host factors (277). The resulting fibrin begins to accumulate and assemble on the surface of *S. aureus* with the assistance of surface proteins clumping factor A, fibronectin-binding protein A and B, and bone sialoprotein binding protein. The agglutination of fibrin on the surface of *S. aureus* protects it from phagocytes. Lastly, SSL10 from *S. aureus* prevents prothrombin autoactivation, preventing activation of other host factors that stimulate the attraction of phagocytes to the entrapped bacteria (306). In summary, *S. aureus* is armed with different mechanisms to avoid coagulation by the host.

Interference with AMP Activity.

Multiple virulence factors and adaptations of *S. aureus* contribute to a collective resistance against different AMPs and antibacterial proteins. Besides its ability to cleave complement proteins, Aureolysin also cleaves the cathelicidin AMP LL-37 and contributes to resistance to this AMP in vitro (259). As mentioned above, *S. aureus* SAK stimulates the protease plasmin to bind and inhibit the activity of α-defensin AMPs (262). Resistance to the antibacterial enzyme lysozyme, was attributed to the function a membrane bound O-acetyltransferase protein that modified the C6 hydroxyl group of muramic acid (280). Moreover, *S. aureus* secretes extracellular adherence protein (Eap) and its related homologs EapH1 and EapH2. Eap, EapH1, and EapH2 inhibit the activity of serine proteases neutrophil elastase, proteinase 3, and cathepsin G that are expressed by neutrophils (281). Furthermore, *S. aureus* uses modifications to wall teichoic acid, LTA, and membrane phospholipids to lower the net negative charge of its membrane. This prevents cationic AMPs from being able to effectively bind to *S. aureus* and cause cell death. The DltABCD proteins, encoded by the *dlt* operon, lead to d-alanine substitutions into wall teichoic acids to reduce negative charge of this membrane component (278). In similar fashion, MprF works to increase the positive charge of phosphatidylglycerol exposed on the outer face of the cytoplasmic membrane by adding a positively charge l-lysine residue (279). In summary, *S. aureus* can either directly target AMPs through virulence factors or modifies its own cellular structures to hinder AMP killing.

Blockade of Neutrophil Migration.

The migration and extravasation of activated neutrophils to the site of infection is a major barrier to *S. aureus* infection. These processes of neutrophils are inhibited by *S. aureus* through the secretion of SSLs, Eap, Staphopain A, chemotaxis inhibitory protein of *S. aureus* (CHIPS), and formyl peptide receptor-like 1 inhibitor (FLIPr) or its homolog (FLIPrL). SSL5, SSL11 and SelX (a staphylococcal enterotoxin-like protein) can bind to P-selectin glycoprotein ligand 1 (PSGL1) on leukocytes (272, 274, 275). PSGL-1 regulates the adhesion and rolling steps of neutrophil extravasation through binding to P-selectin on activated endothelium. Thus, SSL5, SSL11, and SelX binding to PSGL1 interferes with neutrophil extravasation, diminishing the number of neutrophils recruited to the site of infection. Eap blocks neutrophil and leukocyte migration by associating with intercellular adhesion molecule 1 (ICAM1) (282). SSL6 binds to the receptor CD47, which is a common receptor found on most tissues involved in migration, phagocytosis, and proliferation (274). Furthermore, SSL10 interferes with the chemoattraction of neutrophils through the blockade of the C-X-C chemokine receptor 4 (CXCR4) (307). The secreted protease Staphopain A cleaves the N-terminus of CXCR2 chemokines, blocking chemokine signaling and the migration of neutrophils (283). The binding of bacterial formylated proteins to FPR1 and C5a to the C5a receptor potentiate neutrophil chemotaxis and migration. CHIPS is a small protein that can bind to only human formylated peptide receptor 1 (FPR1) and the human complement protein C5a receptor, thereby blocking the neutrophil chemotaxis function induced by these receptors (285). A search for proteins homologous to CHIPS, identified both FLIPr and FLIPrL, which function as antagonists of FPR1 and contribute to blockade of neutrophil chemotaxis

(286). In conclusion, the interference of neutrophil migration is a target of many different *S. aureus* virulence factors.

Toxins of *S. aureus*.

S. aureus directly induces the killing of innate immune cells via PSMs and different toxins. These toxins are arguably the most harmful virulence determinants of *S. aureus*. PSMs are a family of small amphipathic α-helical peptides with broad-range lytic activities. PSMs include both α- and β-type PSMs and the delta-toxin – a member of the α-PSMs. α-PSMs are 20-25 amino acids in length and are usually either neutral or positively charged. In contrast, β-PSMs are twice the size of α-PSMs at around 43-45 amino acids and have a negative net charge. Focusing on just the PSM cell lysing activities, they are reported to lyse osteoblasts, endothelial cells, epithelial cells, monocytes, erythrocytes, and importantly PMNs. The targeting of all these diverse cell types is likely to be a receptor-independent process that relies on membrane insertion and pore formation (308). This is in contrast to other *S. aureus* cytolytic toxins, such as alpha-hemolysin (Hla) or the bicomponent leukotoxins, which are highly specific for a particular cell type and host species.

Hla binds to the receptor A Disintegrin and Metalloproteinase Domain-containing protein 10 (ADAM10), which is expressed on the surface of myeloid cells, including neutrophils, epithelial cells and the vascular endothelium (289). Hla can lyse rabbit erythrocytes to a significantly greater degree compared to human erythrocytes. After binding to ADAM10, Hla assembles into a heptameric pore and through the metalloproteinase activity of ADAM10, triggers the lysis of epithelial cells or modulate the activity of innate immune cells (309).

Another highly destructive group of toxins are the bicomponent pore-forming leukotoxins, which have host species specific targets. These toxins consist of two monomeric subunits that target receptors on immune cells and kill by forming β-barrel pores that span the phospholipid bilayer (310). There are five known leukotoxins that associate with human infection, HlgAB, HlgCB, LukAB/HG, LukED, and Panton-Valentine leukocidin (PVL) (311). All strains of *S. aureus* that infect humans produce at least three leukotoxins (HlgAB, HlgCB, and LukAB/HG), while the most highly virulent human isolates produce all five human-associated leukotoxins (311). LukMF' and LukPQ are two other leukotoxins that are made by *S. aureus* but are only associated with zoonotic infections and rarely humans (312, 313). There are a diverse range of proteinaceous receptors that these leukotoxins bind to, conferring cell-specific targets for lysis. HlgAB binds to chemokine receptors CXCR1, CXCR2, and CCR2, as well as the Duffy antigen receptor for chemokines (DARC) (314, 315). HlgCB and PVL uses chemokine receptors C5aR1 and C5aR2 to associate with target cells (315). LukED also targets chemokine receptors, mainly CCR5, CXCR1, and CXCR2 on myeloid cells as well as DARC on erythrocytes (314, 316, 317). LukAB/HG binds to the myeloid marker CD11b and thus targets a range of phagocytic leukocytes (318). Receptor targeting by the five different human leukotoxins allows for lysis of a large number of immune cells, such as neutrophils, monocytes, macrophages, dendritic cells, T cells, and natural killer cells. In summary, *S. aureus* lytic molecules and toxins are collectively a major destructive group of virulence factors that have the potential to induce major host damage.

Mitigating Oxidative Stress in the Phagosome.

S. aureus withstands and survives an onslaught of host destructive mechanisms within the phagosome of neutrophils and macrophages through various adaptations and virulence factors. The host produces adenosine in response to hypoxia, ROS exposure or tissue damage. Adenosine recognition by the host during an active infection, signals that the level of inflammation to control disease is becoming self-harming. As a consequence of adenosine-based signaling, it can stop platelet aggregation and limit respiratory burst of neutrophils. *S. aureus* uses this system to its advantage and generates adenosine during infection through adenosine synthase A (294). The production of *S. aureus*-derived adenosine facilitates its survival within neutrophils likely through inhibition of respiratory burst (294) .

Many virulence factors help *S. aureus* combat the antibacterial effects of ROS within the phagosome. The golden carotenoid pigment of *S. aureus*, staphyloxanthin, functions as an antioxidant protecting against damaging hydroxyl radicals (295). Furthermore, harmful effects by hydrogen peroxide are mitigated through the functions of *S. aureus* catalase and alkylhydroperoxide reductase (296). To withstand ROS toxicity, *S. aureus* also produces two superoxide dismutases, SodA and SodM, which work to eliminate superoxide production (297). Methionine residues in proteins can be targeted by ROS, leading to harmful oxidation. *S. aureus* encodes a methionine sulfoxide reductase or Msr that can repair the oxidized methionine residues (298). A surface protein of *S. aureus* named surface factor promoting resistance to oxidative killing or Sok is involved in resistance to ROS generated by neutrophils (299). Besides ROS, $NO^{\bullet}$ and RNS induce nitrosative stress against *S. aureus*. One way that *S. aureus*

mediates $NO^{\bullet}$ resistance is by the flavohemoglobin Hmp that scavenges $NO^{\bullet}$ (300). Furthermore, a lactate dehydrogenase, Ldh1, is induced in response to $NO^{\bullet}$ to circumvent the disruption of redox homeostasis within *S. aureus* and regenerate NADH and NAD^{+} (301). The mechanisms that facilitate the detoxification of ROS and avoidance of nitrosative stress within the phagosome clearly contribute to the ability of *S. aureus* to resist killing.

S. aureus Survival in Immune Cells.

S. aureus is considered to be an extracellular pathogen, yet a growing body of evidence suggests that it is able to survive within various cell types including macrophages and neutrophils (123, 125, 291, 319, 320). To cope with the harsh environment within the phagosome, *S. aureus* can differentiate into small-colony variants (321). These small-colony variants are in a metabolically dormant state, can withstand stressors, and are highly resistant to antibiotics. Furthermore, residence in a host cell also can protect bacteria from antibiotics (322). Thus, the small-colony variant phenotype of intracellular *S. aureus* and the resulting protection from antibiotics may contribute to its survival within host cells. This has led to the hypothesis that *S. aureus* uses host cells such as neutrophils to support its dissemination during bloodstream infection to other parts of the host (323). Support for this hypothesis comes from a study that isolated neutrophils from the peritoneal cavity of mice infected with *S. aureus* that harbored viable bacteria and were able to cause disease when administered to naïve mice (324). To aid in the escape from within neutrophils, *S. aureus* increases the production of PSMs and LukAB/GH to mediate cell lysis and subsequent escape from neutrophils (325, 326). Although the immune system has dedicated cells such as

neutrophils to mediate bacterial-killing, *S. aureus* can hijack these cells with its virulence factors and use them for protection from other host defenses.

Concluding Remarks.

S. aureus has a large array of virulence factors that can target numerous parts of the innate response to infection. As a consequence, *S. aureus* can often easily escape and disseminate causing severe disease. Furthermore, a vast majority of the evasion mechanisms introduced focus on how *S. aureus* counters neutrophil immune responses. Comparatively less is known about specific virulence factors that can subvert macrophage immune responses. A major goal of this thesis is to identify novel ways in which *S. aureus* evades macrophage immune responses.

Section 6: *S. aureus* Metabolism and Pathogenesis

Trace Metal Acquisition.

Besides the numerous innate immune evasion adaptations of *S. aureus*, it also harnesses a diverse repertoire of traits that aid in nutrient acquisition. The acquisition of trace metals such as iron, manganese, zinc, and copper during infection are crucial for survival of *S. aureus*, as numerous studies detail that deficiency in acquiring these metals leads to a defect in pathogenesis (327-336). As mentioned before, the host produces multiple metal binding proteins such as calprotectin, lactoferrin, or transferrin to outcompete bacterial sequestering mechanisms. Overcoming iron limitation is required to infect a host. *S. aureus* utilizes siderophores and a heme acquisition system to promote survival. Staphyloferrin A and staphyloferrin B are two siderophores secreted by *S. aureus* that bind to iron with high affinity, providing the bacterium with iron (337, 338). Both of these siderophores can remove and acquire iron from human

transferrin. Though siderophore-mediated iron acquisition supports growth of *S. aureus*, it prefers to use heme as a source of iron (339). Heme is the primary source of iron within vertebrate hosts, and *S. aureus* has a dedicated heme scavenging and heme uptake system (340, 341). Once heme enters the bacterial cell, the tetrapyrrole ring is degraded to liberate iron (342). Like iron, both manganese and zinc are required for *S. aureus* pathogenesis. Manganese is acquired through two transporters, MntABC and MntH, and zinc is imported through AdcABC and CntABCDF (327, 329). Loss of any of these transporters or importers in *S. aureus* compromises pathogenesis. Copper is a cofactor for various proteins in *S. aureus*. Currently the exact mechanism of copper acquisition in the host and the relevance of copper import to pathogenesis in *S. aureus* is unknown. However, two proteins CopA and CopZ are hypothesized to maintain copper homeostasis within *S. aureus*, as loss of these proteins leads to intracellular copper accumulation and toxicity (343).

Acquisition of Other Nutrients.

In addition to trace metal acquisition adaptations by *S. aureus*, the bacterium also needs to import other molecules involved in metabolism such as carbohydrates and inorganic phosphate. Recent work identified 11 carbohydrate transporters in *S. aureus*, four of which can import glucose (344). Elimination of some of these carbohydrate transporters severely limits the amount of imported glucose and diminishes the pathogenesis of *S. aureus* during skin and soft-tissue infection. Similarly, *S. aureus* encodes three different inorganic phosphate transporters (PstSCAB, PitA, and NptA) and elimination of one is not sufficient to cause attenuation of disease (345, 346). Rather, deletion of NptA and either remaining transporter conferred a defect

during *S. aureus* infection. These mechanisms facilitate the ability of *S. aureus* to overcome host imposed nutritional immunity.

Moonlighting Proteins.

As described in detail above, *S. aureus* has a dedicated arsenal of virulence factors that perform distinct functions to promote microbial survival. However, a growing number of proteins outside this array of virulence factors have been identified that are able to carry out secondary activities, including the ability to promote virulence (347, 348). Proteins possessing additional biological activities beyond their primary function are described as having moonlighting activity (349). These moonlighting proteins are emerging as important mediators of virulence in many bacterial pathogens. Proteins with moonlighting activity span all kingdoms of life. Most of the eukaryotic and prokaryotic moonlighting proteins are well-known metabolic enzymes or molecular chaperones. Many bacterial moonlighting proteins have primary functions as metabolic enzymes in the bacterial cytosol; however, inexplicably, these proteins are also commonly found in the extracellular environment where they contribute to bacterial virulence. For example, the glycolytic enzyme glyceraldehyde-3-phosphate dehydrogenase (GAPDH), which is present on the cell surface of streptococci and other bacteria, facilitates bacterial adhesion to a variety of ligands including the major host adhesive glycoprotein, fibronectin, as well as lysozyme, actin, and myosin (350). *S. aureus* GAPDH can bind to host transferrin, which sequesters iron away from bacteria (351). Enolase, an enzyme involved in glycolysis, is also found on the surface of *S. aureus* where it is hypothesized to bind to laminin (352). It is unknown whether the ability of GAPDH or enolase to bind transferrin or laminin has physiological relevance

during *S. aureus* infection. Moreover, as described with GAPDH of streptococci and *S. aureus*, the homologs of moonlighting proteins in other species are often found to retain their secondary functions highlighting their conservation.

Up to 25% of the secretome of *Escherichia coli*, *Bacillus subtilis* and *S. aureus* were identified as cytoplasmic proteins that function in metabolic pathways (353-356). What is so unusual, is that these extracellular cytoplasmic proteins do not contain any discernable secretion signals. This release of cytoplasmic proteins is specific, as not every cytoplasmic protein is found in the extracellular environment (357). Currently, the mechanism for surface display and/or secretion of cytoplasmic proteins is not well characterized. What is known is that the presence of extracellular cytoplasmic proteins from *S. aureus* depends on the activity of the major autolysin, Atl (357). Atl is a peptidoglycan hydrolase and is involved in peptidoglycan remodeling of *S. aureus*. In the absence of Atl, there is a marked decrease in the amount of released cytoplasmic extracellular proteins. Another group concluded that the release of cytoplasmic proteins is not solely dependent on bacterial autolysis, as the abundances of released cytoplasmic proteins occur over time throughout growth and are in similar abundance compared to a naturally secreted protein (358). Furthermore, they show that some released cytoplasmic proteins congregate at the septum region of dividing cells. Also, in *Listeria monocytogenes* the surface display of certain cytoplasmic proteins partially depend on the SecA2 accessory secretion protein (359). Again, although the exact mechanism behind cytoplasmic protein release into the extracellular environment is unknown, it is appreciated that this is likely an active process.

Concluding Remarks.

If *S. aureus* cannot acquire essential nutrients such as trace metals in the host, it cannot effectively replicate and cause disease. Moreover, metabolic proteins are found to be present in the extracellular environment and may facilitate pathogenesis. The processes of trace nutrient acquisition and metabolic moonlighting proteins suggest that bacterial metabolism facilitates pathogenesis either directly or indirectly. In the next section, we will introduce a trace nutrient called lipoic acid that our laboratory has found to be essential for *S. aureus* pathogenesis.

Section 7: Lipoic Acid and *S. aureus*

Overview of Lipoic Acid.

An essential trace nutrient that *S. aureus* must acquire is the metabolic cofactor lipoic acid. Lipoic acid is an organosulfur-containing molecule that is covalently linked to proteins in large multi-subunit enzymatic complexes and is involved in redox coupling during oxidative and one carbon metabolism (Figure 2A) (360). This cofactor is found in nearly all kingdoms of life, including bacteria, yeast, and higher order eukaryotes. Five multi-subunit complexes contain lipoic acid: pyruvate dehydrogenase complex (PDH), 2-Oxoglutarate dehydrogenase (OGDH), branched-chain 2-Oxoacid dehydrogenase (BCODH), the glycine cleavage system (GCS) and acetoin dehydrogenase complex (AoDH) (361). *S. aureus* has all of these complexes except AoDH. In these complexes, lipoic acid serves as an electrophile that can bind reaction intermediates and shuttle substrates between the active sites of different subunits (362, 363). Due to this crucial function, without lipoic acid, these enzyme complexes do not work. The 2-oxoacid decarboxylases (PDH, OGDH, BCODH) are comprised of E1, E2, and E3 subunits

(361, 364). The core of the enzyme structure is provided by the E2 subunit, and often these 2-oxoacid decarboxylases carry multiple copies of the E2 component. In Gram-positive bacteria, the core of PDH is comprised of 60 E2 subunits arranged with icosahedral symmetry (365). The GCS has four main subunits, the pyridoxal phosphate-containing protein (P protein), hydrogen carrier protein (H protein), tetrahydrofolate-containing protein (T protein), and lipoamide dehydrogenase (L protein). Lipoyl moieties are found covalently linked to a conserved lysine within the E2 or H subunit of these complexes. The number of lipoyl domains on PDH varies from one to three, while all OGDH and BCODH E2 subunits contain just one domain (361). PDH catalyzes the oxidative decarboxylation of pyruvate to form acetyl coenzyme A, feeding several metabolic pathways in the cells, including the tricarboxylic acid (TCA) cycle, fatty acid biosynthesis, and arms of isoprenoid biosynthesis. OGDH converts α-ketoglutarate to succinyl-coA, which is consumed by the TCA cycle or can be diverted for heme and amino acid biosynthesis. BCODH participates in the degradation of branched-chain amino acids to generate branched-chain coenzyme A intermediates needed for fatty acid synthesis. The GCS in bacteria degrades glycine and produces 5,19-methylene-tetrahydrofolate, a one carbon donor involved in synthesis in serine, thymidine, and purines (366). In mammals, GCS prevents the buildup of toxic levels of glycine. Despite the conservation of lipoic acid, the mechanisms of lipoic acid acquisition show considerable diversity.

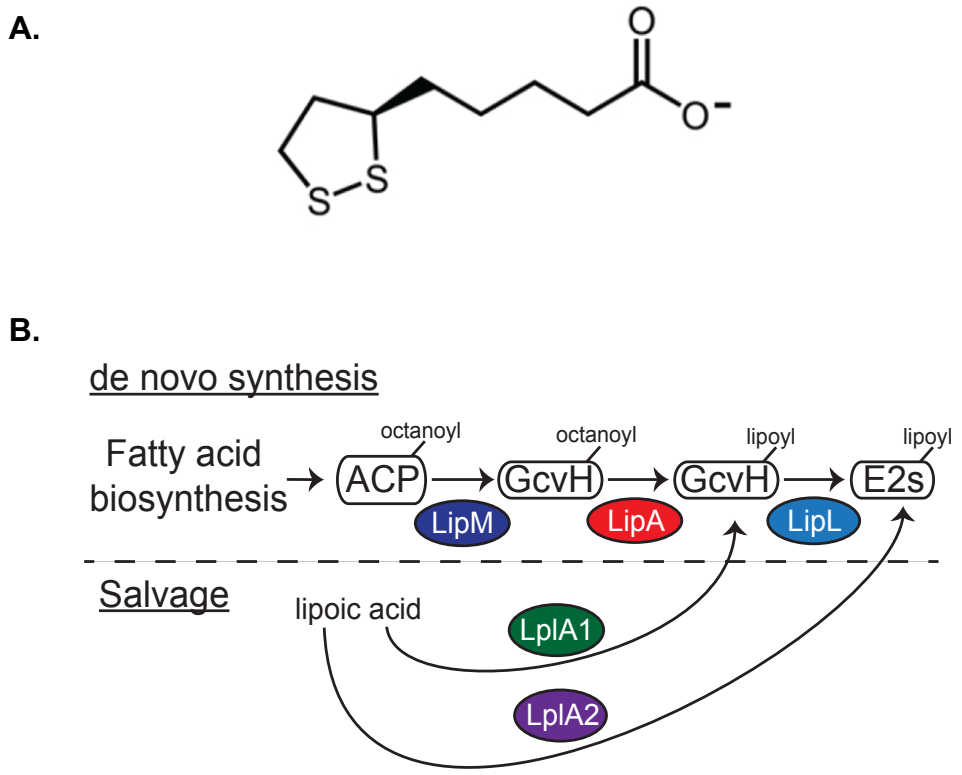

Figure 2. Lipoic Acid Acquisition in *S. aureus*. (A) Structure of lipoic acid. (B) Model of the *S. aureus* lipoic acid synthesis and salvage pathways. ACP, Acyl carrier protein; GcvH, H protein of the glycine cleavage system; E2s, E2 subunits of PDH, OGDH, and BCODH. LipM, octanoyl transferase; LipA, lipoyl synthetase; LipL, lipoyl transferase; LplA1/A2, lipoate protein ligases. (A) Reprinted with permission from Spalding and Prigge, 2010 (360). (Figure 42-Appendix A)

Acquisition of Lipoic Acid.

Bacteria acquire lipoic acid through the use of two different mechanisms: *de novo* synthesis or salvage from the environment. Though lipoic acid is an essential cofactor needed for viability, some bacteria such as *Helicobacter pylori* have adapted alternative non-lipoic acid dependent metabolic enzymes to facilitate cellular viability (367, 368). Lipoic acid acquisition and the proteins involved are best characterized in *E. coli*, *B. subtilis*, and *L. monocytogenes* (369-372). Recent work from our laboratory has

characterized lipoic acid acquisition schemes in *S. aureus.* Like *B. subtilis*, *S. aureus* engages in both *de novo* synthesis and salvage of lipoic acid (Figure 2B) (373, 374). Using genetic and biochemical studies, we have determined that synthesis of lipoic acid depends on the enzymes LipA, LipM, and LipL (373, 374). The salvage of lipoic acid occurs through the action of two ligases, LplA1 and LplA2. Lipoic acid synthesis starts with the transfer of octanoic acid, a medium chain fatty acid, from its acyl carrier protein (ACP) to GcvH by LipM, an octanoyl transferase. The lipoic acid synthase LipA then inserts two sulfur atoms into the octanoyl-precursor forming a dithiolane ring yielding lipoic acid. The amidotransferase LipL transfers the lipoyl moiety from GcvH to conserved lysine residues on the E2 subunits of PDH, OGDH, and BCODH (373, 374). In the scavenging pathway, the ligase LplA1 scavenges free lipoic acid from the environment and attaches it to GcvH where the lipoyl moiety is then transferred to its cognate E2 subunits (373, 374). Another ligase, LplA2, also scavenges free lipoic acid but it bypasses GcvH and directly attaches the lipoyl moiety to E2-PDH, E2-OGDH, and E2-BCODH (373, 374).

Lipoic Acid in Pathogenesis.

Given the significance of lipoic acid in bacterial metabolism, it is no surprise that acquisition of lipoic acid contributes to pathogenesis. For example, lipoic acid salvage enzymes promote the pathogenesis of *Listeria monocytogenes* and *Chlamydia trachomatis* (369, 375-377). In *Plasmodium*, the salvage enzyme ortholog LplA1 contributes to the survival of the parasite during expansion within red blood cells during infection (378, 379). As of 2014, there was no data in the literature to suggest how lipoic acid acquisition in *S. aureus* contributes to virulence during infection. However

published work and preliminary studies from our laboratory indicate lipoic acid synthesis and salvage pathways are crucial for infection by *S. aureus* (373). We have found that in bloodstream infection, perturbations of lipoic acid synthesis and salvage can lead to tissue-specific defects where infection of the kidney depends on salvage, but infection of the heart requires *de novo* synthesis (373). These data suggest there is varied dependency on *de novo* lipoic acid synthesis or salvage for *S. aureus* survival that depends on the tissue site.

Immunosuppressive Properties of Lipoic Acid.

Aside from the central role of lipoic acid in metabolism, it also possesses immunosuppressive traits. High concentrations of free lipoic acid reduce the respiratory burst of neutrophils through its antioxidant properties and block the translocation of the transcription factor, NFκB, to the nucleus (380-383). Intriguingly, high concentrations of free lipoic acid also can activate Akt (384). This stimulates the phosphoinositide 3-kinase/Akt signaling axis, which has a range of biological effects; but, in terms of lipoic acid activation, it was demonstrated to limit inflammatory cytokine production. Another described immunosuppressive activity of free lipoic acid, is the inhibition of iNOS activity at the protein level when induced by IL-1β (385). However, free lipoic acid is not a physiologically relevant form as lipoic acid is always bound to a protein via an amide bound. The relevance of lipoic acid immunosuppressive abilities has never been tested in vivo during the course of a bacterial infection.

Summary

S. aureus is a human pathogen that can infect almost every tissue site in the host and cause significant disease. The innate immune system of the host is a fast-acting

initial line of defense that can recognize and utilize many diverse mechanisms to limit infection. However, *S. aureus* has evolved and acquired an array of virulence factors that can inhibit innate immune cell recruitment and antimicrobial activity, or directly target and kill phagocytic leukocytes thereby facilitating pathogenesis. In order to successfully infect the host, *S. aureus* must be able to acquire trace nutrients. How evasion of host innate responses and acquisition of trace nutrients in *S. aureus* dictates pathogenesis is largely understudied. Moreover, a majority of what is known about innate immune evasion and *S. aureus* focuses on countering neutrophil activity and not macrophages.

Thus, this thesis sought to identify novel host innate evasion mechanisms of *S. aureus* that are directed at curbing macrophage immune responses. We found that the function of the lipoic acid synthetase, LipA, is necessary to dampen macrophage activation by *S. aureus* PAMPs. This occurs through the release of a metabolic protein into the extracellular environment, E2-PDH, which is modified with lipoic acid. The lipoic acid modified E2-PDH moonlights by restricting TLR1/2 activation of macrophages. During infection, the production of lipoic acid is crucial to dampen the inflammatory responses of macrophages. In the absence of this lipoic acid-based restriction of macrophage inflammatory responses during infection, macrophages are better able to control infection. In summary, this thesis has identified a novel innate immune evasion mechanism of *S. aureus* closely associated with bacterial metabolism.

CHAPTER TWO

MATERIALS AND EXPERIMENTAL METHODS

Bacterial Strains and Culture Conditions

All bacterial strains and oligonucleotides used in this thesis are listed in Table 3. The WT and parental strain used to generate all *S. aureus* mutants used in this study was the pulse field gel electrophoresis type USA300 isolate LAC cured of its plasmids (wild type – AH1263), unless noted otherwise. *S. aureus* RN4220 is a NCTC8325 derivative which is restriction deficient for passage of plasmid. The T7 expressing *Escherichia coli* strain*, lysY/I*^{q}*,* was used as a host to overexpress and purify recombinant 6x-Histidine tagged *S. aureus* E2-PDH. All *S. aureus* strains were either grown in rich medium - Tryptic Soy Broth (TSB) (Criterion), or in defined medium lacking lipoic acid - Roswell Park Memorial Institute 1640 medium (RPMI) (Corning) supplemented with 1% casamino acids (Amresco). *E. coli* was cultivated in Lysogeny Broth, Miller formulation (LB) (BD Biosciences). Unless noted, all bacteria were grown at 37°C in a shaking incubator at 200 rpm in tubes kept at a 45° angle. When solid medium was required, agar (Amresco) was supplemented into TSB and LB at 1.5%. Where necessary, media was supplemented with antibiotics at the following final concentrations for *S. aureus*: erythromycin (Erm), 3 µg/mL (Amresco); kanamycin (Kan), 50 µg/mL (Amresco); neomycin (Neo), 50 µg/mL (Amresco); and chloramphenicol (Cam), 10 µg/mL (Amresco). Antibiotics for *E. coli* were supplemented at the following final concentrations: ampicillin (Amp), 100 µg/mL (Gold Biotechnology); Kan, 10 or 25

μg/mL (Amresco); and Neo, 10 or 25 μg/mL (Amresco). RPMI medium used to bypass the requirement for lipoic acid (RPMI+BCFA) was supplemented with the following branched-chain carboxylic acids: 11.23 mM isobutyric acid (Sigma), 9.5 mM 2-methylbutyric acid (Alfa Aesar), 9.69 mM isovaleric acid (Sigma), and 10 mM sodium acetate (Amresco), pH 7.4-7.5.

Molecular Genetic Techniques

S. aureus chromosomal DNA was isolated using the Wizard Genomic DNA purification kit (Promega) following the manufacturer's protocol with minor modifications. 1.2 mL of an overnight culture was pelleted by centrifugation at 14000 rpm for 3 minutes at room temperature and resuspended in 200 μL of TSM buffer (50 mM Tris, 0.5 M D-Sucrose,10 mM $MgCl_2$ pH 7.5) followed by addition of 2.5 μL of lysostaphin (Ambi Products, NY) stock solution (2 mg/mL in 20 mM sodium acetate, pH 4.5) and incubation at 37°C for 15 minutes to digest the cell wall. The bacteria were then pelleted by centrifugation at 14000 rpm for 5 minutes at room temperature and the chromosomal DNA was extracted as detailed by the manufacturer's instructions. Recombinant plasmids and DNA from agarose gels were recovered using miniprep/midiprep and gel extraction kits from QIAGEN following the supplied protocol. Polymerase chain reaction was conducted using GoTaq polymerase (Promega) or Phusion High-Fidelity DNA polymerase (New England Biolabs) with oligonucleotide primers from Eurofin Genomics (Table 4), and dNTPs from Quanta Biosciences. DNA digestion was performed using restriction enzymes purchased from New England Biolabs. When digesting plasmids shrimp alkaline phosphatase (Amresco) was supplemented into the digests. Ligations were conducted using T4 DNA Ligase (New England Biolabs) at 16°C overnight.

Table 3. List of Strains

Designation	Description	Strain
WT AH-LAC	*S. aureus* USA300 Strain LAC. Plasmid cured.	USA300 AH-LAC
WT LAC	*S. aureus* USA300 Strain LAC	USA300 WT LAC
Transposon mutant library	Nebraska Transposon Mutant Library of USA300 JE2 (386)	USA300 JE2
WT JE2	*S. aureus* USA300 Strain JE2	USA300 JE2
DH5α	*E. coli* strain used for propagating pIMAY in *S. aureus*	DH5α
lysY/I^{q}	*E. coli lysY/I*^{q} strain used for expression of E2-PDH	*lysY/I*^{q}
RN4220	Restriction deficient *S. aureus* for plasmid propagation	RN4220
∆*lipA*	AH-LAC with in-frame deletion of *lipA*	FA-S831*
Δ*lipA* + Δ*lipA*	FA-S831 complemented with pJC1112-*lipA*	FA-S877*
Δ*E2-PDH*::*kan*	AH-LAC with gene replacement of *e2-pdh* with the kanamycin resistance cassette	FA-S1041
Δ*E2-OGDH*::*kan*	AH-LAC with gene replacement of *e2-ogdh* with the kanamycin resistance cassette	FA-S1042
∆*gcvH*::*kan*	AH-LAC with gene replacement of *gcvH* with the kanamycin resistance cassette	FA-S1038
Δ*lipM*	AH-LAC with an in-frame deletion of *lipM*	FA-S842*
Δ*lipL*	AH-LAC with an in-frame deletion of *lipL*	FA-S1176*
Δ*lplA1*	AH-LAC with an in-frame deletion of *lplA1*	FA-S841*
Δ*lplA2*	AH-LAC with an in-frame deletion of *lplA2*	FA-S837*
atl::*erm*	Transposon insertion into *atl* from the Nebraska Transposon Mutant Library of USA300 JE2	NE460
secA2::*erm*	Transposon insertion into *secA2* from the Nebraska Transposon Mutant Library of USA300 JE2	NE66
Δ*lipA*::*kan E.coli*	Δ*lipA*::*kan* LysY I^{Q} *E. coli*	FA-E1344
6x-His-PDH	pET15b encoding 6x-His-PDH transformed into Δ*lipA*::*kan* LysY I^{Q} *E. coli*	FA-S1359
SitC-6x-His	RN4220 with pOS1-P_{sarA}-sod_{Rbs}-*SitC-6x-His*	FA-S1424*

*denotes strains generated by current and former members of the Alonzo Lab: Ryan Novak, Azul Zorzoli, and Xi Chen.

E. coli Competent Cell Preparation

A 5 mL O/N culture of *E. coli* in LB was grown at 37°C with shaking at 200 rpm. The overnight culture was diluted 1:55 into a 250 mL flask containing 200 mL of LB, and then grown at 37°C with shaking at 200 rpm until cultures reached an OD600 0.3-0.4 (around 2.5 hours). The culture was divided equally into four pre-chilled 50 mL conical tubes and incubated on ice for 10 minutes. The tubes were centrifuged at 4000 rpm for 10 minutes at 4°C. Supernatant was discarded and the pellets were resuspended in 10 mL of Transformation Buffer 1 (30 mM KOAc, 100 mM $RbCl_2$, 10 mM $CaCl_2$, 50 mM $MnCl_2$, 15% glycerol, pH to 5.8 using 0.2 M acetic acid) and incubated on ice for 10 minutes. These washed cells were then centrifuged at 4000 rpm for 5 minutes at 4°C. Supernatant was discarded and the pellets were resuspended in 1 mL of Transformation Buffer 2 (10 mM MOPS, 75 mM $CaCl_2$, 10 mM $RbCl_2$, 15% glycerol, pH to 6.5 with KOH) and transferred to 1.5 mL microcentrifuge tubes. The competent cell preparations were stored at -80°C for future use.

E. coli Transformation

5 µL of a ligation reaction or 1 µL of purified plasmid were added to 50 µL of competent *E. coli* in microcentrifuge tubes on ice for 20 minutes. Bacterial cells were then heat-shocked for 45 seconds at 42°C and immediately placed on ice for 2 minutes. For recovery, 250 µL of SOC medium (0.5% tryptone, 0.5% yeast extract, 0.05% NaCl, 250 mM KCl, adjusted to a pH 7.0 using 5M NaOH followed by addition of 20 mL 1M glucose) was added to the bacterial cells and incubated at 37°C with shaking at 200 rpm for 2 hours. After incubation, 100 µL of the transformation mixture was plated on LB plates with relevant antibiotics to select for transformants.

Preparation of *S. aureus* Electrocompetent Cells

A 5 mL O/N culture of *S. aureus* in TSB was grown at 37°C with shaking at 200 rpm. The next day, 300 µL of the overnight culture was added to 30 mL of fresh TSB and grown for 3 hours at 37°C with shaking at 200 rpm. The culture was centrifuged for 10 minutes at 8000 rpm for 10 minutes at 4°C. Supernatant was decanted and the bacterial pellet was washed in 30 mL ice-cold 10% glycerol, followed by another centrifugation at 8000 rpm for 10 minutes at 4°C. This washing step was repeated once more. Cells were then resuspended in 15 mL 10% glycerol followed by additional centrifugation at 8000 rpm for 10 minutes. Lastly, cells were suspended in 3 mL 10% glycerol and aliquoted into 1.5 mL microcentrifuge tubes and stored at -80°C until use.

S. aureus Electroporation

To transform *S. aureus*, 50 µL of thawed *S. aureus* competent cells was mixed with ~1 µg of purified plasmid by gentle agitation and incubated at room temperature for 30 minutes. The mixture was transferred to a 2 mm electroporation cuvette (VWR) and pulsed with a GenePulserXcell BioRad electroporator at 1800 V, 10 µF, 600 Ω. After pulsing, cells we allowed to recover in 750 µL of TSB for 1.5 hours at 30°C with shaking at 200 rpm. After incubation, 100 µL of the bacteria was plated onto TSA plates supplemented with appropriate antibiotics. The remaining bacteria were first pelleted by centrifugation at 10000 rpm for 2 minutes and the supernatant was removed until 100 µL remained. The pellet was resuspended in this remaining 100 µL and plated onto TSA plates supplemented with appropriate antibiotics. Plates were incubated for 1-2 days at 30°C.

Construction of Marked Deletion Mutants

Two fragments corresponding to 500 base pairs upstream of the start codon and 500 base pairs downstream of the stop codon of *e2-pdh*, *e2-ogdh*, and *gcvH* were amplified by polymerase chain reaction (PCR). The upstream fragment was PCR amplified from WT *S. aureus* genomic DNA using primer 0791SOE1-Kpn/0995SOE1-Kpn/1305SOE1-Kpn and primer 0791SOE2-Kas/0995SOE2-Kas/1305SOE2-Kas (Table 4). The downstream fragment was also PCR amplified from WT *S. aureus* genomic DNA using primer 0791SOE3-Kas/0995SOE3-Kas/1305SOE3-Kas and primer 0791SOE4-Sac/0995SOE4-Sac/1305SOE4-Sac (Table 4). The resulting fragments were purified and used as templates in a splicing by overlap extension (SOEing) PCR reaction to generate the final amplicon for mutagenesis. This amplicon was then cloned into pIMAY using the KpnI and SacI restriction enzymes and propagated in *E. coli*.

To construct pIMAY mutagenesis plasmids containing an antibiotic resistance marker, *aphA3* (kan^R) was PCR amplified from the plasmid pBTK with oligonucleotides KanF-Kas and KanR-Kas (Table 4). We then sub-cloned the kan^R gene into a unique KasI site engineered between the upstream and downstream regions of homology previously cloned into pIMAY. Once constructed, the pIMAY gene replacement constructs were transformed into *E. coli* and selected for chloramphenicol (Cam) resistance. The pIMAY plasmids were propagated in *E. coli* and purified for electroporation into the restriction deficient *S. aureus* strain RN4220. The pIMAY plasmids were isolated from RN4220 and then electroporated into WT *S. aureus* LAC as described above. The pIMAY plasmid replicates at 28°C and integrates into the *S. aureus* chromosome at 37°C so it was maintained at 28°C until performing

mutagenesis. Allelic replacement was carried out by shifting to the non-permissive temperature for pIMAY replication (37°C) in the presence of Cam. This allows for pIMAY to integrate into the genome at the cloned homologous sites. The strains were then cultured at 28°C without Cam selection to facilitate a second recombination event and subsequent excision of the plasmid from the genome. To counter-select for bacteria that have lost the pIMAY plasmid, bacteria are plated on anhydrous tetracycline (AnTet). At the same time, the bacteria were selected on Kan/Neo plates to select for successful gene replacement events. Colonies that were Cam sensitive, AnTet resistant, and Kan/Neo resistant were analyzed by PCR for deletion of the relevant genes. This procedure was used to generate the following mutant strains: Δ*e2-pdh*::*kan*, Δ*e2-ogdh*::*kan*, and Δ*gcvH*::*kan*.

Bacterial Growth Curves

Growth curves of WT, Δ*lipA*, or Δ*lipA*+*lipA* were carried out in TSB and RPMI, RPMI supplemented with 25 nM α-lipoic acid (Sigma), or RPMI supplemented with BCFA (RPMI+BCFA). Overnight cultures were prepared in triplicate in either TSB or RPMI+BCFA in a 96-well round-bottom polystyrene plate (CellTreat). The next day, cultures were washed three times in TSB or RPMI and the triplicate samples were subcultured 1:100 and grown in a 96-well flat-bottom polystyrene plate at 37°C with shaking at 200 rpm. Bacterial growth was assessed hourly for 10 hours by measuring optical density at 600 nm (OD600) using an ELx800 microplate reader (BioTek) until reaching stationary phase (~10 hours).

Table 4. List of Primers

Name	Sequence
LipAP1F	ATTGAATTGAAACGCTTTCCTTCGTAATTCGCAACTGGAACACGCACGC TGTGTAGGCTGGAGCTGCTTC
LipAP2R	CTTCAAAAAGCGGGTTTTTTATCAGACAGATGTAAGTAATTATTACAGGA ATGGGAATTAGCCATGGTCC
LipAF	ATTGAATTGAAACGCTTTCCTTCGT
LipAR	CTTCAAAAAGCGGGTTTTTTATCAG
995hisN/CF	ATATCATATGGCATTTGAATTTAGATTACCC
995hisNR	ATATGGATCCTTACCCCTCCATTAATAATAA
SitC1	ATATCTGCAGCTGATATTTTTGACT
SitC2	TAATAAAGGTACTAATTTTTTCATAAATAATCATCCTCCTAAGGT
SitC3	ACCTTAGGAGGATGATTATTTATGAAAAAATTAGTACCTTTATTA
SitC4	ATATGTCGACTTAGTGATGGTGATGGTGATGTTTCATGCTTCCGTGTAC AG
NE66F	GATATTGTGGATTATGAGTAT
NE66R	AAACCGAGACGTCCATTAGT
NE460F	AATATTTTTCATTAATTAAGTC
NE460R	ATAATTATAGTTATGATCAATT
0791SOE1-Kpn	CCC-GGTACC(KpnI)-AGGTTGCAGTCGTATGATTA
0791SOE2-Kas	ATTAAGGAGTTACACGGTGA-GGCGCC(KasI)- GAGAATCCCCTCCTAATTAA
0791SOE3-Kas	TTAATTAGGAGGGGATTCTC-GGCGCC(KasI)- TCACCGTGTAACTCCTTAAT
0791SOE4-Sac	CCC-GAGCTC(SacI)-CAGACATTCCATACATTTGATC
0995SOE1-Kpn	CCC-GGTACC(KpnI)-TGAAGAAGTACCTGAAGAAG
0995SOE2-Kas	GAAATCTCCAACTACCATGTT-GGCGCC(KasI)- GTTTTTGCCCTCCTAAGATT
0995SOE3-Kas	AATCTTAGGAGGGCAAAAAC-GGCGCC(KasI)- AACATGGTAGTTGGAGATTTC
0995SOE4-Sac	CCC-GAGCTC(SacI)-TACTTCTTGTAAGTTTAAAGCA
1305SOE1-Kpn	CCC-GGTACC(KpnI)-TGCACAAGCGGCTAGTTTA
1305SOE2-Kas	TAAACTATTTTGTGTTGTGGA-GGCGCC(KasI)- GACTTATTTCCCCCTAGTTA
1305SOE3-Kas	TAACTAGGGGGAAATAAGTC-GGCGCC(KasI)- TCCACAACACAAAATAGTTTA
1305SOE4-Sac	CCC-GAGCTC(SacI)-AATCATAAATTATAGAATATCGG
KanF-Kas	TCCCGGCGCCCTCGACGATAAACCCAGCGAAC
KanR-Kas	TCCCGGCGCCCTTTTTAGACATCTAAATCTAGGTAC

Isolation of Bone Marrow-Derived Macrophages

Primary murine bone marrow macrophages (BMM) were derived from bone marrow progenitor cells isolated from the femurs and tibias of C57BL/6 (WT, TLR2$^{-/-}$, TLR4$^{-/-}$, MyD88$^{-/-}$) mice. 5 x 10^6 progenitor cells were plated in 100 x 26-mm Petri dishes

containing 15 mL bone marrow macrophage medium (BMM medium - DMEM (CellGro) + 1 mM Sodium Pyruvate (CellGro) + 1 mM HEPES Buffer (CellGro) + 2 mM L-glutamine (CellGro) + 20% heat inactivated FBS (Seradigm) + 30% L929 fibroblast cell supernatant + 100 µg/ml Penicillin/Streptomycin (Pen/Strep) (CellGro) + 50 µM β-mercaptoethanol (Amresco)). After 3 days at 37°C, 5% CO_2, 10 mL of fresh BMM medium was added and macrophages were allowed to differentiate for 6 more days. To remove differentiated BMM from petri dishes, the cells were rinsed with 10 mL 1X PBS and incubated with 10 mL 1X PBS at 4°C for 30 minutes. Following incubation, cells were removed by manual pipetting and 1 x 10^7 cells were resuspended in BMM medium containing 10% DMSO (Sigma) for storage in liquid nitrogen. For experiments using frozen BMM, the frozen vial was thawed at 37°C and then slowly diluted dropwise into fresh BMM medium, pelleted by centrifugation at 1500 rpm at 4°C for 5 minutes, and then resuspended in 10 mL of fresh BMM medium. The cell suspension was subsequently split into two 100 x 26-mm Petri plates containing 10 mL BMM medium with 100 µg/mL penicillin/streptomycin and was cultured for 3 days at 37°C, 5% CO_2 before use.

Isolation of Bone Marrow Neutrophils

Murine bone marrow neutrophils were isolated from the femurs and tibias of C57BL/6 WT mice by flushing out the bone marrow cells with DMEM + 10% heat inactivated FBS. Cells were then centrifuged at 1500 rpm at 4°C for 5 minutes, the supernatant was decanted, and red blood cells were lysed with ACK lysing buffer (Lonza) by resuspending the pellet in 2 mL of lysis buffer and incubating for 2 minutes at room temperature. Cell lysis was stopped by adding 8 mL of 1X sterile PBS, mixing

gently, and pelleting by centrifugation at 1500 rpm, 4°C for 5 minutes. The cells were then resuspended in 10 mL of DMEM + 10% heat inactivated FBS, counted, and resuspended in 1 mL of 1X PBS after pelleting by centrifugation at 1500 rpm at 4°C for 5 minutes. To isolate neutrophils, we used density gradient centrifugation. 3 mL of Histopaque 1077 (density 1.077 g/mL) (Sigma) was gently overlaid on 3 mL of Histopaque 1119 (density 1.119 g/mL) (Sigma) followed by addition of the bone marrow cell suspension on top of the Histopaque 1077 layer. The samples were then centrifuged for 30 minutes at 2000 rpm 25°C without brake and neutrophils were collected at the interface between the Histopaque 1119 and 1077 layers. Purified neutrophils were then washed twice by centrifugation at 1500 rpm at 4°C for 5 minutes and resuspending with DMEM + 10% heat inactivated FBS supplemented with 100 µg/mL Pen/Strep (Corning) and 50 µg/mL gentamicin (Amresco). Neutrophils were then seeded at 65000 cells per well into 96-well flat-bottom tissue culture treated plates (Corning) in 90 µL DMEM + 10% heat inactivated FBS supplemented with 100 µg/mL Pen/Strep and 50 µg/mL gentamicin. The neutrophils were activated with 10 µL OD-normalized supernatants from 9 hour *S. aureus* cultures followed by incubation at 37°C, 5% CO_2 for 12 hours. Macrophage supernatants were then removed and either used immediately or stored at -80°C. To measure the levels of cytokines and chemokines in the neutrophil supernatants, a custom Cytometric Bead Array Flex set (BD Biosciences) was used according to manufacturer's specifications. Bead and supernatant mixtures were incubated for 1.5 hours at 25°C at 600 rpm using a Thermo Mixer C (Eppendorf) in a 96-well V-bottom plate (Corning). Samples were then washed using FACS Wash Buffer (1X PBS + 2% heat inactivated FBS + 0.05% (w/v) Sodium Azide), data collected

on a LSRFortessa (BD Biosciences), and analyzed using FlowJo software (FlowJo, LLC) by gating on individual bead populations and calculating the geometric mean of fluorescence relative to protein standards.

To measure the purity of the isolated bone marrow neutrophils, 100000 cells were transferred to a 96-well V-bottom plate (Corning) for cell surface staining. Prior to staining, immune cells were incubated with 50 µL of FACS Wash Buffer containing 0.2 µg/mL of anti-CD16/CD32 (93) (BioLegend) for 30 minutes on ice to block Fc receptors followed by washing with FACS Wash Buffer and surface staining with the following antibodies from BioLegend: anti-CD11b-FITC (M1/70) and anti-Ly6G-APC (1A8) for 30 minutes on ice and washed twice with FACS Wash Buffer. Samples were then washed twice and fixed using FACS Fixing Buffer (1X PBS + 2% heat inactivated FBS + 2% Paraformaldehyde + 0.05% (w/v) sodium azide). Data was collected on a LSRFortessa (BD Biosciences) and subsequently analyzed using FlowJo software (FlowJo, LLC). Isolated bone marrow neutrophils were 85-90% pure.

Transposon Mutant Library Screen on BMM

An annotated transposon mutant library generated in USA300 strain JE2 was used for screening (BEI resources repository) by Francis Alonzo. Overnight cultures were prepared by inoculating polystyrene plates (Corning) containing sterile TSB with transposon mutants that had been spot plated and grown on solid agar in 12x8 arrays (20 plates, each containing a single 12x8 array of mutant strains) the night prior. Following overnight growth at 37°C, the mutant library was subcultured 1:100 by inoculating 2 µL of a well-mixed overnight culture into 198 µL fresh TSB in 96-well polystyrene plates (Corning). The cultures were allowed to grow for 9 hours (OD600 =

1.2) at 37°C with shaking at 200 rpm. After 9 hours, the OD600 of the strains was measured using an Envision 2103 plate reader (Perkin-Elmer) and the bacteria were pelleted by centrifugation at 3700 rpm for 15 minutes at 4°C. Cell free supernatant was collected and used immediately for screening or stored at -80°C. 65000 BMM derived from bone marrow of 6-8 week old male and female C57BL/6 mice were seeded into 96-well flat-bottom tissue culture treated plates (Corning) in BMM medium with 100 µg/mL Pen/Strep (Corning) and 50 µg/mL gentamicin (Amresco) the day before use. The following day, supernatants isolated from 9 hour cultures of *S. aureus* transposon mutants were thawed from storage at -80°C on ice followed by addition of 10 µL OD normalized supernatants to macrophages in 90 µL BMM medium and incubation at 37°C, 5% CO_2 for 24 hours. Macrophage supernatants were then removed and either used immediately in cytometric bead array or stored at -80°C for later analysis.

To measure the levels of cytokines and chemokines in the macrophage supernatants, a custom Cytometric Bead Array Flex set (BD Biosciences) was used according to manufacturer's specifications. Bead and supernatant mixtures were incubated for 1.5 hours at 25°C at 600 rpm using a Thermo Mixer C (Eppendorf) in a 96-well V-bottom plate (Corning). Samples were then washed using FACS Wash Buffer (1X PBS + 2% heat inactivated FBS + 0.05% (w/v) Sodium Azide), data collected on a LSRFortessa (BD Biosciences), and analyzed using FlowJo software (FlowJo, LLC) by gating on individual bead populations and calculating the geometric mean of fluorescence relative to protein standards. From the 1920 mutants in the library, 96 were initially selected for rescreening based upon an altered abundance that fell at least 1 standard deviation outside the average response induced by all 1920 mutants. These 96 mutants were

rescreened. Those mutants whose cytokine abundance remained 1 standard deviation above or below that of wild type induction levels were selected and are displayed in Table 5. ++ and -- in Table 5 refers to those mutants whose cytokine levels fell one standard deviation beyond wild type in the positive or negative direction respectively. For an NE264 mutant, MCP1 and KC levels were highly variable between biological replicates, therefore these cytokine changes were designated ++/ND in Table 5. All 21 mutants were rescreened in triplicate to confirm statistically significant enhancement or diminution of cytokine secretion relative to WT controls. After confirmation, the mutations were subsequently transduced into *S. aureus* USA300 strain LAC to confirm phenotypes before moving forward with prioritization of mutants for further studies. All transduced mutants were screened in triplicate and assessed for statistically significant differences in cytokine abundance compared to wildtype. This screen was conducted by Dr. Francis Alonzo.

S. aureus **Cell Free Supernatant Preparation**

S. aureus overnight cultures were prepared in triplicate by inoculating three wells with an individual bacterial colony in a 96-well round-bottom polystyrene plate containing RPMI+BCFA medium that was filtered sterilized using a 0.22 μM PES syringe filter (Corning) into a plastic conical tube. Following overnight growth at 37°C with shaking at 200 rpm, triplicate samples were subcultured by inoculating 3 μL of a well-mixed overnight culture into 147 μL RPMI+BCFA. The cultures were allowed to grow for 3, 5, or 9 hours at 37°C with shaking at 200 rpm. After 3, 5 or 9 hours, the OD600 of the strains were measured using an ELx800 microplate reader (BioTek) for OD normalization and the bacteria were pelleted by centrifugation at 3700 rpm for 15

minutes at 4°C. Cell free supernatant was collected and used immediately or stored at -80°C.

Purification of *S. aureus* Lipoyl-E2-PDH

Recombinant E2-PDH was expressed and purified from *E. coli lysY/I^q* containing a Δ*lipA::kan* mutation. The Δ*lipA::kan* mutant was generated using lambda red mutagenesis. In brief, a primer pair (LipAP1F/LipAP2R) was designed containing 50 bp of homology upstream and downstream to the *lipA* gene in *E. coli* and homology to the priming regions of pKD4. These primers were then used to PCR amplify the kanamycin resistance cassette encoded in pKD4. Lambda red mutagenesis was carried out by electroporating this amplicon into competent lysY/*I^q* expressing pKD46 and plating on LB containing either 10 or 25 μg/mL of Kan and Neo. Antibiotic resistant colonies were patched and subsequently assessed for replacement of the *lipA* gene with the pKD4 Kan resistance cassette using PCR with primer pair LipAF/LipAR. To generate a 6x-His-Tagged E2-PDH expression plasmid, WT genomic DNA was isolated and amplified with the primer pair 0995hisN/CF/0995hisNR to generate an E2-PDH encoding amplicon flanked by NdeI and BamHI restriction sites. This amplicon was ligated into a pET15b expression plasmid which was subsequently transformed into the Δ*lipA::kan lysY/I^q* strain. To confirm expression of the N terminal 6x Histidine tagged E2-PDH, protein production was assessed after induction with 1 mM IPTG at 37°C for 3 hours (Gold Biotechnology).

To purify E2-PDH, *lysY/I^q* Δ*lipA::kan E. coli* containing the pET15b-6x-His-E2-PDH plasmid was grown overnight in 30 mL LB (BD Biosciences) supplemented with 100 μg/mL ampicillin (Gold Biotechnology) at 37°C, 220 rpm. The following day, the

bacteria were subcultured 1:100 in 4 L fresh LB medium and grown for 20 hours at 37°C until reaching an OD600 of 0.25-0.3 followed by addition of IPTG (0.5 mM) (Gold Biotechnology) and incubation for 4 hours at 37°C at 220 rpm. Bacteria were pelleted by centrifugation at 8500 rpm for 10 minutes at 4°C followed by storage at -80°C. The following day, bacterial pellets were thawed at 37°C and resuspended in lysis buffer (25 mM imidazole (Alfa Aesar), 50 mM Tris-HCL, 300 mM NaCl (Amresco), pH 8) supplemented with 1 mM dithiothreitol (DTT) (Amresco) and 1 mM phenylmethane sulfonyl fluoride (PMSF) (Acròs Organics). Bacteria were lysed on ice using a sonicator (Branson) at 20-second intervals with a rate of 0.8 seconds per pulse and an output of 340 W for a total of 15 minutes. The bacterial debris was pelleted by centrifugation for 45 minutes at 11000 rpm, filtered through a 0.45 μm filter followed by incubation of the clarified supernatant for 1 hour with 1 mL nickel-NTA resin (Qiagen). The resin was washed with 150 mL 50 mM imidazole, 1 mM DTT, 50 mM Tris-HCL, 300 mM NaCl, pH 8 followed by elution in the same buffer containing 500 mM imidazole. The purified protein was dialyzed using snakeskin dialysis tubing (10 kDa MWCO, Thermo Scientific) into 100 mM imidazole + 50 mM Tris-HCL, 300 mM NaCl, pH 8.0 for 3 hours; 25 mM imidazole + 50 mM Tris-HCL, 300 mM NaCl, pH 8.0 overnight; and 50 mM Tris-HCL, 300 mM NaCl, pH 8 for an additional 3 hours. The concentration of the purified protein was measured using a bicinchoninic acid (BCA) kit (Thermo Scientific) and stored at -80°C.

To lipoylate purified 6x-His-E2-PDH 4x50 μl reactions were set up in 50 mM Tris-HCl, 300 mM NaCl, pH 8.0 supplemented with 6 mM ATP (Amresco), 1 mM DTT, 1 mM $MgCl_2$ (Amresco), 1 μM recombinant purified lipoate protein ligase, 20 μM E2-PDH, and

2.4 mM lipoic acid. The reactions were incubated for 2 hours at 37°C shaking at 600 rpm. After incubation, the reaction mixtures were loaded onto a Superdex 100 Increase 3.2/300 Gel Filtration column and fractionated by size exclusion chromatography using an AKTA FPLC system (GE Healthcare) to purify lipoyl-E2-PDH in a final buffer containing 50 mM Tris-HCl, 300 mM NaCl, pH 8.0. Protein purity and lipoylation were confirmed by sodium dodecyl sulfate polyacrylamide gel electrophoresis (SDS-PAGE) and Coomassie staining with GelCode Blue stain reagent (Thermo Scientific), or via immunoblot with anti-lipoic acid antibody as described in detail below. The methods for purification and lipoylation of E2-PDH were devised by Irina Laczkovich.

Purification of *S. aureus* Lipoprotein SitC

Recombinant SitC was expressed and purified from *S. aureus* strain RN4220. To generate a plasmid capable of expressing SitC harboring a C-terminal 6x-His tag we first amplified the *S. aureus sarA* promoter (P_{sarA}) linked to the ribosome binding site of the *S. aureus* superoxide dismutase (sod_{Rbs}) using primer pair SitC1/SitC2 and the plasmid pOS1-P_{sarA}-sod_{Rbs}-*sGFP* as template. We then amplified the *sitC* from *S. aureus* LAC gDNA using primer pair SitC3/SitC4. SitC4 contains coding sequence for a 6x-His tag embedded in the primer. The resulting amplicons from these PCRs were used in a SOEing PCR reaction to generate a single amplicon harboring P_{sarA}-sod_{Rbs}*SitC-6xHis* flanked by restriction endonuclease cut sites Pst1 and Sal1. The P_{sarA}-sod_{Rbs}*SitC-6xHis* was digested, ligated into the pOS1 plasmid, and transformed into DH5α *E. coli*. The pOS1- P_{sarA}-sod_{Rbs}*SitC-6xHis* plasmid, was then purified from *E. coli* and electroporated into RN4220.

To purify SitC, *S. aureus* RN4220 containing the pOS1- P_{sarA}-sod_{Rbs}*SitC-6xHis* plasmid was grown overnight at 37°C, 220 rpm in TSB supplemented with 10 µg of chloramphenicol (Amresco). The following day, the bacteria were subcultured 1:100 into 2 liters of fresh TSB medium (Criterion) supplemented with 10 µg of chloramphenicol (Amresco) and grown for 8 hours at 37°C. Bacteria were pelleted by centrifugation at 8500 rpm for 10 minutes at 4°C and then stored at -80°C overnight. Bacteria pellets were thawed on ice and resuspended in lysis buffer (20mM Tris-HCL (Alfa Aesar), 50mM NaCl (Amresco), pH 8.0). The resuspended cells were treated with 200 µl lysostaphin (Ambi Products, NY) (2mg/mL in 20mM sodium acetate pH 4.5) and incubated at 37°C for 1 hour. The cells were supplemented with 2 mM phenylmethane sulfonyl fluoride (PMSF) and lysed on ice via sonication (Branson) at 20-second intervals with a rate of 0.8 seconds per pulse and an output of 340W for a total of 30 minutes. The bacterial debris was pelleted by centrifugation for 1 hour at 11000 rpm and cell-free supernatants were collected followed by isolation of membranes by ultracentrifugation at 39000 rpm for 1 hour. Membrane pellets were solubilized in extraction buffer (20mM Tris-HCl, 50mM NaCl, 2% TritonX-100 (Amresco), pH 8.0) for 18 hours at 4°C. 1mL of Nickel-NTA resin (Qiagen) was equilibrated in the same extraction buffer for 18 hours at 4°C. The following day, the solubilized membrane pellets were centrifuged at 11000 rpm for 1 hour to remove any insoluble debris, filtered through a 0.45 µM syringe filter, and incubated with Nickel-NTA resin for 1 hour at room temperature. The resin was washed four times with wash buffer (20mM Tris-HCl, 50mM NaCl, 0.25% TritonX-100, 40mM imidazole (Amresco)) prior to elution in the same buffer containing 400 mM imidazole. The purified protein was dialyzed using snakeskin

dialysis tubing (10kDa MWCO, Thermo Scientific) into 100mM imidazole, 20mM Tris-HCl, 50mM NaCl ,0.25% TritonX-100 pH 8.0 3 hours at 4°C; 25mM imidazole, 20mM Tris-HCl, 50mM NaCl, 0.25% TritonX-100 pH 8.0 3 hours at 4°C; 20mM Tris-HCl, 50mM NaCl 0.25% TritonX-100 pH 8.0 overnight at 4°C. The concentration of the purified SitC was measured using a bicinchoninic acid (BCA) kit (Thermo Scientific) and determined to be 2mg/mL. The purified protein was stored at -80°C until use where it was diluted 20,000-fold before addition to cells so that the final TritonX-100 concentration was 0.00001% with no adverse effects on mammalian cells. Protein purity was confirmed by SDS-PAGE and Coomassie staining. Purification of SitC was performed by Xi Chen.

Exoprotein Isolation and Immunoblotting

To isolate *S. aureus* exoproteins, strains were first grown overnight in 5 mL TSB or RPMI+BCFA in conical tubes. The following morning the bacteria were subcultured 1:100 into conical tubes containing 5 mL fresh TSB or RPMI+BCFA and allowed to grow for 9 hours at 37°C with shaking at 200 rpm. After 9 hours, the OD600 was measured using a Genesys 10S UV-Vis spectrophotometer (Thermo Scientific). The cultures were pelleted by centrifugation at 4200 rpm at 4°C for 15 minutes. After pelleting the bacteria, 1.3 mL cell free supernatant was removed followed by the addition of trichloroacetic acid (TCA) (Alfa Aesar) to 10% final volume and subsequent incubation at 4°C overnight. The following day, samples were centrifuged at 13000 rpm at 4°C for 15 minutes and 1 mL of 100% EtOH was added followed by incubation at 4°C for 30 minutes. The precipitated proteins were centrifuged at 13000 rpm at 4°C for 15 minutes and EtOH was removed, followed by an additional centrifugation at 15000 rpm for 2 minutes at room temperature and removal of any excess ethanol. The pellets were then

left to air dry for 1 hour, followed by resuspension in 30 µL of TCA-SDS buffer (2X SDS buffer + β-mercaptoethanol diluted 1:1 with 0.5M Tris-HCl buffer (pH 8.0) + 4% SDS) and boiling for 10 minutes at 100°C. Samples were normalized to the highest OD600 and separated by SDS-PAGE in 10% or 12% polyacrylamide gels followed by Coomassie staining with GelCode Blue stain reagent (Thermo Scientific).

For immunoblotting, strains were first grown overnight in RPMI+BCFA. The following morning, overnights were subcultured 1:100 in 50 mL flasks containing 5 mL of RPMI+BCFA with reduced branched chain fatty acid precursors (1.123 mM isobutyric acid, 1.0 mM 2-methylbutyric acid, 1.0 mM isovaleric acid and 1.0 mM Na acetate) to reduce background on immunoblots. After 9 hours, the OD600 was measured and bacteria from 4 mL culture volume were pelleted by centrifugation at 4200 rpm at 4°C for 15 minutes. 1.3 mL cell free supernatant was removed followed by the addition of 10% TCA and isolation of secreted proteins as described above. To detect lipoyl proteins in the supernatant, samples were loaded based on OD normalization to account for minor differences in final optical density, resolved on 10% or 8% SDS-PAGE gels, followed by transfer to 0.2 µm PVDF membrane (EMD Millipore) at 200V for 1.5 hours in a Quadra Mini-Vertical PAGE/Blotting System (CBS Scientific). Membranes were then incubated overnight in PBST (PBS + 0.1% Tween-20) with 5% Bovine Serum Albumin (BSA) (Amresco) or with 5% BSA in TBST (Tris-buffered saline + 1% Tween-20) at 4°C overnight. The following day, membranes were blocked with 0.9 mg/mL human IgG (Sigma) for 1 hour to mitigate nonspecific binding to *S. aureus* antibody binding proteins. Membranes were washed three times in PBST or TBST for 15 minutes each followed by addition of a 1:5,000 dilution of rabbit anti-lipoic acid antibody (EMD

Millipore) in 10 mL of PBST + 5% BSA or TBST + 5% BSA. After 1 hour, membranes were washed three times with PBST or TBST for 15 minutes each, incubated with a 1:400 dilution of goat anti-rabbit IgG (H+L) HRP conjugate (Thermo Scientific) in 10mL of PBST + 5% BSA for 1 hour or 1:5000 goat anti-rabbit IgG (H+L) Alkaline Phosphatase (Thermo Scientific) in 10mL of TBST + 5% BSA secondary antibodies depending on the detection method, followed by an additional three 15 minute washes in PBST or TBST. Immunoblots were visualized using a FluorChemE System (Protein Simple) or exposed to film (Dot Scientific), and developed using an Alphatek Ax390 SE autoprocessor using Pierce ECL Western Blotting Substrate (Thermo Scientific) or after addition of 35 µL of a 50 mg/mL stock of 5-bromo-4-chloro-3-indoyl phosphate (Amresco) and 66 µL of a 50mg/mL stock of nitro blue tetrazolium (Amresco) to 10mL of 100 mM Tris pH 9.5 + 100 mM NaCl + 5 mM $MgCl_2$ (AP Buffer) to membranes followed by incubation for 1-2 minutes.

Isolation of Surface Proteins

To isolate proteins on the surface of *S. aureus*, 5 mL cultures of strains were grown overnight in RPMI+BCFA. The following morning, the OD600 of the cultures were measured and then pelleted by centrifugation at 4200 rpm at 4°C for 15 minutes. The supernatant was decanted, and the cell pellets were resuspended in 200 µL of a 125 mM Tris-HCL (pH 7.0) + 2% SDS solution. Samples were transferred to 1.5 mL microcentrifuge tubes, and boiled for 3 minutes at 95°C. After boiling, samples were spun at 10,000 g for 10 minutes. 180 µL of supernatant containing surface proteins was collected and boiled at 100°C for 10 minutes in 6X SDS sample buffer (30% (v/v) glycerol (Amresco) + 0.5M Tris (Amresco) + 10% (w/v) SDS (Amresco) + 5% (v/v) β-

mercaptoethanol + 0.012% (w/v) bromophenol blue (Amresco)) followed by storage at -20°C or immediate use in SDS-PAGE. Samples were loaded based on OD normalization to account for minor differences in final optical density and loaded onto 12% SDS-PAGE gels followed either by Coomassie staining with GelCode Blue stain reagent or transfer to 0.2 µm PVDF membrane at 200V for 1 hour. Membranes were then blocked overnight with 5% BSA in TBST (Tris-buffered saline + 1% Tween-20) at 4°C. Immunoblotting was conducted as described above using 0.9 mg/mL of human IgG for blocking, 1:3000 rabbit anti-lipoic acid primary antibody, and 1:5000 goat anti-rabbit IgG (H+L) Alkaline Phosphatase (Thermo Scientific) secondary antibody. Immunoblot were then developed after addition of 35 µL of a 50 mg/mL stock of 5-bromo-4-chloro-3-indoyl phosphate (Amresco) and 66 µL of a 50mg/mL stock of nitro blue tetrazolium (Amresco) to 10mL of 100 mM Tris pH 9.5 + 100 mM NaCl + 5 mM $MgCl_2$ (AP Buffer) to membranes followed by incubation for 1-2 minutes.

Quantification of Lipoyl-E2-PDH

To quantify the amount of lipoyl E2-PDH released by *S. aureus*, WT *S. aureus* was first grown overnight in RPMI+BCFA. The following morning, overnights were subcultured 1:100 in 50 mL flasks containing 5 mL of RPMI+BCFA with reduced branched chain fatty acid precursors. After 9 hours, the bacteria were pelleted by centrifugation at 4200 rpm at 4°C for 15 minutes. 1.3 mL cell free supernatant was removed followed by the addition of 10% TCA and secreted proteins were isolated as described above. 2.5 µL of WT TCA precipitated supernatant was loaded onto a 10% SDS-PAGE gel and resolved with a titration of purified recombinant lipoyl-E2-PDH. After performing an immunoblot to detect lipoyl-E2-PDH as described above, the amount of

lipoyl E2-PDH was estimated based on the intensity of the bands and found to be present in the range of approximately 25-50 nM.

Immunoblotting for Cytosolic Lipoyl-Proteins

To assess cytosolic lipoyl-protein profiles, strains were grown overnight in RPMI+BCFA. The next day cultures were diluted 1:100 in 5 mL RPMI+BCFA and grown for 9 hours at 37°C with shaking at 200 rpm. After 9 hours, OD600 was measured and the strains were pelleted by centrifugation at 4200 rpm for 15 minutes at 4°C. The spent culture medium was aspirated and the bacterial pellets were resuspended in 250 µL of sterile 1X PBS. The bacterial suspensions were transferred into screw-cap microcentrifuge lysing tubes (Fisher Scientific) containing 250 µL of 0.1 mm glass cell disruption beads (Scientific Industries, Inc.) and lysed using a Fast Prep-24 5G (MP Biomedicals) bead disruption system at setting 5.0 for 20 seconds followed by a 5 minute incubation on ice and additional disruption at setting 4.5 for 20 seconds. Tubes were centrifuged at 13000 rpm for 15 minutes at 4°C to pellet debris and 100 µL of clarified lysates were boiled at 100°C for 10 minutes in 6X SDS sample buffer (30% (v/v) glycerol (Amresco) + 0.5M Tris (Amresco) + 10% (w/v) SDS (Amresco) + 5% (v/v) β-mercaptoethanol + 0.012% (w/v) bromophenol blue (Amresco)) followed by storage at -20°C or immediate use in SDS-PAGE. Samples were loaded based on OD normalization to account for minor differences in final optical density and loaded onto 12% SDS-PAGE gels followed either by Coomassie staining with GelCode Blue stain reagent (Thermo Scientific) or transfer to 0.2 µm PVDF membrane at 200V for 1 hour. Membranes were then blocked overnight with 5% BSA in PBST or with 5% BSA in TBST (Tris-buffered saline + 1% Tween-20) at 4°C. Immunoblotting was conducted as

described above using 0.9 mg/mL human IgG for blocking, 1:3000 rabbit anti-lipoic acid primary antibody, and either 1:200 goat anti-rabbit IgG (H+L) HRP conjugate or 1:5000 goat anti-rabbit IgG (H+L) Alkaline Phosphatase (Thermo Scientific) secondary antibodies depending on the detection method. Immunoblots were developed after addition of Pierce ECL Western Blotting Substrate, exposure to film (Dot Scientific), and developed using an Alphatek Ax390 SE autoprocessor, or after addition of 35 µL of a 50 mg/mL stock of 5-bromo-4-chloro-3-indoyl phosphate (Amresco) and 66 µL of a 50mg/mL stock of nitro blue tetrazolium (Amresco) to 10mL of 100 mM Tris pH 9.5 + 100 mM NaCl + 5 mM $MgCl_2$ (AP Buffer) to membranes followed by incubation for 1-2 minutes.

In vitro Macrophage Experiments

65000 macrophages were seeded into 96-well flat-bottom tissue culture treated plates (Corning) in 90 µL BMM medium supplemented with 100 µg/mL Pen/Strep and 50 µg/mL gentamicin (Amresco) the day before use. The following day, supernatants isolated from 9 hour cultures of *S. aureus* were thawed from storage at -80°C on ice and 10 µL was added to BMMs following OD normalization between strains to ensure equivalent content followed by incubation at 37°C, 5% CO_2 for 24 hours. Macrophage supernatants were then removed and either used immediately or stored at -80°C. In experiments using either purified recombinant E2-PDH or synthetic DKA and DK^LA (AnaSpec), proteins were pretreated with 20 µg/mL of Polymyxin B sulfate (Alfa Aesar) for 1-2 hours at 37°C to mitigate aberrant LPS activation. Treated protein samples were then added to the macrophages in triplicate along with the TLR agonists Pam2CSK4 (1 ng/mL) or Pam3CKS4 (3 ng/mL) (Invivogen) where indicated. In the experiments with

SitC, the recombinant lipoprotein was treated with polymyxin B sulfate as described and added to the macrophages at a concentration 0.1 ng/mL for measurement of CCL3 and CCL4 production and 1 ng/mL for measurement of IL-6 and TNF production. In the indicated experiments 250 ng/mL of *E. coli* serotype 0111:B4 lipopolysaccharide (Enzo Life Sciences) or 250 ng/mL of flagellin isolated from the Gram-negative bacterium *Salmonella enterica* serovar Typhimurium (InvivoGen) was added to cells in the absence or presence of with 3 mM α-lipoic acid (Sigma). All BMMs were activated for 24 hours at 37°C, 5% CO_2, followed by removal of macrophage supernatant and immediate use or storage at -80°C.

To measure the levels of cytokines and chemokines in the macrophage supernatants, a custom Cytometric Bead Array Flex set (BD Biosciences) was used according to manufacturer's specifications. Bead and supernatant mixtures were incubated for 1.5 hours at 25°C at 600 rpm using a Thermo Mixer C (Eppendorf) in a 96-well V-bottom plate (Corning). Samples were then washed using FACS Wash Buffer (1X PBS + 2% heat inactivated FBS + 0.05% (w/v) Sodium Azide), data collected on a LSRFortessa (BD Biosciences), and analyzed using FlowJo software (FlowJo, LLC) by gating on individual bead populations and calculating the geometric mean of fluorescence relative to protein standards.

To measure bacterial survival upon infection of activated macrophages, 65000 BMM were first seeded into 96-well flat-bottom plates in BMM-medium without antibiotic. The following day cells were treated with 10% *S. aureus* cell free supernatant and incubated for 16 hours to induce macrophage activation. The day after activation, overnight cultures of WT and Δ*lipA S. aureus* were normalized to an OD600 of 0.32-

0.33 ($1x10^8$ CFU/mL) in PBS, added to macrophages at a multiplicity of infection of 1, and spun for 7 minutes at 1500 rpm to synchronize the infection. Infections were carried out at 37°C, 5% CO_2 for 30 minutes, washed 3X with 1X PBS and incubated with gentamicin (50 µg/mL) at 37°C, 5% CO_2 for an additional 30 minutes. Cells were washed 3X with 1X PBS and placed in BMM medium without antibiotic. After an additional hour of incubation, saponin (0.1%) was added to the wells and incubated on ice for 30 minutes, followed by plating onto BCFA-containing tryptic soy agar plates to enumerate bacterial CFU.

Detection of Lipoyl-Peptide Binding

A competition enzyme-linked immunosorbent assay (ELISA) plate-based assay was used to assess if lipoyl-peptides bound to TLR1/2 heterodimers. A 96-well EIA/RIA plate (Corning, cat# 3591) was coated with 50 µL containing 5 µg/mL of recombinant human TLR1/Fc chimera (R&D systems) and 4 µg/mL of recombinant mouse TLR2/Fc chimera (R&D systems). The ELISA plate was covered in parafilm and stored at 4°C to coat the wells overnight. The next day, the ELISA plate was washed three times in 200 µL of 1X PBS + 0.05% Tween-20. After the final wash, wells were blocked in StartingBlock blocking buffer (Thermo Scientific) per manufacturers protocol. After blocking, the ELISA plate was washed three times in 200 µL of 1X PBS + 0.05% Tween-20. 100 µL of Pam3CSK4-biotin (Tocris Bioscience) was added to the wells in the presence of a serially diluted amount of synthetic DKA and DK^LA (AnaSpec) in 100 µL 1X PBS and incubated for 1 hour at 37°C 5% CO_2. After incubation, the ELISA plate was washed five times in 200 µL of 1X PBS + 0.05% Tween-20 followed by addition of HRP Streptavidin (1:5000) (BioLegend) in 100 µL StartingBlock blocking buffer and

incubation at room temperature for 1 hour. After incubation, the ELISA plate was washed seven-eight times in 200 µL of 1X PBS + 0.05% Tween-20 and 100 µL of 3,3',5,5'-tetramethylbenzidine liquid substrate (Sigma) was added to the wells for 30 minutes at room temperature, followed by addition of 2M sulfuric acid to stop the reaction. Color change was quantified by measuring the absorbance of the sample at 450 nm using an ELx800 microplate reader (BioTek).

NFκB Activation Assay

To measure the activation of the transcription factor NFκB, the RAW-Blue macrophage cell line harboring an NFκB inducible chromosomally integrated secreted embryonic alkaline phosphatase (SEAP) reporter construct (Invivogen) was grown to about 50-70% confluency in DMEM (Corning) + 10% heat inactivated FBS in tissue culture treated T75 flasks (Corning). Media was removed from the flask and the cells were washed with 2mL of 0.05% trypsin + 0.53 mM EDTA (Corning). 2mL of fresh 0.05% trypsin + 0.53 mM EDTA was added to the RAW cells for 5-10 minutes and cells were dissociated from the surface of the flasks by gentle agitation. Dissociated cells were then resuspended in DMEM + 10% heat inactivated FBS and centrifuged for 5 minutes at 1500 rpm. Cells were then counted and seeded into 96-well flat-bottom tissue culture treated plates (Corning) at 50,000 cells per well in 90 µL of DMEM + 10% heat inactivated FBS supplemented with 100 µg/mL Pen/Strep (Corning) and 50 µg/mL gentamicin (Amresco) the day before use. The following day, supernatants isolated from 9 hour cultures of *S. aureus* were thawed from storage at -80°C on ice and added to the RAW cells following OD normalization between strains to ensure equivalent loading followed by incubation at 37°C, 5% CO_2 for 24 hours. Treated RAW-Blue cell

supernatants were collected and subsequently heated at 68°C for 30 minutes to deactivate endogenous phosphatases. 50 µL of the deactivated RAW cell supernatants were mixed with an equal volume of 1-Step PNPP (Thermo Scientific) in a 96-well polystyrene plate. After 2-3 hours of incubation, color change was quantified by measuring the absorbance of the sample at 450 nm using an ELx800 microplate reader (BioTek).

Murine Infection Models

Single colonies of freshly struck out bacteria were inoculated in TSB with shaking at 37°C and grown overnight. The overnight culture was subcultured 1:100 in 15mL fresh TSB and incubated at 200 rpm at 37°C for 3 hours. Cultures were then centrifuged for 5 minutes at 4200 rpm at 4°C, and the resulting cell pellets were washed 3 times in 1X sterile PBS. Bacterial suspensions were then normalized to an OD600 of 1.1-1.2 (~1 x 10^9 CFU/mL) for intraperitoneal infection or to an OD600 of 0.32-0.33 (~1 x 10^8 CFU/mL) for intravenous infection. Five to eight week old female Swiss Webster mice (Envigo) were then injected intraperitoneally with 100 µL of PBS containing 1 x 10^8 CFU of *S. aureus.* For intravenous infection, five to eight week old female Swiss Webster mice were anesthetized with 2,2,2-tribromoethanol (Avertin) (250 mg/kg) (Sigma), via intraperitoneal injection followed by inoculation with 100 µL PBS containing 1 x 10^7 CFU of *S. aureus* directly into the bloodstream via retro-orbital sinus. After infection, the remaining bacterial suspensions were plated onto TSA plates to ensure accuracy of infection inoculums. Mice were monitored daily and after 16 or 72 hours for IP infection and 96 hours for IV infection, serum was collected via the facial vein and mice were immediately euthanized by CO2 narcosis followed by aseptic isolation of kidneys and

lavage samples. Lavage samples were isolated by flushing the peritoneal cavity with 7 mL of 1x sterile PBS. Kidneys were homogenized, and lavage fluid and kidney homogenates were serially diluted onto TSA plates followed by incubation at 37°C overnight to enumerate CFU.

To deplete mice of macrophages, dichloromethane bisphosphonate (clodronate) loaded into liposomes (Liposoma) was administered [1mL/100g (~150 µL/mouse)] by i.p. injection. After three days, bacteria were cultured as described above and normalized to an OD600 of 0.32-0.33 (~1 x 10^8 CFU/mL). Mice were injected i.p. with 100 µL of PBS containing 1 x 10^7 CFU of *S. aureus*. Mice were monitored until 16 hours or 72 hours post-infection followed by enumeration of bacterial loads from the lavage and kidneys as described above.

For *S. aureus* re-challenge models, six to eight week old male and female Swiss Webster mice were immunized by i.p. injection with 100 µL of PBS containing 1 x 10^8 CFU of WT or Δ*lipA S. aureus* or sterile PBS. 7- or 14-days after immunization, mice were anesthetized with 2,2,2-tribromoethanol (Avertin) (250 mg/kg) (Sigma), via i.p. injection followed by inoculation with 100 µL PBS containing 1 x 10^7 CFU of *S. aureus* directly into the bloodstream via retro-orbital sinus. Mice were monitored daily and then euthanized either 24, 72, 96, or 120 hours post infection. Kidneys or hearts were isolated and bacterial loads in the kidneys or the hearts was quantified as described above.

Flow Cytometry of Immune Cells

Assessment of immune cell recruitment to the peritoneal cavity was determined by performing a lavage of the peritoneal cavity of euthanized mice 16- or 72-hours post-

infection with 7 mL of 1X sterile PBS in a 10 mL sterile syringe with an 18-gauge needle. Isolated cells were pelleted by centrifugation at 1500 rpm at 4°C for 5 minutes, supernatant was decanted, and red blood cells were lysed with ACK lysing buffer (Lonza) by resuspending the pellet in 2 mL of lysing buffer and incubating for 2 minutes at room temperature. Cell lysis was stopped by adding 8 mL of 1X sterile PBS, mixing gently, and pelleting by centrifugation at 1500 rpm at 4°C for 5 minutes. Cells were then suspended in 1X sterile PBS and kept on ice while they were counted. 1-2 million cells were transferred to a 96-well V-bottom plate (Corning) for cell surface staining. Prior to staining, immune cells were incubated with 50 µL of FACS Wash Buffer containing 0.2 µg/mL of anti-CD16/CD32 (93) (BioLegend) for 30 minutes on ice to block Fc receptors followed by washing with FACS Wash Buffer and surface staining with the following antibodies from BioLegend: anti-CD11b-Pacific Blue (M1/70), anti-Ly6G-PE (1A8), anti-DX5-APC-Cy7 (DX5), anti-CD206-FITC (C068C2), anti-CD11c-Alexa700 (N418), anti-I-A/I-E-Alexa647 (M5/114.15.2), anti-F4/80-PE-Cy7 (BM8), anti-CCR5-biotin (HM-CCR5) for 30 minutes on ice and washed twice with FACS Wash Buffer. To stain for CCR5, streptavidin conjugated PerCP-Cy5.5 was added on ice for 30 minutes. Samples were then washed twice and fixed using FACS Fixing Buffer (1X PBS + 2% heat inactivated FBS + 2% Paraformaldehyde + 0.05% (w/v) sodium azide). Data was collected on a LSRFortessa (BD Biosciences) and subsequently analyzed using FlowJo software (FlowJo, LLC).

To assess the immune cells recruited to the kidneys in intravenously infected mice after 96 hours, immune cell suspensions were purified using a 40/80 Percoll (GE Healthcare) density gradient centrifugation. Kidneys were isolated and homogenized

using glass mortar and pestle homogenizers (Kontes Glass Co) in 5 mL of RPMI (Corning). Kidney homogenate was then transferred to a 50 mL conical tube and centrifuged at 1500 rpm, 4°C for 5 minutes. Supernatant was decanted and red blood cells were lysed with ACK lysing buffer (Lonza) by resuspending the pellet in 2 mL of lysis buffer and incubating for 2 minutes at room temperature. Cell lysis was stopped by adding 8 mL of RPMI (Corning), mixing gently, and pelleting by centrifugation at 1500 rpm, 4°C for 5 minutes. Cells were resuspended in 10 mL RPMI (Corning) and passed through a 70 μM nylon mesh cell strainer (Corning). A 100% Percoll solution was made by mixing 9 parts Percoll with 1 part 10X PBS (Corning), and then diluted to 80% or 40% in RPMI + 10% heat inactivated FBS. Cells were then centrifuged at 1500 rpm at 4°C for 5 minutes, resuspended in 5 mL of 40% RPMI Percoll solution, and overlaid carefully on top of 5 mL of the 80% RPMI Percoll solution. Percoll gradients were rested at room temperature for 10 minutes and then centrifuged for 20 minutes 2500 rpm at room temperature with no brake. The top layer of parenchymal cells was aspirated off, and the immune cells present at the 40%/80% Percoll interface were collected. The immune cells were then washed twice in RPMI + 10% heat inactivated FBS and stained for flow cytometry as described above.

Measurement of Macrophage Surface Marker Expression

To assess the levels of various surface markers on BMMs, 300000 BMMs were seeded into 24-well non-tissue culture treated plate (Corning) in 300 μL BMM medium supplemented with 100 μg/mL Pen/Strep and 50 μg/mL gentamicin (Amresco) the day before use. The following day, supernatants isolated from 9 hour cultures of *S. aureus* were thawed from storage at -80°C on ice and 30 μL supernatant was added to BMMs

following OD normalization between strains to ensure administration of equivalent content followed by incubation at 37°C, 5% CO_2 for 1, 2, 4, and 24 hours. In some instances 3mM α-lipoic acid (Sigma) was added to BMM for the same incubation times. Media was then removed from the BMMs and washed three times in 1 mL of sterile 1X PBS. After the last wash, 250 µL of sterile 1X PBS was added to the BMMs and incubated at 4°C for 30 minutes. Following incubation, cells were removed by manual pipetting and transferred to a 96-well V-bottom plate (Corning) for cell surface staining. Prior to staining, cells were incubated with 50 µL of sterile 1X PBS containing 0.2 µg/mL of anti-CD16/CD32 (93) (BioLegend) for 30 minutes on ice to block Fc receptors followed by washing with sterile 1X PBS and surface staining with the following antibodies from BioLegend: anti-CD11b-APC-Cy7 (M1/70), anti-F4/80-PE-Cy7 (BM8), anti-CD80- PerCP-Cy5.5 (16-10A1), anti-CD86-APC (GL-1), anti-TLR2-FITC (T2.5), and anti-TLR1-PE (TR23) (eBioscience). A fixable viability dye, eFluor 450, (eBioscience) was also included in the staining panel. Samples were incubated on ice for 30 minutes, washed twice with sterile 1X PBS, and fixed with FACS Fixing Buffer. Data was collected on a LSRFortessa (BD Biosciences) and subsequently analyzed using FlowJo software (FlowJo, LLC).

S. aureus Survival in F4/80$^+$ Sorted Cells

Five to eight week old female Swiss Webster mice were infected via the peritoneal route as described previously with WT and Δ*lipA S. aureus* or sterile 1X PBS. 72 hours post infection mice were euthanized and peritoneal cells were isolated by lavaging the peritoneal cavity with 7 mL of 1X sterile PBS in a 10 mL sterile syringe with an 18-gauge needle. Cells were then pelleted by centrifugation at 1500 rpm at 4°C for 5

minutes followed by decanting the supernatant and resuspending in 5 mL complete RPMI cell culture medium (Corning) (RPMI + 10% heat inactivated FBS) supplemented with 100 µg/mL Pen/Strep and 50 µg/mL gentamicin and incubated on ice for 30 minutes to 1 hour. After incubation, cells were washed 3X in complete RPMI medium without antibiotics and incubated for 30 minutes in the antibiotic free medium. Cells were then washed once and resuspended in FACS wash buffer without sodium azide for magnetic bead sorting. F4/80$^+$ cells were sorted from total peritoneal cells using BD Imag Cell Separation (BD Biosciences) after incubation with anti-CD16/CD32 (93) (BioLegend) and biotinylated anti-F4/80 antibody (BM8) (BioLegend). In brief, streptavidin-conjugated magnetic beads were added to cells and allowed to bind to a magnet for 8 minutes followed by removal of the unbound fraction. Bound beads were then resuspended in FACS wash buffer without sodium azide and allowed to re-bind to the magnet for 6 minutes. This washing step was repeated once more to ensure purity of the bound fraction. Sorted cells were stored in FACS wash buffer without sodium azide overnight at 4°C. The following day an overnight culture of WT LAC grown in TSB was washed 3 times in 5 mL sterile 1X PBS, normalized to an OD600 of ~0.32 (~1.0x10^8 CFU/mL), and opsonized by incubation with 10% mouse serum for 30 minutes at 37°C followed by washing 3 times in 1 mL sterile 1X PBS. The sorted F4/80$^+$ cells were pelleted by centrifugation at 1500 rpm at 4°C for 5 minutes, resuspended in fresh complete RPMI medium, and counted. The opsonized bacteria were then used to infect sorted F4/80$^+$ cells at a multiplicity of infection 1 or 0.1 for 30 minutes at 37°C in sterile 1.5 mL microcentrifuge tubes placed on a rotisserie. Following the 30-minute infection, samples were centrifuged at 1500 rpm at room temperature in a benchtop

centrifuge (Eppendorf) for 5 minutes and washed 3 times in sterile 1X PBS. Samples were then resuspended in 1 mL complete RPMI medium and placed at 37°C on a rotisserie. In certain experiments ROS production was blocked by addition of 2 μM diphenyleneiodonium (DPI; Sigma), mROS production was blocked by addition of 10 μM Necrox5 (Cayman Chemical), iNOS was blocked by the addition of 500 μM N6-(1-Iminoethyl)-lysine hydrochloride (L-NIL; Tocris), or vehicle controls were added to the culture medium. *S. aureus* CFU were enumerated hourly by removing 100 μl aliquots, lysing with 0.1% saponin (Sigma) for 20 minutes on ice, followed by serial diluting and plating the dilutions on TSA plates supplemented with 50 μg/mL of Kan and Neo.
For experiments in which NADPH oxidase activity was blocked the following modifications were performed. Prior to infection, F4/80$^+$ cells were treated with 50 μM gp91ds-tat (Anaspec) or vehicle control for 1 hour in RPMI serum free medium to allow for entry of the inhibitor into cells. Treated cells were then centrifuged at 1500 rpm at room temperature in a benchtop centrifuge for 5 minutes and washed 3 times in sterile 1X PBS. Washed cells were resuspended in complete RPMI medium containing opsonized bacteria at a MOI of 1 and allowed to infect for 30 minutes at 37°C under constant rotation. The remainder of the experiment was conducted as described above.

Assessment of ROS Production

Three days after i.p. infection with WT, Δ*lipA*, or Δ*lipA* + *lipA* strains, peritoneal cells were isolated by lavage of the peritoneal cavity followed by magnetic sorting of F4/80$^+$ macrophages as detailed above. To measure changes in the oxidative state of isolated peritoneal F4/80$^+$ macrophages (ROS production), 5x10^5 F4/80$^+$ cells were infected with WT *S. aureus* at a MOI of 0.1 for 30 minutes under constant rotation at

37°C. Cells were washed free of bacteria followed by incubation in medium containing 1.25 μM CellROX deep red (Thermo Fisher Scientific) for 1 hour under constant rotation at 37°C. Cells were then washed 3X with 200 μL of sterile 1X PBS. Fluorescence was measured using a LSRFortessa (BD Biosciences) and data were analyzed using FlowJo software (FlowJo, LLC). Fold changes in the geometric means of CellROX fluorescence were assessed in infected cells and compared to uninfected F4/80$^+$ cells.

Griess Test for NO$^\bullet$ Production

Three days after i.p. infection with WT, Δ*lipA*, or Δ*lipA* + *lipA* strains, peritoneal cells were isolated by lavage of the peritoneal cavity followed by magnetic sorting of F4/80$^+$ macrophages as described above. Immediately after sorting, isolated F4/80$^+$ macrophages were counted and 100,000 cells were plated in a 96 well plate (Corning) in 100 μL complete RPMI medium. Heat-killed WT *S. aureus* was prepared by incubating a PBS-washed overnight culture for 1hr at 60°C. Sterility of the heat-killed bacteria was confirmed by enumeration of CFU on a TSA plate. Sorted F4/80$^+$ macrophages were then stimulated with the heat-killed bacteria at a MOI of 10 or left unstimulated. After overnight incubation at 37°C in 5% CO_2, 50 μL of supernatant was removed and a Griess test was performed to measure nitrite, which is a breakdown product of nitric oxide. 50 μL of 1% sulfanilic acid (Sigma) in 5% phosphoric acid (Fischer Scientific) was added to the supernatant samples followed by incubation for 5 minutes followed by addition of 50 μL of 0.1% N-alpha-naphthyl-ehtylenediamine (Sigma) in sterile water and incubation for an additional 5 minutes. To quantify the amount of nitrite present in the cell culture medium 100mM sodium nitrate (Sigma) was diluted 1:1 and used to make a standard curve. After incubation, sample absorbance

was measured at OD550 using an ELx800 microplate reader (BioTek). Fold increase in nitrite (nitric oxide) levels of F4/80$^+$ macrophages was determined by comparing nitrite production in heat-killed *S. aureus* stimulated cells compared to non-stimulated cells isolated from the same original infection condition (WT, Δ*lipA*, or Δ*lipA* + *lipA*).

Quantification and Statistical Analysis

All experiments were repeated at least three independent times. Statistical analysis was conducted using Prism software (GraphPad) and the specific tests used are indicated in the figure legends. Statistical significance was defined as $P<0.05$. The number of animals per treatment group is indicated as "n" in the figure legends. For any data without the use of animal models, we assumed a Gaussian distribution and used 1-way ANOVA with Bonferonni-Sidak post-test for pair-wise comparison. For any data with the use of animal models, we assumed a non-Gaussian distribution and used non-parametric 1-way ANOVA (Kruskal-Wallis Test) with Dunn's post-test unless otherwise noted. For *S. aureus* ex vivo survival/growth assays with F4/80$^+$ sorted cells a 2-way ANOVA with Tukey's multiple comparison test was used.

CHAPTER THREE

EXPERIMENTAL RESULTS

Portions of this Chapter are Reprinted with Modifications from Grayczyk et al. 2017 (387)

Introduction

The innate immune system is a fast-acting initial line of defense to prevent infection. In order to withstand innate defenses, bacterial pathogens such as the Gram-positive bacterium *S. aureus*, produce a wide array of virulence factors that inhibit innate immune cell recruitment and antimicrobial activity, or directly target and kill phagocytic leukocytes thereby facilitating pathogenesis. As previously introduced, a large amount of work has been done to understand how *S. aureus* evades neutrophil responses. Comparatively less is known about avoidance of macrophage responses. Macrophages are professional phagocytic leukocytes that are central to antimicrobial innate defenses. Besides the pathogen killing capacity of macrophages, they also produce and secrete a variety of cytokines and chemokines that help to regulate both the innate and adaptive immune system. Though less efficient than dendritic cells, activated macrophages are capable of presenting antigens to engage with T cells and promote their activation. Given their potent antimicrobial activities and critical immune signaling functions, macrophages are a significant mediator of the immune response to infection that *S. aureus* must overcome in order to cause disease. A growing body of work has begun to uncover mechanisms used by *S. aureus* to evade macrophages.

Nevertheless, the repertoire of extracellular *S. aureus* virulence factors that disrupt macrophage functions remains understudied.

Dr. Francis Alonzo conducted a forward genetic screen to identify *S. aureus* secreted factors that perturb macrophage inflammatory responses. To determine if *S. aureus* releases extracellular factors that perturb macrophage activation, Dr. Alonzo devised a forward genetic screen using cell free supernatants derived from 1920 annotated transposon mutants of the epidemic *S. aureus* clone, USA300 (JE2) (386). Supernatants were added to murine bone marrow derived macrophages (BMM) followed by measuring pro-inflammatory cytokine production using multiplexed cytokine bead arrays as outlined in Figure 3. 21 mutants were identified that enhanced or reduced macrophage cytokine secretion, representing potential gene products that interact with macrophages (Table 5). In the screen, already known mechanisms that altered macrophage responses were identified, such as an insertion in the gene that encodes the lipoprotein signal peptidase (*lspA*), NE1757. Deletion of *lspA* led to reduced macrophage activation consistent with its role in processing lipoproteins – the bacterial PAMP recognized by TLR1/2 and TLR2/6 heterodimers – and therefore served as an internal validation of the screen (Figure 4) (388-390).

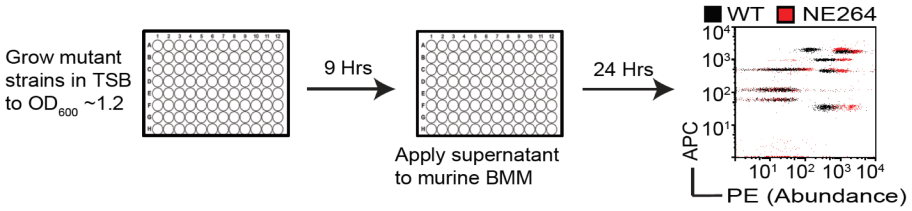

Figure 3. Transposon Mutant Screen. Design of screen used to identify macrophage immunomodulatory factors. Transposon mutants were grown to an OD600 of ~1.2, followed by addition of cell free supernatants to BMM for 24 hours. BMM supernatants were collected and assessed for cytokine and chemokine secretion using cytometric bead array (CBA).

Table 5. Identification of *S. aureus* Transposon Mutants that Enhance/Reduce Macrophage Activation

Mutant #	Accession #	Gene Name	Gene description	IL1β	IL6	KC	MCP1	CCL3	CCL4	TNF
NE95	SAUSA300_1989	*agrB*	accessory gene regulator protein B	++	--	--	--	--	--	ND
NE1262	SAUSA300_1984	Hypothetical	Hypothetical protein	++	--	--	--	--	--	ND
NE1908	SAUSA300_1911	--	ABC Transporter ATP-binding protein	++	--	--	--	--	--	ND
NE1714	SAUSA300_1590	--	GTP pyrophospokinase	ND	--	--	--	--	--	--
NE1757	SAUSA300_1089	*lspA*	lipoprotein signal peptidase	ND	--	--	--	--	--	--
NE1684	SAUSA300_1308	*arlR*	response regulator	++	++	++	++	ND	++	++
NE592	SAUSA300_2060	*atpA*	ATP synthase F1, α subunit	++	++	++	++	ND	++	++
NE481	SAUSA300_0645	--	DNA binding response regulator	ND	++	++	++	++	++	++
NE264	**SAUSA300_0829**	***lipA***	**lipoic acid synthetase**	**ND**	**++**	**++/ND**	**++/ND**	**++**	**++**	**++**
NE1296	SAUSA300_0690	*saeS*	sensor histidine kinase	ND	++	++	++	++	++	++
NE1622	SAUSA300_0691	*saeR*	response regulator	ND	++	++	++	++	++	++
NE1775	SAUSA300_0320	*geh*	triacylglycerol lipase	ND	++	++	++	++	++	++
NE1555	SAUSA300_1148	*codY*	transcriptional repressor	ND	ND	ND	ND	++	++	ND
NE1607	SAUSA300_2025	*rsbU*	sigma B regulation protein	ND	ND	ND	ND	++	++	ND
NE1833	SAUSA300_2026	--	PemK family protein	ND	ND	ND	ND	++	++	ND
NE1872	SAUSA300_2024	*rsbV*	anti-sigma-B factor, antagonist	ND	ND	ND	ND	++	++	ND
NE229	SAUSA300_1119	Hypothetical	Hypothetical protein	++	++	ND	++	ND	++	++
NE292	SAUSA300_0539	*ilvE*	branched chain amino acid amino-transferase	ND	ND	ND	++	++	++	ND
NE912	SAUSA300_0752	*clpP*	Clp protease	ND	ND	ND	++	ND	++	ND
NE1193	SAUSA300_0605	*sarA*	accessory regulator A	++	++	++	++	++	++	++
NE1909	SAUSA300_1720	Hypothetical	Hypothetical protein	ND	++	ND	ND	ND	++	++

*ND – No difference from WT; ++, Increased compared to WT; --, decreased compared to WT; ++/ND, variable response

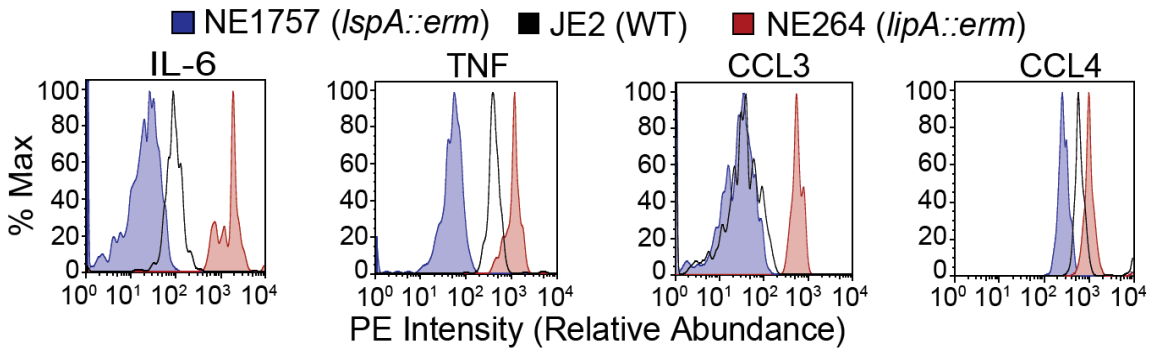

Figure 4. Transposon Mutants Induce Higher or Lower BMM Cytokine and Chemokine Production. Relative abundance of IL-6, TNF, CCL3, and CCL4 produced by macrophages after addition of cell free supernatants from JE2 (WT), NE1757 (*lspA::erm*), NE264 (*lipA::erm*).

Of the other mutants identified, Dr. Alonzo found the transposon mutant NE264 had a marked induction of IL-6, TNF, CCL3, and CCL4 relative to supernatant derived from the JE2 WT strain (Figure 4). Due to this increased macrophage response to the NE264 transposon mutant, this mutant was the selected for further assessment. NE264 contains an insertion in the gene that encodes the lipoic acid synthetase, LipA, an enzyme required for synthesis of lipoic acid (361, 373).

To confirm that disruption of *lipA* led to heightened macrophage activation, we used an in-frame deletion mutant (Δ*lipA*) and complementation strain that harbors a chromosomally integrated plasmid with *lipA* under the control of its predicted native promoter (Δ*lipA*+*lipA*). We assessed the growth dynamics of a Δ*lipA* mutant and found that a Δ*lipA* mutant grew identically to WT in tryptic soy broth (TSB), but not in Roswell Park Memorial Institute (RPMI) medium lacking free lipoic acid (Figure 5A and 5B). When free lipoic acid was supplemented into RPMI, a Δ*lipA* mutant grew identically to the WT strain bypassing the need for lipoic acid synthesis, as lipoic acid can be

acquired through the salvage pathway (Figure 2 and 5B) (373). The growth defect of a Δ*lipA* mutant was rescued in RPMI bypass medium containing branched chain carboxylic acids and sodium acetate (RPMI + BCFA) (Figure 5C). The complementation strain, Δ*lipA*+*lipA*, fully complemented the growth defect of a Δ*lipA* mutant and mimicked WT growth (Figure 5A-C). To test if cell free supernatant from the Δ*lipA* mutant leads to hyper-activation of BMMs like the transposon insertion mutant, we added Δ*lipA* cell free supernatant derived from cultures grown in RPMI + BCFA medium to BMMs. The supernatant enhanced the secretion of the pro-inflammatory cytokines and chemokines IL-6, TNF, CCL3, and CCL4 (Figure 6), verifying the results from the screen. Furthermore, the enhanced activation of BMMs by Δ*lipA* mutant supernatant was complemented using the Δ*lipA*+*lipA* strain. Together, these data imply that LipA is required for synthesis of lipoic acid and suppresses BMM activation.

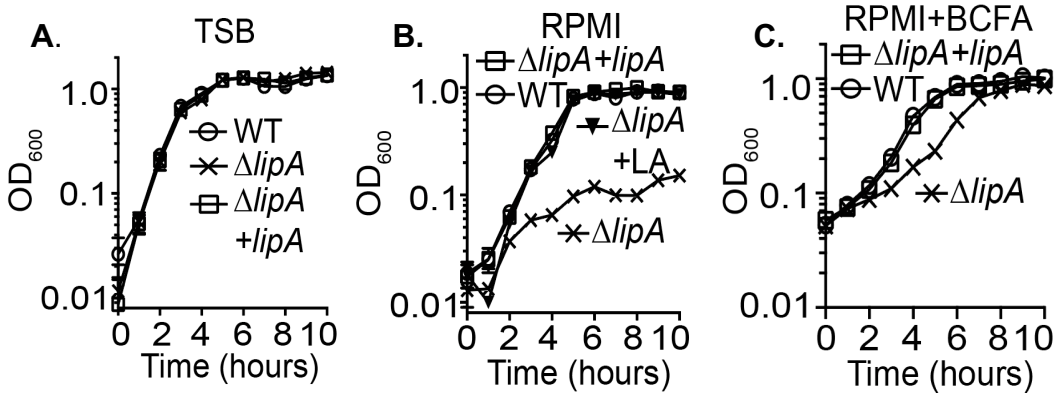

Figure 5. Growth Dynamics of a Δ*lipA* Mutant in Various Media. (A-C) Growth curves of WT, Δ*lipA*, or Δ*lipA*+*lipA* in TSB, RPMI medium with and without 25 nM lipoic acid (LA), or RPMI medium supplemented with branched chain fatty acid precursors and sodium acetate (RPMI+BCFA), which bypasses the requirement for lipoic acid.

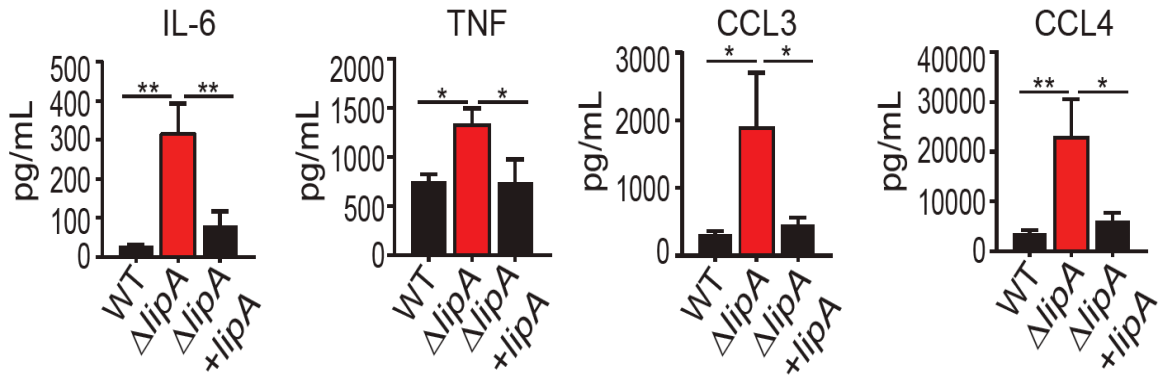

Figure 6. Lipoic Acid Synthesis is Required for Suppression of BMM Activation. IL-6, TNF, CCL3, and CCL4 production (pg/mL) by BMMs after addition of supernatant from WT*,* Δ*lipA*, or Δ*lipA*+*lipA* grown in RPMI+BCFA. Data shown are from one of at least three experiments conducted in triplicate. Means ± SD are shown (n = 3). *, *P*<0.05; **, *P*<0.01 by 1-way ANOVA with Bonferonni-Sidak post-test.

The purpose of this thesis is to characterize and identify the mechanism behind the hyper-inflammatory macrophage response elicited by a Δ*lipA* mutant. In addition, we sought to elucidate if this modulation of macrophage immune responses imparted by LipA activity influences the pathogenesis of *S. aureus* using murine infection models. In summary, this dissertation reports on a novel innate immune evasion mechanism of *S. aureus* conferred through the function of the lipoic acid synthetase and adds to the growing body of work highlighting the crucial roles for bacterial metabolism in evasion of host immunity.

LipA Restriction of Innate Immune Cell Activation Occurs through TLR2

Immune cells sense and respond to *S. aureus* through TLR2-based recognition of lipoproteins and subsequent signaling through the adaptor protein MyD88 (391). To determine if *lipA*-mediated immune suppression occurs via a TLR2-dependent pathway, we evaluated activation of WT, TLR2$^{-/-}$, TLR4$^{-/-}$ or MyD88$^{-/-}$ BMMs treated with

supernatant from WT, Δ*lipA,* or Δ*lipA*+*lipA*. Use of TLR2$^{-/-}$ and MyD88$^{-/-}$ BMMs abrogated the enhanced secretion of IL-6, TNF, CCL3, and CCL4 elicited by Δ*lipA* mutant supernatant (Figure 7). Signaling through TLR2 leads to NFκB activation and induction of pro-inflammatory cytokine and chemokine gene expression. We tested if macrophages treated with Δ*lipA* mutant supernatant have higher NFκB activation. The increased production of IL-6, TNF, CCL3, and CCL4 elicited by Δ*lipA* mutant supernatant correlated with increased NFκB dependent gene expression (Figure 8). These data suggest that LipA limits macrophage activation through a TLR2/MyD88 dependent pathway.

Neutrophils, like macrophages, express PRRs such as TLR2. To assess if other TLR2 expressing cells have enhanced activation in response to Δ*lipA* mutant supernatant, we tested the activation of neutrophils in response to Δ*lipA* mutant supernatant. We found that the enhanced activation caused by Δ*lipA* mutant supernatant is not limited to macrophages as murine neutrophils purified from the bone marrow also exhibited enhanced inflammatory chemokine secretion (Figure 9). These data indicate that other cells expressing TLR2-expressing cells respond better to supernatant derived from a Δ*lipA* mutant.

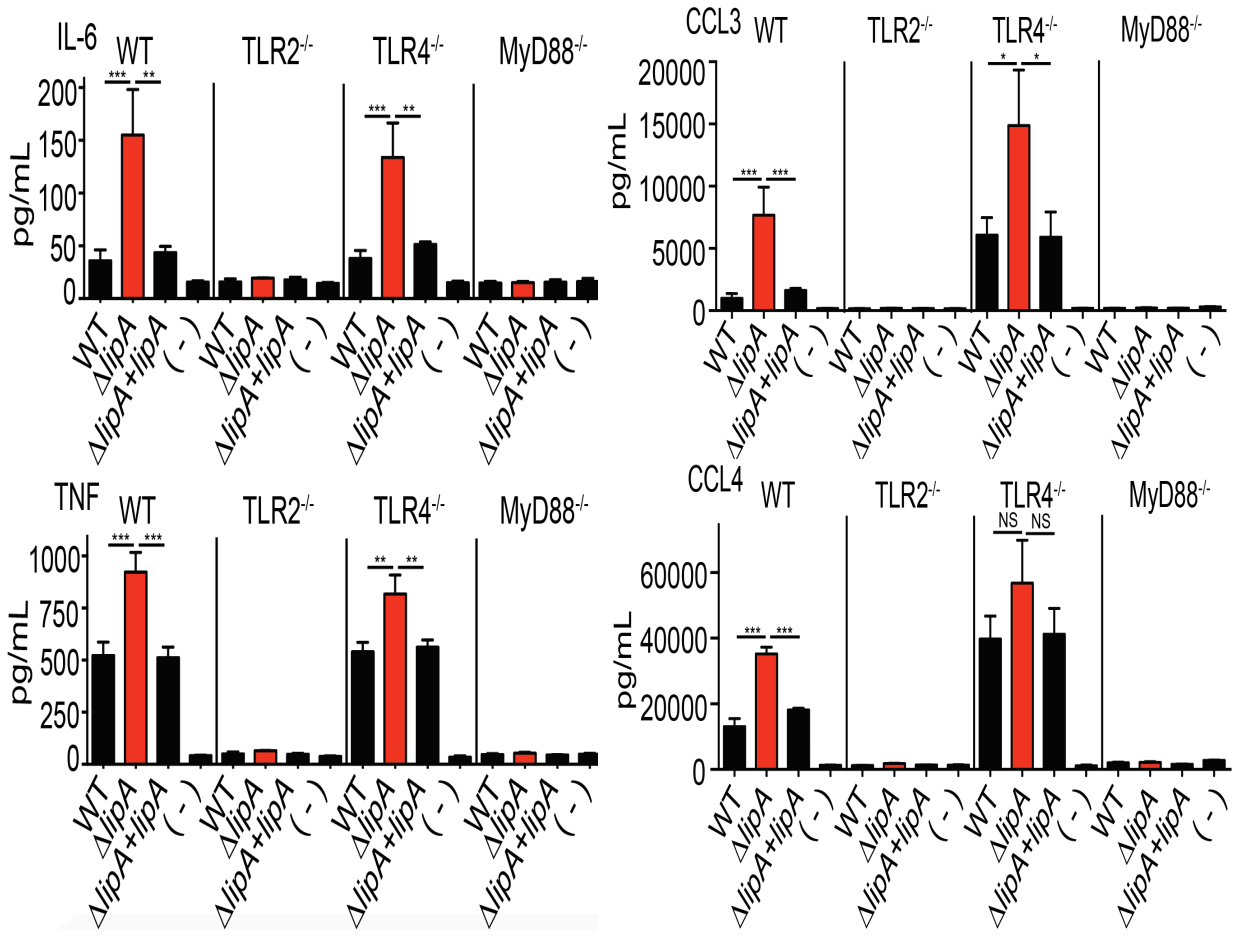

Figure 7. TLR2 and MyD88 are Required for Δ*lipA* Hyper-Activation of BMMs. Production of IL-6, TNF, CCL3, and CCL4 (pg/mL) after addition of cell-free supernatant from WT, Δ*lipA*, or Δ*lipA*+*lipA* to WT, TLR2$^{-/-}$, TLR4$^{-/-}$, or MyD88$^{-/-}$ BMMs. Data shown are from one of at least three experiments conducted in triplicate. (-), media alone. Means ± SD are shown (n=3). NS, not significant; *, P<0.05; **, P<0.01; ***, P<0.001, by 1-way ANOVA with Bonferonni-Sidak post-test.

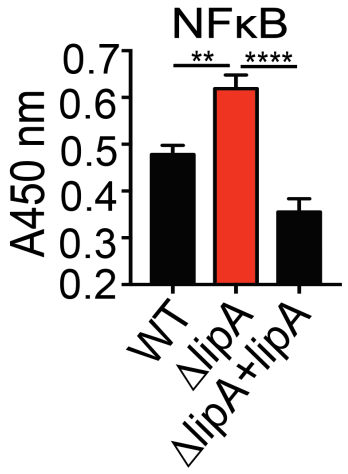

Figure 8. NFκB Activation is Induced by Δ*lipA* Mutant Supernatant. NFκB activation after treatment of RAW 264.7 cells, containing an NFκB-inducible secreted embryonic alkaline phosphatase reporter, with cell-free supernatant from WT, Δ*lipA*, or Δ*lipA*+*lipA*. Relative reporter activity (Absorbance 450 nm) from one of two experiments conducted in triplicate is shown. Means ± SD are shown. **, *P*<0.01; ****, *P*<0.0001, by 1-way ANOVA with Bonferonni-Sidak post-test.

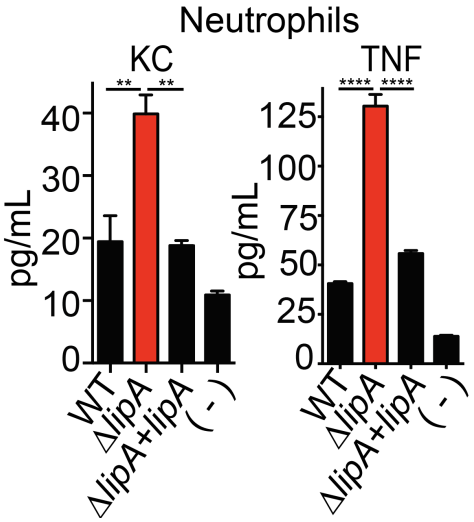

Figure 9. Neutrophils Secrete Greater Amounts of Cytokines in Response to Δ*lipA* Mutant Supernatant. KC and TNF production (pg/mL) of primary murine neutrophils after 24 hour stimulation with cell-free supernatant from the indicated strains. (-), media alone. Means ± SD are shown (n=3). **, *P*<0.01; ****, *P*<0.0001, by 1-way ANOVA with Bonferonni-Sidak post-test.

S. aureus Release of Lipoyl-E2-PDH Coincides with Macrophage Suppression

As cell free supernatants are used in all immune cell activation studies, we hypothesized that the secretome of *S. aureus* could be disrupted in a Δ*lipA* mutant leading to enhanced TLR2-dependent macrophage activation. However, we found that a Δ*lipA* mutant does not exhibit major alterations in its exoprotein profile when grown in either TSB or RPMI + BCFA compared to WT (Figure 10). Thus, the heightened activation of macrophages is not due to the hyper-secretion of TLR2 activating proteins as detected by Coomassie staining.

There are four cytosolic lipoylated proteins (E2-PDH, E2-OGDH, E2-BCODH, and GcvH) produced by *S. aureus* that rely on the lipoic acid synthase activity of LipA for lipoylation when there is no available exogenous lipoic acid (Figure 11A). We wondered if one of these four lipoylated proteins in the cytosol of WT *S. aureus* may be released into the supernatant. Indeed, we found that of the four cytosolic lipoylated proteins produced by *S. aureus*, one 72 kilodalton protein is released into the supernatant and contains a lipoyl moiety, but is absent in a Δ*lipA* mutant. This protein is similar in size to E2-PDH and immunoblot of exoproteins from a Δ*E2-pdh* mutant indicated that this released lipoyl-protein is E2-PDH (Figure 11B). In summary, these data suggest that WT *S. aureus* releases lipoyl-E2-PDH.

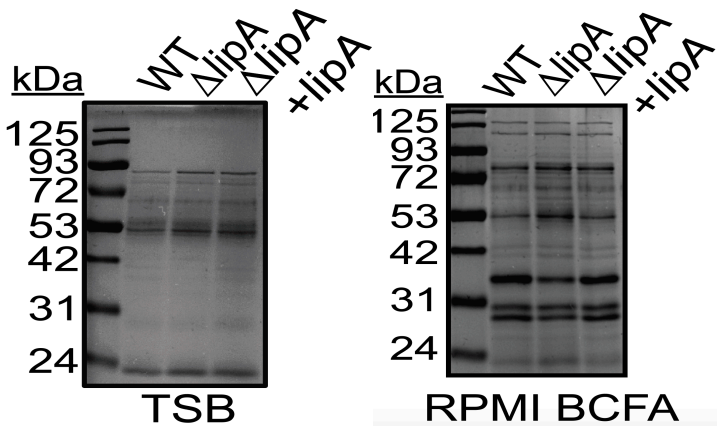

Figure 10. Exoprotein Profiles of WT, Δ*lipA*, and Δ*lipA* + *lipA* Strains. Coomassie stained SDS-PAGE gels of TCA precipitated exoproteins after 9 hours growth of the indicated strains in TSB or RPMI+BCFA.

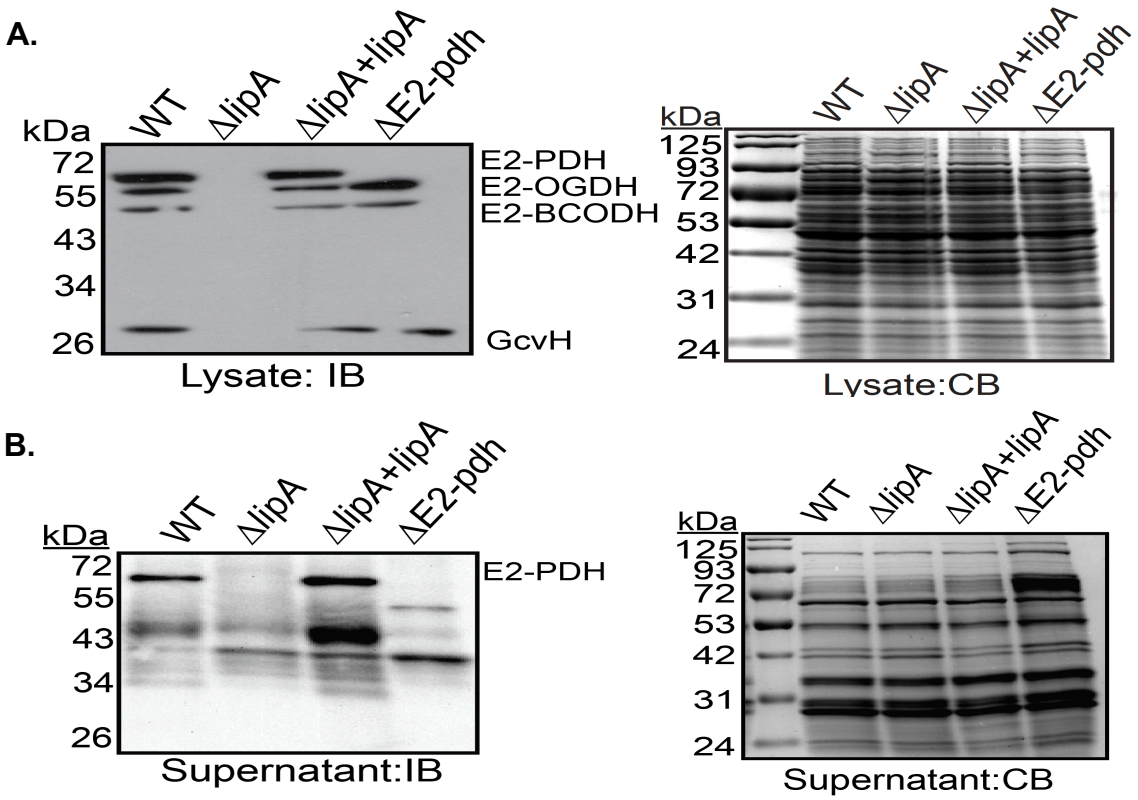

Figure 11. WT *S. aureus* Releases Lipoyl-E2-PDH into the Supernatant. Coomassie-blue stained SDS-PAGE gels (CB) or α-lipoic acid immunoblots (IB) of cell lysate (A) or TCA precipitated supernatant (B) proteins isolated after growing WT, Δ*lipA*, Δ*lipA*+*lipA*, and Δ*E2-pdh* in RPMI+BCFA for 9 hours. Other bands in supernatant IB appear to be non-specific.

Lipoic acid acquisition by *S. aureus* occurs through either synthesis or salvage ((373) and Figure 2). LipA, LipM, and LipL are required for synthesis, while LplA1 and LplA2 are involved in salvage. LipA and LipM contribute to the direct synthesis of the lipoyl moiety and LipL is required for its transfer to E2-PDH and E2-BCODH. We hypothesized that deletion of *lipM* or *lipL* would phenocopy the inflammatory response elicited by BMMs treated with Δ*lipA* supernatant. We found that all mutants lacking lipoyl-E2-PDH (Δ*lipA,* Δ*lipM,* and Δ*lipL*), but not mutants of the salvage pathway (Δ*lplA1* and Δ*lplA2*) elicited higher activation of BMMs (Figure 12A and B). A Δ*lipL* mutant enhanced macrophage activation even with lipoyl-E2-OGDH and lipoyl-GcvH present in the cytosol (Figure 12B). These data indicate that *de novo* lipoic acid synthesis is required to suppress BMM activation and specifically links the presence of lipoyl-E2-PDH in the supernatant to suppression of macrophage activation.

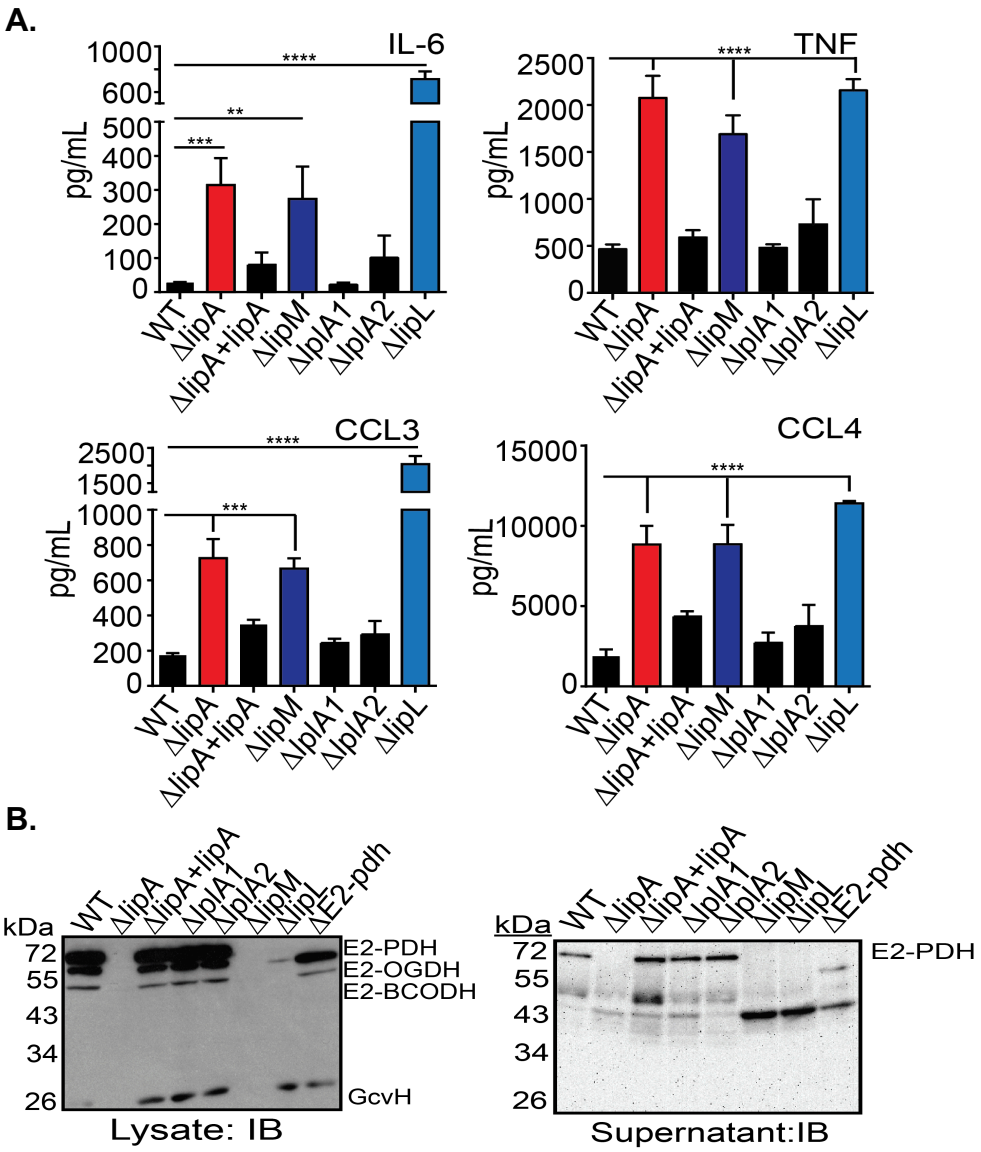

Figure 12. Lipoic Acid Synthesis and Release of Lipoyl-E2-PDH Correlate with Dampening of BMM Activation. (A) IL-6, TNF, CCL3, and CCL4 production (pg/mL) by BMMs after addition of supernatant from the indicated strains. Data shown are from one of at least three experiments conducted in triplicate. Means ± SD are shown (n = 3). **, *P*<0.01; ***, *P*<0.001; ****, *P*<0.0001 by 1-way ANOVA with Bonferonni-Sidak post-test. (B) Whole cell lysates or TCA precipitated exoproteins from the indicated *S. aureus* strains collected after growth in RPMI+BCFA followed by immunoblotting for lipoic acid-containing proteins. Other bands in supernatant IB appear to be non-specific.

Lipoyl-E2-PDH is Released During *S. aureus* Growth

The detection of cytosolic proteins in the extracellular environment, such as E2-PDH, has been observed for numerous bacteria even though they do not contain a secretion signal (357, 359, 392, 393).To test if the release of lipoyl-E2-PDH is an active process or due to cell lysis during bacterial growth, we assessed lipoyl-E2-PDH release in the supernatant over various timepoints. We were able to detect E2-PDH in supernatant as early as 5 hours and by 9 or 24 hours we saw the highest levels of released E2-PDH (Figure 13A). Since the release of lipoyl-E2-PDH occurs earlier than 9 hours during growth, we surmised that Δ*lipA* mutant supernatant harvested prior to 9 hours, which lacks lipoyl-E2-PDH, could enhance the activation of macrophages. Macrophages treated with supernatants from Δ*lipA* mutant supernatant after 3, 5, and 9 hours of culture in RPMI + BCFA enhanced macrophage activation (Figure 13B). Comparisons to purified recombinant lipoyl-E2-PDH suggest that *S. aureus* supernatant contains ~25-50 nM released lipoyl-E2-PDH (Figure 14). Thus, *S. aureus* releases nanomolar amounts of lipoyl-E2-PDH throughout its growth cycle.

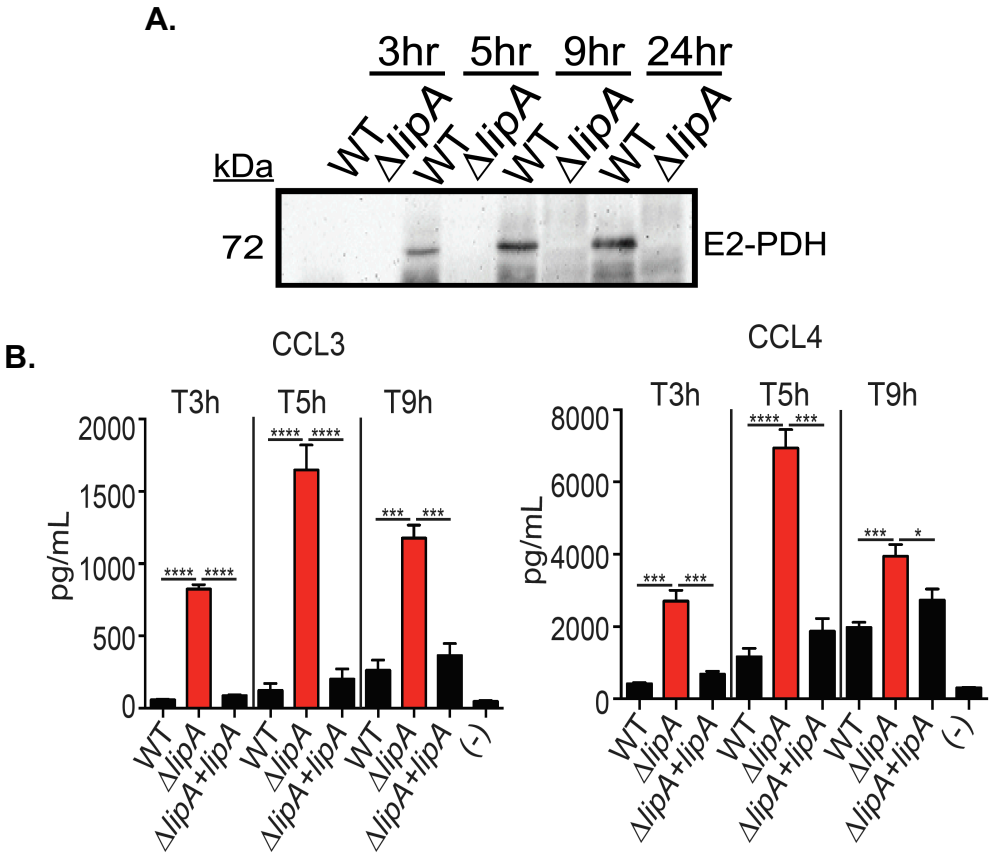

Figure 13. Release of Lipoyl-E2-PDH and Suppression of BMM Activation Occurs During Bacterial Growth. (A) Exoproteins were TCA precipitated from cell free supernatants of WT or Δ*lipA* S. aureus after 3, 5, 9, and 24 hours of growth in RPMI+BCFA followed by immunoblotting for lipoic acid-containing proteins. (B) CCL3 and CCL4 production (pg/mL) by BMMs after addition of T3h, T5h, or T9h supernatant from the indicated strains. Data shown are from one out of at least three experiments conducted in triplicate. (-), media alone. Means ± SD are shown (n=3). *, *P*<0.05; ***, *P*<0.001; ****, *P*<0.0001 by 1-way ANOVA with Bonferonni-Sidak post-test.

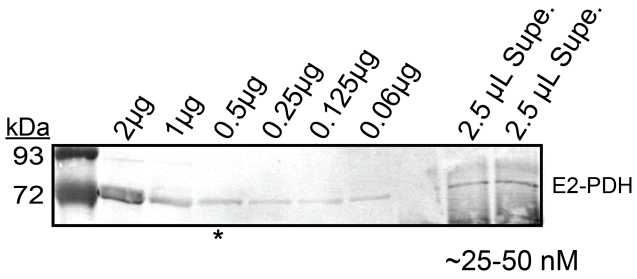

Figure 14. WT *S. aureus* Releases Nanomolar Amounts of Lipoyl-E2-PDH into the Supernatant. Immunoblot to quantify lipoyl-E2-PDH in *S. aureus* supernatant. To quantify the amount of lipoyl-E2-PDH released by *S. aureus* a titration of purified lipoyl-E2-PDH was compared to released lipoyl-E2-PDH in the supernatant.

E2-PDH and GcvH are Detectable on the Bacterial Surface

Extracellular detection of cytoplasmic proteins, though unusual, is not uncommon. A majority of these extracellular proteins are found to be expressed on the surface of bacteria. For example, E2-PDH has been detected on the surface of *L. monocytogenes* and *Mycoplasma pneumonia* (359, 391, 392).Therefore, we assessed if lipoyl-E2-PDH is also present on the surface of *S. aureus*. Visualization of surface extracted proteins show that E2-PDH and perhaps GcvH are present on the surface of WT *S. aureus* and its Δ*lipA* mutant (Figure 15). Furthermore, by immunoblot, we could see lipoyl-E2-PDH and lipoyl-GcvH in WT *S. aureus*, but not in a Δ*lipA* mutant (Figure 15). This is surprising, as we did not see lipoyl-GcvH released into the supernatant of WT *S. aureus* by our detection methods. No lipoyl-E2-PDH was present on the surface of a Δ*gcvH* mutant, as GcvH is necessary to shuttle lipoic acid to E2-PDH (373, 374). Additionally, surface expression of E2-PDH and GcvH were not dependent on the lipoyl moiety, as we still saw both E2-PDH and GcvH on the surface of a Δ*lipA* mutant (Figure 15). *L. monocytogenes* surface expression of E2-PDH is partially dependent on the secondary secretion system, SecA2 (359), whereas the autolysin Atl is required for the release of some cytosolic proteins in *S. aureus* (357). Using transposon mutants of *atl* and *secA2*, we found that SecA2 likely contributes to, while Atl may be necessary for the release of lipoyl-E2-PDH (Figure 16). All together, these data suggest lipoyl-E2-PDH is on the surface of *S. aureus* and potentially requires Atl-dependent lysis for release.

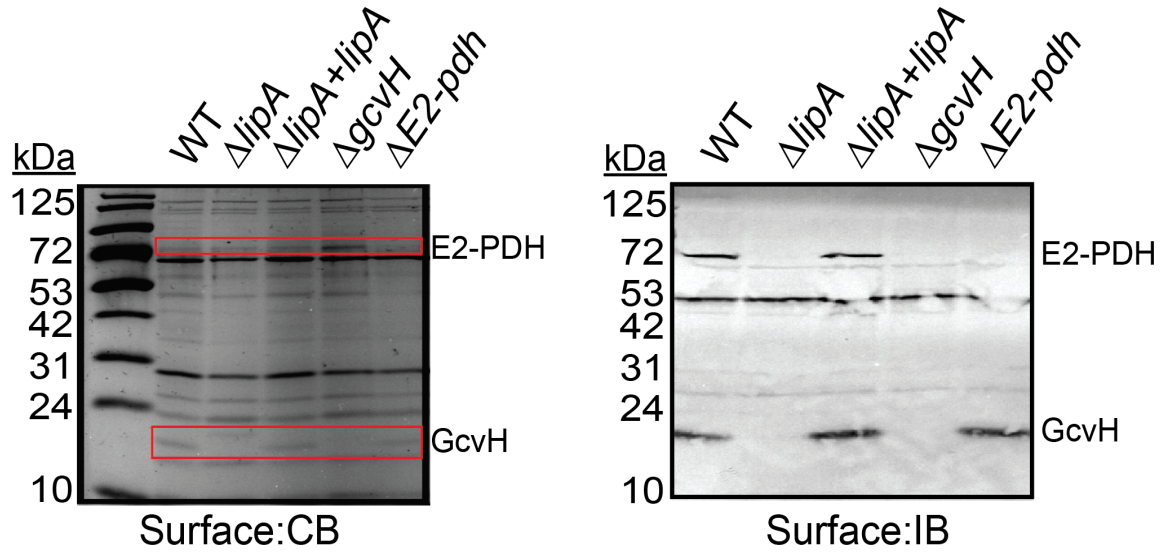

Figure 15. Surface Display of E2-PDH and GcvH. Coomassie-blue stained SDS-PAGE gels (CB) or α-lipoic acid immunoblots (IB) of surface proteins isolated after growing WT, Δ*lipA*, Δ*lipA+lipA*, Δ*gcvH*, and Δ*E2-pdh* in RPMI+BCFA. Boxed regions in CB represents E2-PDH and GcvH location. Dominant band in IB appears to be non-specific.

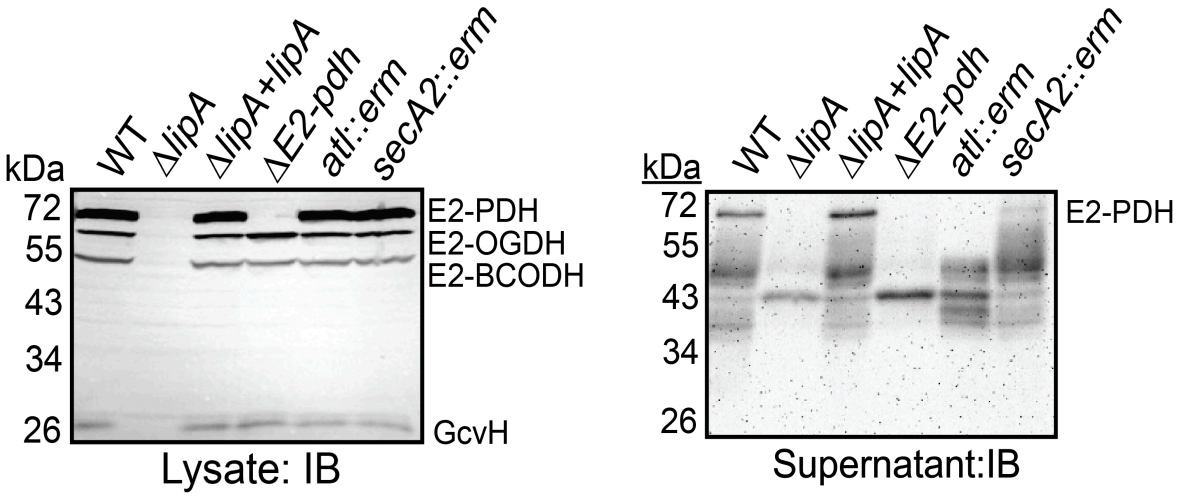

Figure 16. Release of Lipoyl-E2-PDH Likely Requires Atl and Potentially SecA2. Whole cell lysates or TCA precipitated exoproteins from the indicated *S. aureus* strains collected after growth in RPMI+BCFA followed by immunoblotting (IB) for lipoic acid-containing proteins. Other bands in supernatant IB appear to be non-specific.

Free Lipoic Acid Restricts the Activation of Macrophages

Free lipoic acid suppresses the respiratory burst of innate cells when used at high concentrations (394, 395). Therefore, we hypothesized that release of lipoyl-E2-PDH by *S. aureus* might confer immunosuppressive properties. We first determined if free lipoic acid suppresses BMM activation by *S. aureus* secreted factors. Supplementation of Δ*lipA* mutant supernatant with 3 mM free lipoic acid reduced BMM secretion of IL-6, TNF, CCL3, and CCL4 (Figure 17). 3 mM free lipoic acid also diminished the activation of BMMs by Pam2CSK4 and Pam3CSK4, synthetic diacylated or triacylated lipopeptides that induce TLR2/6 or TLR1/2 heterodimer signaling (Figures 18). As free lipoic acid could suppress TLR2-based activation of macrophages, we wondered if lipoic acid also impairs recognition of other surface TLRs, such as TLR4 and TLR5. Activation of BMMs with the TLR4 ligand lipopolysaccharide or the TLR5 ligand flagellin in the presence of 3 mM free lipoic acid reduced the activation of BMMs, as determined by lower cytokine secretion (Figure 19). These data indicate free lipoic acid suppresses TLR2-dependent and other TLR-based activation pathways of BMMs when applied at supraphysiologic concentrations.

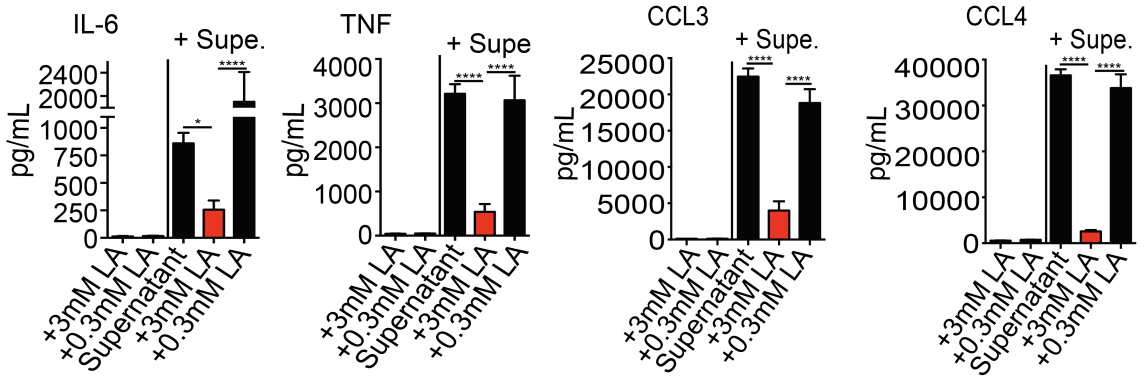

Figure 17. Free Lipoic Acid Diminishes BMM Activation by Δ*lipA* Mutant Supernatant IL-6, TNF, CCL3, and CCL4 production (pg/mL) after addition of Δ*lipA* supernatant to BMMs in the presence of free lipoic acid (LA) (3 mM or 0.3 mM). Data shown are from one of at least three experiments conducted in triplicate. Means ± SD are shown (n=3). *, *P*<0.05; ****, *P*<0.0001 by 1-way ANOVA with Bonferonni-Sidak post-test.

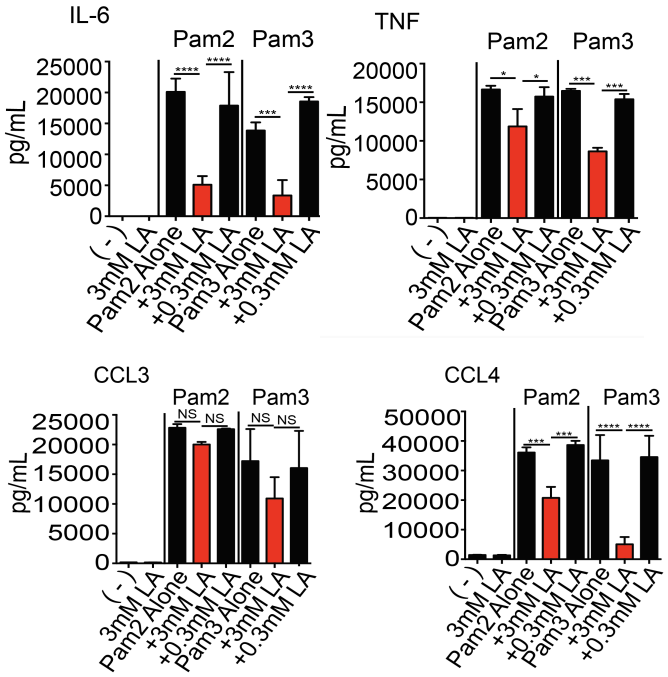

Figure 18. Free Lipoic Acid Restricts TLR2-Dependent BMM Activation. IL-6, TNF, CCL3, and CCL4 production (pg/mL) after addition of 3 ng/mL Pam2CKS4 (Pam2) and 30 ng/mL of Pam3CSK4 (Pam3) to BMMs in the presence of free lipoic acid (3 mM or 0.3 mM). (-), media alone. Data shown are from one of at least three experiments conducted in triplicate. Means ± SD are shown (n=3). NS, not significant; *, *P*<0.05; ***, *P*<0.001; ****, *P*<0.0001 by 1-way ANOVA with Bonferonni-Sidak post-test.

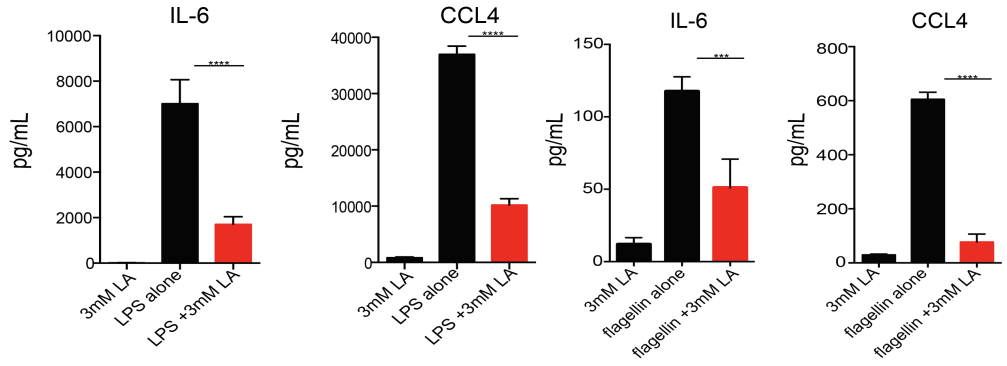

Figure 19. Free Lipoic Acid Blunts TLR4- and TLR5-Dependent BMM Activation. IL-6 and CCL4 production (pg/mL) after addition of 250 ng/mL lipopolysaccharide (LPS) and 250 ng/mL of flagellin to BMMs in the presence of 3mM free lipoic acid. Data shown are from one of at least three experiments conducted in triplicate. Means ± SD are shown (n=3). ***, $P<0.001$; ****, $P<0.0001$ by 1-way ANOVA with Bonferonni-Sidak post-test.

Lipoyl-E2-PDH Diminishes the TLR1/2 Activation of Macrophages

Since free lipoic acid suppresses macrophage activation, we wondered whether lipoylated proteins – the main form of lipoic acid in living systems – from *S. aureus* are sufficient to suppress BMM activation at physiologically meaningful concentrations. We tested if lipoyl-E2-PDH suppresses BMM activation by first purifying recombinant *S. aureus* lipoyl-E2-PDH and lipoylating it in vitro (purification and lipoylation technique devised by Irina Laczkovich) (Figure 20). Next, we activated BMMs with Pam2CSK4 and Pam3CSK4 in the presence of recombinant lipoyl-E2-PDH and monitored cytokine secretion. We found that 10 nM lipoyl-E2-PDH suppressed TLR1/2 activation, but not TLR2/6 activation (Figure 21). To test if the lipoyl moiety is necessary for the restriction of BMM activation we used a synthetic tripeptide containing a lipoyl-lysine residue, $DK^{L}A$, and found that it is sufficient to suppress TLR1/2 dependent macrophage activation at 10 nM concentration but not the unmodified tripeptide, DKA (Figure 22). $DK^{L}A$ also suppressed macrophage activation by SitC, a TLR1/2 activating triacylated

lipoprotein produced by *S. aureus* (160, 161) (Figures 23). These data indicate that lipoyl-E2-PDH is sufficient to suppress TLR1/2 activation of macrophages and that immune suppression is directly linked to the lipoyl modification.

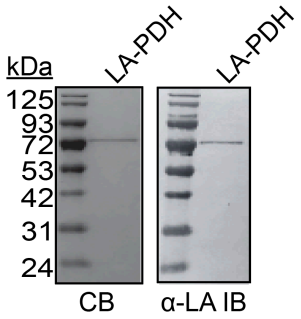

Figure 20. Purified Lipoyl-E2-PDH. S. aureus E2-PDH purified from E. coli. Coomassie-stained SDS-PAGE gel of 1 µg lipoyl-E2-PDH (CB) and lipoyl moiety detection by immunoblot with anti-lipoic acid antibody (α-LA IB).

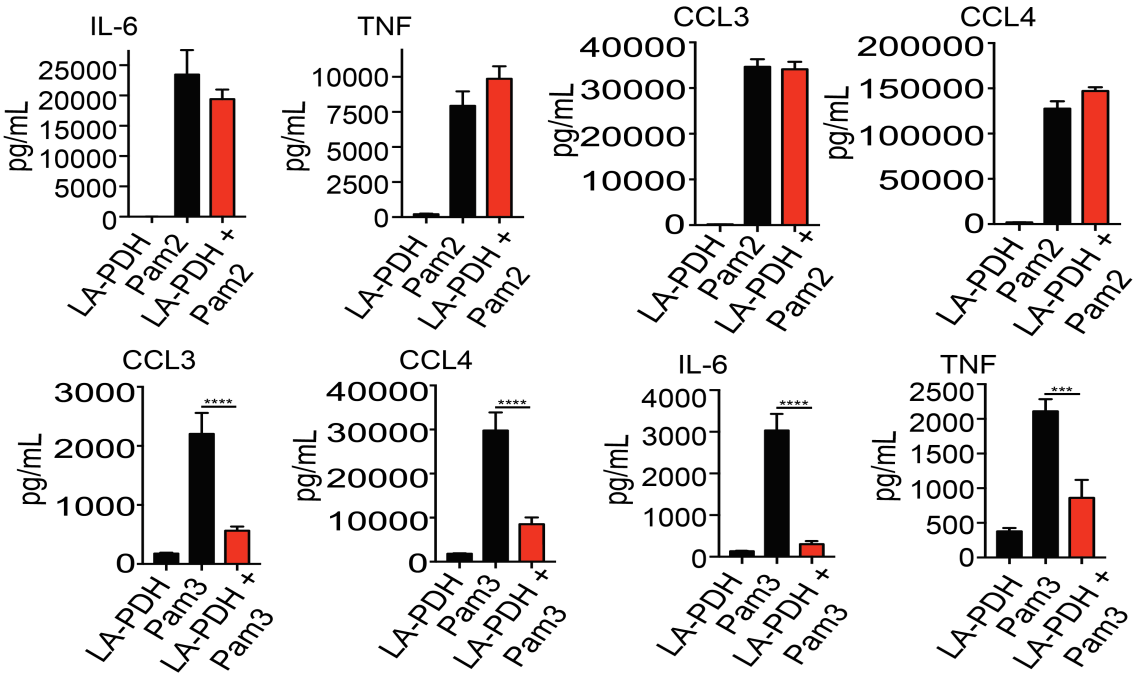

Figure 21. Purified Lipoyl-E2-PDH Dampens TLR1/2 Activation of BMMs. IL-6, TNF, CCL3, CCL4 production (pg/mL) after addition of 10 nM lipoyl-E2-PDH (LA-PDH) to BMMs in the presence of 1 ng/mL of Pam2 or 3 ng/mL of Pam3. Data shown are from one of at least three experiments conducted in triplicate. Means ± SD are shown (n=3). ***, *P*<0.001; ****, *P*<0.0001 by 1-way ANOVA with Bonferonni-Sidak post-test.

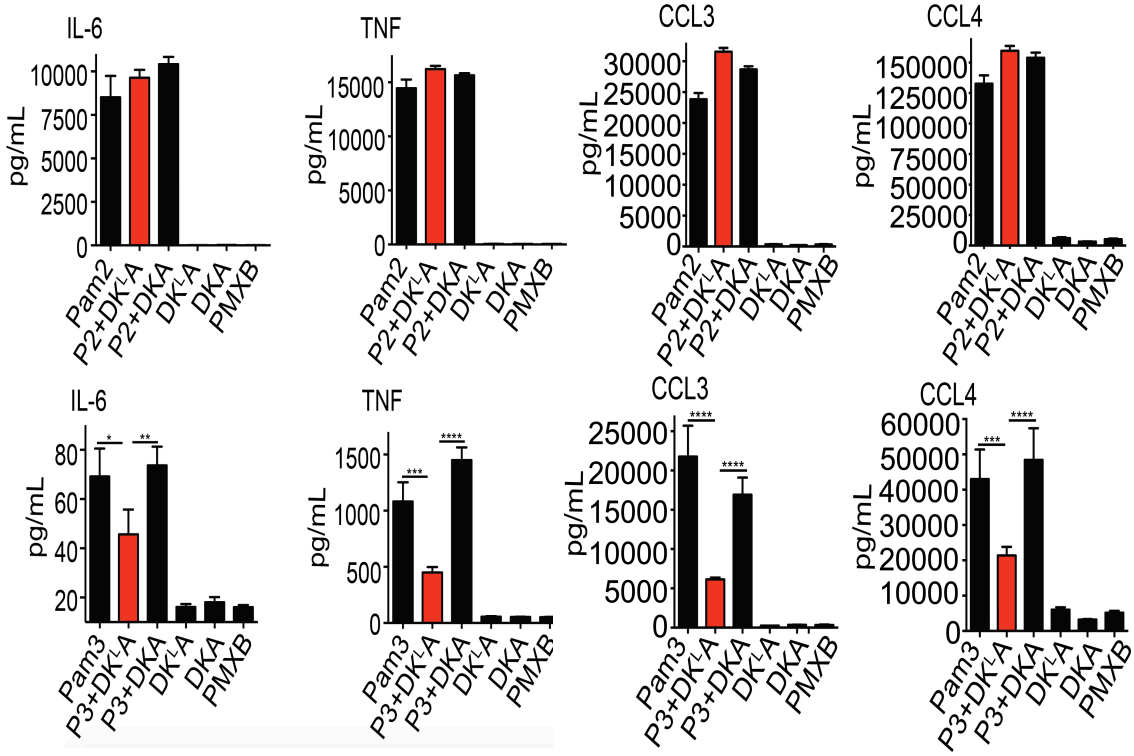

Figure 22. The Lipoyl Moiety is Necessary for Restriction of TLR1/2 Activation BMMs. IL-6, TNF, CCL3, and CCL4 production (pg/mL) after addition of 10 nM synthetic tripeptides $DK^{L}A$ and DKA to BMMs in the presence of 1 ng/mL of Pam2 or 3 ng/mL of Pam3. Data shown are from one of at least three experiments conducted in triplicate. Means ± SD are shown (n=3). *, $P<0.05$; **, $P<0.01$; ***, $P<0.001$; ****, $P<0.0001$ by 1-way ANOVA with Bonferonni-Sidak post-test.

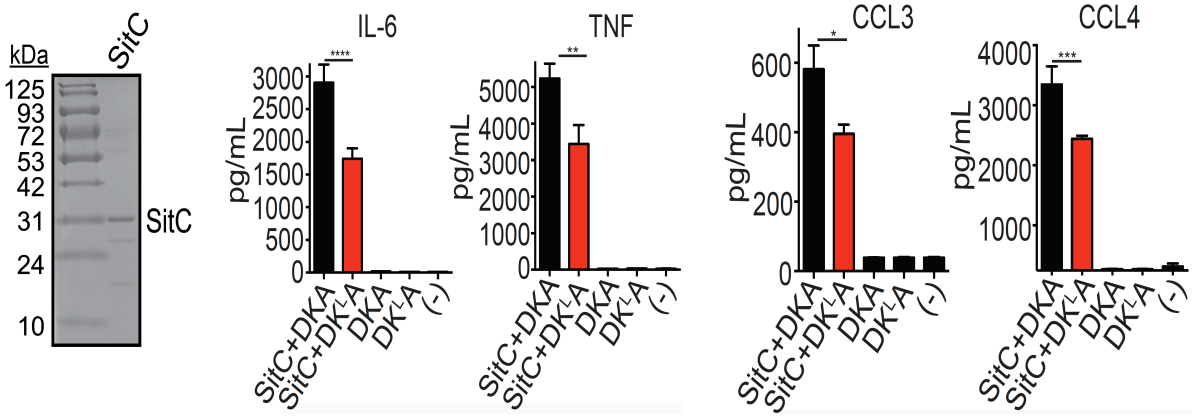

Figure 23. Lipoyl-Peptide DK^{L}A Dampens SitC Activation of BMMs. Coomassie-stained SDS-PAGE gel of 500 ng purified SitC. IL-6, TNF, CCL3, and CCL4 production (pg/mL) after addition of SitC (0.1 ng/ml for CCL3/CCL4 and 1.0 ng/ml for IL-6/TNF) to BMM in the presence of 10 nM synthetic tripeptides DK^{L}A and DKA. Data shown are from one of at least three experiments conducted in triplicate. Means ± SD are shown (n=3). *, *P*<0.05; **, *P*<0.01; ***, *P*<0.001; ****, *P*<0.0001 by 1-way ANOVA with Bonferonni-Sidak post-test.

Mechanism of TLR1/2 Restriction by Lipoyl-Protein

Restriction of BMMs by lipoyl-E2-PDH only occurs through TLR1/2 and not TLR2/6, suggesting a mechanism of suppression specific to TLR1 or TLR2. We hypothesized that free lipoic acid or lipoyl-peptides either stimulates changes in TLR1 or TLR2 surface display, or directly interferes with the interaction of natural ligands with TLR1/2 by competing for similar binding sites. We tested this idea by assessing the levels of TLR1 or TLR2 on the surface of BMMs treated with supernatant derived from WT or Δ*lipA S. aureus,* as well as in the presence of free lipoic acid given that lipoyl-proteins and free lipoic acid have different immunosuppressive functions. We found that there are no differences after treatment with supernatant from *S. aureus* that lack lipoyl proteins (Δ*lipA*) on the surface expression levels of TLR1 or TLR2 (Figure 24). Furthermore, we found that treatment of BMMs with free lipoic acid decreases the

amount of surface TLR2 on BMMs and not TLR1 (Figure 24). Next, we assessed if WT or Δ*lipA* supernatant or free lipoic acid could modulate the surface expression of other pro-inflammatory surface markers of BMMs such as CD80 and CD86. Again, there are no differences between surface CD80 or CD86 levels of BMMs treated with WT or Δ*lipA* supernatant. Interestingly, we found that free lipoic acid decreases the surface expression of CD86 but not CD80 relative to the media control condition (Figure 24). Like supernatant from *S. aureus*, free lipoic acid increased the surface levels of TLR1 and CD80 (Figure 24). In summary, these data suggest that supernatant from a Δ*lipA* mutant does not modulate the levels of TLR1, TLR2, CD80, or CD86. Moreover, these data demonstrate that free lipoic acid reduces TLR2 and CD86 on BMMs, highlighting the broad immunosuppressive functions of free lipoic acid.

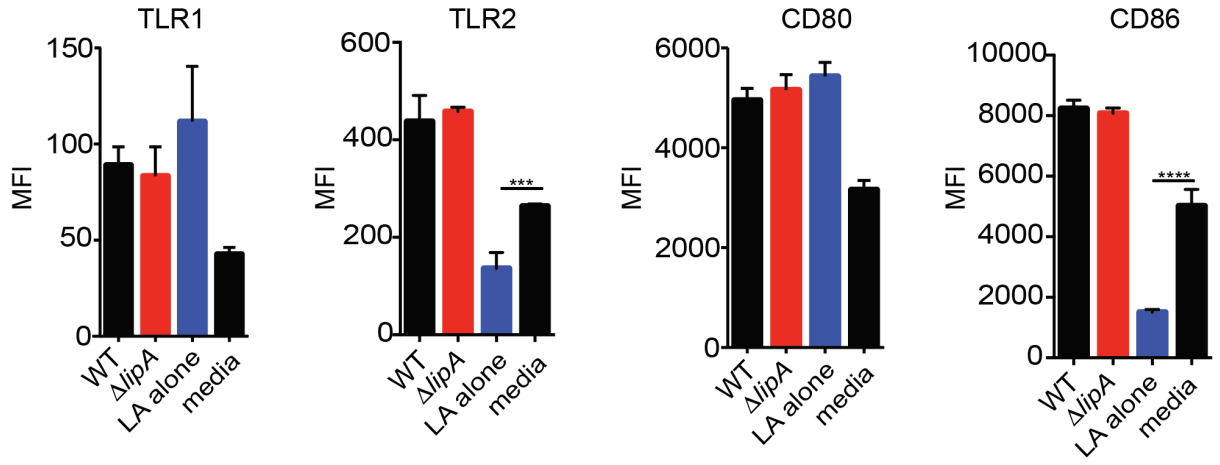

Figure 24. Surface Expression of TLR1, TLR2, CD80, or CD86 are Not Modulated by Δ*lipA* Mutant Supernatant. BMMs were treated in the presence of WT or Δ*lipA* supernatant or 3 mM free lipoic acid (LA) for 18-24 hours followed by assessment of surface levels of TLR1 or TLR2, CD80, and CD86 by flow cytometry. Data shown are from one of at least three experiments conducted in triplicate. Means ± SD are shown (n=3). ***, $P<0.001$; ****, $P<0.0001$ by 1-way ANOVA with Bonferonni-Sidak post-test.

To determine if lipoyl-peptides directly interfere with the interaction of natural ligands with TLR1/2 by competing for similar binding sites, we used an enzyme linked immunosorbent assay-based approach. Recombinant TLR1 and TLR2 were bound in a well overnight, followed by competing of binding for TLR1/2 between Pam3CSK4 and DKA or DK^{L}A. If the lipoyl peptide DK^{L}A binds to TLR1 or TLR2, then we expect to see a reduction in the binding of the native TLR1/2 ligand Pam3CSK4 in the presence of DK^{L}A but not DKA. We found that an excess of DK^{L}A, but not DKA, reduces the binding ability of Pam3CSK4 (Figure 25). However, as we titrated out the amounts of tripeptide, we observed high variability in the binding of Pam3CSK4. These data suggest that at high concentrations, the lipoyl moiety on DK^{L}A may bind to TLR1/2 and compete for binding. However, this approach to determine if lipoyl-peptides bind to TLR1/2 to compete for binding sites with native ligands was limited and needs to be further refined.

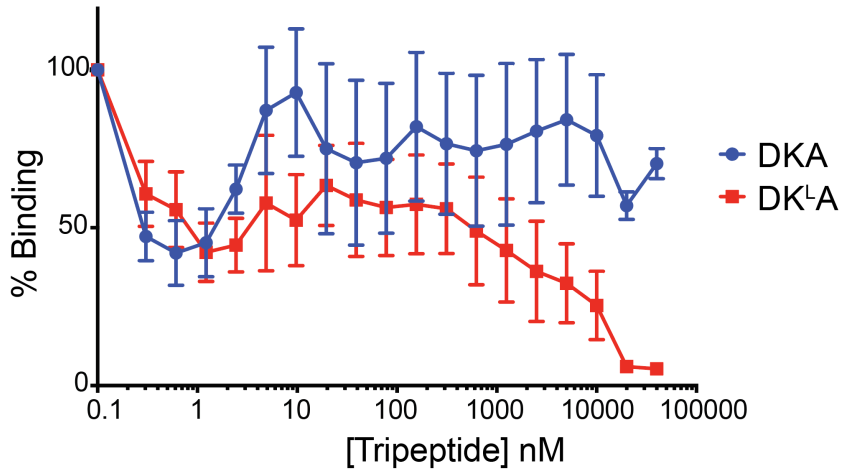

Figure 25. Binding of DK^{L}A and DKA to Recombinant TLR1/2. 750 nM of biotinylated Pam3CSK4 binding to recombinant TLR1 and TLR2 in the presence of various amounts of the synthetic tripeptides DKA or DK^{L}A. Percent binding determined by dividing the average absorbance of wells with Pam3CSK4 and titrated peptides by the absorbance of Pam3CSK4 binding alone. Pam3CSK4 binding to TLR1/2 alone was set as 100% binding. Means ± SD are shown (n=5).

Activity of the Lipoic Acid Synthetase Promotes *S. aureus* Pathogenesis

Previous work in the lab conducted by Azul Zorzoli found that, during bloodstream infection, *S. aureus* mutants with defects in bacterial lipoic acid synthesis and salvage lead to tissue-specific virulence defects where infection of the kidney depends on lipoic acid salvage enzymes, but infection of the heart requires LipA (373). These observations suggest there is varied dependency on *de novo* lipoic acid synthesis for *S. aureus* survival in different tissue sites. Given the strong in vitro dampening of TLR1/2 activation of macrophages, we surmised that this immunosuppression could alter the host's ability to limit infection by macrophage antimicrobial responses. To determine if lipoyl-protein immunosuppression occurs in vivo, we induced systemic infection in mice by intraperitoneal injection of WT, Δ*lipA*, or Δ*lipA*+*lipA* and determined the levels of macrophage chemokines in the serum. After 16 hours, animals infected with a Δ*lipA* mutant had more CCL3 and CCL4 in the serum, whereas at 72 hours chemokine levels were similar (Figure 26). CCL3 and CCL4 are chemokines for macrophages and monocytes in addition to other innate immune cells through interaction with the CCR5 receptor. We then surveyed if the population of immune cells recruited to the site of infection were different between the infected animals. At 16 hours, the proportion of pro-inflammatory macrophages ($CD11b^+$, $F4/80^+$, $CCR5^+$, I-A/I-E^{high}, $Ly6G^-$) in the peritoneal cavity were identical among the infection groups (Figure 27). However, at 72 hours, Δ*lipA* mutant-infected animals had more I-A/I-E^{high}/$CCR5^+$ activated macrophages and I-A/I-E^{high} dendritic cells (Figure 27 and 28). Although CCL3 and CCL4 recruit other innate immune cells, the total number of recruited macrophages, neutrophils, and dendritic cells were the same in all infection

groups at both 16 hours and 72 hours post-infection (Figure 29). In summary, the proportion of activated pro-inflammatory phagocytes is larger in Δ*lipA* mutant-infected animals.

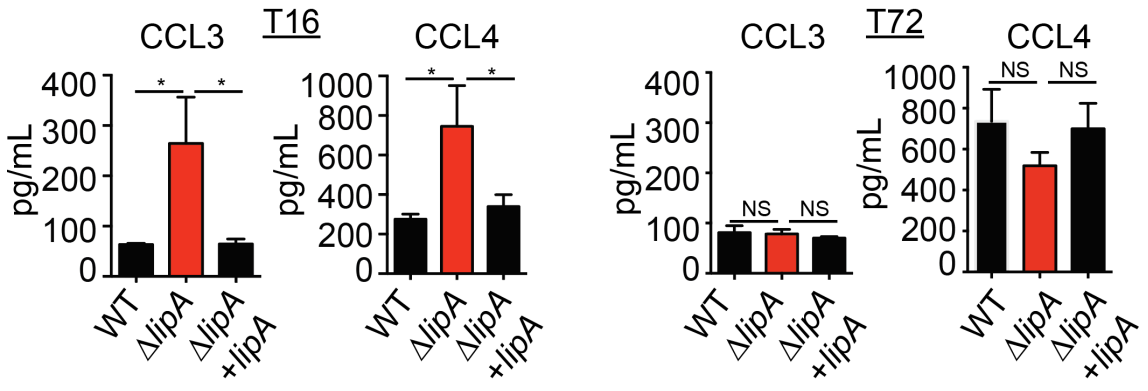

Figure 26. Serum Levels of CCL3 and CCL4 Chemokines are Higher in Δ*lipA* Mutant-Infected Mice 16 Hours Post-Infection. Serum CCL3 and CCL4 levels (pg/mL) 16 hours or 72 hours post-infection. Means ± SD are shown (WT and Δ*lipA* n=10, Δ*lipA*+*lipA* n=7). NS, not significant; *, *P*<0.05 by 1-way ANOVA with Bonferonni-Sidak post-test.

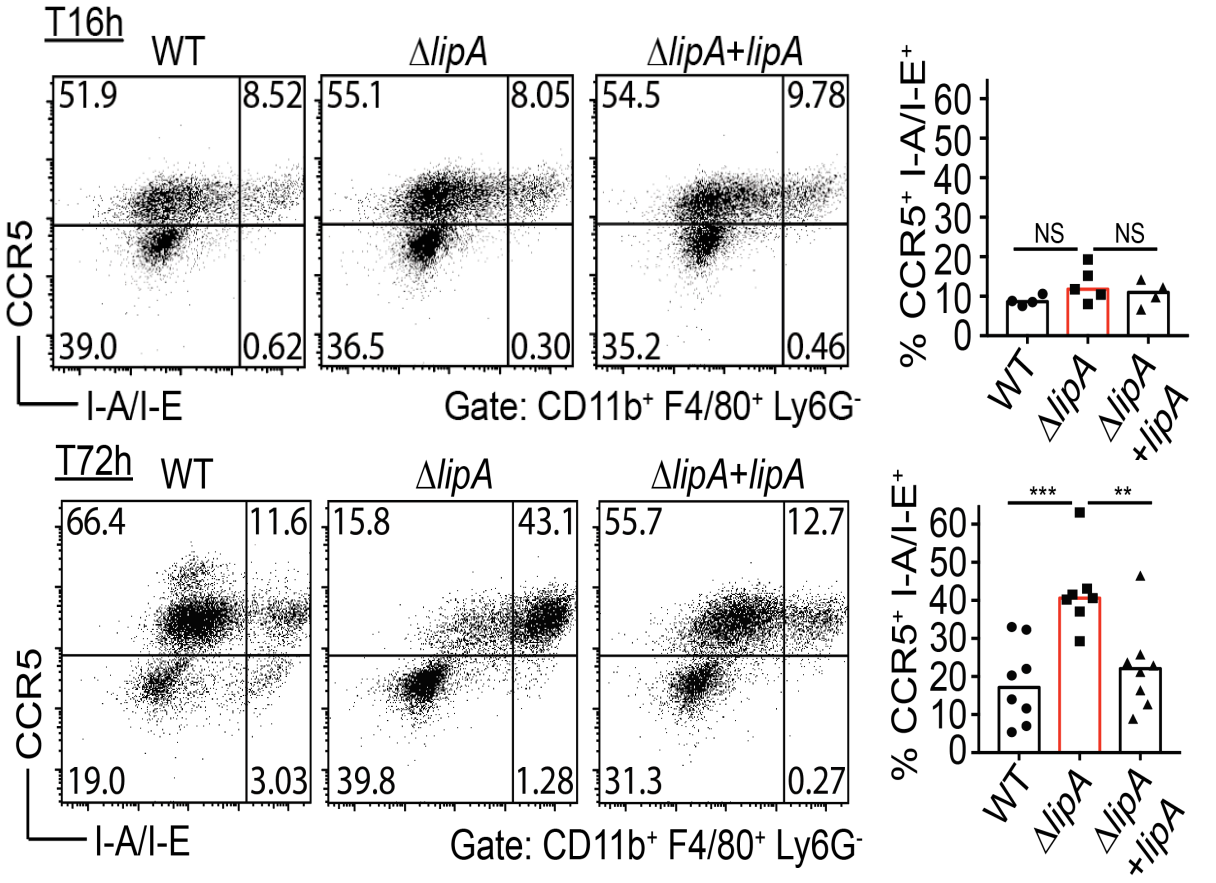

Figure 27. Greater Amounts of Pro-Inflammatory Macrophages are Recruited to the Site of Infection with a Δ*lipA* Mutant 72 Hours Post-Infection. Pro-inflammatory macrophages in the peritoneal cavity at 16 hours and 72 hours post-infection. Macrophages were gated on CD11b^{+} F4/80^{+} Ly6G^{-} cells followed by assessment of CCR5^{+} I-A/I-E^{hi} cells. Flow cytometry plots are representative of 4-8 animals per group. Scatter plots display percent CCR5^{+}/I-A/I-E^{hi} cells within the CD11b^{+} F4/80^{+} Ly6G^{-} gate. Bars display the median. NS, not significant; **, P<0.01; ***, P<0.001 by 1-way ANOVA with Bonferonni-Sidak post-test.

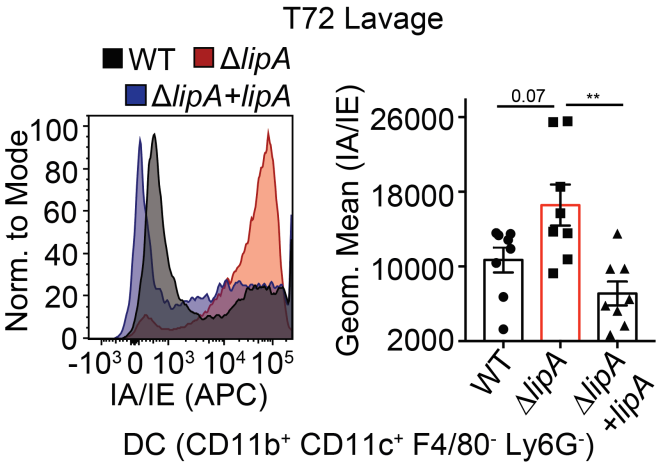

Figure 28. Greater Amounts of IA/IE$^+$ Dendritic Cells are Recruited to the Site of Infection with a Δ*lipA* Mutant 72 Hours Post-Infection. Measurement of dendritic cells (CD11b$^+$ CD11c$^+$ F4/80$^-$ Ly6G$^-$) expressing MHCII (I-A/I-E^{hi}) in the peritoneal cavity 72 hours post-infection. Histogram is representative of 8 animals per group. Scatter plots display geometric mean of I-A/I-E^{hi} cells within the CD11b$^+$ CD11c$^+$ F4/80$^-$ Ly6G$^-$ gate for all animals - WT (n=8), Δ*lipA* (n=8), and Δ*lipA* + *lipA* (n=8). Means ± SD are shown. **, *P*<0.01 by 1-way ANOVA with Bonferonni-Sidak post-test or *P* values are shown.

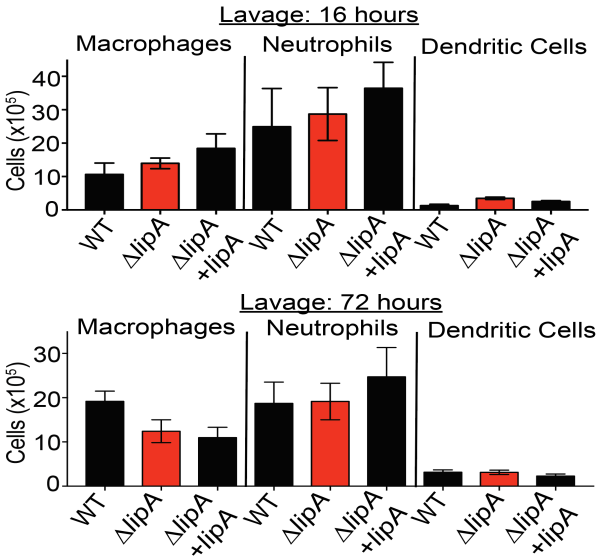

Figure 29. The Total Number of Macrophages, Neutrophils, and Dendritic Cells are Not Different Between Infected Mice. Total cell numbers of macrophages, neutrophils, and dendritic cells in the peritoneal cavity of mice infected intraperitoneally with 1x10^8 CFU of WT, Δ*lipA*, or Δ*lipA* + *lipA S. aureus* 16- or 72-hours post-infection. Macrophages:CD11b$^+$ F4/80$^+$. Neutrophils: CD11b$^+$ Ly6G$^+$. Dendritic cells: CD11b$^+$ CD11c$^+$. Means ± SD are shown.

A Δ*lipA* Mutant is Attenuated During Infection

Pro-inflammatory activated macrophages have a higher propensity to kill bacteria, and because we see higher proportions of activated macrophages recruited to the site of infection in animals infected with Δ*lipA* mutant-infected animals, we hypothesized there could be lower burdens of bacteria in the intraperitoneal infection model. Indeed, Δ*lipA* mutant-infected animals had significantly fewer bacteria at 16- and 72-hours post-infection in the lavage fluid and kidney compared to WT or Δ*lipA*+*lipA* (Figure 30A). After 72 hours, a substantial number of the Δ*lipA* mutant-infected animals had undetectable bacteria in both the lavage fluid (N=7) and the kidneys (N=6) (Figure 30A). By 72 hours, the median bacterial colony forming units (CFU) in Δ*lipA* mutant-infected animals was near or at the limit of detection in both sites, while the median bacterial CFU of the WT and complement infected animals remained 1-2 logs higher, indicating LipA may promote bacterial survival during infection (Figure 30B). With these data, we cannot rule out the possibility that the attenuation of a ∆*lipA* mutant in vivo may stem either from observed metabolic deficiencies associated with lipoic acid limitation, or from improved clearance of bacteria by activated macrophages.

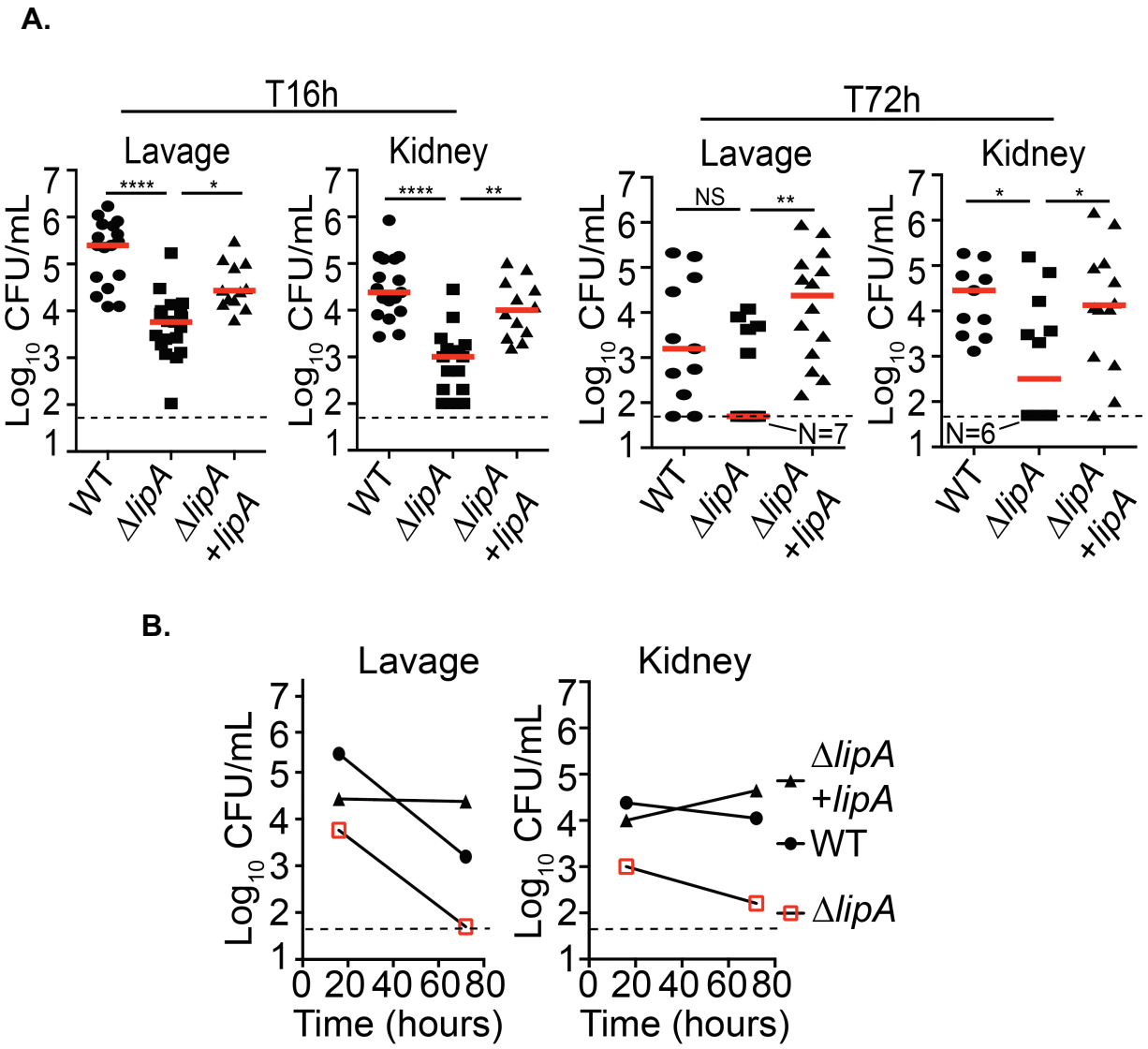

Figure 30. A Δ*lipA* Mutant is Attenuated During Infection. Bacterial burden (A) and medians of bacterial burden (B) in the peritoneal cavity and kidneys of mice 16 hours - WT (n=17), Δ*lipA* (n=19), Δ*lipA*+*lipA* (n=12), and 72 hours - WT (n=11), Δ*lipA* (n=12), Δ*lipA*+*lipA* (n=14) post IP infection. NS, not significant; *, $P<0.05$; **, $P<0.01$; ****, $P<0.0001$ by non-parametric 1-way ANOVA (Kruskal-Wallis Test) with Dunn's post-test. Dashed lines, limit of detection. N=7 and N=6 in the 72 hour dataset are the number of animals with undetectable CFU (A).

As mentioned earlier, during bloodstream infection, a Δ*lipA* mutant is not attenuated in the kidneys (373). In this bloodstream model, kidney abscesses readily form where phagocytic leukocytes are excluded from the abscess (396, 397). Therefore, we wondered if there are greater proportions of pro-inflammatory macrophages in kidneys during bloodstream infection with a Δ*lipA* mutant that cannot penetrate this abscess, leading to failure to clear a Δ*lipA* mutant. To test this, we systemically infected mice via injection into the bloodstream with WT or Δ*lipA* and assessed the proportion of pro-inflammatory macrophages in the kidneys. As expected, we found no differences in bacterial burdens in the kidney; however, we observed macrophages expressing higher amounts of IA/IE, suggesting greater macrophage activation in the kidneys of Δ*lipA* mutant-infected animals (Figure 31). These data imply that, in the absence of macrophage infiltration, a growth defect imparted by lack of LipA activity is likely not sufficient for attenuation.

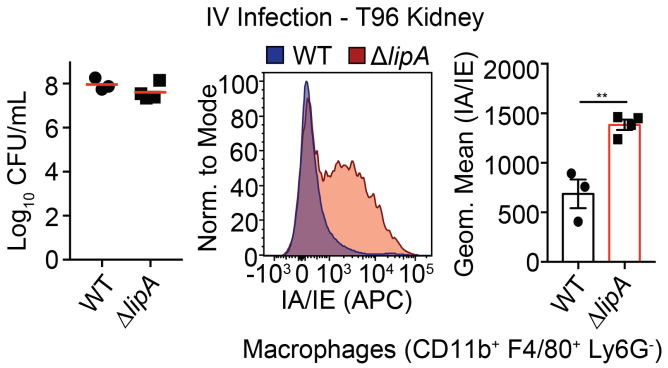

Figure 31. A Δ*lipA* Mutant is Not Attenuated in Kidneys During Bloodstream Infection, but Recruits Pro-Inflammatory Macrophages Bacterial burden (CFU/mL) in the kidneys of mice 96 hours post IV infection- WT (n=3) and Δ*lipA* (n=4). Pro-inflammatory macrophages (CD11b$^+$ F4/80$^+$ Ly6G$^-$) expressing I-A/I-E in kidneys of mice 96 hours post-infection. Histogram is representative of 3-4 animals per group. Scatter plots display geometric mean of I-A/I-E^{hi} cells within the CD11b$^+$ F4/80$^+$ Ly6G$^-$ gate for all animals. Means ± SD are shown. **, P<0.01 by 1-way ANOVA with Bonferonni-Sidak post-test.

Macrophages are Responsible for Attenuation of a Δ*lipA* Mutant During Systemic Infection

To test if the observed attenuation of a Δ*lipA* mutant is due to the antimicrobial activity of activated macrophages, we depleted mice of macrophages and their precursors by administering clodronate-loaded liposomes three days prior to infection with $1x10^7$ CFU of WT, Δ*lipA*, or Δ*lipA* + *lipA* strains. We first determined if clodronate treatment depleted macrophages in our infection model by assessing the proportion of macrophages recovered from *S. aureus* infected mice that were pre-treated with clodronate or PBS three days prior to infection. Clodronate treated mice had significantly reduced proportions of macrophages ($CD11b^+$ $Ly6G^-$ $Ly6C^-$ $Gr1^-$ $F4/80^+$) in the peritoneal cavity compared to non-treated mice (Figure 32A). We then infected clodronate-treated mice with WT, Δ*lipA*, or Δ*lipA* + *lipA* strains and enumerated CFU at 16 hours and 72 hours post-infection. After 16 hours, we recovered near identical CFU from the peritoneal cavities or kidneys of macrophage-depleted mice despite a large distribution of bacterial loads (Figure 32B). At 72 hours post-infection, there were no discernable differences in CFU recovered from the lavage or the kidneys of infected clodronate-treated mice regardless of the strain used for infection (Figure 32C). We also observe a large distribution in CFU recovered from clodronate treated-mice at 72 hours post-infection; however, there were no differences in the average CFU recovered from infected animals. In summary, these data suggest that, in a peritonitis infection model, macrophages are a primary mediator of clearance in Δ*lipA* mutant-infected animals as opposed to a metabolic defect associated with lipoic acid limitation and macrophages are instrumental to control bacterial loads during infection.

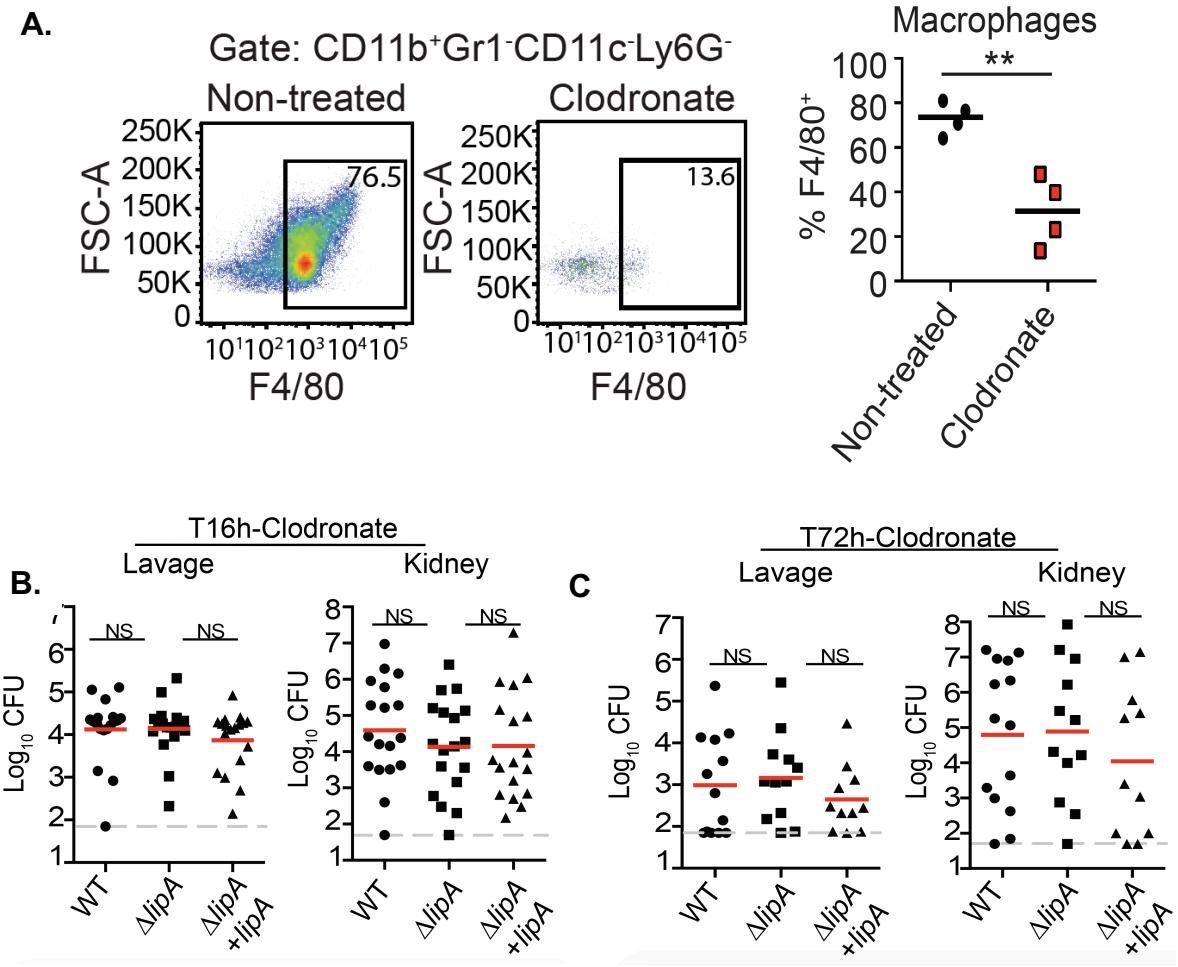

Figure 32. A Δ*lipA* Mutant is Not Attenuated in Macrophage-Depleted Mice. (A) Abundance of macrophages ($CD11b^+$ $Gr1^-$ $CD11c^-$ $Ly6G^-$ $F4/80^+$) in the peritoneal cavity of clodronate-treated mice or non-treated mice 72 hours post-intraperitoneal infection with WT *S. aureus*. Bar represent medians. Data were analyzed using unpaired, two-tailed Student's *t* test. **, $P<0.01$. (B and C) the bacterial burden (Log_{10} CFU) in the peritoneal cavity and kidneys of clodronate treated mice 16 hours (B) post-intraperitoneal infection with WT (n=18), Δ*lipA* (n=18), Δ*lipA* + *lipA* (n=18) or 72 hours (C) post-intraperitoneal infection with WT (n=13), Δ*lipA* (n=12), Δ*lipA* + *lipA* (n=11). Bars represent means. NS, not significant by non-parametric 1-way ANOVA (Kruskal-Wallis Test) with Dunn's post-test. Dashed lines represent limit of detection.

Macrophages from Δ*lipA* Mutant-Infected Mice Control the Outgrowth of *S. aureus*

Because a greater proportion of macrophages in Δ*lipA*-infected mice have enhanced pro-inflammatory characteristics, we reasoned that these macrophages might have greater bactericidal activity. To test this hypothesis, we isolated F4/80$^+$ peritoneal cells elicited to the peritoneal cavity 72 hours after infection with WT and Δ*lipA S. aureus*, or mock infected with PBS. After antibiotic treatment to kill bacteria used for elicitation, we infected the sorted population of F4/80$^+$ cells with WT *S. aureus*. The F4/80$^+$ peritoneal cells elicited after infection with a Δ*lipA* mutant inhibited the growth of *S. aureus* better than F4/80$^+$ peritoneal cells elicited from WT or PBS treated mice (Figure 33). Consistent with our in vitro findings, these data indicate macrophage activation is increased in Δ*lipA* mutant-infected mice and coincides with better infection control.

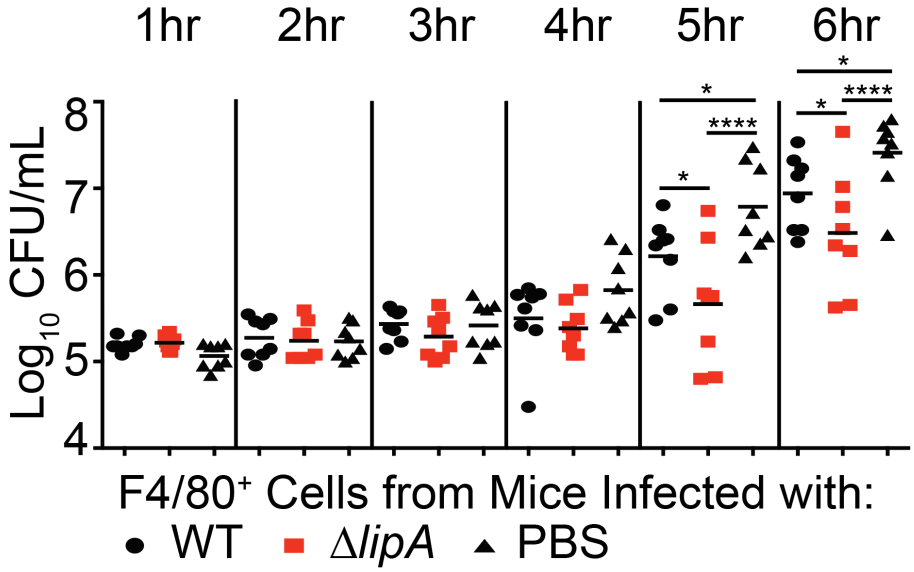

Figure 33. Macrophages Isolated from Δ*lipA* Mutant-Infected Mice Control the Outgrowth of *S. aureus*. Survival/outgrowth of WT *S. aureus* after infecting WT (n=8), Δ*lipA* (n=8), or PBS (n=8) elicited F4/80$^+$ cells. *, $P<0.05$, ****; $P<0.0001$ by 2-way ANOVA with Tukey's post-test.

Macrophages from Δ*lipA* Mutant-Infected Mice Produce More ROS to Restrict *S. aureus* Growth

As the pro-inflammatory macrophages recruited to the site of infection with a Δ*lipA* mutant better restrict bacterial growth ex vivo and are instrumental to bacterial clearance, we sought to determine the mechanism by which these macrophages have an enhanced restrictive capacity. Macrophages generate ROS as one of a variety of mechanisms used to inhibit the growth of engulfed pathogens. To test if ROS production by macrophages is increased in Δ*lipA* mutant-infected mice, we elicited macrophages to the peritoneal cavity using WT, Δ*lipA,* or Δ*lipA* + *lipA* strains and re-infected the isolated macrophages ex vivo with WT *S. aureus* followed by quantitation of ROS, using an indicator dye that fluoresces upon oxidation. Upon re-infection, macrophages sourced from WT-infected mice had a net decrease in mean fluorescent intensity (MFI) (Figure 34). In contrast, macrophages isolated from Δ*lipA* mutant-infected mice had, on average, a positive fold change in MFI, suggesting that these macrophages have a higher oxidative state (Figure 34). This was partially complemented by the Δ*lipA* + *lipA* strain (Figure 34). These data suggest that macrophages from Δ*lipA* mutant-infected mice produce greater amounts of ROS.

To test if the increased ROS generation by macrophages isolated from Δ*lipA* mutant-infected mice is necessary to restrict *S. aureus* growth, we first inhibited ROS production using diphenyleneiodonium chloride (DPI) and compared the ability to restrict growth relative to macrophages isolated from WT-infected or mock-infected (PBS) mice. As seen previously, ROS replete cells from Δ*lipA* mutant-infected mice

slow the outgrowth of *S. aureus* compared to macrophages isolated from WT-infected mice (Figure 35). Upon inhibition of ROS production by DPI treatment, the macrophages isolated from Δ*lipA*-infected mice no longer restricted *S. aureus* outgrowth compared to WT-infected or mock-infected mice (Figure 35). These data suggest that increased ROS production contributes to the heightened ability of macrophages isolated from Δ*lipA* mutant-infected mice to control bacterial outgrowth.

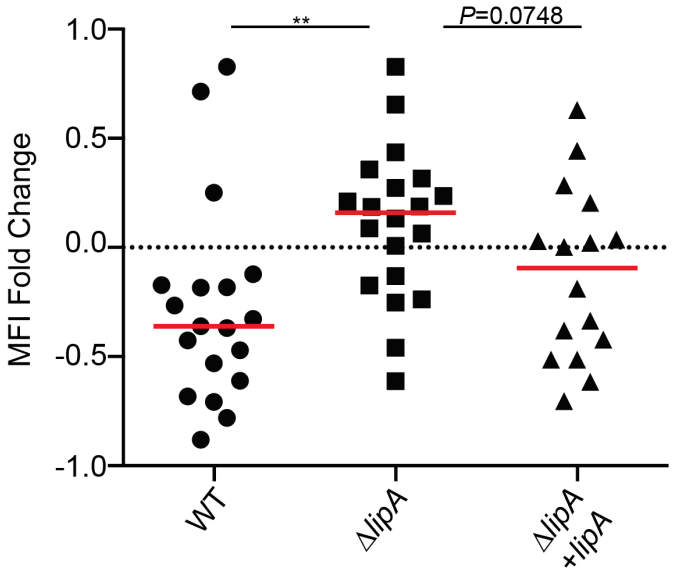

Figure 34. Macrophages from Δ*lipA* Mutant-Infected Mice Produce Greater Amounts of ROS. F4/80$^+$ macrophages were sorted from immune cells harvested from the peritoneal cavity of mice 72 hours post-intraperitoneal infection with WT (n=19), Δ*lipA* (n=20), Δ*lipA* + *lipA* (n=16) and infected ex vivo with WT *S. aureus* at a MOI of 0.1. Macrophages were stained with the ROS indicator CellROX deep red and analyzed by flow cytometry. Fold changes in the geometric means of CellROX fluorescence were assessed in infected cells and compared to uninfected F4/80$^+$ cells. **, $P<0.01$ by non-parametric 1-way ANOVA (Kruskal-Wallis Test) with Dunn's post-test. Dashed line is at zero, bars represent the median.

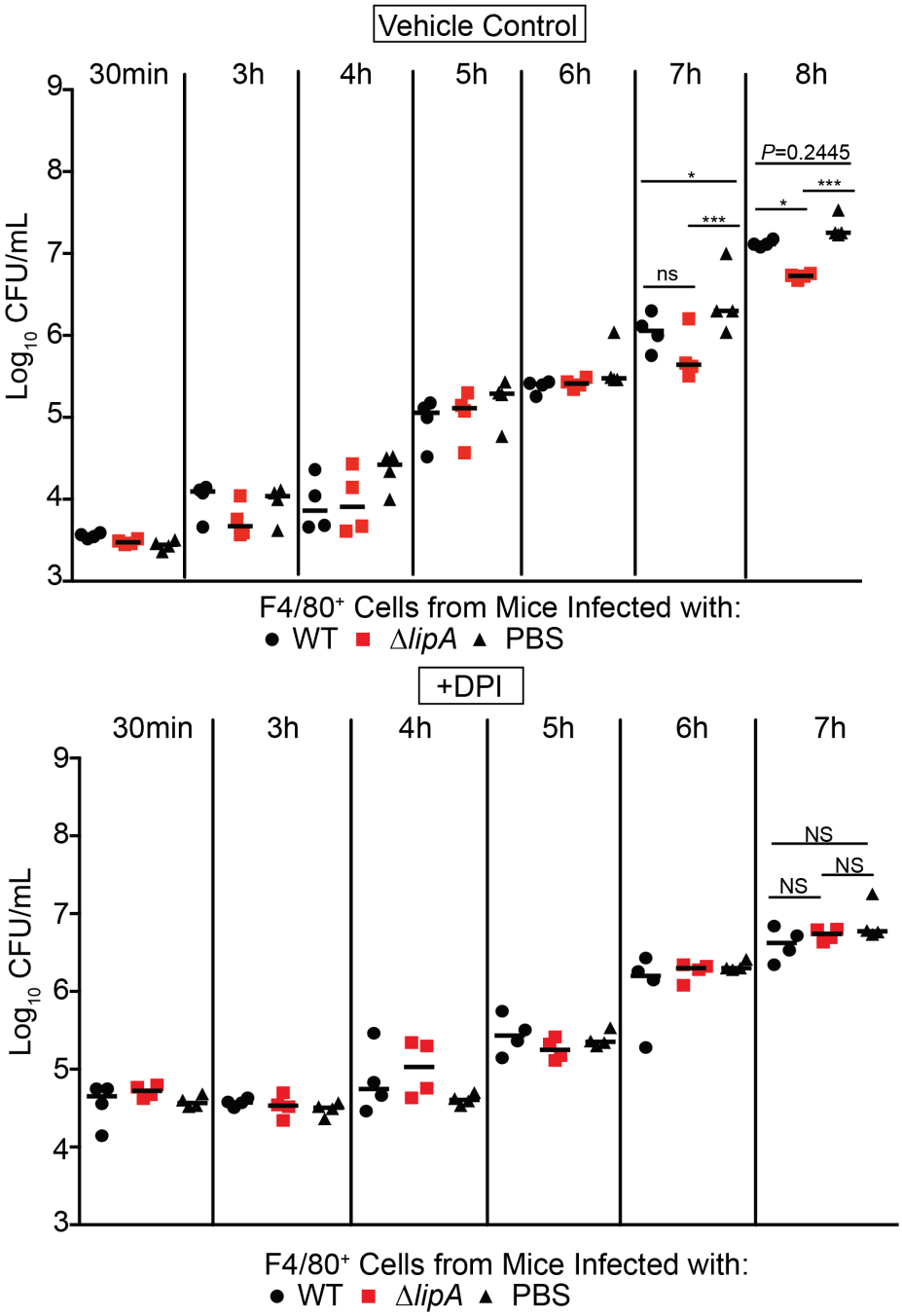

Figure 35. ROS Production Contributes to the Heightened Ability of Macrophages Isolated from Δ*lipA* Mutant-Infected Mice to Control Bacterial Outgrowth. Outgrowth (Log_{10} CFU/mL) of WT *S. aureus* after infecting F4/80$^+$ cells isolated from mice 72 hours post-intraperitoneal infection with WT (n=4), Δ*lipA* (n=4), or PBS (n=4) treated with DMSO vehicle control or ROS inhibitor DPI. Bars represent medians. NS, not significant; *, $P<0.05$; ***, $P<0.001$ by 2-way ANOVA with Tukey's post-test. Data shown are from one of at least three independent experiments.

Δ*lipA* Mutant-Induced Antibacterial ROS Are Generated by NADPH Oxidase

Although DPI is commonly used to inhibit production of ROS, it can have off-target effects that lead to the inhibition of mitochondrial respiration, which interferes with mROS generation (398). Therefore, DPI cannot conclusively determine whether ROS derived from the mitochondria or NADPH oxidase facilitates restriction of bacterial growth. However, recent studies have found that delivery of mROS to the phagosome is important for the antimicrobial response to internalized *S. aureus*, suggesting mROS are important in bacterial clearance (251, 252). We asked if macrophages from Δ*lipA* mutant-infected mice use mROS or NADPH oxidase-derived ROS to restrict bacterial growth. We inoculated mice with WT *S. aureus* or a Δ*lipA* mutant, isolated macrophages, and determined if inhibition of mROS using the inhibitor Necrox-5 abrogated growth restriction. Generation of mROS facilitated the killing of *S. aureus* within macrophages, as *S. aureus* survival was greater in Necrox-5 treated macrophages compared to vehicle treated macrophages (Figure 36A). However, in the presence of Necrox-5, macrophages isolated from Δ*lipA*-infected mice still restricted the outgrowth of *S. aureus* to a greater degree than macrophages from WT- or mock-infected mice (Figure 36B-C). These data suggest that, while production of mROS contributes to control of *S. aureus* within the macrophage, they are not involved in the improved restrictive capacity of macrophages isolated from Δ*lipA* mutant-infected mice.

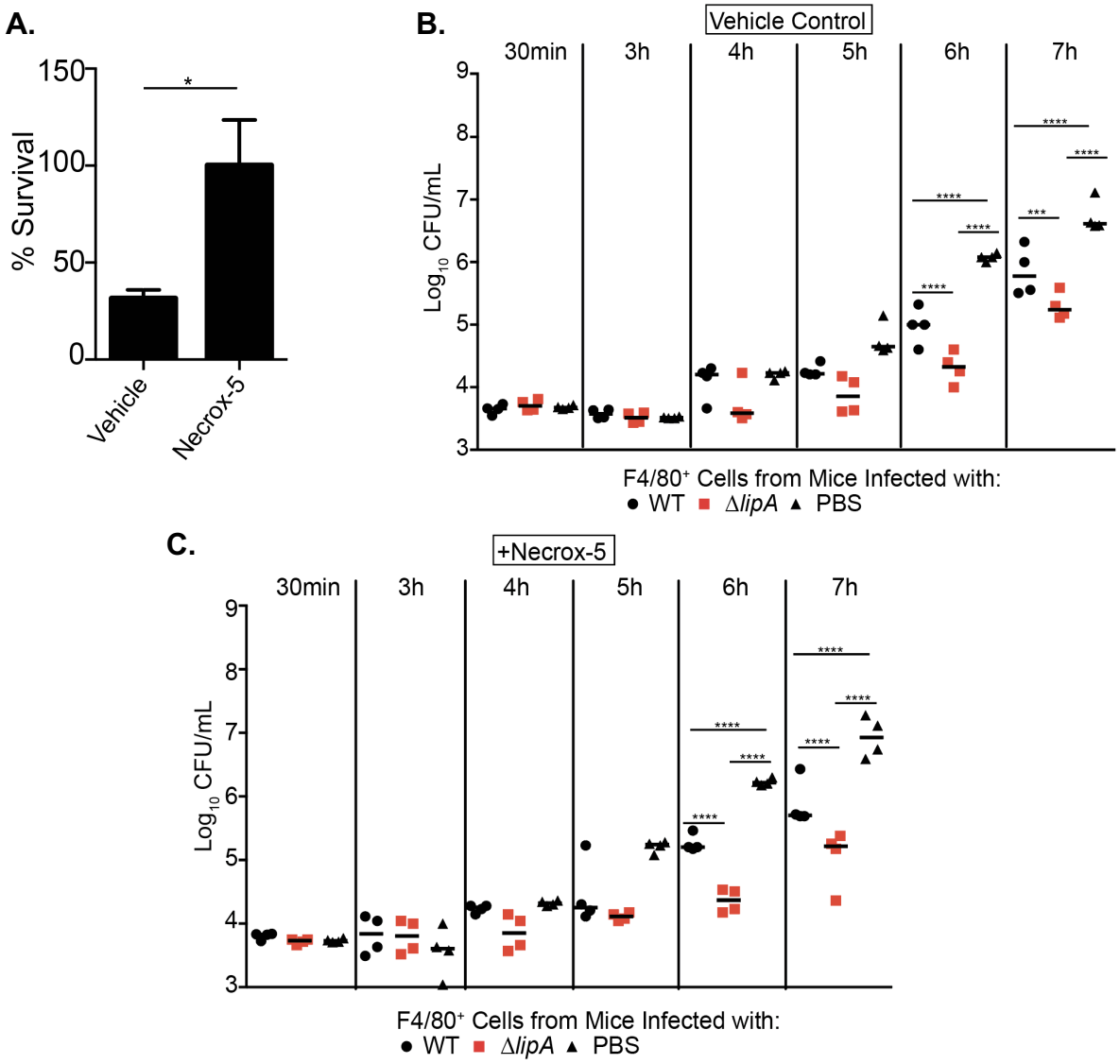

Figure 36. Macrophages Isolated from Δ*lipA* Mutant-Infected Mice Do Not Use mROS to Restrict Bacterial Outgrowth. (A) Percent survival of WT *S. aureus* 8 hours after infecting F4/80$^+$ cells isolated from mice treated with DMSO vehicle control or mROS inhibitor Necrox-5. n=8, error bars represent SEM. Data were analyzed using unpaired, two-tailed Student's *t* test. *, *P*<0.05. (B and C) Outgrowth (Log_{10} CFU/mL) of WT *S. aureus* after infecting F4/80$^+$ cells isolated from mice 72 hours post-intraperitoneal infection with WT (n=4), Δ*lipA* (n=4), or PBS (n=4) treated with (B) DMSO vehicle control or (C) Necrox-5. Bars represent medians. ***, *P*<0.001; ****, *P*<0.0001 by 2-way ANOVA with Tukey's post-test. Data shown are from one of at least two independent experiments.

Since mROS do not appear to play a role in the improved restrictive function, we wondered if NADPH oxidase-dependent ROS production contributes to the greater ability of macrophages sourced from Δ*lipA* mutant-infected mice to restrict bacterial growth. To test this, we used a specific peptide-based inhibitor of NADPH oxidase, gp91ds-tat (399). This NADPH oxidase assembly inhibitor is a chimeric peptide containing an amino acid sequence with high affinity for the gp91-*phox* subunit of NADPH oxidase linked with the tat peptide sequence from human immunodeficiency virus, which facilitates entry into cells (399, 400). We isolated macrophages from WT, Δ*lipA*, and mock (PBS) infected mice followed by re-infection with WT *S. aureus* ex vivo and monitored bacterial outgrowth hourly. Macrophages from Δ*lipA* mutant-infected mice better restricted the outgrowth of *S. aureus* compared to macrophages isolated from WT and mock-infected mice (Figure 37A). Treatment of macrophages sourced from WT, Δ*lipA*, or mock-infected mice with gp91ds-tat prevented enhanced growth restriction of *S. aureus* compared to macrophages isolated from WT and mock-infected mice (Figure 37B). In summary, these data suggest that the ROS generated from NADPH oxidase are necessary for the increased growth restriction of macrophages isolated from Δ*lipA* mutant-infected mice.

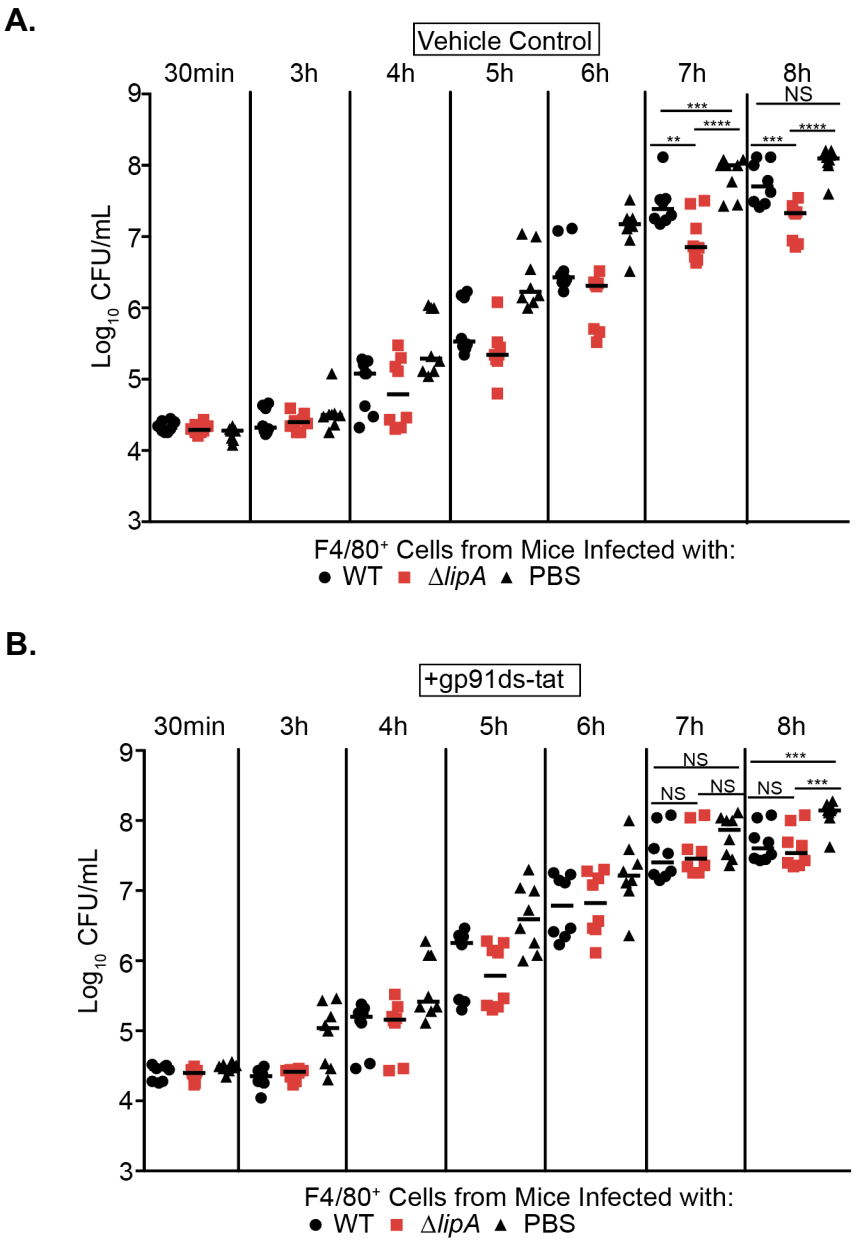

Figure 37. NADPH Oxidase Derived ROS Contributes to Improved Control of Bacterial Outgrowth by Macrophages Isolated from Δ*lipA* Mutant-Infected Mice. (A and B) Outgrowth (Log_{10} CFU/mL) of WT *S. aureus* after infecting F4/80$^+$ cells isolated from mice 72 hours post-intraperitoneal infection with WT (n=8), Δ*lipA* (n=8), or PBS (n=8) treated with (A) water vehicle control or (B) NADPH oxidase inhibitor gp91ds-tat. Bars represent medians. NS, not significant; **, P<0.01; ***, P<0.001; ****, P<0.0001 by 2-way ANOVA with Tukey's post-test.

RNS Contributes to the Enhanced Ability of Macrophages from Δ*lipA* Mutant-infected Mice to Slow Bacterial Outgrowth

Besides ROS, which forms in the phagosome to kill engulfed pathogens, the generation of $NO^{\bullet}$ and RNS by iNOS also controls pathogen growth (237). Our data thus far suggest that blockade of NADPH oxidase activity abrogates the restrictive capacity of macrophages from Δ*lipA* mutant-infected mice, implicating ROS in this process. However, antimicrobial RNS such as $ONOO^-$ may depend on NADPH oxidase derived $O_2^{-\bullet}$ (254). Thus, macrophages treated with NADPH oxidase inhibitors may also generate fewer antimicrobial RNS. Therefore, we tested if macrophages recruited to the site of infection with a Δ*lipA* mutant produce greater amounts of $NO^{\bullet}$ in addition to ROS that together might lead to growth restriction. We stimulated macrophages isolated from WT, Δ*lipA*, or Δ*lipA* + *lipA* infected mice ex vivo with heat-killed *S. aureus* and measured $NO^{\bullet}$ production by the Griess test (401). Upon re-stimulation, macrophages from Δ*lipA* mutant-infected mice produced three times greater levels of nitrite, a stable breakdown product of $NO^{\bullet}$ compared to WT or the complement strain (Figure 38). These data suggest that macrophages from Δ*lipA* mutant-infected mice produce greater amounts of $NO^{\bullet}$.

Given the increased production of $NO^{\bullet}$ in macrophages isolated from Δ*lipA* mutant-infected mice, we tested whether RNS contributes to growth restriction. We monitored the growth of WT *S. aureus* in macrophages isolated from WT, Δ*lipA*, or mock-infected mice in the presence of a specific iNOS inhibitor, N6-(1-Iminoethyl)-lysine hydrochloride (L-NIL), which prevents $NO^{\bullet}$ production and thus RNS generation. We found that iNOS inhibition by L-NIL abrogated the improved growth restriction of *S.*

aureus by Δ*lipA* mutant-elicited macrophages compared to macrophages isolated from WT or mock-infected mice (Figure 39). Together, our data demonstrate that $NO^{\bullet}$ production and iNOS activity are also necessary for macrophages isolated from Δ*lipA* mutant-infected mice to limit *S. aureus* growth ex vivo.

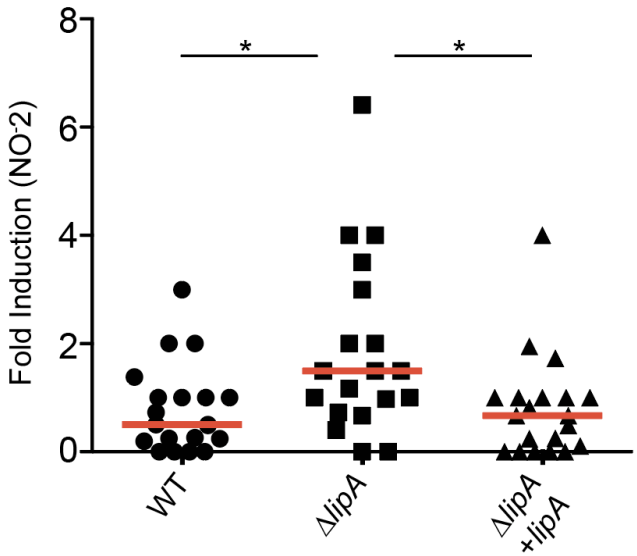

Figure 38. Macrophages Isolated from Δ*lipA* Mutant-Infected Mice Produce Greater Levels of Nitric Oxide. $F4/80^{+}$ macrophages were sorted from immune cells harvested from the peritoneal cavity of mice 72 hours post-intraperitoneal infection with WT (n=20), Δ*lipA* (n=19), Δ*lipA* + *lipA* (n=20) and stimulated overnight ex vivo with heat-killed WT *S. aureus* at a MOI of 10. Nitrite levels, a breakdown of nitric oxide production, were measured by Griess test. Fold induction of nitric oxide production was determined by comparing levels of nitrite produced by infected cells to uninfected $F4/80^{+}$ cells. *, $P<0.05$ by non-parametric 1-way ANOVA (Kruskal-Wallis Test) with Dunn's post-test. Bars represent the median.

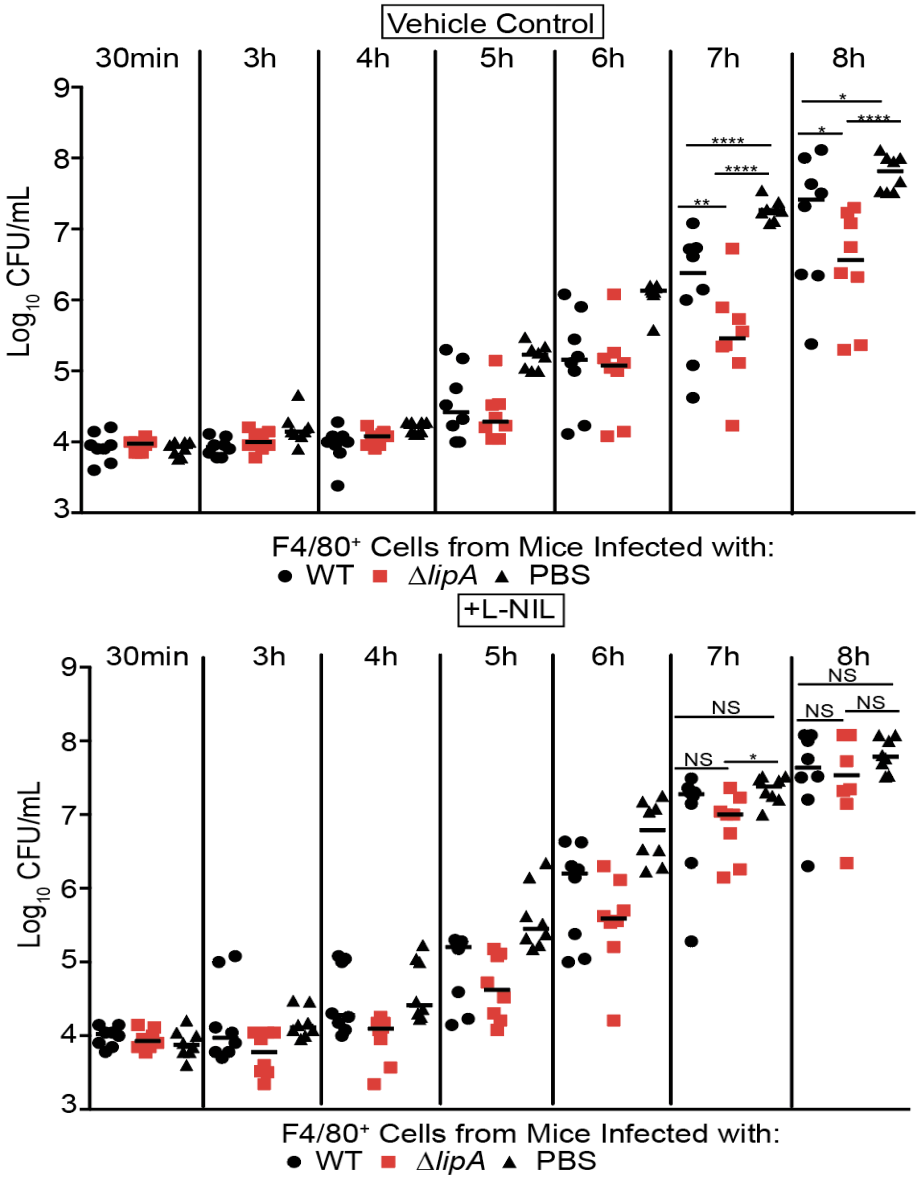

Figure 39. RNS are Important for Restriction of Bacterial Growth by Macrophages Isolated from Δ*lipA* Mutant-Infected Mice. Outgrowth (Log_{10} CFU/mL) of WT *S. aureus* after infecting F4/80$^+$ cells isolated from mice 72 hours post-intraperitoneal infection with WT (n=8), Δ*lipA* (n=8), or PBS (n=8) treated with water vehicle control or iNOS inhibitor L-NIL. Bars represent medians. NS, not significant; *, $P<0.05$; **, $P<0.01$; ****, $P<0.0001$ by 2-way ANOVA with Tukey's post-test.

Primary Infection with a Δ*lipA* Mutant Fails to Protect Mice from Secondary *S. aureus* Challenge

We have observed that a Δ*lipA* mutant not only increases macrophage ROS and RNS production to enhance bacterial killing, but also leads to (i) greater neutrophil cytokine and chemokine release (Figure 9) and (ii) elicits dendritic cells and macrophages with large amounts of the antigen presenting molecule major histocompatibility complex II (MHC-II) during infection (Figure 28). Thus, we wondered if infection with a Δ*lipA* mutant might improve protective recall responses upon *S. aureus* re-infection. We immunized mice with WT, a Δ*lipA* mutant, or PBS (mock) and allowed infection to clear over seven days. After seven days, mice were re-challenged with WT *S. aureus* and CFU were quantified in the kidney over time. Mice immunized with a Δ*lipA* mutant had equivalent CFU in the kidney compared to mice immunized with WT or mice that were not immunized at all time points (Figure 40A). Moreover, upon extension of the immunization time-course to two weeks, we noted that re-infection continues to yield identical CFU in the kidney regardless of whether or not the mice received primary immunization with WT or a Δ*lipA* mutant (Figure 40B). Interestingly, in mice immunized over the course of two weeks, we see higher levels of bacterial loads in the heart if mice received a primary immunization with a Δ*lipA* mutant (Figure 40B). In summary, these data suggest that despite the greater host innate response elicited during infection with a Δ*lipA* mutant, no improved response or potentially a worse recall response follows.

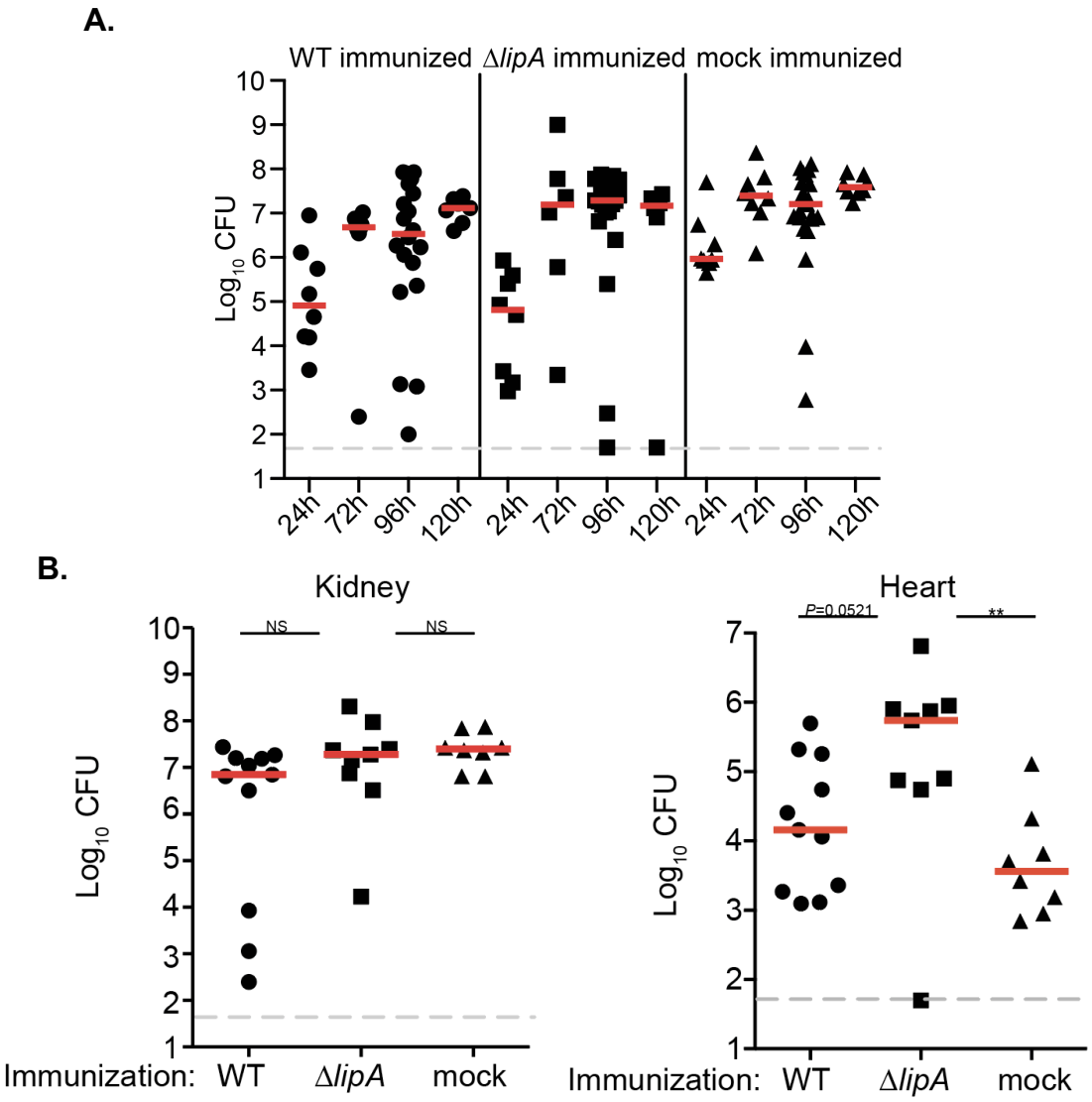

Figure 40. Immunization of Mice with a Δ*lipA* Mutant Does Not Confer Protection from Secondary Challenge. (A and B) Mice were immunized by intraperitoneal injection with either 1 x 10^8 CFU of WT or Δ*lipA S. aureus* or sterile PBS (mock immunized). Either 7- (A) or 14- (B) days after immunization, mice were re-challenged via injection into the retro-orbital sinus with 1 x 10^7 CFU of WT *S. aureus*. Bacterial burden (Log_{10} CFU) in the kidneys (A and B) or hearts (B) of mice assessed (A) 24 hours (WT: n=8, Δ*lipA*: n=8, PBS: n=8), 72 hours (WT: n=8, Δ*lipA*: n=6, PBS: n=8), 96 hours (WT: n=20, Δ*lipA*: n=23, PBS: n=23), 120 hours (WT: n=7, Δ*lipA*: n=6, PBS: n=8) or (B) 96 hours (WT: n=11, Δ*lipA*: n=9, PBS: n=8) post-secondary challenge. Bars represent medians and dashed lines represent the limit of detection. NS, not significant; **, *P*<0.01; by non-parametric 1-way ANOVA (Kruskal-Wallis Test) with Dunn's post-test.

CHAPTER FOUR

DISCUSSION

Introduction

For a pathogen to infect and replicate in the host, it is often necessary to impede host immune defenses. The human pathogen *S. aureus* has armed itself with a repertoire of virulence factors to promote immune evasion. Many virulence factors counter neutrophil responses to infection, as these cells constitute the initial cellular response to *S. aureus* infection. Macrophages are another cellular component of the innate immune system with critical antimicrobial functions. In addition to their killing capacity, macrophages also produce cytokines and chemokines to promote key functions of both innate and adaptive immunity. Thus, macrophages are a key cell for *S. aureus* to overcome during infection. The goal of this thesis was to identify and characterize a novel extracellular virulence factor of *S. aureus* that counters macrophage immune responses.

Using a transposon mutant library of the USA300 strain JE2, Dr. Alonzo found numerous mutants that elicited reduced or enhanced production of pro-inflammatory cytokines and chemokines by BMMs. Of interest, was the hyper-activation of BMMs caused by addition of supernatant from a *S. aureus* mutant with a mutation in the *lipA* gene. The *lipA* gene encodes for lipoic acid synthetase, which synthesizes the essential metabolic cofactor lipoic acid. In this work, we found that suppression of macrophage activation correlated with the ability of *S. aureus* to release a lipoic acid-modified metabolic enzyme subunit, E2 PDH, into the supernatant where it moonlights by

restricting the TLR1/2 activation of macrophages. We show that dampening of macrophage function by LipA activity is necessary for optimal *S. aureus* pathogenesis. In the absence of lipoic acid synthesis in *S. aureus*, we saw that a Δ*lipA* mutant is more readily cleared by the host and elicits greater proportions of pro-inflammatory macrophages. Upon isolation of these macrophages, they restrict the outgrowth of *S. aureus* ex vivo better than macrophages from WT infected mice. The impedance of macrophage antimicrobial functions by LipA is mediated by reductions in the generation of ROS and RNS by NADPH oxidase and iNOS, respectively, leading to improved survival of *S. aureus* during infection. This suppressive function is lost upon infection with a Δ*lipA* mutant, whose clearance is dramatically improved due to enhanced production of ROS and RNS by macrophages at the site of infection. Despite the induction of a more robust antimicrobial immune response during infection with a Δ*lipA* mutant, the host is unable to mount a successful recall response, likely due to rapid clearance of the microbe. Figure 41 depicts a graphical model for how we imagine lipoic acid synthesis alters macrophage immune responses. On the whole, the work in this thesis demonstrates that synthesis of bacterial-derived lipoic acid by LipA confers immunosuppressive properties on macrophages and emphasizes the close associations between bacterial metabolism and evasion of innate immunity.

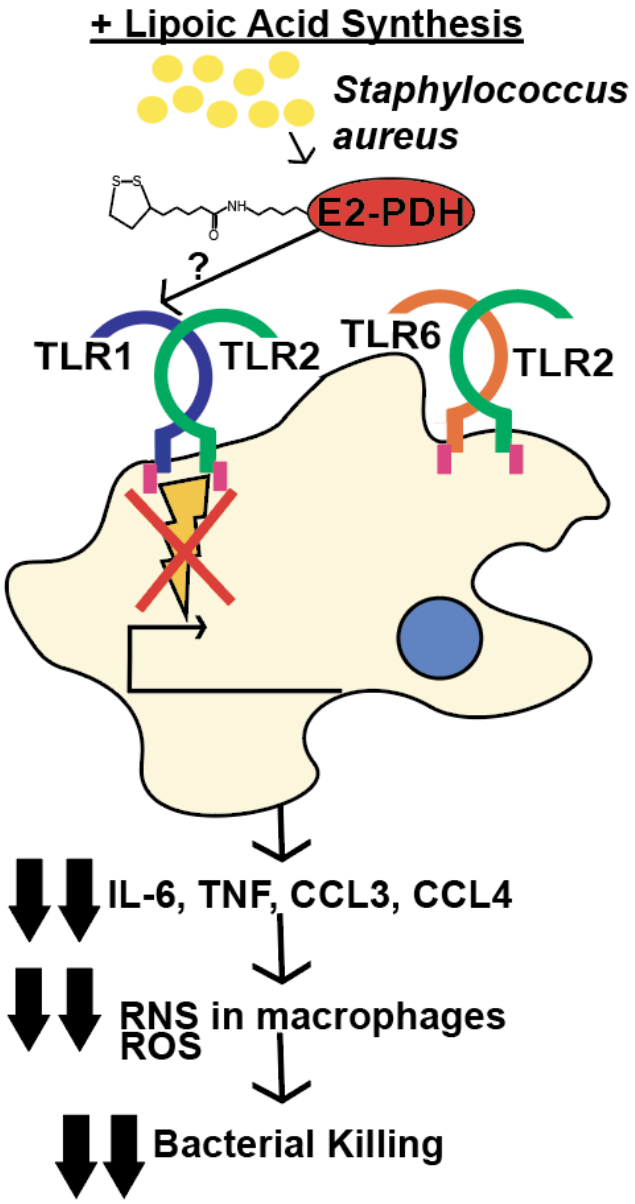

Figure 41. Model of Lipoic Acid Synthesis Modulation of Macrophage Responses. WT *S. aureus* uses lipoic acid synthesis to attach a lipoyl moiety to E2-PDH, which is released into the supernatant. Lipoyl-E2-PDH blocks TLR1/2 activation of macrophages, perhaps through binding competition with native ligands, leading to reduction in pro-inflammatory cytokines and chemokines IL-6, TNF, CCL3 and CCL4. As a result of LipA-mediated immunosuppression, macrophages produce less antimicrobial RNS and ROS and fail to efficiently kill bacteria.

Release of Lipoyl-E2-PDH

In order for *S. aureus* to dampen the activation of macrophages, it needs to release lipoyl-E2-PDH. Once outside of the bacterial cell, our data suggests that lipoyl-E2-PDH can block TLR1/2 activation of macrophages. Normally, lipoyl-E2-PDH functions within the PDH complex present in the cytoplasm of *S. aureus.* The PDH complex catalyzes the oxidative decarboxylation of pyruvate to form acetyl coenzyme A, feeding several metabolic pathways in the cells, including the TCA cycle, fatty acid biosynthesis, and parts of isoprenoid biosynthesis. E2-PDH is not predicted to be secreted by *S. aureus* as it does not have a secretion sequence. Thus, it is unexpected to see a subunit of this cytoplasmic enzyme complex in the cell-free supernatant of *S. aureus*. In this section, we will discuss the release of lipoyl-E2-PDH by *S. aureus*.

Excretion of Cytoplasmic Proteins.

Our detection methods for identifying lipoylated proteins in the supernatant of *S. aureus* indicates that, of the four cytosolic lipoylated proteins, E2-PDH is the only subunit released by the bacterium (Figure 11). The extracellular detection of lipoyl-E2-PDH is unusual, considering it lacks a discernable secretion sequence and is predominantly thought to function in the cytosol as a component of the PDH complex. However, metabolic enzymes and subunits of metabolic complexes, like PDH, are routinely found in the extracellular environment in numerous bacteria and eukaryotes (347, 348). E2-PDH was found on the surface of *L. monocytogenes,* where it depends on the SecA2 accessory secretion system for surface display (359). Furthermore, E2-PDH is present on the surface of *M. pneumoniae,* where it is hypothesized to bind human plasminogen (392, 393). In prior studies, it was shown that *S. aureus* can

release cytoplasmic proteins into the extracellular environment including E2-PDH (357, 358). This release of cytoplasmic proteins into the extracellular environment correlated with cell division and is linked to the activity of the peptidoglycan modifying enzyme, Atl (357). Not every cytoplasmic protein of *S. aureus* is found extracellularly, suggesting that this phenomenon is specific and not exclusively due to lysis of the bacterial cell. Indeed, our studies support data in literature, as we saw the release of lipoyl-E2-PDH requires Atl and to a lesser extent SecA2, despite the presence of cytosolic lipoyl-E2-PDH in Δ*atl* and Δ*secA2* mutants (Figure 16). The roles of Atl and SecA2 in E2-PDH release are yet to be confirmed through genetic complementation of the Δ*atl* and Δ*secA2* mutant strains. The exact mechanism by which particular cytoplasmic proteins like lipoyl-E2-PDH are selected for extracellular release and then allowed to traverse across the bacterial membrane also needs to be studied. One way to approach this would be to fluorescently tag E2-PDH with a protein such as green fluorescent protein. Then, we could observe the localization dynamics of this tagged E2-PDH during phases of *S. aureus* growth with fluorescence microscopy. Furthermore, protein secretion in bacteria can require the assistance of chaperone proteins. Thus, it is possible that chaperone proteins or other proteins besides the other subunits of PDH interact with E2-PDH to facilitate its release into the extracellular environment.

Surface Display of E2-PDH and GcvH.

It is unknown how cytoplasmic proteins, like E2-PDH, that lack a discernable secretion sequence are released by bacteria. However, what we do know is that, as mentioned previously, other bacteria express cytoplasmic proteins on their surface. Our data confirm this happens in *S. aureus*, as we saw E2-PDH on the cell surface (Figure

15). In addition to E2-PDH, we find GcvH on the surface though we cannot detect it in the supernatant by immunoblot. It needs to be tested if the presence of E2-PDH and GcvH on the surface changes during the growth of *S. aureus*. Moreover, we wondered if the lipoyl moiety of E2-PDH is necessary for its release into the extracellular environment. However, our data indicates that the lipoyl moiety of E2-PDH and GcvH do not appear to be necessary for surface display, as we can detect both E2-PDH and GcvH on the surface a Δ*lipA* mutant (Figure 15). We surmise that both E2-PDH and GcvH on the surface of a Δ*lipA* mutant are modified with the medium chain fatty acid precursor to lipoic acid, octanoic acid. It is possible that the modification of octanoic acid on E2-PDH and GcvH facilitates their localization to the surface. We could test this possibility by substituting alanine for the conserved modified lysine residues of E2-PDH and GcvH and then assess the surface display of the non-modified E2-PDH and GcvH. If the modification of octanoic acid is necessary for the surface display of E2-PDH and GcvH, then we expect mutation of the modified conserved lysine residues would disrupt surface display. Along these lines, it remains to be explored if a Δ*lipA* mutant could release non-lipoyl-E2-PDH into the extracellular environment or if E2-PDH stays associated with the bacterial surface. More sensitive detection methods, such as mass spectrometry of exoproteins, could reveal if other lipoyl-proteins are present in the supernatant and if a Δ*lipA* mutant releases non-lipoyl modified versions of E2-PDH.

Why E2-PDH?

Out of the four lipoyl-proteins in the cytosol of *S. aureus*, we identified that only lipoyl-E2-PDH is released during growth in our conditions. PDH is one of the largest cellular machines in Gram-positive bacteria, as it contains 60 copies of E1 and E2

subunits, and 6-12 copies of the E3 subunit (365, 402). This is in contrast to the other lipoic acid modified subunits of enzyme complexes that contain fewer copies (~24 for E2-OGDH) of the lipoylated subunits (361). Thus, the high abundance of lipoyl-E2-PDH copies in the cytosol may explain why this protein is the primary released lipoyl-protein. The higher abundance of lipoyl-E2-PDH in the cytosol is evident in our immunoblots, as E2-PDH is the most intense band on the immunoblot (Figure 11A).

Our studies determined that a synthetic tripeptide containing the lipoyl-lysine residue, $DK^{L}A$, but not the unmodified tripeptide, DKA, is sufficient to restrict macrophage activation (Figure 22 and 23). This indicates the lipoyl moiety is required for immune suppression rather than a unique property of the lipoyl-E2-PDH protein itself. Since a lipoyl modification is sufficient for blunting macrophage activation, we believe that it is possible for any lipoyl protein, where the domain is accessible, to restrict macrophage activation. Future studies will need to test if any of the other three lipoyl-proteins of *S. aureus* (E2-OGDH, E2-BCODH, and GcvH) can confer immunosuppressive properties.

Concluding Remarks.

In summary, *S. aureus* is able to release lipoyl-E2-PDH into the supernatant through an unknown mechanism. Because lipoyl-E2-PDH is an easily detectable protein, it can serve as a tool to more carefully delineate the process by which bacteria, like *S. aureus,* release a subset of cytoplasmic proteins without a discernable secretion signal.

Lipoic Acid and Lipoyl-Protein Suppression of Macrophage Activation

In this thesis, we provide data to support the hypothesis that bacterial derived lipoic acid can suppress the activation of innate immune cells. Lipoic acid derived from bacteria encounters immune cells in a form that is covalently attached to conserved lysine residues in the E2 subunit of PDH. Our data indicate that free lipoic acid and protein-linked lipoic acid confer different immunosuppressive properties on macrophages. Therefore, free lipoic acid and lipoyl-proteins may use different methods to exert their immunosuppressive functions on macrophages. In this section, we speculate on what the mechanisms for free lipoic acid and lipoyl-protein based immunosuppression could be.

Lipoic Acid Suppression of BMM Activation.

Millimolar concentrations of free lipoic are needed to suppress the activation of BMMs by either *S. aureus* supernatant, or TLR1/2, TLR2/6, TLR4, and TLR5 agonists (Figure 17-19). We only tested if free lipoic acid could block the activation of TLRs present on the surface of macrophages. However, due to the broad suppressive effects of lipoic acid, we expect that it could likely block other TLR activation pathways or other PRRs expressed by macrophages. To assess if free lipoic acid can limit the activation of other TLRs, such as TLR3, TLR7, TLR8, and TLR9, which are expressed intracellularly, one could stimulate macrophages with TLR3/7/8/9 agonists in the presence or absence of free lipoic acid and determine macrophage activation by cytokine secretion. Moreover, it would be valuable to test if free lipoic acid can block the activation of other inflammatory pathways, such as the inflammasome, by stimulating macrophages with inflammasome agonists in the presence of free lipoic acid.

Besides TLR based suppression, we found that free lipoic acid reduces the surface expression of TLR2 and CD86 on BMMs (Figure 24). Our data indicate that free lipoic acid reduced expression of only certain surface molecules, like TLR2 and CD86 but not TLR1 nor CD80. Therefore, we hypothesize that there are other markers of BMMs that may be regulated by lipoic acid through an undetermined mechanism. RNAseq could be a useful approach to understand the broad modulatory effects of free lipoic acid on expression of the full range of BMM transcripts or those of other innate immune cells. Data from RNAseq could determine if free lipoic acid can polarize macrophages to a more pro-inflammatory or anti-inflammatory state. Moreover, others found that high concentrations of free lipoic acid reduce the respiratory burst of neutrophils through its antioxidant properties and block the translocation of the transcription factor, NFκB, to the nucleus (380-383). Also, free lipoic acid can activate the phosphoinositide 3-kinase/Akt signaling pathway to reduce inflammatory cytokine production (384). The perturbation of respiratory burst, blockade of NFκB translocation, and activation of the phosphoinositide 3-kinase/Akt signaling pathway all occur internally within immune cells. Because free lipoic acid can block these internal processes of inflammation, it must be able to enter eukaryotic cells to do so. Little insight has been made into how free lipoic acid or lipoyl proteins can enter into eukaryotic cells. In enterocytes and hepatocytes, the sodium-dependent multivitamin transport system (SMVT) transports biotin and patothenate and is reported to be used by lipoic acid or lipoyl proteins to enter these eukaryotic cells (403-405). It is unknown if macrophages express or utilize the SMVT system; thus, free lipoic acid may gain entry

into macrophages by other means, such as passive diffusion, which would necessitate the high concentrations needed for immunosuppression in our studies.

Lipoyl-E2-PDH Restriction of BMM Activation.

In contrast to free lipoic acid, which can limit the activation of BMMs through multiple TLRs, we found that purified lipoyl-E2-PDH limitsTLR1/2 activation of macrophages by Pam3CSK4 (Figure 22). For free lipoic acid to exert its TLR-restrictive function, millimolar quantities were needed. In contrast, nanomolar quantities of lipoyl-E2-PDH or $DK^{L}A$ were sufficient to reduce TLR1/2 activation of BMMs. We hypothesize that a 1000-fold less lipoyl-protein is required for immunosuppression compared to free lipoic acid possibly due to the hydrophobic nature of free lipoic acid. The protein-bound form of lipoic acid would be more stable in solution and could access the macrophage more easily compared to hydrophobic free lipoic acid. Moreover, free lipoic acid could possibly diffuse across cellular membranes where it is then attached to host metabolic proteins, whereas the protein or peptide-bound form cannot readily do so.

TLR2 Activation by *S. aureus*.

To speculate about why lipoyl-E2-PDH only blocks TLR1/2 activation of BMMs, we need to revisit how the innate immune system mainly recognizes *S. aureus*. *S. aureus* produces numerous PAMPs that are recognized by TLR2 like peptidoglycan and lipoteichoic acid (132, 163, 164). However, the biological relevance of these PAMPs is questioned as the concentrations of peptidoglycan and lipoteichoic acid needed to activate TLR2 are not physiological (406). Treatment of peptidoglycan purification preparations with hydrofluoric acid to degrade LTA and lipoproteins completely abrogates the TLR2-activating effects of this purified peptidoglycan (165). Similarly,

treatment of *S. aureus* cell wall components with lipase to degrade the lipoproteins also abrogated the TLR2 activating ability of the purified cell wall fractions (166, 167). The consensus for *S. aureus*-based TLR2 activation is that lipoproteins are the most potent PAMPs that activate TLR2. These abundant lipoproteins from *S. aureus* can be diacylated or triacylated and are recognized by TLR1/2 and TLR2/6, respectively (158). *S. aureus* is reported to predominantly synthesize lipoproteins in their triacylated form in standard growth conditions (160, 161). Thus, TLR1/2 heterodimerization is a presumed major pathway of immune activation in *S. aureus*, necessitating adaptations by this pathogen to overcome TLR1/2 recognition.

TLR1/2 Restriction by Lipoyl-E2-PDH.

Triacylated lipoproteins and peptides bind to TLR1 and TLR2 via interactions of the amide-linked acyl chain with TLR1 and the cysteine-linked diacylglycerol with TLR2 (157, 162). Lipoyl-PDH and lipoyl peptides suppress macrophage activation by Pam3CSK4, but not Pam2CSK4, suggesting a mechanism of blockade that is specific to TLR1/2. We found that the lipoyl moiety on $DK^{L}A$ is necessary to block the TLR1/2 activation by the native triacylated lipoprotein SitC from *S. aureus* (Figure 23). The crystal structure of TLR1/2 with Pam3CSK4 revealed a hydrophobic binding pocket in TLR1 that interacts with the amide bound lipid of Pam3CSK4 (157). This hydrophobic interaction is reminiscent of how amide-linked lipoic acid binds within the hydrophobic pocket of E1 subunits (407, 408). This is in contrast to the binding pocket of TLR6, which is much shorter and is truncated by bulky phenylalanine side chains (162). Furthermore, TLR1 is thought to preferentially bind to peptide-bound medium chain fatty acids (> 6 carbons), resulting in activation of immune cells (409-411). We surmise that

the lipid-like structure of lipoic acid may facilitate E2-PDH and $DK^{L}A$ binding in the TLR1 lipid binding pocket in order to compete with triacylated lipoproteins/peptides to prevent TLR1/2 activation. We tested this hypothesis by assessing if $DK^{L}A$ but not DKA could reduce the binding of Pam3CSK4 to TLR1/2. Using an enzyme-linked immunosorbent assay, we found that high molar excess concentrations (~20 times) of $DK^{L}A$, but not DKA, were able to reproducibly block Pam3CSK4 binding to TLR1/2 (Figure 25). However, upon diluting out the competing tripeptides, we experienced variability between technical and biological replicates. This perhaps is due to lack of optimal dimerization between recombinant TLR1 and TLR2, which could lower the binding efficacy of Pam3CSK4 in the various replicates. Furthermore, this approach fails to distinguish if blocking of Pam3CKS4 binding is occurring in the ligand binding site of TLR1 or TLR2. We suggest that more sensitive biochemical approaches such as isothermal titration calorimetry, using only TLR1 or TLR2 with $DK^{L}A$ or DKA to measure binding events could decipher if the lipoyl moiety binds to TLR1 or TLR2. To determine if the lipoyl moiety binds within the pocket of TLR1, we could systematically mutate residues that comprise the binding pocket of TLR1 and assess by isothermal titration calorimetry if binding between $DK^{L}A$ with TLR1 still occurs. Also, if isothermal titration calorimetry indicates an interaction between TLR1 and $DK^{L}A$, we could perform protein X-ray crystallography of TLR1 co-crystallized with $DK^{L}A$ to see where $DK^{L}A$ may be binding.

The biologically active form of lipoic acid is not a linear fatty acid as it contains a dithiolane ring. This dithiolane ring may sterically hinder the insertion of lipoic acid within the TLR1 binding pocket. However, the disulfide bond in the dithiolane ring can be

reduced in certain conditions, breaking up the ring structure in the head group of lipoic acid (360). Although the extracellular environment is thought to be mainly oxidizing, the effect of the redox state of the lipoyl moiety on proteins to confer immunosuppressive functions needs to be considered. To test this, we could treat $DK^{L}A$ with a reducing agent such as dithiothreitol and assess by isothermal titration calorimetry the difference of binding between dithiothreitol treated and untreated $DK^{L}A$ with TLR1.

Concluding Remarks.

Free lipoic acid and protein-bound lipoic acid derived from bacteria confer different immunosuppressive functions. We found that free lipoic acid can broadly suppress surface TLR activation by macrophages, as well as modulate the surface expression levels of certain markers on macrophages. This is in contrast to lipoyl-E2-PDH, which we found only blocks TLR1/2 activation. Future studies will need to be conducted to determine how free lipoic acid can exert its broad anti-inflammatory activities on macrophages. Furthermore, we need to test how lipoyl-E2-PDH and the lipoyl-peptide $DK^{L}A$ only restricts TLR1/2 activation of macrophages.

Breadth of Lipoic Acid Synthesis Dependent Suppression of Immune Cells

Though macrophages were used throughout this thesis, we observed that a Δ*lipA* mutant increased the activation of neutrophils as well as dendritic cells. Since lipoyl-proteins restrict TLR1/2 activation, any cell that expresses TLR1/2, such as neutrophils and dendritic cells, may be modulated by LipA activity. Other innate immune cells that express TLR1/2 need to be tested to determine if their functions are also modulated by LipA-mediated mechanisms. Additionally, non-immune cells such as keratinocytes in the skin or epithelial cells can express TLR1/2 (412). Therefore, it would be interesting

to assess if activity of LipA modulates functions of these barrier cells that can encounter *S. aureus* during an infection. This could be tested by treating keratinocytes with supernatant from a Δ*lipA* mutant and then measure cytokine secretion as a readout of activation.

Use of lipoic acid as cofactor in PDH is conserved in all kingdoms of life, though some bacterial species such as *H. pylori* do not use lipoic acid as a metabolic cofactor. It is unknown if lipoic acid synthesis in other Gram-positive or Gram-negative pathogens confers immunosuppressive functions to facilitate pathogenesis. Given the conservation of lipoic acid, we posit that any bacterial pathogen that activates the innate immune system through TLR1/2 and uses lipoic acid as a metabolic cofactor could use it a mechanism to evade TLR1/2 activation. However, the ability of lipoyl-E2-PDH or lipoyl-proteins to moonlight depends on the extracellular presence of lipoylated metabolic proteins. As mentioned previously, E2-PDH is found on the surface of *L. monocytogenes* and *M. pneumoniae*. It is unknown if surface-associated E2-PDH is ever released from the surface of these bacteria into the extracellular environment, like we saw with *S. aureus*. Thus, we need to assess if other bacteria, such as *L. monocytogenes* and *M. pneumoniae*, release lipoylated-E2-PDH or other lipoyl-proteins into the extracellular environment during growth.

Other TLR2-based Evasion Mechanisms.

S. aureus has evolved in other ways to evade TLR2 recognition by the innate immune system. For example, the superantigen-like protein SSL3 is known to bind to the extracellular domain of TLR2 and function as an antagonist (276). Additionally, recent work conducted by Xi Chen in the Alonzo laboratory identified that the glycerol

ester hydrolase (Geh) of *S. aureus* prevents activation of macrophages by both diacylated and triacylated lipopeptides likely through cleavage of the two ester-bound lipid chains in the lipopeptides (413). The activity of SSL3, Geh, and LipA all seem to mask the TLR2-dependent activation of innate immune cells through slightly different mechanisms. For example, Geh only cleaves ester-bound lipid chains in triacylated lipoproteins, which are recognized by TLR2. We believe that the lipoyl moiety interferes with TLR1 recognition of the amide-linked lipid chain of the triacylated lipoprotein. Therefore, the activities of Geh and LipA are likely both important for blocking TLR2-based recognition of *S. aureus*. Due to the broad immunosuppressive functions of lipoic acid, we believe that LipA could alter the pathogenesis of *S. aureus* in a non-TLR2 dependent manner. We need to determine if a Δ*lipA* mutant is compromised for infection in TLR2 knockout animals as we know that a Δ*geh* mutant can colonize TLR2 knockout animals to the same level as WT *S. aureus* (413). The combined contribution of all three known TLR2-based evasion mechanisms in *S. aureus* during infection needs to be further explored. This could be assessed by creating a triple mutant strain of *S. aureus* that contains deletions of the genes that encode for LipA, Geh, and SSL3 and assessing infection outcomes.

Concluding Remarks.

In this thesis, we primarily focused on how lipoic acid synthesis in *S. aureus* suppresses the activation of macrophages. This finding could have broad implications in the sense that many bacterial species use lipoic acid as a metabolic cofactor. Thus it is possible that other bacteria could use lipoic acid as means to dampen macrophage activation. Furthermore, other cells in the innate immune system can recognize and

become activated by *S. aureus*. Though we predominantly use macrophages in this thesis, other cells that express TLR1/2 could be blocked by lipoyl protein production. Lastly, *S. aureus* has more than one way to block TLR2 activation by innate immunity. It needs to be considered how other TLR2 evasion of mechanisms work either individually or together in the context of infection to evade the innate immune system.

Importance of Lipoic Acid Synthesis in *S. aureus* Pathogenesis

An important outcome of this thesis was our ability to demonstrate that lipoic acid synthesis can influence the virulence of *S. aureus* through its immunosuppressive abilities. Although lipoic acid synthesis is intimately linked to bacterial metabolism, the ability of lipoic acid to dampen macrophage antibacterial activities is crucial to the ability of *S. aureus* to survive in the host. In this section, we discuss the implications of lipoic acid synthesis in promoting *S. aureus* pathogenesis.

Inflammation Dynamics in Δ*lipA* Mutant-Infected Mice.

A Δ*lipA* mutant elicited heightened levels of CCL3 and CCL4 in the serum early in infection and greater proportions of activated macrophages ($CCR5^{+}$ IA/IE^{hi}) at the site of infection were not seen until later in the infection time-course (Figure 26 and 27). However, CCL3 and CCL4 levels were indistinguishable later in infection. We posit that the early increase in macrophage chemokines is likely a meaningful early signature that promotes the enhanced recruitment and activation of macrophages seen at 72 hours in Δ*lipA*-infected animals. At later time points of infection, when many Δ*lipA*-infected mice have undetectable infection, the effects of lipoyl-E2-PDH on chemokine secretion are less clear.

During infection, circulating monocytes in the blood are recruited into the peritoneal cavity and differentiate into F4/80-expressing macrophages (111). These recruited monocytes that differentiate into macrophages are recruited by the chemokine CCL2, and these cells also express the CCR2 receptor (114, 115). We did not test for CCL2 levels in the serum of Δ*lipA* mutant-infected animals nor assess CCR2 levels on the macrophage population at the site of infection. Though we see differences in the proportion of pro-inflammatory macrophages during infection, at both early and later stages of infection, the total number of macrophages, neutrophils, and dendritic cells were not different between the infection groups. These data are somewhat counterintuitive as presence of macrophage chemokines CCL3 and CCL4 in the serum would presumably recruit more macrophages and other innate immune cells to the site of infection with a Δ*lipA* mutant. Perhaps our assessment of immune cell numbers at 16- or 72-hours post-infection failed to capture the proper timeframe in which increased cell numbers are present in Δ*lipA* mutant-infected animals if at all. We can test some of these ideas by assessing CCR2 levels on macrophages and CCL2 levels in the serum after infection with a Δ*lipA* mutant, and determine cell counts of the immune cells present earlier than 16 hours post-infection.

Activated Macrophages by a Δ*lipA* Mutant Control Infection.

Mice infected with a Δ*lipA* mutant of *S. aureus* more readily clear infection than mice infected with WT *S. aureus* (Figure 30). The clearance of bacteria in Δ*lipA* mutant-infected animals correlated with the presence of greater proportions of activated macrophages. Upon isolation, these cells exhibited a greater ability to limit bacterial growth ex vivo (Figure 33). Using clodronate to deplete mice of macrophages, we

determined that the attenuation of a Δ*lipA* mutant during peritoneal infection is mediated almost exclusively by activated macrophages (Figure 32). This was surprising, as we surmised a proportion of the virulence defect of a Δ*lipA* mutant was derived from compromised metabolism due to lipoic acid limitation (373). During bloodstream infection, *S. aureus* mutants with defects in bacterial lipoic acid synthesis and salvage lead to tissue-specific virulence defects where infection of the kidney depends on lipoic acid salvage enzymes, but infection of the heart requires LipA (373). These observations suggest there is varied dependency on *de novo* lipoic acid synthesis for *S. aureus* survival in different tissue sites. Although virulence defects in the heart were previously attributed to lipoic acid auxotrophy, data in this thesis suggest the alternative possibility that LipA-dependent enhancement of antimicrobial innate immunity promotes infection persistence. To test this, we could systemically infect mice that are depleted of macrophages through treatment with liposomes containing clodronate and then measure the bacterial loads in the heart. We found that LipA is not necessary for bacterial survival in the peritoneal cavity in the absence of macrophages (Figure 32B and 32C). We surmise that either an alternative metabolism takes over to allow survival in the absence of lipoic acid, or that sufficient trace lipoic acid is available to maintain metabolic activity (414-417). Incorporation of trace lipoic acid, while sufficient to maintain growth, appears to be insufficient to suppress immune responses in macrophage depleted mice.

Clodronate Depletion.

To deplete mice of macrophages, we administered clodronate-containing liposomes (86, 121, 122). At 72 hours post-infection in the peritoneal cavity of

macrophage depleted mice, we saw complete clearance of bacteria in some animals. Clodronate is used extensively to deplete macrophages, but other cells such as monocytes can also be depleted (418). Neutrophils, on the other hand, are still present in clodronate-treated mice, possibly in even greater amounts after *S. aureus* infection (121). The presence of neutrophils in the peritoneal cavity, given their crucial role in protection from *S. aureus* infection (86, 87), could account for clearance observed in some of the macrophage depleted mice. Though we have noted that lipoic acid synthesis interferes with neutrophil cytokine and chemokine secretion, this did not translate to enhanced clearance of a Δ*lipA* mutant compared to WT in macrophage depleted mice. To assess if neutrophils account for the clearance of bacteria in macrophage depleted mice, we could deplete mice of both macrophages and neutrophils and determine if mice are still able to clear bacteria after infection. Nonetheless, our studies show macrophage activity primarily leads to the virulence defect of a Δ*lipA* mutant.

LipA Activity Modulates Macrophage ROS and RNS.

Our data indicate that macrophages from Δ*lipA* mutant-infected mice are primed to produce higher amounts of ROS and $NO^{\bullet}$. Moreover, inhibition of NADPH oxidase activity by gp91ds-tat and iNOS activity by L-NIL abolished the greater restrictive capacity of macrophages from Δ*lipA* mutant-infected mice. Because both inhibitors abrogate bacterial growth defects when used separately, we assume that NADPH oxidase-derived ROS and iNOS-derived $NO^{\bullet}$ are both required for *S. aureus* growth restriction. It is known that $NO^{\bullet}$ alone is not a highly reactive molecule and has an expansive range of cellular functions (254). Rather, $NO^{\bullet}$ becomes highly reactive when

it is converted to oxidative products such as $ONOO^-$ from superoxide (254). The resulting powerfully reactive $ONOO^-$ leads to microbial destruction by reacting with iron/sulfur metal centers, causing tyrosine nitration, triggering lipid peroxidation, and damaging DNA (237). As such, elimination of either ROS production or $NO^\bullet$ production has the potential to compromise generation of potent antimicrobials, such as $ONOO^-$. We propose a mechanism based on our data where the immunosuppressive effects of lipoic acid synthesis by *S. aureus* leads to reduced generation of the highly antimicrobial RNS derived from NADPH oxidase superoxide and $NO^\bullet$. The assessment of specific RNS species production using boronate-containing fluorescent probes (ESIPT) in macrophages isolated from WT and Δ*lipA*-infected animals needs to be tested, although this may be difficult due to the short half-life of species such as $ONOO^-$ (419, 420).

TLR2 Activation of ROS.

Lipoic acid synthesis is necessary to dampen TLR1/2 activation of BMMs through the release of lipoyl-E2-PDH by WT *S. aureus*. Besides leading to the production of pro-inflammatory cytokines and chemokines, TLR2 can mediate the induction of ROS generation. Recognition of *Mycobacterium tuberculosis* by TLR2 leads to a direct interaction between TLR2 and NADPH oxidase to ultimately stimulate ROS production (421, 422). Similarly, activation of TLR2 by heat-killed *L. monocytogenes* induces an autophagy-associated protein, Rubicon, which interacts with the p22*phox* subunit of NADPH oxidase to aid in its phagosomal trafficking and subsequent superoxide production (423). Furthermore, TLR2 is necessary for efficient NADPH oxidase-dependent killing of *S. aureus* in murine neutrophils (424). Indeed, our data aligns with these studies and suggests that LipA-dependent inhibition of TLR1/2 signaling by lipoyl-

E2-PDH prevents activation of NADPH oxidase and thus ROS generation. This can be tested by treating macrophages with supernatant from a Δ*lipA* mutant and assessing levels of the NADPH oxidase complex proteins by immunoblot.

Effects of Free Lipoic Acid on NADPH Oxidase and iNOS.

In order to activate NADPH oxidase, Akt (protein kinase B) must phosphorylate p47*phox* (425). As mentioned before, high concentrations of free lipoic acid can activate Akt by increasing the levels of phosphorylated Akt (384). Because a Δ*lipA* mutant cannot synthesize lipoic acid, one might assume lower Akt activation and NADPH oxidase activity during infection. Our data does not support this assumption, as we see higher NADPH oxidase-derived ROS in macrophages from Δ*lipA* mutant-infected mice. We know that *S. aureus* derived lipoic acid is bound to proteins; thus, we believe the effects on Akt likely are not manifested in our infection system. In regard to iNOS activity, free lipoic acid can inhibit the induction of iNOS activity by IL-1β at the protein level (385). Thus, a Δ*lipA* mutant is likely more predisposed to activate iNOS activity leading to the observed higher $NO^{\bullet}$ production. To test if a Δ*lipA* mutant may modulate Akt or iNOS activity, we can treat macrophages with supernatant from a Δ*lipA* mutant and then assess levels of phosphorylated Akt and the abundance of iNOS by immunoblot. Finally, free lipoic acid is known to have antioxidant activity that diminishes the respiratory burst of phagocytes (381, 383). Therefore, mice infected with a Δ*lipA* mutant may also be less likely to detoxify macrophage ROS or RNS. The detailed cellular mechanism behind how *S. aureus* lipoic acid synthesis interferes with ROS and RNS generation in macrophages during infection needs to be investigated. To test this, we can first activate macrophages with *S. aureus* supernatant to generate ROS and

RNS and treat these activated macrophages with free lipoic acid or lipoyl-E2-PDH. Then we could use fluorescent probes that measure ROS such as Cellrox or perform a Griess test to measure RNS production to determine if free lipoic acid or lipoyl-E2-PDH treatment modulates ROS or RNS levels.

mROS Inhibition of *S. aureus*.

Upon stimulation of macrophages through TLR1/2/4, mitochondria are recruited to the phagosome and can produce mROS which are known to contribute to the killing of *S. aureus* within the phagosome (248, 251, 252). Curiously, we found that mROS do not contribute to the ability of macrophages from Δ*lipA*-infected mice to restrict bacterial outgrowth. $NO^{\bullet}$ and the resulting $ONOO^{-}$ are capable of interfering with the mitochondrial electron transport chain and perturb mitochondria respiration (254). However, this disruption of electron transfer by $NO^{\bullet}$ can markedly increase the leakage of electrons resulting in enhanced formation of superoxide in the mitochondrial matrix (254). In a recent study, it was found that alpha-hemolysin activates the inflammasome in macrophages, leading to sequestration of mitochondria away from the phagosomes (252). These authors believe that the failure of mitochondria to localize and deliver mROS into the phagosome contributes to *S. aureus* survival in macrophages (252). Thus, it is possible the secretion of alpha-hemolysin could interfere with mROS-mediated killing during infection in our ex vivo survival experiments. Nonetheless, we saw that mROS production in macrophages contributed to growth restriction of *S. aureus* (Figure 36A), but our data suggests that the greater ROS-related restrictive function of macrophages from Δ*lipA*-infected mice is mediated by NADPH oxidase derived ROS.

Macrophage Restriction of *S. aureus*.

Infection with WT or Δ*lipA S. aureus* elicits macrophages that possess a greater intrinsic ability to restrict growth compared to macrophages from mock-infected mice. Inhibition of mROS, NADPH oxidase or iNOS in macrophages from *S. aureus*-infected mice (WT or Δ*lipA*) still retain their greater restrictive capacity relative to the macrophages from mock-infected mice. Thus, *S. aureus* infection elicits macrophages that upon isolation and re-infection are more predisposed to produce greater ROS from the mitochondria or NADPH oxidase and RNS from iNOS activity that coalesce to hinder bacterial growth. In each instance where one main source of antimicrobial activity is blocked (ROS, mROS, or RNS), the other two pathways are sufficient to hinder bacteria growth. However, only upon treatment of macrophages with DPI, which blocks all ROS production and iNOS activity through off-target effects (398, 426), do we see no differences in growth restrictive function between *S. aureus* elicited macrophages or macrophages from mock-infected mice (Figure 35). These data highlight how *S. aureus* infection elicits macrophages that have ROS and RNS dependent restrictive functions.

A Δ*lipA* Mutant Fails to Prime the Adaptive Immune System

Macrophages play a major role in the activation of the adaptive immune system through production of cytokines and chemokines that regulate T cell function and facilitate dendritic cell maturation, leading to antigen presentation and induction of adaptive immunity (90, 427). Despite the improved activation of innate immunity and microbial clearance after infection with a Δ*lipA* mutant, we found that prior infection failed to protect the host or even lead to more severe infection after secondary challenge. We suspect that the explanation for such poor immunity to infection centers

on the fact that *S. aureus* is destroyed too rapidly after infection with a Δ*lipA* mutant, a consequence of improved macrophage activation. The robust and destructive oxidative burst of macrophages interferes with optimal antigen presentation due to rapid phagolysosome fusion and destruction of antigenic peptides, lowering their ability to optimally present antigen (427). This contrasts with dendritic cells, which have drastically different phagosomal environments. Dendritic cell phagosomes are less destructive and can conserve antigenic information from engulfed pathogens thereby promoting efficient antigen presentation (427). Studies on early antibiotic intervention in *Salmonella* and *Chlamydia* infections found that early administration shortened the duration of antigen presentation, leading to poor protective memory (428). This observation supports our hypothesis that activated macrophages destroy antigen too quickly during infection with a Δ*lipA* mutant, leading to poor protective memory. Our data also demonstrate that $NO^{\bullet}$ production is increased upon infection with a Δ*lipA* mutant, which is in part responsible for the antimicrobial function of recruited macrophages. Beyond its importance in the generation of RNS, $NO^{\bullet}$ has diverse signaling functions that can dramatically affect adaptive immune responses such as inhibition of T cell proliferation (429-431). Thus, it is possible that the greater $NO^{\bullet}$ produced by macrophages during infection with a Δ*lipA* mutant may interfere with optimal T cell proliferation. Whatever the ultimate mechanism, what seems clear is that improved activation of innate immune responses is unable to facilitate acquired immunity to *S. aureus* infection in mice.

Summary

In this thesis, we provided evidence for a novel *S. aureus* macrophage evasion mechanism. We found that synthesis of the metabolic cofactor lipoic acid by LipA is necessary for the suppression of macrophage inflammatory responses. This is mediated by the release of lipoyl-E2-PDH by *S. aureus* where it moonlights by restricting the TLR1/2 activation by triacylated lipoproteins of macrophages. Moreover, *S. aureus* lipoyl-protein production in vivo results in impaired activation of inflammatory ROS and RNS responses of macrophages and leads to reduced host control of bacterial growth and dissemination. Additionally, increased macrophage responses do not necessarily translate to protection against reinfection.

Bacterial pathogens are a significant cause of mortality and morbidity in human health. Modern medicine is faced with a crisis concerning the development of bacterial resistance to common treatment methods such as antibiotics. It is imperative to develop new therapeutics that target novel bacterial targets that do not lead to resistance. To begin to undercover novel therapeutics against bacterial pathogens, we must fundamentally understand how these pathogens interact with the host to cause disease. Thus, the scope of this thesis encompassed three main objectives: (1) to understand how bacteria cause disease; (2) to study how the host responds to bacterial disease; and (3) to uncover novel mechanisms by which bacterial pathogens evade the host response to infection. By understanding the interaction between the host and the pathogen, we can potentially identify new means to treat these infections. In line with these objectives, the work in this thesis has broadened our understanding that bacterial metabolism is closely linked with the evasion of innate immune responses by virtue of

the moonlighting activity of a metabolic protein. The metabolic disadvantage coupled with the observed heightened innate immune response associated with a *S. aureus* strain containing a mutation in the gene encoding for the lipoic acid synthetase, highlights a possibly lucrative therapeutic target for *S. aureus* infections that may cripple bacterial replication but still enhance host immunity. This work could have broad applications to other bacterial pathogens as well given that lipoic acid is a highly conserved metabolic cofactor in many human pathogens.

APPENDIX A

PERMISSION TO REPRODUCE COPYRIGHTED CONTENT

Figure 42. Permission to Reproduce Copyrighted Content. Reprinted with permission from Spalding and Prigge, 2010 (360). See figure 2A.

REFERENCE LIST

1. Ogston A. 1880. Ueber Abscesse. Arch Klin Chir. 25:588-600.

2. Newsom S. 2008. Ogston's coccus. Journal of Hospital Infection. 70:369-372.

3. Mehraj J, Witte W, Akmatov MK, Layer F, Werner G, Krause G. 2016. Epidemiology of *Staphylococcus aureus* nasal carriage patterns in the community. Current Topics in Microbiology and Immunology. 398:55-87.

4. Kluytmans J, Belkum A, Verbrugh H. 1997. Nasal carriage of *Staphylococcus aureus*: epidemiology, underlying mechanisms, and associated risks. Clinical Microbiology Reviews. 10:505-520.

5. Turner NA, Sharma-Kuinkel BK, Maskarinec SA, Eichenberger EM, Shah PP, Carugati M, Holland TL, Fowler VGJ. 2019. Methicillin-resistant *Staphylococcus aureus*: an overview of basic and clinical research. Nature Reviews. Microbiology. 17:203-218.

6. Currie A, Davis L, Odrobina E, Waldman S, White D, Tomassi J, Katz KC. 2008. Sensitivities of Nasal and Rectal Swabs for Detection of Methicillin-Resistant *Staphylococcus aureus* Colonization in an Active Surveillance Program. Journal of Clinical Microbiology. 46:3101-3103.

7. Batra R, Eziefula A, Wyncoll D, Edgeworth J. 2008. Throat and rectal swabs may have an important role in MRSA screening of critically ill patients. Intensive Care Med. 34:1703-1706.

8. Mermel LA, Cartony JM, Covington P, Maxey G, Morse D. 2011. Methicillin-Resistant *Staphylococcus aureus* Colonization at Different Body Sites: a Prospective, Quantitative Analysis. Journal of Clinical Microbiology. 49:1119-1121.

9. Popovich KJ, Aroutcheva A, Hota B, Beavis KG, Hayden MK, Weinstein RA. 2014. Anatomic Sites of Colonization with Community-Associated Methicillin-Resistant *Staphylococcus aureus*. Infection Control and Hospital Epidemiology. 35:1192-1194.

10. Ehrenkranz JN. 1964. Person-to-Person Transmission of *Staphylococcus aureus*. The New England Journal of Medicine. 271:225-23.

11. van Hal SJ, Jensen SO, Vaska VL, Espedido BA, Paterson DL, Gosbell IB. 2012. Predictors of Mortality in *Staphylococcus aureus* Bacteremia. Clinical Microbiology Reviews. 25:362-386.

12. Malani PN. 2014. National burden of invasive methicillin-resistant *Staphylococcus aureus* infection. Jama. 311:1438-1439.

13. Kourtis AP, Hatfield K, Baggs J, Mu Y, See I, Epson E, Nadle J, Kainer MA, Dumyati G, Petit S, Ray SM, Ham D, Capers C, Ewing H, Coffin N, McDonald LC, Jernigan J, Cardo D. 2019. Vital Signs: Epidemiology and Recent Trends in Methicillin-Resistant and in Methicillin-Susceptible *Staphylococcus aureus* Bloodstream Infections - United States. MMWR. Morbidity and Mortality Weekly Report. 68:214-219.

14. Barber M, Rozwadowska-Dowzenko M. 1948. Infection by penicillin-resistant staphylococci. Lancet. 2:641-4.

15. Kirby W. 1944. Extraction of a highly potent penicillin inactivator from penicillin resistant staphylococci. Science. 99:452-453.

16. Barber M. 1961. Methicillin-resistant staphylococci. J. Clin. Pathol. 14:385-393.

17. Katayama Y, Ito T, Hiramatsu K. 2000. A New Class of Genetic Element, Staphylococcus Cassette Chromosome mec, Encodes Methicillin Resistance in *Staphylococcus aureus*. Antimicrobial Agents and Chemotherapy. 44:1549-1555.

18. Ito T, Katayama Y, Asada K, Mori N, Tsutsumimoto K, Tiensasitorn c, Hiramatsu K. 2001. Structural Comparison of Three Types of Staphylococcal Cassette Chromosome mec Integrated in the Chromosome in Methicillin-Resistant *Staphylococcus aureus*. Antimicrobial Agents and Chemotherapy. 45:1323-1336.

19. Iandolo JJ, Worrell V, Groicher KH, Qian Y, Tian R, Kenton S, Dorman A, Ji H, Lin S, Loh P, Qi S, Zhu H, Roe BA. 2002. Comparative analysis of the genomes of the temperate bacteriophages Phi 11, Phi 12 and Phi 13 of *Staphylococcus aureus* 8325. Gene. 289:109-118.

20. Weigel LM, Clewell DB, Gill SR, Clark NC, McDougal LK, Flannagan SE, Kolonay JF, Shetty J, Killgore GE, Tenover FC. 2003. Genetic Analysis of a High-Level Vancomycin-Resistant Isolate of *Staphylococcus aureus*. Science. 302:1569-1571.

21. Hiramatsu K, Aritaka N, Hanaki H, Kawasaki S, Hosoda Y, Hori S, Fukuchi Y, Kobayashi I. 1997. Dissemination in Japanese hospitals of strains of *Staphylococcus aureus* heterogeneously resistant to vancomycin. The Lancet. 350:1670-1673.

22. Lentino JR, Narita M, Yu L. 2008. New antimicrobial agents as therapy for resistant gram-positive cocci. Eur J Clin Microbiol Infect Dis. 27:3-15.

23. Pan A, Lorenzotti S, Zoncada A. 2008. Registered and Investigational Drugs for the Treatment of Methicillin-Resistant *Staphylococcus aureus* Infection. Recent Patents on Anti-Infective Drug Discovery. 3:10-33.

24. Anderson SD, Gums JG. 2008. Ceftobiprole: An Extended-Spectrum Anti–Methicillin-Resistant *Staphylococcus aureus* Cephalosporin. Annals of Pharmacotherapy. 42:806-816.

25. Parish D, Scheinfeld N. 2008. Ceftaroline fosamil, a cephalosporin derivative for the potential treatment of MRSA infection. Current Opinion in Investigational Drugs. 9(2):201-9.

26. Chambers HF, DeLeo FR. 2009. Waves of resistance: *Staphylococcus aureus* in the antibiotic era. Nat. Rev. Microbiol. 7:629-641.

27. Enright MC, Day NP, Davies CE, Peacock SJ, Spratt BG. 2000. Multilocus sequence typing for characterization of methicillin-resistant and methicillin-susceptible clones of *Staphylococcus aureus*. Journal of Clinical Microbiology. 38:1008-1015.

28. Edward J. Feil, Bao C. Li, David M. Aanensen, William P. Hanage, Brian G. Spratt. 2004. eBURST: Inferring Patterns of Evolutionary Descent among Clusters of Related Bacterial Genotypes from Multilocus Sequence Typing Data. Journal of Bacteriology. 186:1518-1530.

29. Feil EJ, Cooper JE, Grundmann H, Robinson AD, Enright MC, Berendt T, Peacock SJ, Smith JM, Murphy M, Spratt BG, Moore CE, Day N. 2003. How Clonal Is *Staphylococcus aureus*? Journal of Bacteriology. 185:3307-3316.

30. Planet PJ, Mathema B, Boundy S, Archer G, Narechania A, Chen L, Kreiswirth B. 2016. Architecture of a Species: Phylogenomics of *Staphylococcus aureus*. Trends in Microbiology. 25:153-166.

31. Shopsin B, Gomez M, Montgomery SO, Smith DH, Waddington M, Dodge DE, Bost DA, Riehman M, Naidich S, Kreiswirth BN. 1999. Evaluation of Protein A Gene Polymorphic Region DNA Sequencing for Typing of *Staphylococcus aureus* Strains. Journal of Clinical Microbiology. 37:3556-3563.

32. McDougal LK, Steward CD, Killgore GE, Chaitram JM, McAllister SK, Tenover FC. 2003. Pulsed-Field Gel Electrophoresis Typing of Oxacillin-Resistant *Staphylococcus aureus* Isolates from the United States: Establishing a National Database. Journal of Clinical Microbiology. 41:5113-5120.

33. Murchan S, Aucken HM, O'Neill GL, Ganner M, Cookson BD. 2004. Emergence, Spread, and Characterization of Phage Variants of Epidemic Methicillin-Resistant *Staphylococcus aureus* 16 in England and Wales. Journal of Clinical Microbiology. 42:5154-5160.

34. O'Neill GL, Murchan S, Gil-Setas A, Aucken HM. 2001. Identification and Characterization of Phage Variants of a Strain of Epidemic Methicillin-Resistant *Staphylococcus aureus* (EMRSA-15). Journal of Clinical Microbiology. 39:1540-1548.

35. Tenover FC, Goering RV. 2009. Methicillin-resistant *Staphylococcus aureus* strain USA300: origin and epidemiology. Journal of Antimicrobial Chemotherapy. 64:441-446.

36. Centers for Disease Control And Prevention. 2001. Methicillin-Resistant *Staphylococcus aureus* Skin or Soft Tissue Infections in a State Prison — Mississippi, 2000. Morbidity and Mortality Weekly Report. 50:919-922.

37. Gantz N, Harmon H, Handy J, Gershman K. 2003. Methicillin-Resistant *Staphylococcus aureus* Infections Among Competitive Sports Participants — Colorado, Indiana, Pennsylvania, and Los Angeles County, 2000–2003. Morbidity and Mortality Weekly Report. 52:793-795.

38. John JF, Lindsay JA. 2008. Clones and Drones: Do Variants of Panton-Valentine Leukocidin Extend the Reach of Community-Associated Methicillin-Resistant *Staphylococcus aureus*? The Journal of Infectious Diseases. 197:175-178.

39. van der Mee-Marquet N, Poisson D-, Lavigne J-, Francia T, Tristan A, Vandenesch F, Quentin R, Bertrand X. 2015. The incidence of *Staphylococcus aureus* ST8-USA300 among French pediatric inpatients is rising. Eur J Clin Microbiol Infect Dis. 34:935-942.

40. Glaser P, Martins-Simões P, Villain A, Barbier M, Tristan A, Bouchier C, Ma L, Bes M, Laurent F, Guillemot D, Wirth T, Vandenesch F. 2016. Demography and Intercontinental Spread of the USA300 Community-Acquired Methicillin-Resistant *Staphylococcus aureus* Lineage. mBio. 7:e02183-15.

41. Planet PJ, Diaz L, Kolokotronis S, Narechania A, Reyes J, Xing G, Rincon S, Smith H, Panesso D, Ryan C, Smith DP, Guzman M, Zurita J, Sebra R, Deikus G, Nolan RL, Tenover FC, Weinstock GM, Robinson DA, Arias CA. 2015. Parallel Epidemics of Community-Associated Methicillin-Resistant *Staphylococcus aureus* USA300 Infection in North and South America. The Journal of Infectious Diseases. 212:1874-82.

42. Popovich KJ, Snitkin ES, Hota B, Green SJ, Pirani A, Aroutcheva A, Weinstein RA. 2017. Genomic and Epidemiological Evidence for Community Origins of

Hospital-Onset Methicillin-Resistant *Staphylococcus aureus* Bloodstream Infections. The Journal of Infectious Diseases. 215:1640-1647.

43. Francis JS, Doherty MC, Lopatin U, Johnston CP, Sinha G, Ross T, Cai M, Hansel NN, Perl T, Ticehurst JR, Carroll K, Thomas DL, Nuermberger E, Bartlett JG. 2005. Severe Community-Onset Pneumonia in Healthy Adults Caused by Methicillin-Resistant *Staphylococcus aureus* Carrying the Panton-Valentine Leukocidin Genes. Clinical Infectious Diseases. 40:100-107.

44. Davis SL, Perri MB, Donabedian SM, Manierski C, Singh A, Vager D, Haque NZ, Speirs K, Muder RR, Robinson-Dunn B, Hayden MK, Zervos MJ. 2007. Epidemiology and Outcomes of Community-Associated Methicillin-Resistant *Staphylococcus aureus* Infection. Journal of Clinical Microbiology. 45:1705-1711.

45. Centers for Disease Control and Prevention. 2013. Antibiotic resistance threats in the United States, 2013. Cdc. 1-114.

46. Niyonsaba F, Ogawa H. 2005. Protective roles of the skin against infection: Implication of naturally occurring human antimicrobial agents β-defensins, cathelicidin LL-37 and lysozyme. Journal of Dermatological Science. 40:157-168.

47. Ogawa H, Miyazaki H, Kimura M. 1971. Isolation and Characterization of Human Skin Lysozyme. Journal of Investigative Dermatology. 57:111-116.

48. Dominiecki ME, Weiss J. 1999. Antibacterial Action of Extracellular Mammalian Group IIA Phospholipase A2 against Grossly Clumped *Staphylococcus aureus*. Infection and Immunity. 67:2299-305.

49. Cartron ML, England SR, Chiriac AI, Josten M, Turner R, Rauter Y, Hurd A, Sahl H, Jones S, Foster SJ. 2014. Bactericidal activity of the human skin fatty acid cis-6-hexadecanoic acid on *Staphylococcus aureus*. Antimicrobial Agents and Chemotherapy. 58:3599-3609.

50. Bardan A, Nizet V, Gallo RL. 2004. Antimicrobial peptides and the skin. Expert Opinion on Biological Therapy. 4:543-549.

51. Hamann KJ, Barker RL, Ten RM, Gleich GJ. 1991. The Molecular Biology of Eosinophil Granule Proteins. International Archives of Allergy and Immunology. 94:202-209.

52. Blanchard C, Rothenberg ME. 2009. Biology of the Eosinophil. Adv Immunol. 101:81-121.

53. Kozlowski E, Lee JJ, Kelly AM, Gold JA, Yousefi S, Reichenbach J, Simon H, Gleich GJ, Straumann A, Andina N, Schmid I. 2008. Catapult-like release of

mitochondrial DNA by eosinophils contributes to antibacterial defense. Nature Medicine. 14:949-953.

54. Min B. 2008. Basophils: what they 'can do' versus what they 'actually do'. Nature Immunology. 9:1333-1339.

55. Stone KD, Prussin C, Metcalfe DD. 2010. IgE, mast cells, basophils, and eosinophils. Journal of Allergy and Clinical Immunology, The. 125:S73-80.

56. Baker BS. 2006. The role of microorganisms in atopic dermatitis. 144:1-9.

57. Prince LR, Graham KJ, Connolly J, Anwar S, Ridley R, Sabroe I, Foster SJ, Whyte M. 2012. *Staphylococcus aureus* Induces Eosinophil Cell Death Mediated by α-hemolysin. PLoS One. 7:e31506.

58. Marone G, Tamburini M, Giudizi MG, Biagiotti R, Almerigogna F, Romagnani S. 1987. Mechanism of activation of human basophils by *Staphylococcus aureus* Cowan 1. Infection and Immunity. 55:803-809.

59. Rocha-de-Souza CM, Berent-Maoz B, Mankuta D, Moses AE, Levi-Schaffer F. 2008. Human Mast Cell Activation by *Staphylococcus aureus*: Interleukin-8 and Tumor Necrosis Factor Alpha Release and the Role of Toll-Like Receptor 2 and CD48 Molecules. Infection and Immunity. 76:4489-4497.

60. Abel J, Goldmann O, Ziegler C, Höltje C, Smeltzer MS, Cheung AL, Bruhn D, Rohde M, Medina E. 2011. *Staphylococcus aureus* Evades the Extracellular Antimicrobial Activity of Mast Cells by Promoting Its Own Uptake. Journal of Innate Immunity. 3:495-507.

61. Rönnberg E, Johnzon C, Calounova G, Garcia Faroldi G, Grujic M, Hartmann K, Roers A, Guss B, Lundequist A, Pejler G. 2014. Mast cells are activated by *Staphylococcus aureus* in vitro but do not influence the outcome of intraperitoneal S. aureus infection in vivo. Immunology. 143:155-163.

62. Steinman RM, Cohn ZA. 1973. Identification of a novel cell type in peripheral lymphoid organs of mice. I. Morphology, quantitation, tissue distribution. J Exp Med. 137:1142-62.

63. Steinman RM, Cohn ZA. 1974. Identification of a novel cell type in peripheral lymphoid organs of mice. II. Functional properties in vitro. The Journal of Experimental Medicine. 139:380-397.

64. Théry C, Amigorena, S. 2001. The cell biology of antigen presentation in dendritic cells. 13:45-51.

65. Joffre OP, Segura E, Savina A, Amigorena S. 2012. Cross-presentation by dendritic cells. Nature Reviews. Immunology. 12:557-569.

66. Fujii SI, Liu K, Smith C, Bonito AJ, Steinman RM. 2004. The Linkage of Innate to Adaptive Immunity via Maturing Dendritic Cells In Vivo Requires CD40 Ligation in Addition to Antigen Presentation and CD80/86 Costimulation. Journal of Experimental Medicine. 199:1607-1618.

67. Heufler C, Koch F, Stanzl U, Topar G, Wysocka M, Trinchieri G, Enk A, Steinman RM, Romani N, Schuler G. 1996. Interleukin-12 is produced by dendritic cells and mediates T helper 1 development as well as interferon-γ production by T helper 1 cells. European Journal of Immunology. 26:659-668.

68. Wu X, Xu F. 2014. Dendritic cells during *Staphylococcus aureus* infection: subsets and roles. Journal of Translational Medicine. 12:358.

69. Hong SJ, Kim SK, Ko EB, Yun C, Han SH. 2017. Wall teichoic acid is an essential component of *Staphylococcus aureus* for the induction of human dendritic cell maturation. Molecular Immunology. 81:135-142.

70. Cruciani M, Etna MP, Camilli R, Giacomini E, Percario ZA, Severa M, Sandini S, Rizzo F, Brandi V, Balsamo G, Polticelli F, Affabris E, Pantosti A, Bagnoli F, Coccia EM. 2017. *Staphylococcus aureus* Esx Factors Control Human Dendritic Cell Functions Conditioning Th1/Th17 Response. Frontiers in Cellular and Infection Microbiology. 7:330.

71. Schindler D, Gutierrez MG, Beineke A, Rauter Y, Rohde M, Foster S, Goldman O, Medina E. 2012. Dendritic Cells Are Central Coordinators of the Host Immune Response to *Staphylococcus aureus* Bloodstream Infection. American Journal of Pathology, The. 181:1327-1337.

72. Berends ETM, Zheng X, Zwack EE, Ménager MM, Cammer M, Shopsin B, Torres VJ. 2019. *Staphylococcus aureus* Impairs the Function of and Kills Human Dendritic Cells via the LukAB Toxin. mBio. 10:1918.

73. Borregaard N. 2010. Neutrophils, from Marrow to Microbes. Immunity. 33:657-670.

74. Doeing DC, Borowicz JL, Crockett ET. 2003. Gender dimorphism in differential peripheral blood leukocyte counts in mice using cardiac, tail, foot, and saphenous vein puncture methods. BMC Clinical Pathology. 3:3.

75. Mestas J, Hughes CCW. 2004. Of Mice and Not Men: Differences between Mouse and Human Immunology. The Journal of Immunology. 172:2731-2738.

76. Summers C, Rankin SM, Condliffe AM, Nanak S, Peters MA. 2010. Neutrophil kinetics in health and disease. Trends in Immunology. 31:318-324.

77. Peters AM. 1998. Just How Big is the Pulmonary Granulocyte Pool? Clinical Science. 94:7-19.

78. Haeger M, Cowland JB, Borregaard N. 2010. Neutrophil granules in health and disease. Journal of Internal Medicine. 268:25-34.

79. Galli SJ, Borregaard N, Wynn TA. 2011. Phenotypic and functional plasticity of cells of innate immunity: macrophages, mast cells and neutrophils. Nature Immunology. 12:1035-1044.

80. Colotta F, Re F, Polentarutti N, Sozzani S, Mantovani A. 1992. Modulation of granulocyte survival and programmed cell death by cytokines and bacterial products. Blood. 80:2012-20.

81. Vestweber D. 2007. Adhesion and signaling molecules controlling the transmigration of leukocytes through endothelium. 218:178-196.

82. Zarbock A, Ley K, McEver RP, Hidalgo A. 2011. Leukocyte ligands for endothelial selectins: specialized glycoconjugates that mediate rolling and signaling under flow. Blood. 118:6743-6751.

83. Moore KL, Patel KD, Bruehl RE, Li F, Johnson DA, Lichenstein HS, Cummings RD, Bainton DF, McEver RP. 1995. P-selectin glycoprotein ligand-1 mediates rolling of human neutrophils on P-selectin. The Journal of Cell Biology. 128:661-671.

84. Campbell JJ, Hedrick J, Zlotnik A, Siani MA, Thompson DA, Butcher EC. 1998. Chemokines and the Arrest of Lymphocytes Rolling Under Flow Conditions. Science. 279:381-384.

85. Phillipson M, Heit B, Colarusso P, Liu L, Ballantyne CM, Kubes P. 2006. Intraluminal crawling of neutrophils to emigration sites: a molecularly distinct process from adhesion in the recruitment cascade. Journal of Experimental Medicine. 203:2569-2575.

86. Pollitt EJG, Szkuta PT, Burns N, Foster SJ. 2018. *Staphylococcus aureus* infection dynamics. 14:e1007112.

87. Mölne L, Verdrengh M, Tarkowski A. 2000. Role of Neutrophil Leukocytes in Cutaneous Infection Caused by *Staphylococcus aureus*. Infection and Immunity. 68:6162-6167.

88. Tsuda Y, Takahashi H, Kobayashi M, Hanafusa T, Herndon DN, Suzuki F. 2004. Three Different Neutrophil Subsets Exhibited in Mice with Different Susceptibilities to Infection by Methicillin-Resistant *Staphylococcus aureus*. Immunity. 21:215-226.

89. Metchnikoff E. 1883. Untersuchungen ueber die mesodermalen Phagocyten einiger Wirbeltiere. Biologisches Centralblatt. 3:560-5.

90. Mosser DM, Edwards JP. 2008. Exploring the full spectrum of macrophage activation. Nat. Rev. Immunol. 8:958-969.

91. Okabe Y, Medzhitov R. 2014. Tissue-specific signals control reversible program of localization and functional polarization of macrophages. Cell. 157:832-844.

92. Ginhoux F, Jung S. 2014. Monocytes and macrophages: developmental pathways and tissue homeostasis. Nature Reviews: Immunology. 14:392-404.

93. Epelman S, Lavine K, Randolph G. 2014. Origin and Functions of Tissue Macrophages. Immunity. 41:21-35.

94. Hashimoto D, Chow A, Noizat C, Teo P, Beasley M, Leboeuf M, Becker C, See P, Price J, Lucas D, Greter M, Mortha A, Boyer S, Forsberg E , Tanaka M, van Rooijen N, García-Sastre A, Stanley E , Ginhoux F, Frenette P, Merad M. 2013. Tissue-Resident Macrophages Self-Maintain Locally throughout Adult Life with Minimal Contribution from Circulating Monocytes. Immunity. 38:792-804.

95. Yona S, Kim K, Wolf Y, Mildner A, Varol D, Breker M, Strauss-Ayali D, Viukov S, Guilliams M, Misharin A, Hume D, Perlman H, Malissen B, Zelzer E, Jung S. 2013. Fate Mapping Reveals Origins and Dynamics of Monocytes and Tissue Macrophages under Homeostasis. Immunity. 38:79-91.

96. Sieweke MH, Allen JE. 2013. Beyond Stem Cells: Self-Renewal of Differentiated Macrophages. Science. 342:946.

97. Gautier EL, Shay T, Miller J, Greter M, Jakubzick C, Ivanov S, Helft J, Chow A, Elpek KG, Gordonov S, Mazloom AR, Ma'ayan A, Chua W, Hansen TH, Turley SJ, Merad M, Randolph GJ. 2012. Gene-expression profiles and transcriptional regulatory pathways that underlie the identity and diversity of mouse tissue macrophages. Nature Immunology. 13:1118-1128.

98. Gosselin D, Link VM, Romanoski C, Fonseca G, Eichenfield D, Spann N, Stender J, Chun H, Garner H, Geissmann F, Glass C. 2014. Environment Drives Selection and Function of Enhancers Controlling Tissue-Specific Macrophage Identities. Cell. 159:1327-1340.

99. Lavin Y, Winter D, Blecher-Gonen R, David E, Keren-Shaul H, Merad M, Jung S, Amit I. 2014. Tissue-Resident Macrophage Enhancer Landscapes Are Shaped by the Local Microenvironment. Cell. 159:1312-1326.

100. Gorgani NN, Ma Y, Clark HF. 2008. Gene signatures reflect the marked heterogeneity of tissue-resident macrophages. Immunology and Cell Biology. 86:246-254.

101. Simonet WS, Lacey DL, Boyle WJ. 2003. Osteoclast differentiation and activation. Nature. 423:337-342.

102. Parkhurst C, Yang G, Ninan I, Savas J, Yates J, Lafaille J, Hempstead B, Littman D, Gan W. 2013. Microglia Promote Learning-Dependent Synapse Formation through Brain-Derived Neurotrophic Factor. Cell. 155:1596-1609.

103. Hussell T, Bell TJ. 2014. Alveolar macrophages: plasticity in a tissue-specific context. Nature Reviews: Immunology. 14:81-93.

104. Wardle EN. 1987. Kupffer cells and their function. Liver. 7:63-75.

105. Edelson BT, Mejia C, Frazier WA, Murphy KM, Ise W, Murphy TL, Wilker PR, Kohyama M, Hildner K. 2009. Role for Spi-C in the development of red pulp macrophages and splenic iron homeostasis. Nature. 457:318-321.

106. Cassado ADA, D'Império Lima MR, Bortoluci KR. 2015. Revisiting Mouse Peritoneal Macrophages: Heterogeneity, Development, and Function. Frontiers in Immunology. 6:225.

107. Ghosn E, Cassado AA, Govon GG, Fukuhara T, Yang Y, Monack DM, Bortoluci KR, Almeida SR, Herzenberg LA. 2010. Two Physically, Functionally, and Developmentally Distinct Peritoneal Macrophage Subsets. Proceedings of the National Academy of Sciences of the United States of America. 107:2568-2573.

108. Jenkins SJ, Ruckerl D, Thomas GD, Hewitson JP, Duncan S, Brombacher F, Maizels RM, Hume DA, Allen JE. 2013. IL-4 directly signals tissue-resident macrophages to proliferate beyond homeostatic levels controlled by CSF-1. Journal of Experimental Medicine. 210:2477-2491.

109. Geissmann F, Jung S, Littman DR. 2003. Blood Monocytes Consist of Two Principal Subsets with Distinct Migratory Properties. Immunity. 19:71-82.

110. Passlick B, Flieger D, Ziegler-Heitbrock HW. 1989. Identification and characterization of a novel monocyte subpopulation in human peripheral blood. Blood. 74:2527-34.

111. Randolph GJ, Inaba K, Robbiani DF, Steinman RM, Muller WA. 1999. Differentiation of Phagocytic Monocytes into Lymph Node Dendritic Cells In Vivo. Immunity. 11:753-761.

112. Serbina NV, Jia T, Hohl TM, Pamer EG. 2008. Monocyte-Mediated Defense Against Microbial Pathogens. Annual Review of Immunology. 26:421-452.

113. Avraham-Davidi I, Yona S, Grunewald M, Landsman L, Cochain C, Silvestre JS, Mizrahi H, Faroja M, Strauss-Ayali D, Mack M, Jung S, Keshet E. 2013. On-site education of VEGF-recruited monocytes improves their performance as angiogenic and arteriogenic accessory cells. Journal of Experimental Medicine. 210:2611-2625.

114. Ziegler-Heitbrock L. 2014. Monocyte subsets in man and other species. Cellular Immunology. 289:135-139.

115. Auffray C, Fogg D, Garfa M, Elain G, Join-Lambert O, Kayal S, Sarnacki S, Cumano A, Lauvau G, Geissmann F. 2007. Monitoring of Blood Vessels and Tissues by a Population of Monocytes with Patrolling Behavior. Science. 317:666-670.

116. Mills CD, Kincaid K, Alt JM, Heilman MJ, Hill AM. 2000. M-1/M-2 Macrophages and the Th1/Th2 Paradigm. The Journal of Immunology. 164:6166-6173.

117. Mackaness GB. 1977. Cellular immunity and the parasite. Advances in Experimental Medicine and Biology. 93:65-73.

118. Gordon S. 2003. Alternative activation of macrophages. Nature Reviews Immunology. 3:23-35.

119. Cao Q, Wang Y, Zheng D, Sun Y, Wang Y, Lee VWS, Zheng G, Tan TK, Ince J, Alexander SI, Harris DCH. 2010. IL-10/TGF-beta-modified macrophages induce regulatory T cells and protect against adriamycin nephrosis. Journal of the American Society of Nephrology: JASN. 21:933-942.

120. Stout RD, Jiang C, Matta B, Tietzel I, Watkins SK, Suttles J. 2005. Macrophages Sequentially Change Their Functional Phenotype in Response to Changes in Microenvironmental Influences. The Journal of Immunology. 175:342-349.

121. Brown AF, Murphy AG, Lalor SJ, Leech JM, O'Keeffe KM, Mac Aogáin M, O'Halloran DP, Lacey KA, Tavakol M, Hearnden CH, Fitzgerald-Hughes D, Humphreys H, Fennell JP, Wamel W, Foster TJ, Geoghegan JA, Lavelle EC, Rogers TR, McLoughlin RM. 2015. Memory Th1 Cells Are Protective in Invasive *Staphylococcus aureus* Infection. PLoS Pathogens. 11:e1005226.

122. Martin FJ, Parker D, Harfenist BS, Soong G, Prince A. 2011. Participation of CD11c+ Leukocytes in Methicillin-Resistant *Staphylococcus aureus* Clearance from the Lung. Infection and Immunity. 79:1898-1904.

123. Flannagan RS, Heit B, Heinrichs DE. 2016. Intracellular replication of *Staphylococcus aureus* in mature phagolysosomes in macrophages precedes host cell death, and bacterial escape and dissemination. Cellular Microbiology. 18:514-535.

124. Kubica M, Guzik K, Koziel J, Zarebski M, Richter W, Gajkowska B, Golda A, Maciag-Gudowska A, Brix K, Shaw L, Foster T, Potempa J. 2008. A Potential New Pathway for *Staphylococcus aureus* Dissemination: The Silent Survival of S. aureus Phagocytosed by Human Monocyte-Derived Macrophages. PLoS One. 3:e1409.

125. Li C, Wu Y, Riehle A, Ma J, Kamler M, Gulbins E, Grassme H. 2017. *Staphylococcus aureus* Survives in Cystic Fibrosis Macrophages, Forming a Reservoir for Chronic Pneumonia. Infection and Immunity. 85:e00883-16.

126. Chan LC, Rossetti M, Miller LS, Filler SG, Johnson CW, Lee HK, Wang H, Gjertson D, Fowler VG, Reed EF, Yeaman MR. 2018. Protective immunity in recurrent *Staphylococcus aureus* infection reflects localized immune signatures and macrophage-conferred memory. Proceedings of the National Academy of Sciences of the United States of America. 115:e11119.

127. Akira S, Uematsu S, Takeuchi O. 2006. Pathogen Recognition and Innate Immunity. Cell. 124:783-801.

128. Lemaitre B, Nicolas E, Michaut L, Reichhart J, Hoffmann JA. 1996. The Dorsoventral Regulatory Gene Cassette spätzle/Toll/cactus Controls the Potent Antifungal Response in Drosophila Adults. Cell. 86:973-983.

129. Takeuchi O, Sato S, Horiuchi T, Hoshino K, Takeda K, Dong Z, Modlin RL, Akira S. 2002. Cutting Edge: Role of Toll-Like Receptor 1 in Mediating Immune Response to Microbial Lipoproteins. The Journal of Immunology. 169:10-14.

130. Aderem A, Underhill DM, Stevens A, Hajjar AM, Wilson CB, Bassetti M, Ozinsky A. 1999. The Toll-like receptor 2 is recruited to macrophage phagosomes and discriminates between pathogens. Nature. 401:811-815.

131. Schwandner R, Dziarski R, Wesche H, Rothe M, Kirschning CJ. 1999. Peptidoglycan- and Lipoteichoic Acid-induced Cell Activation Is Mediated by Toll-like Receptor 2. Journal of Biological Chemistry. 274:17406-17409.

132. Takeuchi O, Hoshino K, Kawai T, Sanjo H, Takada H, Ogawa T, Takeda K, Akira S. 1999. Differential Roles of TLR2 and TLR4 in Recognition of Gram-Negative and Gram-Positive Bacterial Cell Wall Components. Immunity. 11:443-451.

133. Aliprantis AO, Yang R, Mark MR, Suggett S, Devaux B, Radolf JD, Klimpel GR, Godowski P, Zychlinsky A. 1999. Cell Activation and Apoptosis by Bacterial Lipoproteins Through Toll-like Receptor-2. Science. 285:736-739.

134. Medzhitov R, Alexopoulou L, Flavell RA, Holt AC. 2001. Recognition of double-stranded RNA and activation of NF-κB by Toll-like receptor 3. Nature. 413:732-738.

135. Poltorak A, He X, Smirnova I, Liu M, Huffel CV, Du X, Birdwell D, Alejos E, Silva M, Galanos C, Freudenberg M, Ricciardi-Castagnoli P, Layton B, Beutler B. 1998. Defective LPS Signaling in C3H/HeJ and C57BL/10ScCr Mice: Mutations in Tlr4 Gene. Science. 282:2085-2088.

136. Akira S, Goodlett DR, Hayashi F, Yi EC, Eng JK, Hawn TR, Underhill DM, Smith KD, Aderem A, Ozinsky A. 2001. The innate immune response to bacterial flagellin is mediated by Toll-like receptor 5. Nature. 410:1099-1103.

137. Schwandner R, Dziarski R, Wesche H, Rothe M, Kirschning CJ. 1999. Peptidoglycan- and Lipoteichoic Acid-induced Cell Activation Is Mediated by Toll-like Receptor 2. Journal of Biological Chemistry. 274:17406-17409.

138. Takeuchi O, Kawai T, Muehlradt PF, Morr M, Radolf JD, Zychlinsky A, Takeda K, Akira S. 2001. Discrimination of bacterial lipoproteins by Toll-like receptor 6. International Immunology. 13:933-940.

139. Diebold SS, Kaisho T, Hemmi H, Akira S, Reis e Sousa C. 2004. Innate Antiviral Responses by Means of TLR7-Mediated Recognition of Single-Stranded RNA. Science. 303:1529-1531.

140. Heil F, Hemmi H, Hochrein H, Ampenberger F, Kirschning C, Akira S, Lipford G, Wagner H, Bauer S. 2004. Species-Specific Recognition of Single-Stranded RNA via Toll-like Receptor 7 and 8. Science. 303:1526-1529.

141. Bergstroem B, Aune MH, Awuh JA, Kojen JF, Blix KJ, Ryan L, Flo TH, Mollnes TE, Espevik T, Stenvik J. 2015. TLR8 Senses *Staphylococcus aureus* RNA in Human Primary Monocytes and Macrophages and Induces IFN- beta Production via a TAK1-IKK beta -IRF5 Signaling Pathway. Journal of Immunology. 195:1100-1111.

142. Kaisho T, Hoshino K, Takeuchi O, Matsumoto M, Wagner H, Kawai T, Sato S, Akira S, Hemmi H, Sanjo H, Takeda K. 2000. A Toll-like receptor recognizes bacterial DNA. Nature. 408:740-745.

143. Zhang D, Zhang G, Hayden MS, Greenblatt MB, Bussey C, Flavell RA, Ghosh S. 2004. A Toll-like Receptor That Prevents Infection by Uropathogenic Bacteria. Science. 303:1522-1526.

144. Yarovinsky F, Zhang D, Andersen JF, Bannenberg GL, Serhan CN, Hayden MS, Hieny S, Sutterwala FS, Flavell RA, Ghosh S, Sher A. 2005. TLR11 Activation of Dendritic Cells by a Protozoan Profilin-Like Protein. Science. 308:1626-1629.

145. Koblansky A , Jankovic D, Oh H, Hieny S, Sungnak W, Mathur R, Hayden M, Akira S, Sher A, Ghosh S. 2013. Recognition of Profilin by Toll-like Receptor 12 Is Critical for Host Resistance to Toxoplasma gondii. Immunity. 38:119-130.

146. Oldenburg M, Krüger A, Ferstl R, Kaufmann A, Nees G, Sigmund A, Bathke B, Lauterbach H, Suter M, Dreher S, Koedel U, Akira S, Kawai T, Buer J, Wagner H, Bauer S, Hochrein H, Kirschning CJ. 2012. TLR13 Recognizes Bacterial 23S rRNA Devoid of Erythromycin Resistance—Forming Modification. Science. 337:1111-1115.

147. Fournier B, Philpott DJ. 2005. Recognition of *Staphylococcus aureus* by the Innate Immune System. Clinical Microbiology Reviews. 18:521-540.

148. Parker D, Prince A. 2012. *Staphylococcus aureus* Induces Type I IFN Signaling in Dendritic Cells Via TLR9. Journal of Immunology. 189:4040-4046.

149. Caruso R, Warner N, Inohara N, Núñez G. 2014. NOD1 and NOD2: Signaling, Host Defense, and Inflammatory Disease. Immunity. 41:898-908.

150. Takeda K, Akira S. 2004. Toll-like receptor signaling. Nature Reviews Immunology. 4:499-511.

151. Matsushima N, Tanaka T, Enkhbayar P, Mikami T, Taga M, Yamada K, Kuroki Y. 2007. Comparative sequence analysis of leucine-rich repeats (LRRs) within vertebrate toll-like receptors. BMC Genomics. 8:124.

152. Bowie A, O'Neill LA. 2000. The interleukin-1 receptor/Toll-like receptor superfamily: signal generators for pro-inflammatory interleukins and microbial products. Journal of Leukocyte Biology. 67:508-514.

153. O'Neill LAJ, Bowie AG. 2007. The family of five: TIR-domain-containing adaptors in Toll-like receptor signalling. Nature Reviews Immunology. 7:353-364.

154. Liu L, Botos I, Wang Y, Leonard JN, Shiloach J, Segal DM, Davies DR. 2008. Structural Basis of Toll-Like Receptor 3 Signaling with Double-Stranded RNA. Science. 320:379-381.

155. Kim HM, Kim J, Kim SE, Park BS, Lee H, Lee J, Lee J, Oh SC, Enkhbayar P, Matsushima N, Yoo OJ. 2007. Crystal Structure of the TLR4-MD-2 Complex with Bound Endotoxin Antagonist Eritoran. Cell. 130:906-917.

156. Jin MS, Lee JO. 2008. Structures of the Toll-like Receptor Family and Its Ligand Complexes. Immunity. 29:182-191.

157. Jin MS, Kim SE, Heo JY, Lee ME, Kim HM, Paik SG, Lee H, Lee JO. 2007. Crystal Structure of the TLR1-TLR2 Heterodimer Induced by Binding of a Tri-Acylated Lipopeptide. Cell. 130:1071-1082.

158. Beutler B, Jiang Z, Georgel P, Crozat K, Croker B, Rutschmann S, Du X, Hoebe K. 2006. Genetic Analysis of Host Resistance: Toll-Like Receptor Signaling and Immunity at Large. Annual Review of Immunology. 24:353-389.

159. Buwitt-Beckmann U, Heine H, Wiesmaller KH, Jung G, Brock R, Akira S, Ulmer AJ. 2006. TLR1- and TLR6-independent Recognition of Bacterial Lipopeptides. Journal of Biological Chemistry. 281:9049-9057.

160. Asanuma M, Kurokawa K, Ichikawa R, Ryu KH, Chae JH, Dohmae N, Lee BL, Nakayama H. 2011. Structural evidence of a-aminoacylated lipoproteins of *Staphylococcus aureus*. Febs J. 278:716-728.

161. Nguyen MT, Gotz F. 2016. Lipoproteins of gram-positive bacteria: Key players in the immune response and virulence. Microbiol. Mol. Biol. Rev. 80:891-903.

162. Kang JY, Nan X, Jin MS, Youn SJ, Ryu YH, Mah S, Han SH, Lee H, Paik SG, Lee JO. 2009. Recognition of Lipopeptide Patterns by Toll-like Receptor 2-Toll-like Receptor 6 Heterodimer. Immunity. 31:873-884.

163. Ozinsky A, Underhill DM, Fontenot JD, Hajjar AM, Smith KD, Wilson CB, Schroeder L, Aderem A. 2000. The Repertoire for Pattern Recognition of Pathogens by the Innate Immune System is Defined by Cooperation between Toll-Like Receptors. Proceedings of the National Academy of Sciences of the United States of America. 97:13766-13771.

164. Yoshimura A, Lien E, Ingalls RR, Tuomanen E, Dziarski R, Golenbock D. 1999. Cutting edge: recognition of Gram-positive bacterial cell wall components by the innate immune system occurs via Toll-like receptor 2. Journal of Immunology. 163:1-5.

165. Travassos LH, Girardin SE, Philpott DJ, Blanot D, Nahori MA, Werts C, Boneca IG. 2004. Toll-like receptor 2-dependent bacterial sensing does not occur via peptidoglycan recognition. EMBO Reports. 5:1000-1006.

166. Hashimoto M, Furuyashiki M, Kaseya R, Fukada Y, Akimaru M, Aoyama K, Okuno T, Tamura T, Kirikae T, Kirikae f, Eiraku N, Morioka H, Fujimoto Y, Fukase K, Takashige K, Moriya Y, Kusumoto S, Suda Y. 2007. Evidence of Immunostimulating Lipoprotein Existing in the Natural Lipoteichoic Acid Fraction. Infection and Immunity. 75:1926-1932.

167. Hashimoto M, Tawaratsumida K, Kariya H, Aoyama K, Tamura T, Suda Y. 2006. Lipoprotein is a predominant Toll-like receptor 2 ligand in *Staphylococcus aureus* cell wall components. International Immunology. 18:355-362.

168. Dziarski R, Gupta D. 2005. *Staphylococcus aureus* Peptidoglycan Is a Toll-Like Receptor 2 Activator: a Reevaluation. Infection and Immunity. 73:5212-5216.

169. Asong J, Wolfert MA, Maiti KK, Miller D, Boons GJ. 2009. Binding and Cellular Activation Studies Reveal That Toll-like Receptor 2 Can Differentially Recognize Peptidoglycan from Gram-positive and Gram-negative Bacteria. Journal of Biological Chemistry. 284:8643-8653.

170. Iyer JK, Khurana T, Langer M, West CM, Ballard JD, Metcalf JP, Merkel TJ, Coggeshall KM. 2010. Inflammatory Cytokine Response to *Bacillus anthracis* Peptidoglycan Requires Phagocytosis and Lysosomal Trafficking. Infection and Immunity. 78:2418-2428.

171. Wolf AJ, Underhill DM. 2018. Peptidoglycan recognition by the innate immune system. Nature Reviews. Immunology. 18:243-254.

172. Hoebe K, Shamel L, Zähringer U, Mudd S, Du X, Beutler B, Georgel P, Crozat K, Hartung T, Sovath S, Rutschmann S. 2005. CD36 is a sensor of diacylglycerides. Nature. 433:523-527.

173. Nakata T, Yasuda M, Fujita M, Kataoka H, Kiura K, Sano H, Shibata K. 2006. CD14 directly binds to triacylated lipopeptides and facilitates recognition of the lipopeptides by the receptor complex of Toll-like receptors 2 and 1 without binding to the complex. Cellular Microbiology. 8:1899-1909.

174. Cleveland MG, Gorham JD, Murphy TL, Tuomanen E, Murphy KM. 1996. Lipoteichoic acid preparations of gram-positive bacteria induce interleukin-12 through a CD14-dependent pathway. Infection and Immunity. 64:1906-1912.

175. Kusunoki T, Hailman E, Juan T, Lichenstein HS, Wright SD. 1995. Molecules from *Staphylococcus aureus* that bind CD14 and stimulate innate immune responses. Journal of Experimental Medicine. 182:1673-1682.

176. Pugin J, Heumann D, Tomasz A, Kravchenko VV, Akamatsu Y, Nishijima M, Glauser MP, Tobias PS, Ulevitch RJ. 1994. CD14 Is a pattern recognition receptor. Immunity. 1:509-516.

177. Jimenez-Dalmaroni MJ, Xiao N, Corper AL, Verdino P, Ainge GD, Larsen DS, Painter GF, Rudd PM, Dwek RA, Hoebe K, Beutler B, Wilson IA, Unutmaz D. 2009. Soluble CD36 Ectodomain Binds Negatively Charged Diacylglycerol Ligands and Acts as a Co-Receptor for TLR2. PLoS ONE. 4:e7411.

178. Patel SN, Lu Z, Ayi K, Serghides L, Gowda DC, Kain KC. 2007. Disruption of CD36 Impairs Cytokine Response to *Plasmodium falciparum* Glycosylphosphatidylinositol and Confers Susceptibility to Severe and Fatal Malaria In Vivo. The Journal of Immunology. 178:3954-3961.

179. Prince A. 1992. Adhesins and receptors of Pseudomonas aeruginosa associated with infection of the respiratory tract. 13:251-260.

180. Ratner AJ, Bryan R, Weber A, Nguyen S, Barnes D, Pitt A, Gelber S, Cheung A, Prince A. 2001. Cystic Fibrosis Pathogens Activate Ca2+-dependent Mitogen-activated Protein Kinase Signaling Pathways in Airway Epithelial Cells. Journal of Biological Chemistry. 276:19267-19275.

181. Soong G, Reddy B, Sokol S, Adamo R, Prince A. 2004. TLR2 is mobilized into an apical lipid raft receptor complex to signal infection in airway epithelial cells. The Journal of Clinical Investigation. 113:1482-1489.

182. Akira S, Takeda K. 2004. Toll-like receptor signaling. Nat. Rev. Immunol. 4:499-511.

183. Matsui K, Kawai T, Takeuchi O, Kumagai Y, Kato H, Kawagoe T, Saitoh T, Sato S, Akira S, Matsushita K. 2008. Sequential control of Toll-like receptor-dependent responses by IRAK1 and IRAK2. Nature Immunology. 9:684-691.

184. Adhikari A, Xu M, Chen ZJ. 2007. Ubiquitin-mediated activation of TAK1 and IKK. Oncogene. 26:3214-3226.

185. Chen F, Bhatia D, Chang Q, Castranova V. 2006. Finding NEMO by K63-linked polyubiquitin chain. Cell Death and Differentiation. 13:1835-1838.

186. Deng L, Wang C, Spencer E, Yang L, Braun A, You J, Slaughter C, Pickart C, Chen ZJ. 2000. Activation of the IkappaB kinase complex by TRAF6 requires a dimeric ubiquitin-conjugating enzyme complex and a unique polyubiquitin chain. Cell. 103:351.

187. Liu T, Zhang L, Joo D, Sun S. 2017. NF-κB signaling in inflammation. Signal Transduction and Targeted Therapy. 2:17023.

188. Lai Y, Gallo RL. 2009. AMPed up immunity: how antimicrobial peptides have multiple roles in immune defense. Trends in Immunology. 30:131-141.

189. Joo H, Otto M. 2015. Mechanisms of resistance to antimicrobial peptides in staphylococci. BBA - Biomembranes. 1848:3055-3061.

190. Jenssen H, Hamill P, Hancock RE. 2006. Peptide antimicrobial agents. Clin Microbiol Rev. 19:491-511.

191. Yang L, Harroun TA, Weiss TM, Ding L, Huang HW. 2001. Barrel-Stave Model or Toroidal Model? A Case Study on Melittin Pores. Biophysical Journal. 81:1475-1485.

192. Bechinger B, Aisenbrey C, Bertani P. 2004. The alignment, structure and dynamics of membrane-associated polypeptides by solid-state NMR spectroscopy. Biochimica Et Biophysica Acta. 1666:190-204.

193. Brogden KA. 2005. Antimicrobial peptides: pore formers or metabolic inhibitors in bacteria? Nature Reviews Microbiology. 3:238-250.

194. Sarma J, Ward P. 2011. The complement system. Cell Tissue Res. 343:227-235.

195. Noris M, Remuzzi G. 2013. Overview of Complement Activation and Regulation. Seminars in Nephrology. 33:479-492.

196. Sørensen R, Thiel S, Jensenius J. 2005. Mannan-binding-lectin-associated serine proteases, characteristics and disease associations. Springer Semin Immun. 27:299-319.

197. Wallis R. 2007. Interactions between mannose-binding lectin and MASPs during complement activation by the lectin pathway. Immunobiology. 212:289-99.

198. Kemper C, Atkinson JP, Hourcade DE. 2009. Properdin: Emerging Roles of a Pattern-Recognition Molecule. Annual Review of Immunology. 28:131-155.

199. Manthey HD, Woodruff TM, Taylor SM, Monk PN. 2009. Complement component 5a (C5a). International Journal of Biochemistry and Cell Biology. 41:2114-2117.

200. Morgan BP, McGeer PL. 1995. Physiology and Pathophysiology of Complement: Progress and Trends. Critical Reviews in Clinical Laboratory Sciences. 32:265-298.

201. Dinarello CA. 2007. Historical insights into cytokines. European Journal of Immunology. 37:S45.

202. Arango Duque G, Descoteaux A. 2014. Macrophage Cytokines: Involvement in Immunity and Infectious Diseases. Frontiers in Immunology. 5:491.

203. Hurst SM, Wilkinson TS, McLoughlin RM, Jones S, Jones SA, Horiuchi S, Yamamoto N, Rose-John S, Fuller GM, Topley N. 2001. IL-6 and Its Soluble Receptor Orchestrate a Temporal Switch in the Pattern of Leukocyte Recruitment Seen during Acute Inflammation. Immunity. 14:705-714.

204. Scheller J, Chalaris A, Schmidt-Arras D, Rose-John S. 2011. The pro-and anti-inflammatory properties of the cytokinevinterleukin-6. Biochim Biophys Acta. 1813:878-88.

205. Ben-Sasson SZ, Hu-Li J, Quiel J, Cauchetaux S, Ratner M, Shapira I, Dinarello CA, Paul WE. 2009. IL-1 Acts Directly on CD4 T Cells to Enhance Their Antigen-Driven Expansion and Differentiation. Proceedings of the National Academy of Sciences of the United States of America. 106:7119-7124.

206. Gouwy M, Struyf S, Catusse J, Proost P, Van Damme J. 2004. Synergy between proinflammatory ligands of G protein-coupled receptors in neutrophil activation and migration. Journal of Leukocyte Biology. 76:185-194.

207. Starckx S, Van den Steen PE, Wuyts A, Van Damme J, Opdenakker G. 2002. Neutrophil Gelatinase B and Chemokines in Leukocytosis and Stem Cell Mobilization. Leukemia & Lymphoma. 43:233-241.

208. Wang KS, Frank DA, Ritz J. 2000. Interleukin-2 enhances the response of natural killer cells to interleukin-12 through up-regulation of the interleukin-12 receptor and STAT4. Blood. 95:3183-3190.

209. Comerford I, McColl SR. 2011. Mini-review series: focus on chemokines. Immunol Cell Biol. 89:183-4.

210. van Kessel, Kok P M, Bestebroer J, van Strijp, Jos A G. 2014. Neutrophil-Mediated Phagocytosis of *Staphylococcus aureus*. Frontiers in Immunology. 5:467.

211. Patel PC, Harrison RE. 2008. Membrane Ruffles Capture C3bi-opsonized Particles in Activated Macrophages. Molecular Biology of the Cell. 19:4628-4639.

212. Flannagan RS, Harrison RE, Yip CM, Jaqaman K, Grinstein S. 2010. Dynamic macrophage “probing” is required for the efficient capture of phagocytic targets. The Journal of Cell Biology. 191:1205-1218.

213. Bohdanowicz M, Schlam D, Hermansson M, Rizzuti D, Fairn GD, Ueyama T, Somerharju P, Du G, Grinstein S. 2013. Phosphatidic acid is required for the constitutive ruffling and macropinocytosis of phagocytes. Molecular Biology of the Cell. 24:1700-1712.

214. Freeman SA, Grinstein S. 2014. Phagocytosis: receptors, signal integration, and the cytoskeleton. Immunological Reviews. 262:193-215.

215. Jaumouillé V, Farkash Y, Jaqaman K, Das R, Lowell C, Grinstein S. 2014. Actin Cytoskeleton Reorganization by Syk Regulates Fcγ Receptor Responsiveness by Increasing Its Lateral Mobility and Clustering. Developmental Cell. 29:534-546.

216. Greenberg S, El Khoury J, di Virgilio F, Kaplan EM, Silverstein SC. 1991. Ca super(2+)-independent F-actin assembly and disassembly during Fc receptor-mediated phagocytosis in mouse macrophages. Journal of Cell Biology. 113:757-767.

217. Tse SML, Furuya W, Gold E, Schreiber AD, Sandvig K, Inman RD, Grinstein S. 2003. Differential Role of Actin, Clathrin, and Dynamin in Fcγ Receptor-mediated Endocytosis and Phagocytosis. The Journal of Biological Chemistry. 278:3331-3338.

218. Schlam D, Bagshaw RD, Freeman SA, Collins RF, Pawson T, Fairn GD, Grinstein S. 2015. Phosphoinositide 3-kinase enables phagocytosis of large particles by terminating actin assembly through Rac/Cdc42 GTPase-activating proteins. Nature Communications. 6:8623.

219. Desjardins M, Huber LA, Parton RG, Griffiths G. 1994. Biogenesis of phagolysosomes proceeds through a sequential series of interactions with the endocytic apparatus. The Journal of Cell Biology. 124:677-688.

220. Hackam DJ, Rotstein OD, Zhang WJ, Demaurex N, Woodside M, Tsai O, Grinstein S. 1997. Regulation of phagosomal acidification. Differential targeting of Na+/H+ exchangers, Na+/K+-ATPases, and vacuolar-type H+-atpases. The Journal of Biological Chemistry. 272:29810-29820.

221. Jabado N, Jankowski A, Dougaparsad S, Picard V, Grinstein S, Gros P. 2000. Natural resistance to intracellular infections: Natural resistance-associated macrophage protein 1 (Nramp1) functions as a pH-dependent manganese transporter at the phagosomal membrane. Journal of Experimental Medicine. 192:1237-1248.

222. Turk B, Dolenc I, Turk V, Bieth JG. 1993. Kinetics of the pH-induced inactivation of human cathepsin L. Biochemistry. 32:375-380.

223. Brinkmann V, Reichard U, Goosmann C, Fauler B, Uhlemann Y, Weiss DS, Weinrauch Y, Zychlinsky A. 2004. Neutrophil Extracellular Traps Kill Bacteria. Science. 303:1532-1535.

224. Fuchs TA, Abed U, Goosmann C, Hurwitz R, Schulze I, Wahn V, Weinrauch Y, Brinkmann V, Zychlinsky A. 2007. Novel Cell Death Program Leads to Neutrophil Extracellular Traps. The Journal of Cell Biology. 176:231-241.

225. Yipp BG, Petri B, Salina D, Jenne CN, Scott B, Zbytnuik LD, Pittman K, Asaduzzaman M, Wu K, Meijndert CH, Malawista SE, Boisfleury Chevance A, Zhang K, Conly J, Kubes P. 2012. Infection-induced NETosis is a dynamic process involving neutrophil multitasking in vivo. Nature Medicine. 18:1386-1393.

226. Pilsczek FH, Salina D, Poon KK, Fahey C, Yipp BG, Sibley CD, Robbins SM, Green FH, Surette MG, Sugai M, Bowden M, Hussain M, Zhang K, Kubes P. 2010. A Novel Mechanism of Rapid Nuclear Neutrophil Extracellular Trap Formation in Response to *Staphylococcus aureus*. Journal of Immunology. 185:7413-7425.

227. Toonen RFG, Verhage M. 2003. Vesicle trafficking: pleasure and pain from SM genes. Trends in Cell Biology. 13:177-186.

228. Lacy P. 2006. Mechanisms of Degranulation in Neutrophils. Allergy, Asthma, and Clinical Immunology. 2:98-108.

229. Seymour J. Klebanoff. 2005. Myeloperoxidase: friend and foe. Journal of Leukocyte Biology. 77:598-625.

230. Borregaard N, Cowland JB. 1997. Granules of the human neutrophilic polymorphonuclear leukocyte. Blood. 89:3503-21.

231. Corbin BD, Seeley EH, Raab A, Feldmann J, Miller MR, Torres VJ, Anderson KL, Dattilo BM, Dunman PM, Gerads R, Caprioli RM, Nacken W, Chazin WJ, Skaar EP. 2008. Metal Chelation and Inhibition of Bacterial Growth in Tissue Abscesses. Science. 319:962-965.

232. Jabado N, Jankowski A, Dougaparsad S, Picard V, Grinstein S, Gros P. 2000. Natural resistance to intracellular infections: Natural resistance-associated macrophage protein 1 (Nramp1) functions as a pH-dependent manganese transporter at the phagosomal membrane. Journal of Experimental Medicine. 192:1237-1248.

233. Searle S, Bright NA, Roach TI, Atkinson PG, Barton CH, Meloen RH, Blackwell JM. 1998. Localisation of Nramp1 in macrophages: modulation with activation and infection. Journal of Cell Science. 111:2855.

234. Gruenheid S, Pinner E, Desjardins M, Gros P. 1997. Natural resistance to infection with intracellular pathogens: The Nramp1 protein is recruited to the membrane of the phagosome. Journal of Experimental Medicine. 185:717-730.

235. Weinberg ED. 1975. Nutritional Immunity: Host's Attempt to Withhold Iron From Microbial Invaders. Jama. 231:39-41.

236. Sbarra AJ, Karnovsky ML. 1959. The biochemical basis of phagocytosis. I. Metabolic changes during the ingestion of particles by polymorphonuclear leukocytes. The Journal of Biological Chemistry. 234:1355.

237. Fang FC. 2004. Antimicrobial reactive oxygen and nitrogen species: concepts and controversies. Nature Reviews Microbiology. 2:820-832.

238. Vignais PV. 2002. The superoxide-generating NADPH oxidase: structural aspects and activation mechanism. CMLS, Cell. Mol. Life Sci. 59:1428-1459.

239. Babior BM, Lambeth JD, Nauseef W. 2002. The neutrophil NADPH oxidase. Arch Biochem Biophys. 397:342-344.

240. El-Benna J, Dang PM, Gougerot-Pocidalo M, Marie J, Braut-Boucher F. 2009. p47phox, the phagocyte NADPH oxidase/NOX2 organizer: structure, phosphorylation and implication in diseases. Experimental and Molecular Medicine. 41:217-225.

241. Hampton MB, Kettle, AJ, Winterbourn, CC. 1998. Inside the neutrophil phagosome: oxidants, myeloperoxidase, and bacterial killing. 92:3007-3017.

242. Winterbourn CC, Kettle AJ. 2013. Redox Reactions and Microbial Killing in the Neutrophil Phagosome. Antioxidants & Redox Signaling. 18:642-660.

243. Winterbourn CC. 2008. Reconciling the chemistry and biology of reactive oxygen species. Nature Chemical Biology. 4:278-286.

244. Flannagan RS, Cosío G, Grinstein S. 2009. Antimicrobial mechanisms of phagocytes and bacterial evasion strategies. Nature Reviews Microbiology. 7:355-366.

245. Slauch JM. 2011. How does the oxidative burst of macrophages kill bacteria? Still an open question. Mol. Microbiol. 80:580-583.

246. Winkelstein JA, Marino MC, Johnston RJ, Boyle J, Curnutte J, Gallin JI, Malech HL, Holland SM, Ochs H, Quie P, Buckley RH, Foster CB, Chanock SJ, Dickler H. 2000. Chronic Granulomatous Disease: Report on a National Registry of 368 Patients. Medicine. 79:155-169.

247. Buvelot H, Posfay-Barbe KM, Linder P, Schrenzel J, Krause K. 2017. *Staphylococcus aureus*, phagocyte NADPH oxidase and chronic granulomatous disease. FEMS Microbiology Reviews. 41:139-157.

248. West AP, Brodsky IE, Rahner C, Woo DK, Erdjument-Bromage H, Tempst P, Walsh MC, Choi Y, Shadel GS, Ghosh S. 2011. TLR signalling augments macrophage bactericidal activity through mitochondrial ROS. Nature. 472:476-480.

249. Murphy MP. 2009. How mitochondria produce reactive oxygen species. The Biochemical Journal. 417:1-13.

250. Koopman WJH, Nijtmans LGJ, Dieteren CEJ, Roestenberg PMH, Valsecchi F, Smeitink JAM, Willems, P. H. G. M. 2010. Mammalian mitochondrial complex I: biogenesis, regulation, and reactive oxygen species generation. Antioxidants & Redox Signaling. 12:1431-1470.

251. Abuaita BH, Schultz TL, O'Riordan MX. 2018. Mitochondria-Derived Vesicles Deliver Antimicrobial Reactive Oxygen Species to Control Phagosome-Localized *Staphylococcus aureus*. Cell Host & Microbe. 24:636.e5.

252. Cohen TS, Boland BB, Boland ML, Takahashi V, Tovchigrechko A, Lee Y, Wilde AD, Mazaitis MJ, Jones-Nelson O, Tkaczyk C, Raja R, Stover CK, Sellman BR. 2018. S. aureus Evades Macrophage Killing through NLRP3-Dependent Effects on Mitochondrial Trafficking. Cell Reports. 22:2431-2441.

253. Stuehr DJ. 1999. Mammalian nitric oxide synthases. Biochimica Et Biophysica Acta (BBA) - Bioenergetics. 1411:217-230.

254. Pacher P, Beckman JS, Liaudet L. 2007. Nitric Oxide and Peroxynitrite in Health and Disease. Physiological Reviews. 87:315-424.

255. Dedon PC, Tannenbaum, SR. 2004. Reactive nitrogen species in the chemical biology of inflammation. 423:12-22.

256. Wink DA, Mitchell JB. 1998. Chemical biology of nitric oxide: insights into regulatory, cytotoxic, and cytoprotective mechanisms of nitric oxide. Free Radical Biology and Medicine. 25:434-456.

257. Pacelli R, Wink DA, Cook JA, Krishna MC, DeGraff W, Friedman N, Tsokos M, Samuni A, Mitchell JB. 1995. Nitric oxide potentiates hydrogen peroxide-induced killing of *Escherichia coli*. Journal of Experimental Medicine. 182:1469-1479.

258. Laarman AJ, Ruyken M, Malone CL, van Strijp JA, Horswill AR, Rooijakkers SH. 2011. *Staphylococcus aureus* Metalloprotease Aureolysin Cleaves Complement C3 To Mediate Immune Evasion. Journal of Immunology. 186:6445-6453.

259. Sieprawska-Lupa M, Mydel P, Krawczyk K, Wójcik K, Puklo M, Lupa B, Suder P, Silberring J, Reed M, Pohl J, Shafer W, McAleese F, Foster T, Travis J, Potempa J. 2004. Degradation of Human Antimicrobial Peptide LL-37 by *Staphylococcus*

aureus-Derived Proteinases. Antimicrobial Agents and Chemotherapy. 48:4673-4679.

260. Jongerius I, Koehl J, Pandey MK, Ruyken M, van Kessel KP, van Strijp JA, Rooijakkers SH. 2007. Staphylococcal complement evasion by various convertase-blocking molecules. Journal of Experimental Medicine. 204:2461-2471.

261. Rooijakkers SHM, van Wamel, Willem J B, Ruyken M, Presanis JS, Sim RB, Roos A, van Kessel, Kok P M, Daha MR, van Strijp, Jos A G. 2005. Immune evasion by a staphylococcal complement inhibitor that acts on C3 convertases. Nature Immunology. 6:920-927.

262. Jin T, Bokarewa M, Foster T, Mitchell J, Higgins J, Tarkowski A. 2004. *Staphylococcus aureus* Resists Human Defensins by Production of Staphylokinase, a Novel Bacterial Evasion Mechanism. The Journal of Immunology. 172:1169-1176.

263. Rooijakkers SHM, van Wamel WJB, Ruyken M, van Kessel KPM, van Strijp JAG. 2005. Anti-opsonic properties of staphylokinase. Microbes and Infection. 7:476-484.

264. Forsgren A, Quie PG. 1974. Effects of Staphylococcal Protein a on Heat Labile Opsonins. The Journal of Immunology. 112:1177.

265. Forsgren A, Nordstrom K. 1974. Protein A from *Staphylococcus aureus*: the biological significance of its interaction with IgG. Pnas. 236:252-266.

266. Haupt K, Reuter M, van den Elsen J, Burman J, Haelbich S, Richter J, Skerka C, Zipfel PF, Cheung A. 2008. The *Staphylococcus aureus* Protein Sbi Acts as a Complement Inhibitor and Forms a Tripartite Complex with Host Complement Factor H and C3b. PLoS Pathogens. 4:e1000250.

267. Burman JD, Leung E, Atkins KL, O'Seaghdha MN, Lango L, Bernadó P, Bagby S, Svergun DI, Foster TJ, Isenman DE, van den Elsen, Jean M H. 2008. Interaction of human complement with Sbi, a staphylococcal immunoglobulin-binding protein: indications of a novel mechanism of complement evasion by *Staphylococcus aureus*. The Journal of Biological Chemistry. 283:17579-17593.

268. Zhang L, Jacobsson K, Vasi J, Lindberg M, Frykberg L. 1998. A second IgG-binding protein in *Staphylococcus aureus*. Microbiology. 144:985-991.

269. Lee LY, Höök M, Haviland D, Wetsel RA, Yonter EO, Syribeys P, Vernachio J, Brown EL. 2004. Inhibition of Complement Activation by a Secreted *Staphylococcus aureus* Protein. J Infect Dis. 190:571-579.

270. Langley R, Wines B, Willoughby N, Basu I, Proft T, Fraser JD. 2005. The staphylococcal superantigenlike protein 7 binds IgA and complement C5 and inhibits IgA-Fc alpha RI binding and serum killing of bacteria. Journal of Immunology. 174:2926-33.

271. Hermans SJ, Baker HM, Sequeira RP, Langley RJ, Baker EN, Fraser JD. 2012. Structural and Functional Properties of Staphylococcal Superantigen-Like Protein 4. Infection and Immunity. 80:4004-4013.

272. Bestebroer J, Poppelier M, Ulfman LH, Lenting PJ, Denis CV, van Kessel K, van Strijp J, de Haas C. 2007. Staphylococcal superantigen-like 5 binds PSGL-1 and inhibits P-selectin-mediated neutrophil rolling. Blood. 109:2936-2943.

273. Chung MC, Wines BD, Baker H, Langley RJ, Baker EN, Fraser JD. 2007. The crystal structure of staphylococcal superantigen-like protein 11 in complex with sialyl Lewis X reveals the mechanism for cell binding and immune inhibition. Molecular Microbiology. 66:1342-1355.

274. Fevre C, Bestebroer J, Mebius MM, Haas CJC, Strijp JAG, Fitzgerald JR, Haas PA. 2014. *Staphylococcus aureus* proteins SSL6 and SEIX interact with neutrophil receptors as identified using secretome phage display. Cellular Microbiology. 16:1646-1665.

275. Walenkamp AM, Bestebroer J, Boer IG, Kruizinga R, Verheul HM, van Strijp JA, de Haas CJ. 2010. Staphylococcal SSL5 Binding to Human Leukemia Cells Inhibits Cell Adhesion to Endothelial Cells and Platelets. Cellular Oncology. 32:1-10.

276. Yokoyama R, Itoh S, Kamoshida G, Takii T, Fujii S, Tsuji T, Onozaki K. 2012. Staphylococcal Superantigen-Like Protein 3 Binds to the Toll-Like Receptor 2 Extracellular Domain and Inhibits Cytokine Production Induced by *Staphylococcus aureus*, Cell Wall Component, or Lipopeptides in Murine Macrophages. Infection and Immunity. 80:2816-2825.

277. Friedrich R, Bock PE, Panizzi P, Verhamme I, Fuentes-Prior P, Huber R, Kawabata S. 2003. Staphylocoagulase is a prototype for the mechanism of cofactor-induced zymogen activation. Nature. 425:535-539.

278. Peschel A, Otto M, Jack RW, Kalbacher H, Jung G, Götz F. 1999. Inactivation of the dlt operon in *Staphylococcus aureus* confers sensitivity to defensins, protegrins, and other antimicrobial peptides. The Journal of Biological Chemistry. 274:8405-8410.

279. Peschel A, Jack RW, Otto M, Collins LV, Staubitz P, Nicholson G, Kalbacher H, Nieuwenhuizen WF, Jung G, Tarkowski A, van Kessel K, van Strijp J. 2001. *Staphylococcus aureus* Resistance to Human Defensins and Evasion of

Neutrophil Killing via the Novel Virulence Factor MprF Is Based on Modification of Membrane Lipids with L-Lysine. Journal of Experimental Medicine. 193:1067-1076.

280. Bera A, Herbert S, Jakob A, Vollmer W, Götz F. 2005. Why are pathogenic staphylococci so lysozyme resistant? The peptidoglycan O-acetyltransferase OatA is the major determinant for lysozyme resistance of *Staphylococcus aureus*. Molecular Microbiology. 55:778-787.

281. Stapels D, Ramyar KX, Bischoff M, Milder FJ, Ruyken M, Eisenbeis J, McWhorter WJ, Herrmann M, van Kessel K, Geisbrecht BV, Rooijakkers S. 2014. *Staphylococcus aureus* secretes a unique class of neutrophil serine protease inhibitors. Proceedings of the National Academy of Sciences of the United States of America. 111:13187-13192.

282. Chavakis T, Preissner KT, Kanse SM, Bretzel RG, Flock J, Herrmann M, Peters G, Hussain M. 2002. *Staphylococcus aureus* extracellular adherence protein serves as anti-inflammatory factor by inhibiting the recruitment of host leukocytes. Nature Medicine. 8:687-693.

283. Laarman AJ, Mijnheer G, Mootz JM, Van Rooijen, W J M, Ruyken M, Malone CL, Heezius EC, Ward R, Milligan G, Van Strijp, J A G, De Haas, C J C, Horswill AR, Van Kessel, K P M, Rooijakkers SHM. 2012. *Staphylococcus aureus* Staphopain A inhibits CXCR2-dependent neutrophil activation and chemotaxis. Embo J. 31:3607-3619.

284. De Haas, C J C, Veldkamp KE, Peschel A, Weerkamp F, Van Wamel, W J B, Heezius, E C J M, Poppelier, M J J G, Van Kessel, K P M, Van Strijp, J A G. 2004. Chemotaxis Inhibitory Protein of *Staphylococcus aureus*, a Bacterial Antiinflammatory Agent. J. Exp. Med. 199:687-695.

285. Postma B, Poppelier MJ, van Galen JC, Prossnitz ER, van Strijp, Jos A. G, de Haas, Carla J. C, van Kessel, Kok P. M. 2004. Chemotaxis Inhibitory Protein of *Staphylococcus aureus* Binds Specifically to the C5a and Formylated Peptide Receptor. The Journal of Immunology. 172:6994-7001.

286. Prat C, Bestebroer J, de Haas, Carla J. C, van Strijp, Jos A. G, van Kessel, Kok P. M. 2006. A New Staphylococcal Anti-Inflammatory Protein That Antagonizes the Formyl Peptide Receptor-Like 1. The Journal of Immunology. 177:8017-8026.

287. Peschel A, Otto M. 2013. Phenol-soluble modulins and staphylococcal infection. Nature Reviews. Microbiology. 11:667-673.

288. Cheung GYC, Joo H, Chatterjee SS, Otto M. 2014. Phenol-soluble modulins – critical determinants of staphylococcal virulence. FEMS Microbiology Reviews. 38:698-719.

289. Wilke GA, Bubeck Wardenburg J. 2010. Role of a disintegrin and metalloprotease 10 in *Staphylococcus aureus* α-hemolysin–mediated cellular injury. Proceedings of the National Academy of Sciences of the United States of America. 107:13473-13478.

290. Burnet FM. 1930. The Exotoxins of Staphylococcus Pyogenes Aureus. The Journal of Pathology and Bacteriology. 32:717-734.

291. Van de Velde H. 1894. Etude sur le mécanisme de la virulence du Staphylocoque pyogene. Cellule. 10:401-410.

292. Denys J, Van de Velde H. 1895. Sur la production d'une antileucocidine chez les lapin vaccinés contre le Staphylocoque pyogène. Cellule. 11:359-372.

293. Spaan AN, Van Strijp J, Torres VJ. 2017. Leukocidins: staphylococcal bi-component pore-forming toxins find their receptors. Nature Reviews. Microbiology. 15:435-447.

294. Thammavongsa V, Kern JW, Missiakas DM, Schneewind O. 2009. *Staphylococcus aureus* synthesizes adenosine to escape host immune responses. The Journal of Experimental Medicine. 206:2417-2427.

295. Liu GY, Essex A, Buchanan JT, Datta V, Hoffman HM, Bastian JF, Fierer J, Nizet V. 2005. *Staphylococcus aureus* golden pigment impairs neutrophil killing and promotes virulence through its antioxidant activity. Journal of Experimental Medicine. 202:209-215.

296. Cosgrove K, Coutts G, Jonsson IM, Tarkowski A, Kokai-Kun JF, Mond JJ, Foster SJ. 2007. Catalase (KatA) and Alkyl Hydroperoxide Reductase (AhpC) Have Compensatory Roles in Peroxide Stress Resistance and Are Required for Survival, Persistence, and Nasal Colonization in *Staphylococcus aureus*. Journal of Bacteriology. 189:1025-1035.

297. Karavolos MH, Horsburgh MJ, Ingham E, Foster SJ. 2003. Role and regulation of the superoxide dismutases of *Staphylococcus aureus*. Microbiology. 149:2749-2758.

298. Pang YY, Schwartz J, Bloomberg S, Boyd JM, Horswill AR, Nauseef WM. 2014. Methionine Sulfoxide Reductases Protect against Oxidative Stress in *Staphylococcus aureus* Encountering Exogenous Oxidants and Human Neutrophils. Journal of Innate Immunity. 6:353-364.

299. Malachowa N, Kohler PL, Schlievert PM, Chuang ON, Dunny GM, Kobayashi SD, Miedzobrodzki J, .Bohach GA, Seo KS. 2011. Characterization of a *Staphylococcus aureus* Surface Virulence Factor That Promotes Resistance to Oxidative Killing and Infectious Endocarditis. Infection and Immunity. 79:342-352.

300. Gonçalves VL, Nobre LS, Vicente JB, Teixeira M, Saraiva LM. 2006. Flavohemoglobin requires microaerophilic conditions for nitrosative protection of *Staphylococcus aureus*. FEBS Letters. 580:1817-1821.

301. Richardson AR, Libby SJ, Fang FC. 2008. A Nitric Oxide-Inducible Lactate Dehydrogenase Enables *Staphylococcus aureus* to Resist Innate Immunity. Science. 319:1672-1676.

302. O'Riordan K, Lee JC. 2004. *Staphylococcus aureus* Capsular Polysaccharides. Clinical Microbiology Reviews. 17:218-234.

303. Forsgren A, Sjquist J. 1966. "Protein A" from S. aureus. I. Pseudo-immune reaction with human gamma-globulin. J. Immunol. 97:822-827.

304. Williams RJ, Ward JM, Henderson B, Poole S, O Hara BP, Wilson M, Nair SP. 2000. Identification of a Novel Gene Cluster Encoding Staphylococcal Exotoxin-Like Proteins: Characterization of the Prototypic Gene and Its Protein Product, SET1. Infection and Immunity. 68:4407-4415.

305. McCarthy AJ, Lindsay JA. 2013. *Staphylococcus aureus* innate immune evasion is lineage-specific: A bioinfomatics study. Infection, Genetics and Evolution. 19:7-14.

306. Itoh S, Yokoyama R, Kamoshida G, Fujiwara T, Okada H, Takii T, Tsuji T, Fujii S, Hashizume H, Onozaki K. 2013. Staphylococcal Superantigen-like Protein 10 (SSL10) Inhibits Blood Coagulation by Binding to Prothrombin and Factor Xa via Their γ-Carboxyglutamic Acid (Gla) Domain. The Journal of Biological Chemistry. 288:21569-21580.

307. Walenkamp AME, Boer IGJ, Bestebroer J, Rozeveld D, Timmer-Bosscha H, Hemrika W, van Strijp JAG, de Haas CJC. 2009. Staphylococcal Superantigen-like 10 Inhibits CXCL12-Induced Human Tumor Cell Migration. Neoplasia. 11:333-344.

308. Forsman H, Christenson K, Bylund J, Dahlgren C. 2012. Receptor-Dependent and -Independent Immunomodulatory Effects of Phenol-Soluble Modulin Peptides from *Staphylococcus aureus* on Human Neutrophils Are Abrogated through Peptide Inactivation by Reactive Oxygen Species. Infection and Immunity. 80:1987-1995.

309. Song L, Hobaugh MR, Shustak C, Cheley S, Bayley H, Gouaux JE. 1996. Structure of Staphylococcal alpha -Hemolysin, a Heptameric Transmembrane Pore. Science. 274:1859-1866.

310. Miles G, Movileanu L, Bayley H. 2002. Subunit composition of a bicomponent toxin: Staphylococcal leukocidin forms an octameric transmembrane pore. Protein Science. 11:894-902.

311. Alonzo F, Torres VJ. 2014. The bicomponent poreforming leucocidins of *Staphylococcus aureus*. Microbiol. Mol. Biol. Rev. 78:199-230.

312. Koop G, Vrieling M, Storisteanu DM, Lok LS, Monie T, Wigcheren GFv, Raisen C, Ba X, Gleadall N, Hadjirin N, Timmerman AJ, Wagenaar JA, Klunder HM, Fitzgerald JR, Zadoks R, Paterson GK, Torres C, Waller AS, Loeffler A, Loncaric I, Hoet AE, Bergstrom K, Martino L, Pomba C, Lencastre Hd, Slama KB, Gharsa H, Richardson EJ, Chilvers ER, Haas Cd, Kessel Kv, Strijp JAv, Harrison EM, Holmes MA. 2017. Identification of LukPQ, a novel, equid-adapted leukocidin of *Staphylococcus aureus*. Scientific Reports. 7:40660.

313. Prevost G, Bouakham T, Piemont Y, Monteil H. 1995. Characterisation of a synergohymenotropic toxin produced by Staphylococcus intermedius. FEBS Letters. 376:135-140.

314. Lubkin A, Lee WL, Alonzo F, Wang C, Aligo J, Keller M, Girgis NM, Reyes-Robles T, Chan R, O'Malley A, Buckley P, Vozhilla N, Vasquez MT, Su J, Sugiyama M, Yeung ST, Coffre M, Bajwa S, Chen E, Martin P, Kim SY, Loomis C, Worthen GS, Shopsin B, Khanna KM, Weinstock D, Lynch AS, Koralov SB, Loke P, Cadwell K, Torres VJ. 2019. *Staphylococcus aureus* Leukocidins Target Endothelial DARC to Cause Lethality in Mice. Cell Host & Microbe. 25:470.e9.

315. Spaan AN, Vrieling M, Wallet P, Badiou C, Reyes-Robles T, Ohneck EA, Benito Y, de Haas, Carla J C, Day CJ, Jennings MP, Lina G, Vandenesch F, van Kessel, Kok P M, Torres VJ, van Strijp, Jos A G, Henry T. 2014. The staphylococcal toxins γ-haemolysin AB and CB differentially target phagocytes by employing specific chemokine receptors. Nature Communications. 5:5438.

316. Reyes-Robles T, Alonzo F, Kozhaya L, Lacy D , Unutmaz D, Torres V. 2013. *Staphylococcus aureus* Leukotoxin ED Targets the Chemokine Receptors CXCR1 and CXCR2 to Kill Leukocytes and Promote Infection. Cell Host & Microbe. 14:453-459.

317. Alonzo F, Kozhaya L, Rawlings SA, Reyes-Robles T, DuMont AL, Myszka DG, Landau NR, Unutmaz D, Torres VJ. 2013. CCR5 is a receptor for *Staphylococcus aureus* leukotoxin ED. Nature. 493:51-55.

318. DuMont AL, Yoong P, Day CJ, Alonzo FI, McDonald WH, Jennings MP, Torres VJ. 2013. *Staphylococcus aureus* LukAB cytotoxin kills human neutrophils by targeting the CD11b subunit of the integrin Mac-1. Proceedings of the National Academy of Sciences of the United States of America. 110:10794-10799.

319. Garzoni C, Kelley WL. 2008. *Staphylococcus aureus*: new evidence for intracellular persistence. Trends in Microbiology. 17:59-65.

320. Alexander E, Hudson M. 2001. Factors influencing the internalization of *Staphylococcus aureus* and impacts on the course of infections in humans. Appl Microbiol Biotechnol. 56:361-366.

321. Sendi P, Proctor RA. 2008. *Staphylococcus aureus* as an intracellular pathogen: the role of small colony variants. Trends in Microbiology. 17:54-58.

322. Craven N, Anderson JC. 1983. Antibiotic activity against intraleukocytic *Staphylococcus aureus* in vitro and in experimental mastitis in mice. American Journal of Veterinary Research. 44:709.

323. Thwaites GE, Gant V. 2011. Are bloodstream leukocytes Trojan Horses for the metastasis of *Staphylococcus aureus*? Nature Reviews Microbiology. 9:215-222.

324. Gresham HD, Lowrance JH, Caver TE, Wilson BS, Cheung AL, Lindberg FP. 2000. Survival of *Staphylococcus aureus* Inside Neutrophils Contributes to Infection. The Journal of Immunology. 164:3713-3722.

325. DuMont AL, Yoong P, Surewaard B, Benson MA, Nijland R, van Strijp J, Torres VJ. 2013. *Staphylococcus aureus* Elaborates Leukocidin AB To Mediate Escape from within Human Neutrophils. Infection and Immunity. 81:1830-1841.

326. Surewaard BGJ, De Haas, CJC, Vervoort F, Rigby KM, Deleo FR, Otto M, Van Strijp, JAG, Nijland R. 2013. Staphylococcal alpha-phenol soluble modulins contribute to neutrophil lysis after phagocytosis. Cell. Microbiol. 15:1427-1437.

327. Grim KP, San Francisco B, Radin JN, Brazel EB, Kelliher JL, Párraga Solórzano PK, Kim PC, McDevitt CA, Kehl-Fie TE. 2017. The Metallophore Staphylopine Enables *Staphylococcus aureus* To Compete with the Host for Zinc and Overcome Nutritional Immunity. mBio. 8:1281.

328. Horsburgh MJ, Wharton SJ, Cox AG, Ingham E, Peacock S, Foster SJ. 2002. MntR modulates expression of the PerR regulon and superoxide resistance in *Staphylococcus aureus* through control of manganese uptake. Molecular Microbiology. 44:1269-1286.

329. Kehl-Fie TE, Zhang Y, Moore JL, Farrand AJ, Hood MI, Rathi S, Chazin WJ, Caprioli RM, Skaar EP. 2013. MntABC and MntH Contribute to Systemic *Staphylococcus aureus* Infection by Competing with Calprotectin for Nutrient Manganese. Infection and Immunity. 81:3395-3405.

330. Pishchany G, McCoy AL, Torres VJ, Krause JC, Crowe JE, Fabry ME, Skaar EP. 2010. Specificity for Human Hemoglobin Enhances *Staphylococcus aureus* Infection. Cell Host & Microbe. 8:544-550.

331. Dedent A, Cheng AG, McAdow M, Bagnoli F, Missiakas DM, Schneewind O. 2010. IsdA and IsdB antibodies protect mice against *Staphylococcus aureus* abscess formation and lethal challenge. Vaccine. 28:6382-6392.

332. Cheng AG, Kim HK, Burts ML, Krausz T, Schneewind O, Missiakas DM. 2009. Genetic requirements for *Staphylococcus aureus* abscess formation and persistence in host tissues. The FASEB Journal. 23:3393-3404.

333. Torres VJ, Pishchany G, Humayun M, Schneewind O, Skaar EP. 2006. *Staphylococcus aureus* IsdB Is a Hemoglobin Receptor Required for Heme Iron Utilization. Journal of Bacteriology. 188:8421-8429.

334. Speziali CD, Dale SE, Henderson JA, Vines ED, Heinrichs DE. 2006. Requirement of *Staphylococcus aureus* ATP binding cassette-ATPase FhuC for iron-restricted growth and evidence that it functions with more than one iron transporter. J Bacteriol. 188:2048-55.

335. Dale SE, Doherty-Kirby A, Lajoie G, Heinrichs DE. 2004. Role of Siderophore Biosynthesis in Virulence of *Staphylococcus aureus*: Identification and Characterization of Genes Involved in Production of a Siderophore. Infection and Immunity. 72:29-37.

336. Beasley FC, Marolda CL, Cheung J, Buac S, Heinrichs DE. 2011. *Staphylococcus aureus* Transporters Hts, Sir, and Sst Capture Iron Liberated from Human Transferrin by Staphyloferrin A, Staphyloferrin B, and Catecholamine Stress Hormones, Respectively, and Contribute to Virulence. Infection and Immunity. 79:2345-2355.

337. Cheung J, Beasley FC, Liu S, Lajoie GA, Heinrichs DE. 2009. Molecular characterization of staphyloferrin B biosynthesis in *Staphylococcus aureus*. Molecular Microbiology. 74:594.

338. Beasley F, Vinés ED, Grigg JC, Zheng Q, Liu S, Lajole GA, Murphy M, Heinrichs DE. 2009. Characterization of staphyloferrin A biosynthetic and transport mutants in *Staphylococcus aureus*. Molecular Microbiology. 72:947.

339. Skaar EP, Humayun M, Bae T, DeBord KL, Schneewind O. 2004. Iron-Source Preference of *Staphylococcus aureus* Infections. Science. 305:1626-1628.

340. Mazmanian SK, Ton-That H, Su K, Schneewind O. 2002. An Iron-Regulated Sortase Anchors a Class of Surface Protein during *Staphylococcus aureus*

Pathogenesis. Proceedings of the National Academy of Sciences of the United States of America. 99:2293-2298.

341. Muryoi N, Tiedemann MT, Pluym M, Cheung J, Heinrichs DE, Stillman MJ. 2008. Demonstration of the Iron-regulated Surface Determinant (Isd) Heme Transfer Pathway in *Staphylococcus aureus*. Journal of Biological Chemistry. 283:28125.

342. Skaar EP, Gaspar AH, Schneewind O. 2004. IsdG and IsdI, Heme-degrading Enzymes in the Cytoplasm of *Staphylococcus aureus*. Journal of Biological Chemistry. 279:436-443.

343. Sitthisak S, Knutsson L, Webb JW, Jayaswal RK. 2007. Molecular characterization of the copper transport system in *Staphylococcus aureus*. Microbiology. 153:4274-4283.

344. Vitko NP, Grosser MR, Khatri D, Lance TR, Richardson AR. 2016. Expanded Glucose Import Capability Affords *Staphylococcus aureus* Optimized Glycolytic Flux during Infection. mBio. 7:296.

345. Kelliher JL, Radin JN, Grim KP, Párraga Solórzano PK, Degnan PH, Kehl-Fie TE. 2018. Acquisition of the Phosphate Transporter NptA Enhances *Staphylococcus aureus* Pathogenesis by Improving Phosphate Uptake in Divergent Environments. Infection and Immunity. 86:e00631-17.

346. Kelliher JL, Radin JN, Kehl-Fie TE. 2018. PhoPR Contributes to *Staphylococcus aureus* Growth during Phosphate Starvation and Pathogenesis in an Environment-Specific Manner. Infection and Immunity. 86:e00371-18.

347. Henderson B, Martin A. 2011. Bacterial virulence in the moonlight: Multitasking bacterial moonlighting proteins are virulence determinants in infectious disease. Infect. Immun. 79:3476-3491.

348. Henderson B, Martin, A. 2013. Bacterial moonlighting proteins and bacterial virulence. Curr. Top. Microbiol. Immunol. 358:59.

349. Jeffery CJ. 1999. Moonlighting proteins. Trends Biochem. Sci. 24:8-11.

350. Pancholi V, Fischetti VA. 1992. A major surface protein on group A streptococci is a glyceraldehyde-3- phosphate-dehydrogenase with multiple binding activity. Journal of Experimental Medicine. 176:415-426.

351. Modun B, Morrissey, J, Williams, P. 2000. The staphylococcal transferrin receptor: a glycolytic enzyme with novel functions. 8:231-237.

352. Carneiro CRW, Postol E, Nomizo R, Reis LFL, Brentani RR. 2004. Identification of enolase as a laminin-binding protein on the surface of *Staphylococcus aureus*. Microbes and Infection. 6:604-608.

353. Xia X, Han M, Lee SY, Yoo J. 2008. Comparison of the extracellular proteomes of *Escherichia coli* B and K-12 strains during high cell density cultivation. Proteomics. 8:2089.

354. Li M, Rosenshine I, Tung SL, Wang XH, Friedberg D, Hew CL, Leung KY. 2004. Comparative Proteomic Analysis of Extracellular Proteins of Enterohemorrhagic and Enteropathogenic *Escherichia coli* Strains and Their ihf and ler Mutants. Applied and Environmental Microbiology. 70:5274-5282.

355. Tjalsma H, Antelmann H, Jongbloed JD, Braun PG, Darmon E, Dorenbos R, Dubois JY, Westers H, Zanen G, Quax WJ, Kuipers OP, Bron S, Hecker M, Dijl JMv. 2004. Proteomics of protein secretion by Bacillus subtilis: separating the "secrets" of the secretome. Microbiology and Molecular Biology Reviews. 68:207-233.

356. Sibbald MJ, Winter T, van der Kooi-Pol M, Buist G, Tsompanidou E, Bosma T, Schäfer T, Ohlsen K, Hecker M, Antelmann H, Engelmann S, Maarten van Dijl J. 2010. Synthetic Effects of secG and secY2 Mutations on Exoproteome Biogenesis in *Staphylococcus aureus*. Journal of Bacteriology. 194:3788.

357. Pasztor L, Ziebandt A-, Nega M, Schlag M, Haase S, Franz-Wachtel M, Madlung J, Nordheim A, Heinrichs DE, Gtz F. 2010. Staphylococcal major autolysin (Atl) is involved in excretion of cytoplasmic proteins. J. Biol. Chem. 285:36794-36803.

358. Ebner P, Prax M, Nega M, Koch I, Dube L, Yu W, Rinker J, Popella P, Fltenmeyer M, Gotz F. 2015. Excretion of cytoplasmic proteins (ECP) in *Staphylococcus aureus*. Mol. Microbiol. 97:775-789.

359. Lenz LL, Mohammadi S, Geissler A, Portnoy DA. 2003. SecA2-dependent secretion of autolytic enzymes promotes *Listeria monocytogenes* pathogenesis. Proc. Natl. Acad. Sci. U. S. A. 100:12432-12437.

360. Spalding MD, Prigge ST. 2010. Lipoic acid metabolism in microbial pathogens. Microbiol. Mol. Biol. Rev. 74:200-228.

361. Cronan JE. 2016. Assembly of lipoic acid on its cognate enzymes: An extraordinary and essential biosynthetic pathway. Microbiol. Mol. Biol. Rev. 80:429-450.

362. Reed LJ. 2001. A Trail of Research from Lipoic Acid to α-Keto Acid Dehydrogenase Complexes. The Journal of Biological Chemistry. 276:38329-38336.

363. Perham RN. 2000. Swinging arms and swinging domains in multifunctional enzymes: Catalytic Machines for Multistep Reactions. Annual Review of Biochemistry. 69:961-1004.

364. Perham RN. 1991. Domains, motifs, and linkers in 2-oxo acid dehydrogenase multienzyme complexes: a paradigm in the design of a multifunctional protein. Biochemistry. 30:8501-8512.

365. Milne J, Wu X, Borgnia MJ, Lengyel JS, Brooks BR, Shi D, Perham RN, Subramaniam S. 2006. Molecular Structure of a 9-MDa Icosahedral Pyruvate Dehydrogenase Subcomplex Containing the E2 and E3 Enzymes Using Cryoelectron Microscopy. Journal of Biological Chemistry. 281:4364-4370.

366. Kikuchi G, Motokawa Y, Yoshida T, Hiraga K. 2008. Glycine cleavage system: reaction mechanism, physiological significance, and hyperglycinemia. Proceedings of the Japan Academy. Series B, Physical and Biological Sciences. 84:246-263.

367. Kather B, Stingl K, van der Rest, M E, Altendorf K, Molenaar D. 2000. Another unusual type of citric acid cycle enzyme in Helicobacter pylori: the malate : quinone oxidoreductase. Journal of Bacteriology. 182:3204-3209.

368. Hughes NJ, Chalk P, Clayton CL, Kelly DJ. 1995. Identification of carboxylation enzymes and characterization of a novel four-subunit pyruvate:flavodoxin oxidoreductase from Helicobacter pylori. Journal of Bacteriology. 177:3953-3959.

369. Christensen QH, Hagar JA, O'Riordan MXD, Cronan JE. 2011. A complex lipoate utilization pathway in *Listeria monocytogenes*. J. Biol. Chem. 286:31447-31456.

370. Christensen QH, Martin N, Mansilla MC, de Mendoza D, Cronan JE. 2011. A novel amidotransferase required for lipoic acid cofactor assembly in *Bacillus subtilis*. Mol. Microbiol. 80:350-363.

371. Martin N, Christensen QH, Mansilla MC, Cronan JE, de Mendoza D. 2011. A novel two-gene requirement for the octanoyltransfer reaction of *Bacillus subtilis* lipoic acid biosynthesis. Molecular Microbiology. 80:335-349.

372. Christensen QH, Cronan JE. 2009. The *Thermoplasma acidophilum* LplA-LplB complex defines a new class of bipartite lipoate-protein ligases. J. Biol. Chem. 284:21317-21326.

373. Zorzoli A, Grayczyk JP, Alonzo F. 2016. *Staphylococcus aureus* Tissue Infection During Sepsis Is Supported by Differential Use of Bacterial or Host-Derived Lipoic Acid. PLoS Pathog. 12:e1005933.

374. Laczkovich I, Teoh WP, Flury S, Grayczyk JP, Zorzoli A, Alonzo F. 2018. Increased flexibility in the use of exogenous lipoic acid by *Staphylococcus aureus*. Molecular Microbiology. 109:150-168.

375. O'Riordan M, Moors MA, Portnoy DA. 2003. Listeria Intracellular Growth and Virulence Require Host-Derived Lipoic Acid. Science. 302:462-464.

376. Keeney KM, Stuckey JA, O'Riordan MXD. 2007. LplA1-dependent utilization of host lipoyl peptides enables Listeria cytosolic growth and virulence. Mol. Microbiol. 66:758-770.

377. Ramaswamy AV, Maurelli AT. 2010. *Chlamydia trachomatis* serovar L2 can utilize exogenous lipoic acid through the action of the lipoic acid ligase LplA1. J. Bacteriol. 192:6172-6181.

378. Storm J, Mller S. 2012. Lipoic acid metabolism of Plasmodium - a suitable drug target. Curr. Pharm. Des. 18:3480-3489.

379. Gunther S, Matuschewski K, Mller S. 2009. Knockout studies reveal an important role of Plasmodium lipoic acid protein ligase A1 for asexual blood stage parasite survival. PLoS ONE. 4:e5510.

380. Zhang WJ, Frei B. 2001. α-Lipoic acid inhibits TNF-α-induced NF-κB activation and adhesion molecule expression in human aortic endothelial cells. Faseb J. 15:2423-2432.

381. Packer L. 1998. α-Lipoic acid: A metabolic antioxidant which regulates NF-κB signal transduction and protects against oxidative injury. Drug Metab. Rev. 30:245-275.

382. Kim H, Kim H, Park K, Kim Y, Kwon T, Park J, Lee K, Kim J, Lee I. 2007. α-Lipoic acid inhibits matrix metalloproteinase-9 expression by inhibiting NF-κB transcriptional activity. Exp. Mol. Med. 39:106-113.

383. Packer L, Witt EH, Tritschler HJ. 1995. Alpha-lipoic acid as a biological antioxidant. Free Radic. Biol. Med. 19:227-250.

384. Zhang W, Wei H, Hagen T, Frei B. 2007. a-Lipoic acid attenuates LPS-induced inflammatory responses by activating the phosphoinositide 3-kinase/Akt signaling pathway. Proc. Natl. Acad. Sci. U. S. A. 104:4077-4082.

385. Yamada M, Kaibori M, Tanaka H, Habara K, Hijikawa T, Tanaka Y, Oishi M, Okumura T, Nishizawa M, Kwon A. 2012. [alpha]-Lipoic Acid Prevents the Induction of iNOS Gene Expression Through Destabilization of Its mRNA in Proinflammatory Cytokine-Stimulated Hepatocytes. Digestive Diseases and Sciences. 57:943.

386. Fey PD, Endres JL, Yajjala VK, Widhelm TJ, Boissy RJ, Bose JL, Bayles KW. 2013. A genetic resource for rapid and comprehensive phenotype screening of nonessential *Staphylococcus aureus* genes. MBio. 4:e00537-12.

387. Grayczyk JP, Harvey CJ, Laczkovich I, Alonzo F. 2017. A Lipoylated Metabolic Protein Released by *Staphylococcus aureus* Suppresses Macrophage Activation. Cell Host and Microbe. 22:678-687.

388. Takeuchi O, Sato S, Horiuchi T, Hoshino K, Takeda K, Dong Z, Modlin RL, Akira S. 2002. Cutting edge: Role of Toll-like receptor 1 in mediating immune response to microbial lipoproteins. J. Immunol. 169:10-14.

389. Takeuchi O, Kawai T, Mhlradt PF, Morr M, Radolf JD, Zychlinsky A, Takeda K, Akira S. 2001. Discrimination of bacterial lipoproteins by Toll-like receptor 6. Int. Immunol. 13:933-940.

390. Wardenburg JB, Williams WA, Missiakas D. 2006. Host defenses against *Staphylococcus aureus* infection require recognition of bacterial lipoproteins. Proc. Natl. Acad. Sci. U. S. A. 103:13831-13836.

391. Takeuchi O, Hoshino K, Akira S. 2000. Cutting edge: TLR2-deficient and MyD88-deficient mice are highly susceptible to *Staphylococcus aureus* infection. J. Immunol. 165:5392-5396.

392. Grundel A, Friedrich K, Pfeiffer M, Jacobs E, Dumke R. 2015. Subunits of the pyruvate dehydrogenase cluster of *Mycoplasma pneumoniae* are surface-displayed proteins that bind and activate human plasminogen. PLoS ONE. 10:e0126600.

393. Thomas C, Jacobs E, Dumke R. 2013. Characterization of pyruvate dehydrogenase subunit B and enolase as plasminogen-binding proteins in *Mycoplasma pneumoniae*. Microbiology. 159:352-365.

394. Fei M, Xie Q, Zou Y, He R, Zhang Y, Wang J, Bo L, Li J, Deng X. 2016. Alpha-lipoic acid protects mice against concanavalin A-induced hepatitis by modulating cytokine secretion and reducing reactive oxygen species generation. Int. Immunopharmacol. 35:53-60.

395. O'Neill HC, Rancourt RC, White CW. 2008. Lipoic acid suppression of neutrophil respiratory burst: Effect of NADPH. Antioxid. Redox Signal. 10:277-285.

396. Cheng AG, Kim HK, Burts ML, Krausz T, Schneewind O, Missiakas DM. 2009. Genetic requirements for *Staphylococcus aureus* abscess formation and persistence in host tissues. The FASEB Journal. 23:3393-3404.

397. Thammavongsa V, Missiakas DM, Schneewind O. 2013. *Staphylococcus aureus* Degrades Neutrophil Extracellular Traps to Promote Immune Cell Death. Science. 342:863-866.

398. Li Y, Trush MA. 1998. Diphenyleneiodonium, an NAD(P)H oxidase inhibitor, also potently inhibits mitochondrial reactive oxygen species production. Biochem. Biophys. Res. Commun. 253:295-299.

399. Rey FE, Cifuentes ME, Kiarash A, Quinn MT, Pagano PJ. 2001. Novel Competitive Inhibitor of NAD(P)H Oxidase Assembly Attenuates Vascular O 2 − and Systolic Blood Pressure in Mice. Circulation Research. 89:408-414.

400. Stephen Fawell, Joe Seery, Yasmin Daikh, Claire Moore, Chen, Blake Pepinsky, James Barsoum. 1994. Tat-Mediated Delivery of Heterologous Proteins into Cells. Proceedings of the National Academy of Sciences of the United States of America. 91:664-668.

401. Bryan NS, Grisham MB. 2007. Methods to detect nitric oxide and its metabolites in biological samples. Free Radical Biology and Medicine. 43:645-657.

402. Gao H, Jiang X, Pogliano K, Aronson AI. 2002. The E1 and E2 Subunits of the *Bacillus subtilis* Pyruvate Dehydrogenase Complex Are Involved in Regulation of Sporulation. Journal of Bacteriology. 184:2780-2788.

403. Prasad PP, Wang H, Kekuda R, Fujita T, Fei YJ, Devoe LD, Leibach FH, Ganapathy V. 1998. Cloning and Functional Expression of a cDNA Encoding a Mammalian Sodium-dependent Vitamin Transporter Mediating the Uptake of Pantothenate, Biotin, and Lipoate. Journal of Biological Chemistry. 273:7501-7506.

404. Zehnpfennig B, Wiriyasermkul P, Carlson DA, Quick M. 2015. Interaction of α-Lipoic Acid with the Human Na+/Multivitamin Transporter (hSMVT). The Journal of Biological Chemistry. 290:16372-16382.

405. Balamurugan K, Ortiz A, Said HM. 2003. Biotin uptake by human intestinal and liver epithelial cells: role of the SMVT system. American Journal of Physiology - Gastrointestinal and Liver Physiology. 285:73-77.

406. Zahringer U, Lindner B, Inamura S, Heine H, Alexander C. 2008. TLR2-promiscuous or specific? A critical reevaluation of a receptor expressing apparent broad specificity. Immunobiology. 213:205-224.

407. Aevarsson A, Seger K, Turley S, Sokatch JR, Hol WGJ. 1999. Crystal structure of 2-oxoisovalerate and dehydrogenase and the architecture of 2-oxo acid dehydrogenase multienzyme complexes. Nat. Struct. Biol. 6:785-792.

408. Fujiwara K, Toma S, Okamura-Ikeda K, Motokawa Y, Nakagawa A, Taniguchi H. 2005. Crystal structure of lipoate-protein ligase A from *Escherichia coli*: Determination of the lipoic acid-binding site. J. Biol. Chem. 280:33645-33651.

409. Farhat K, Riekenberg S, Heine H, Debarry J, Lang R, Mages J, Buwitt-Beckmann U, Rschmann K, Jung G, Wiesmller K, Ulmer AJ. 2008. Heterodimerization of TLR2 with TLR1 or TLR6 expands the ligand spectrum but does not lead to differential signaling. J. Leukocyte Biol. 83:692-701.

410. Huang S, Rutkowsky JM, Snodgrass RG, Ono-Moore KD, Schneider DA, Newman JW, Adams SH, Hwang DH. 2012. Saturated fatty acids activate TLR-mediated proinflammatory signaling pathways. J. Lipid Res. 53:2002-2013.

411. Lee JY, Zhao L, Youn HS, Weatherill AR, Tapping R, Feng L, Lee WH, Fitzgerald KA, Hwang DH. 2004. Saturated Fatty Acid Activates but Polyunsaturated Fatty Acid Inhibits Toll-like Receptor 2 Dimerized with Toll-like Receptor 6 or 1. J. Biol. Chem. 279:16971-16979.

412. McClure R, Massari P. 2014. TLR-Dependent Human Mucosal Epithelial Cell Responses to Microbial Pathogens. Frontiers in Immunology. 5:386.

413. Chen X, Alonzo F. 2019. Bacterial lipolysis of immune-activating ligands promotes evasion of innate defenses. Proceedings of the National Academy of Sciences of the United States of America. 116:3764-3773.

414. Wilde AD, Snyder DJ, Putnam NE, Valentino MD, Hammer ND, Lonergan ZR, Hinger SA, Aysanoa EE, Blanchard C, Dunman PM, Wasserman GA, Chen J, Shopsin B, Gilmore MS, Skaar EP, Cassat JE. 2015. Bacterial Hypoxic Responses Revealed as Critical Determinants of the Host-Pathogen Outcome by TnSeq Analysis of *Staphylococcus aureus* Invasive Infection. PLoS Pathogens. 11:e1005341.

415. Balasubramanian D, Harper L, Shopsin B, Torres VJ. 2017. *Staphylococcus aureus* pathogenesis in diverse host environments. Pathogens and Disease. 75:005.

416. Yefei Zhu, Renu Nandakumar, Marat R. Sadykov, Nandakumar Madayiputhiya, Thanh T. Luong, Rosmarie Gaupp, Chia Y. Lee, Greg A. Somerville. 2011. RpiR Homologues May Link *Staphylococcus aureus* RNAIII Synthesis and Pentose Phosphate Pathway Regulation. Journal of Bacteriology. 193:6187-6196.

417. Vitko NP, Grosser MR, Khatri D, Lance TR, Richardson AR. 2016. Expanded Glucose Import Capability Affords *Staphylococcus aureus* Optimized Glycolytic Flux during Infection. mBio. 7:296.

418. Sunderkotter C, Nikolic T, Dillon MJ, van Rooijen N, Stehling M, Drevets DA, Leenen PJM. 2004. Subpopulations of Mouse Blood Monocytes Differ in Maturation Stage and Inflammatory Response. The Journal of Immunology. 172:4410-4417.

419. Chen X, Chen H, Deng R, Shen J. 2014. Pros and Cons of Current Approaches for Detecting Peroxynitrite and Their Applications. Biomedical Journal. 37:120-126.

420. Sedgwick AC, Sun X, Kim G, Yoon J, Bull SD, James TD. 2016. Boronate based fluorescence (ESIPT) probe for peroxynitrite. Chemical Communications (Cambridge, England). 52:12350.

421. Yang C, Shin D, Kim K, Lee Z, Lee C, Park SG, Bae YS, Jo E. 2009. NADPH Oxidase 2 Interaction with TLR2 Is Required for Efficient Innate Immune Responses to Mycobacteria via Cathelicidin Expression. The Journal of Immunology. 182:3696-3705.

422. Schuett J, Schuett H, Oberoi R, Koch A, Pretzer S, Luchtefeld M, Schieffer B, Grote K. 2017. NADPH oxidase NOX2 mediates TLR2/6-dependent release of GM-CSF from endothelial cells. FASEB Journal. 31:2612-2624.

423. Yang C, Lee J, Lee J, Lee K, Rodgers M, Min C, Kim H, Kim C, Oh B, Zandi E, Yue Z, Kramnik I, Liang C, Jung J. 2012. Autophagy Protein Rubicon Mediates Phagocytic NADPH Oxidase Activation in Response to Microbial Infection or TLR Stimulation. Cell Host & Microbe. 11:264-276.

424. Jann NJ, Schmaler M, Ferracin F, Landmann R. 2010. TLR2 enhances NADPH oxidase activity and killing of *Staphylococcus aureus* by PMN. Immunology Letters. 135:17-23.

425. Carolyn R. Hoyal, Abel Gutierrez, Brandon M. Young, Sergio D. Catz, Jun-Hsiang Lin, Philip N. Tsichlis, Bernard M. Babior. 2003. Modulation of p47PHOX activity by site-specific phosphorylation: Akt-dependent activation of the NADPH oxidase. Proceedings of the National Academy of Sciences of the United States of America. 100:5130-5135.

426. Mendes F, Carvalho PA, Caramona MM, Lopes CM. 2001. Diphenyleneiodonium inhibits NF-kappaB activation and iNOS expression induced by IL-1beta: involvement of reactive oxygen species. Mediators of Inflammation. 10:209-215.

427. Savina A, Amigorena, S. 2007. Phagocytosis and antigen presentation in dendritic cells. 219:143-156.

428. Benoun JM, Labuda JC, McSorley SJ. 2016. Collateral Damage: Detrimental Effect of Antibiotics on the Development of Protective Immune Memory. mBio. 7:1520.

429. Bingisser RM, Tilbrook PA, Holt PG, Kees UR. 1998. Macrophage-Derived Nitric Oxide Regulates T Cell Activation via Reversible Disruption of the Jak3/STAT5 Signaling Pathway. The Journal of Immunology. 160:5729-5734.

430. Nabeshima S, Nomoto M, Matsuzaki G, Kishihara K, Taniguchi H, Yoshida SI, Nomoto K. 1999. T-Cell Hyporesponsiveness Induced by Activated Macrophages through Nitric Oxide Production in Mice Infected with *Mycobacterium tuberculosis*. Infection and Immunity. 67:3221-3226.

431. Bogdan C. 2015. Nitric oxide synthase in innate and adaptive immunity: an update. Trends in Immunology. 36:161-178.

VITA

James Paul Grayczyk was born on June 9, 1992 in Arlington Heights, Illinois. He attended Iowa State University in Ames, Iowa, where he earned a Bachelor of Science in Microbiology and Genetics in 2014. During his undergraduate studies, James worked and researched in the plant pathology laboratory of Dr. Steven Whitham at Iowa State University. In Dr. Whitham's lab, James studied potential virulence factors from the soybean rust fungus pathogen.

In August 2014, James matriculated into the Integrated Program in Biomedical Sciences at Loyola University Chicago and joined the Department of Microbiology and Immunology. He completed his graduate studies in the laboratory of Dr. Francis Alonzo III, where he focused on investigating evasion of macrophage responses by *Staphylococcus aureus*. James's dissertation research was supported by an NIH T32 Training Grant in Experimental Immunology to Dr. Katherine L. Knight, an American Heart Association Predoctoral Fellowship award, and an NIH R01 awarded to Dr. Francis Alonzo III.

After completion of his graduate studies, James will continue researching bacterial host-pathogen interactions as a Postdoctoral Research Fellow in the laboratory of Dr. Igor Brodsky, at the University of Pennsylvania in Philadelphia, PA.